Characterization of anti-gp120/Env-specific antibody functionality in HIV controllers associated with HIV control

Sanket Kant

Faculty of Medicine, Division of Experimental Medicine

McGill University, Montreal

December 2021

A thesis submitted to McGill University in partial fulfillment of the requirements of the degree of Doctor of Philosophy

Abstract (in English)

Availability of anti-retroviral therapy (ART) has transformed HIV infection from a death sentence into a chronic viral disease. However, a cure for HIV remains elusive. The RV144 Thai HIV vaccine trial demonstrated modest protective vaccine efficacy. Anti-HIV-1 antibodies (Abs) and their functions were identified as correlates of protection. In addition, recent literature has provided more evidence that anti-HIV-1 Abs, specifically non-neutralising Abs to the HIV-1 glycoprotein 120 (gp120)/Envelope (Env) are important actors in the fight against HIV. Upon gp120/Env recognition by the Fab portion of the Abs, the Fc portion engages with the complement system and Fc receptors on several types of innate immune cells. When the Fc receptor on natural killer (NK) cells is cross-linked, these cells are activated for cytolysis and secretion of cytokines and chemokines directed to HIV-infected cells. When the Fc receptor on monocytes is cross-liked, phagocytosis and trogocytosis directed to HIV-infected cells are induced. Overall, these Abs have the potential to target and eliminate HIV-infected cells. HIV-1 elite controllers (ECs) are a rare subset (<0.05%) of HIV-1 infected individuals who can spontaneously control viremia to below the limit of detection of available viral load assays in the absence of ART. The biological mechanism(s) underlying durable and suppressed viremia is an intense area of study. It is implied that the non-neutralising anti-gp120/Env Abs might play a role in the durable suppression in ECs. Nevertheless, antibody dependent (AD) functions have not been characterised in the context of HIV reservoirs.

In this thesis I measured the concentrations of gp120/Env-specific Abs, their non-neutralising functions, and their biophysical characteristics in four HIV-infected populations. The extent of usefulness of non-neutralising of gp120/Env-specific Ab functions in HIV control is not concrete and is strongly debated. Such contradiction may exist in part due to the target cell system used.

Most studies to date have worked with gp120-coated $CD4^+$ cells. It is well known now that depending on the presence of CD4, HIV-1 Env exists in different conformations. Interaction with cell surface CD4 leads to opening up the Env conformation, which exposes hidden conserved regions containing epitopes recognized by the immune system. This is observed in HIV infection models whereby gp120 shed from infected cells binds to neighboring uninfected bystander $CD4^+$ cells. Thus, gp120-coated $CD4^+$ cells represent Env in the open conformation and Abs binding to the open conformation of Env in reality represent Abs targeting the uninfected bystander $CD4^+$ target cells. However, in a productive HIV-1 infection, two HIV-1 proteins, Nef and Vpu are responsible for downregulating CD4 molecule from the cell surface. Therefore, the cell surface Env is present in a closed conformation. In this thesis, we developed a target model, called as the sorted infected CEM (siCEM) cell line, that represents a productively infected HIV-1 model such that the Env is expressed in its closed conformation.

In addition to ECs, we included three additional HIV-infected study groups – untreated progressors (UTPs), treated progressors (TPs) and viremic controllers (VCs) and I measured the concentrations of Abs binding to the open (gp120-coated $CD4^+$ cells) and closed conformation of Env (siCEM cells). We reported that concentration of gp120-specific IgG Abs in plasma from all groups of people living with HIV (PLWH) was significantly greater than concentrations of IgG Abs binding to Env on siCEM cells. Our data also showed that while there were no significant differences between amount of Abs binding to gp120-coated targets or siCEM cells in plasma from UTPs, ECs and VCs, these levels were significantly higher than in plasma from TPs.

The four antibody dependent (AD) functions investigated in the thesis were AD cellular phagocytosis (ADCP), AD complement deposition (ADCD), AD cellular cytotoxicity (ADCC) and AD cellular trogocytosis (ADCT). For the most part, ADCP, ADCC and ADCT function

levels did not differ significantly between the UTPs, ECs and VCs. Yet again, plasma from these 3 study groups had significantly higher AD function level than plasma from TPs. Interestingly, none of the individual or groupings of functions differentiate ECs from the other study groups. However, all methods used to measure HIV-specific Abs and their AD functions in plasma from ECs were significantly correlated with each other, demonstrating that the Ab responses in ECs were highly coordinated and polyfunctional in nature. Significant differences between groups disappeared when the AD functions were normalised to the concentrations of gp120/Env-specific Abs. Thus, the intensity of the functions was determined by the concentration of gp120-/Env-specific Abs present in each participant's plasma.

We also measured the reservoir in ECs and VCs (HIV controllers) by using real-time quantitative DNA polymerase chain reaction (PCR). Our data demonstrated that amongst controllers, those with an HIV reservoir size that was below the limit of detection had significantly higher levels of normalised ADCC function than those with a detectable HIV reservoir size. Ab-normalised ADCP, ADCP and ADCT levels showed non-significant trends towards being higher in controllers with undetectable versus detectable HIV reservoir sizes. This association would be consistent with these functions playing a role on HIV control though the cause and effect relationship between the 2 has yet to be established.

The two biophysical characteristics we measured in this project were the 1) distribution of IgG subclasses specific for several HIV antigens (gp120, gp70V1V2, gp140, gp41, and p24) and 2) proportions of the different glycosylation patterns on gp120-specific IgG Abs. We observed that UTPs had significantly higher amounts of gp70, gp140, & gp41-specific IgG2 and gp120- and gp41-specific IgG4 Abs than ECs. There were no noteworthy correlations between IgG subclass distribution to the various antigens and AD functions, which suggested that while there were

significant differences for IgG2 and IgG4 between UTPs and ECs, they did not associate with AD functions. Unsupervised and supervised clustering methods did not distinguish ECs from other groups of PLWH, which again suggests that the IgG subclass distribution features were not key features that distinguished ECs from the other groups of PLWH. Glycosylation patterns of gp120-specific IgG Abs revealed that the proportion of galactosylated and digalactosylated-sialylated gp120-specific Abs amongst the total gp120-specific IgG Abs were higher in ECs than UTPs. ECs as well had lower proportions of fucosylated gp120-specific IgG Abs. Fucosylated Abs have been shown to impact CD16 engagement on NK cells, which lowers ADCC activity compared to afucosylated Abs. Interestingly, the proportion of sialylated gp120-specific IgG Abs were significantly and positively correlated with AD functions only in ECs. Again, unsupervised, or supervised clustering methods were unable to distinguish ECs from other groups of PLWH based on the glycoforms of anti-gp120 IgG Abs. This implies that glycosylation features were not pertinent in distinguishing ECs from other groups of PLWH.

Résumé (en français)

La disponibilité de la thérapie antirétrovirale (TAR) a transformé l'infection à VIH d'une condamnation à mort en une maladie virale chronique. Cependant, un remède contre le VIH reste insaisissable. L'essai du vaccin Thai RV144 contre le VIH a démontré une efficacité vaccinale protectrice modeste. Les anticorps anti-VIH-1 (Acs) et leurs fonctions ont été identifiés comme des réponses immunitaires responsables de la protection. De plus, la littérature récente a fourni davantage de preuves que les Acs anti-VIH-1, en particulier les Acs non neutralisants aux glycoprotéine 120 (gp120)/Enveloppe (Env) du VIH-1 sont des acteurs importants dans la lutte contre le VIH. Lors de la reconnaissance de gp120/Env par la partie Fab de l'Ac, la partie Fc s'engage avec le système du complément et les récepteurs Fc sur plusieurs types de cellules immunitaires innées. Lorsque le récepteur Fc sur les cellules tueuses naturelles (NK) est cross-linké, ces cellules sont activées pour la cytolyse et la sécrétion de cytokines et de chimiokines dirigées vers les cellules infectées par le VIH. Lorsque le récepteur Fc sur les monocytes est cross-linké, la phagocytose et la trogocytose dirigées vers les cellules infectées par le VIH sont induites. Globalement, ces Acs ont le potentiel de cibler et d'éliminer les cellules infectées par le VIH. Les contrôleurs d'élite (CEs) du VIH-1 sont une sous-population rare (<0,05 %) d'individus infectés par le VIH-1 qui peuvent contrôler spontanément la virémie en dessous de la limite de détection avec des tests de charge virale disponibles en l'absence de TAR. Le ou les mécanismes biologiques sous-jacents à une suppression virale durable constituent un domaine d'étude intense. Il est présumé que les Acs anti-gp120/Env non neutralisants pourraient jouer un rôle dans la suppression durable chez les CEs. Néanmoins, les fonctions dépendantes des anticorps (DA) n'ont pas été caractérisées dans le contexte des réservoirs du VIH.

Dans cette thèse, j'ai mesuré les concentrations d'Acs spécifiques aux gp120/Env, leurs fonctions non neutralisantes et leurs caractéristiques biophysiques dans quatre populations infectées par le VIH. L'étendue de l'utilité des fonctions non neutralisantes des Ac spécifiques aux gp120/Env dans le contrôle du VIH n'est pas concrète et est fortement débattue. Une telle contradiction peut exister en partie dû au système de cellule cible utilisé. La plupart des études réalisées à ce jour ont porté sur des cellules $CD4^+$ recouvertes de gp120. Il est bien connu maintenant qu'en fonction de la présence de CD4, l'Env du VIH-1 existe sous différentes conformations. L'interaction de cette dernière avec la CD4 aux surfaces cellulaires conduit à une conformation ouverte d'Env, qui expose des régions conservées cachées contenant des épitopes reconnus par le système immunitaire. Ceci est observé dans les modèles d'infection par le VIH où la gp120 libérée des cellules infectées se lie aux cellules $CD4^+$ voisines non infectées. Ainsi, les cellules $CD4^+$ recouvertes de gp120 représentent Env dans la conformation ouverte et les Acs se liant à la conformation ouverte d'Env, en réalité, représente les Acs ciblant les cellules cibles $CD4^+$ non infectées. Cependant, dans une infection productive par le VIH-1, deux protéines du VIH-1, Nef et Vpu, sont responsables de la régulation négative des molécules CD4 sur la surface cellulaire. Par conséquent, l'Env à la surface cellulaire est présente dans une conformation fermée. Dans cette thèse, nous avons développé un modèle cible, appelé la lignée cellulaire CEM infectée triée (siCEM, de l'anglais *sorted infected CEM*), qui représente un modèle VIH-1 infecté de manière productive de telle sorte que l'Env est exprimé dans sa conformation fermée.

En plus des CEs, nous avons inclus trois groupes d'étude supplémentaires infectés par le VIH - les progresseurs non traités (PNTs), les progresseurs traités (PTs) et les contrôleurs virémiques (CVs), et j'ai mesuré les concentrations d'Acs se liant à la conformation ouverte (cellules $CD4^+$

recouvertes de gp120) et fermée d'Env (cellules siCEM). Nous avons démontré que la concentration d'Acs IgG spécifiques à la gp120 dans le plasma de tous les groupes de personnes vivant avec le VIH (PVVIH) était significativement supérieure aux concentrations d'Acs IgG se liant à l'Env sur les cellules siCEM. Nos données ont également montré que, bien qu'il n'y ait pas de différences significatives entre la quantité d'Abs se liant aux cibles recouvertes de gp120 ou aux cellules siCEM dans le plasma des PNTs, des CEs et des CVs, elles étaient significativement plus élevées que dans le plasma des PTs.

Les quatre fonctions dépendantes des anticorps (DA) étudiées dans la thèse étaient la phagocytose cellulaire DA (ADCP, de l'anglais *antibody-dependent cellular phagocytosis*), le dépôt de complément DA (ADCD, de l'anglais *antibody-dependent complement deposition*), la cytotoxicité à médiation cellulaire DA (ADCC, de l'anglais *antibody-dependent cellular cytotoxicity*) et la trogocytose cellulaire DA (ADCT, de l'anglais *antibody-dependent cellular trogocytosis*). Pour la plupart, les niveaux de fonction des ADCP, ADCC et ADCT ne différaient pas significativement entre les PNTs, les CEs et les CVs. De plus, le plasma de ces trois groupes d'étude avait un niveau de fonction DA significativement plus élevé que celui des PTs. Fait intéressant, aucune des fonctions individuelles ou de groupes ne différencie les CEs des autres groupes d'étude. Cependant, toutes les méthodes utilisées pour mesurer les Acs spécifiques au VIH ainsi que leurs fonctions DA dans le plasma des CEs étaient significativement corrélées les unes aux autres, démontrant que les réponses des Acs chez les CEs étaient hautement coordonnée et polyfonctionnelle. Des différences significatives entre les groupes ont disparu lorsque les fonctions DA ont été normalisées aux concentrations d'Acs spécifiques aux gp120/Env. Ainsi, le niveau des fonctions a

été déterminée par la concentration d'Acs spécifiques aux gp120/Env présents dans le plasma de chaque participant.

Nous avons également mesuré le réservoir chez les CEs et les CVs (contrôleurs du VIH) en utilisant la réaction en chaîne par polymérase (ACP) à l'ADN quantitative en temps réel. Nos données ont démontré que parmi les contrôleurs, ceux dont la taille du réservoir de VIH était inférieure à la limite de détection avaient des niveaux significativement plus élevés de fonction ADCC normalisée que ceux dont la taille du réservoir de VIH était détectable. Les niveaux d'ADCP, d'ADCD et d'ADCT normalisés aux Acs ont montré des tendances non significatives mais plus élevés chez les contrôleurs avec des tailles de réservoir de VIH indétectables par rapport aux détectables. Cette association serait cohérente avec le fait que ces fonctions jouent un rôle dans le contrôle du VIH bien que la relation de cause à effet entre les deux n’ait pas encore été établie.

Les deux caractéristiques biophysiques que nous avons mesurées dans ce projet étaient 1) la distribution des sous-classes d'IgG spécifiques aux plusieurs antigènes du VIH (gp120, gp70V1V2, gp140, gp41 et p24) et 2) les proportions des différents profils de glycosylation sur les Acs IgG spécifiques à la gp120. Nous avons observé que les PNTs avaient des quantités significativement plus élevées d'IgG2 spécifiques aux gp70, gp140 et gp41, et d'IgG4 spécifiques aux gp120 et gp41 que les CEs. Il n'y avait pas de corrélations notables entre la distribution des sous-classes d'IgG aux divers antigènes et les fonctions DA, ce qui suggère que, bien qu'il y ait des différences significatives au niveau des IgG2 et IgG4 entre les PNTs et les CEs, elles ne sont pas associées aux fonctions DA. Les méthodes de regroupement supervisées et non supervisées n'ont pas permis de distinguer les CEs des autres groupes de PVVIH, ce qui suggère à nouveau que les

caractéristiques de distribution des sous-classes d'IgG n'étaient pas des caractéristiques clés qui distinguaient les CEs des autres groupes de PVVIH. Les profils de glycosylation des Acs IgG spécifiques à la gp120 ont révélé que la proportion d'Acs spécifiques aux gp120 galactosylées et digalactosylées-sialylées parmi les Acs IgG spécifiques aux gp120 totales était plus élevée chez les CEs que chez les PNTs. Les CEs avaient également des proportions plus faibles d'Acs IgG spécifiques aux gp120 fucosylées. Il a été démontré que les Acs fucosylés ont un impact sur l'engagement de CD16 sur les cellules NK, ce qui réduit l'activité d'ADCC par rapport aux Acs afucosylés. Fait intéressant, la proportion d'Ac IgG spécifiques à la gp120 sialylée était significativement et positivement corrélée avec les fonctions DA uniquement chez les CEs. Encore une fois, les méthodes de regroupement non supervisées ou supervisées n'ont pas été en mesure de distinguer les CEs des autres groupes de PVVIH sur la base des glycoformes d'Acs IgG anti-gp120. Cela implique que les caractéristiques de glycosylation n'étaient pas pertinentes pour distinguer les CEs des autres groupes de PVVIH.

This thesis is dedicated to my maternal and paternal grandparents who have only dreamt of me succeeding. I hope I do you proud and I am sure that you are watching over me.

Acknowledgments

First, I would like to express my immense gratitude to my supervisor and mentor, Dr. Nicole Flore Bernard for formulating this incredible idea and for welcoming me into her team. Her scientific aptitude, encouraging words, and trust in me have led to this work. Her scientific and personal support throughout the years has made me the scientist I dreamed of. I am fortunate to have benefited from Dr. Bernard's support. Her scientific vision and drive have a positive impact on me that will last throughout my professional life. She has taught me everything I know about science and academia – from learning how to read a paper, to writing one.

Special thanks to Dr. Franck P. Dupuy for his scientific know-how and critical thinking. I have learnt a great deal about science and the academic world from him. His expertise contributed to the rigor of this body of work. Thank you for answering my questions and in the process, invoking questions which actually taught me how to do "research".

To my committee members, Dr. Jean-Pierre Routy, Dr. Andrés Finzi, Dr. Cecilia Costinuik, and my academic advisor, Dr. Danuta Radzioch – thank you for making me into the scientist I am. My scientific career is wholly indebted to you. Your thoughtful suggestions and critical advice have shaped this body of work. Whenever I close my eyes, I look back at the time of my Comprehensive exams when the committee expressed that I was doing better as the time went by – I will never forget that.

To Tsoarella Mabanga, I am grateful to have you as a colleague and a friend. Your presence was essential to my survival – be it providing cell positions, ordering reagents, or critical life advice. Your empathy and kindness have helped me change and become a different person (for better, I think or at least I hope).

To Louise Gilbert, I am grateful for your technical assistance, which contributed to the results presented in my first published article and for every time you provided me the cell positions. However, I enjoyed your company most whenever we discussed food and cooking. Thank you for sharing your food with me – I will cherish those times.

To Zahra Kiani, your personality was like no one other. I admired and, in the process, learned a great deal from you on how to troubleshoot. Thanks for your support, encouraging words, and good mood.

To Ningyu Zhang and Alexa del Corpo, thank you for your technical help throughout the years. This thesis would not have been completed without your assistance with anti-gp120 plate-based ELISAs – the backbone of all our experiments and analysis.

To Lauren Nagel and Christopher Leeks, thank you for your assistance and help with the various antibody-dependent experiments we performed over the years.

To Dr. Oussama Meziane, your scientific thought, questions, and work ethic was second to none. I want to thank you for teaching me how to organise all the data and text for scientific publications.

To Dr. Makan Golizeh, I am immensely indebted to you for your kind ear, encouraging & uplifting words, and for imparting wisdom.

To Tao Shi, for your scientific expertise and assisting us with translating the abstract of this thesis to French language.

A huge thank you to past and present members of the Bernard lab – Alexandre Barbe and Khlood Al Sulami, for your technical assistance.

I would also like to acknowledge the clinical and administrative teams of, and the samples obtained from the two cohorts whose participants provided biological samples used to generate the research

results presented in this thesis – 1) the Canadian Cohort of HIV^+ Slow Progressors, setup by Dr. Cécile Tremblay and Dr. N.F. Bernard, and 2) the Montreal Primary HIV Infection Cohort, setup by Dr. Jean-Pierre Routy. To all the individuals who were benevolent in providing their samples, words cannot express my gratitude to your unselfishness for the greater good in advancing the field of HIV research. My deepest gratitude to the clinicians, nurses, technicians, data managers, and administrators who worked with these cohorts, clinically following participants, collecting and banking donor biological samples.

I would also like to thank Dr. Costinuik's team (Edwin, Yulia, Sarah, Ralph, and Elaine) for their uplifting mood and technical expertise.

To Dr. Dmitri Kharitidi, former colleague and friend, for all his helpful advice and insight into science. I am fortunate that you were my first friend in Canada.

To Victor and Sout, I am thankful for having found you. You have been super supportive and encouraging and I could not imagine reaching this stage without having you by my side.

I am nothing without my parents' support and guidance. You have been unconditionally supportive of my pursuit of research.

पंख है तो पुरा फेला बस क्या?

Contribution of Authors

The primary author was responsible for writing the entirety of this thesis unless mentioned otherwise. Assistance was obtained throughout the Doctoral degree at various stages with respect to experiments, data analysis and presentations, and writing and editing the manuscripts. I acknowledge Tsoarella Mabanga and Louise Gilbert for providing biological samples and technical assistance with the experiments, and Alexa del Corpo for providing help with aliquoting the samples and assistance with ELISA experiments.

Chapter 1: Introduction and Literature Review

Author contribution: Sanket Kant wrote the chapter. Nicole F. Bernard edited the chapter.

Chapter 2: Quantifying Anti-HIV Envelope-Specific Antibodies in Plasma from HIV Infected Individuals.

Sanket Kant, Ningyu Zhang, Jean-Pierre Routy ,Cécile Tremblay, Réjean Thomas, Jason Szabo, Pierre Côté, Benoit Trottier, Roger LeBlanc, Danielle Rouleau, Marianne Harris, Franck P. Dupuy, and Nicole F. Bernard

Published in Viruses, 28 May 2019. https://doi.org/10.3390/v11060487

Author contribution: Sanket Kant conceived the study, performed, and analysed the experiments, prepared the figures, wrote the first draft and edited the manuscript. Franck P. Dupuy conceived the study, analysed the experiments, prepared the figures, and edited the manuscript. Nicole F. Bernard conceived the study, wrote the first draft, and edited the manuscript, provided clinical material from PLWH enrolled in the study, supervised the project, provided project administration and obtained funding for the study. Ningyu Zhang contributed to the performing a portion of the experiments. Jean-Pierre Routy ,Cécile Tremblay, Réjean Thomas, Jason Szabo, Pierre Côté,

Benoit Trottier, Roger LeBlanc, Danielle Rouleau, and Marianne Harris recruited the PLWH and provided clinical samples and edited the manuscript.

Chapter 3: Polyfunctional Fc Dependent Activity of Antibodies to Native Trimeric Envelope in HIV Elite Controllers

Sanket Kant, Ningyu Zhang, Alexandre Barbé, Jean-Pierre Routy, Cécile Tremblay, Réjean Thomas, Jason Szabo, Pierre Côté, Benoit Trottier, Roger LeBlanc, Danielle Rouleau, Marianne Harris, Franck P. Dupuy, and Nicole F. Bernard

Published in Frontiers in Immunology, 30 September 2020. https://doi.org/10.3389/fimmu.2020.583820

Author contribution: Sanket Kant conceived the study, performed the experiments, analysed the data, prepared figures for publication, wrote the first draft of the manuscript, and edited the manuscript. Franck P. Dupuy conceived the study, contributed partly to the experiments, analysed the data, and edited the manuscript. Nicole F. Bernard conceived the study, wrote the first draft of the manuscript, edited the manuscript, enrolled PLWH and provided clinical samples for the study, supervised the study, and obtained funding for this study. Ningyu Zhang and Alexandre Barbé contributed partly to experiments. Jean-Pierre Routy ,Cécile Tremblay, Réjean Thomas, Jason Szabo, Pierre Côté, Benoit Trottier, Roger LeBlanc, Danielle Rouleau, and Marianne Harris enrolled PLWH, provided us clinical samples for the study, and reviewed and edited the manuscript.

Chapter 4: Biophysical features of gp120-specific Abs in people living with HIV/HIV elite controllers

Manuscript under preparation

Sanket Kant, Caitlyn Linde, Ningyu Zhang, Vicky Roy, Jean-Pierre Routy, Cécile Tremblay, Réjean Thomas, Jason Szabo, Pierre Côté, Benoit Trottier, Roger LeBlanc, Danielle Rouleau, Marianne Harris, Franck P. Dupuy, Galit Alter, and Nicole F. Bernard

Author contribution: Sanket Kant conceived the study, performed a portion of the experiments, analysed the data, prepared figures for publication, wrote the first draft of the manuscript, and edited the manuscript. Caitlyn Linde performed a portion of the experiments in the manuscript. Vicky Roy provided technical assistance to the data generated by Caitlyn Linde. Franck P. Dupuy, Ningyu Zhang contributed partly to experiments. Franck P. Dupuy contributed partially to the data analysis. Nicole F. Bernard conceived the study, wrote the first draft of the manuscript, edited the manuscript, enrolled PLWH, and provided clinical samples for the study, supervised the study, and obtained funding for this study. Galit Alter provided administrative support and Jean-Pierre Routy, Cécile Tremblay, Réjean Thomas, Jason Szabo, Pierre Côté, Benoit Trottier, Roger LeBlanc, Danielle Rouleau, and Marianne Harris enrolled PLWH, provided us clinical samples for the study, and reviewed and edited the manuscript.

Chapter 5: Discussion

Author contribution: Sanket Kant wrote the chapter. Nicole F. Bernard edited the chapter.

Contribution to other articles:

1. **Natural Killer Cells in Antibody Independent and Antibody Dependent HIV control**
   Nicole F. Bernard, Sanket Kant, Zahra Kiani, Cécile Tremblay, and Franck P Dupuy
   Accepted for publication in Frontiers in Immunology on 11 April 2022
   Contribution to study: I contributed to literature review, writing, and revising the manuscript at different stages. I also contributed to preparing figures for this review article.

data analysis of those experiments, assisted in preparing graphs, and reviewed the manuscripts at different stages of preparation

2. **Distinct Plasma Concentrations of Acyl-CoA-Binding Protein (ACBP) in HIV Progressors and Elite Controllers**

Published in Viruses, 23 February 2022. https://doi.org/10.3390/v14030453

Stéphane Isnard, Léna Royston, John Lin, Brandon Fombuena, Simeng Bu, **Sanket Kant**, Tsoarello Mabanga, Carolina Berini, Mohamed El-Far, Madeleine Durand, Cécile L. Tremblay, Nicole F. Bernard, Guido Kroemer, and Jean-Pierre Routy

Contribution to study: I contributed partly to experiments, data analysis of those experiments, and reviewed the manuscripts at different stages of preparation.

3. **Evolution of Antibodies to Native Trimeric Envelope and Their Fc-Dependent Functions in Untreated and Treated Primary HIV Infection**

Published in Journal of Virology, 29 September 2021. https://doi.org/10.1128/JVI.01625-21

Lauren Nagel, **Sanket Kant**, Christopher Leeks, Jean-Pierre Routy, Cécile Tremblay, Réjean Thomas, Jason Szabo, Pierre Côté, Benoit Trottier, Roger LeBlanc, Danielle Rouleau, Franck P Dupuy, Nicole F Bernard, investigators in Montreal Primary HIV Infection cohort

Contribution to study: I contributed to experiments, data analysis of those experiments, assisted in preparing graphs, and reviewed the manuscripts at different stages of preparation.

4. **Anti-cytomegalovirus Immunoglobulin G Is Linked to CD4 T-cell Count Decay in Human Immunodeficiency Virus (HIV) Elite Controllers**

Published in Clinical Infectious Diseases, 5 August 2020. https://doi.org/10.1093/cid/ciaa1129

Stephane Isnard, Rayoun Ramendra, John Lin, **Sanket Kant**, Brandon Fombuena, Jing Ouyang, Xiaorong Peng, Mohamed El Far, Cécile Tremblay, Nicole F Bernard, Jean-Pierre Routy

Contribution to study: I contributed partly to experiments, data analysis of those experiments, and reviewed the manuscripts at different stages of preparation.

5. **Antibody-dependent cellular cytotoxicity-competent antibodies against HIV-1-infected cells in plasma from HIV-infected subjects**

Published in mBio, 17 December 2019. https://doi.org/10.1128/mBio.02690-19

Franck P Dupuy, **Sanket Kant**, Alexandre Barbé, Jean-Pierre Routy, Julie Bruneau, Bertrand Lebouché, Cécile Tremblay, Marzena Pazgier, Andrés Finzi, Nicole F Bernard

Contribution to study: I contributed partly to experiments, data analysis of those experiments, assisted in preparing figures for the publication, and reviewed the manuscripts at different stages of preparation.

6. **Differential contribution of education through KIR2DL1, KIR2DL3, and KIR3DL1 to antibody-dependent (AD) NK cell activation and ADCC**

Published in Journal of Leukocyte Biology, 30 January 2019. https://doi.org/10.1002/JLB.4A0617-242RRR

Irene Lisovsky, **Sanket Kant**, Alexandra Tremblay-McLean, Gamze Isitman, Zahra Kiani, Franck P Dupuy, Louise Gilbert, Julie Bruneau, Naglaa H Shoukry, Bertrand Lebouché, Nicole F Bernard

Contribution to study: I was co-first author on this manuscript, in which I performed experiments, contributed to revisions for the manuscript, analyzed the results, and contributed to manuscript revisions.

7. **Natural Killer (NK) Cell Education Differentially Influences HIV Antibody-Dependent NK Cell Activation and Antibody-Dependent Cellular Cytotoxicity**

Nicole F. Bernard, Zahra Kiani, Alexandra Tremblay-McLean, **Sanket Kant**, Christopher E. Leeks and Franck P. Dupuy

Published in Frontiers in Immunology, 24 August 2017, https://doi.org/10.3389/fimmu.2017.01033

Contribution to study: I contributed to performing the literature review, writing, and editing the manuscript.

Abbreviations

Ab: Antibody

AD: Antibody dependent

Ad5: Adenovirus serotype 5

Ad26: Adenovirus serotype 26

ADCC: Antibody dependent cellular cytotoxicity

ADCD: Antibody dependent complement deposition

ADCP: Antibody dependent cellular phagocytosis

ADCT: Antibody dependent cellular trogocytosis

ADCVI: Antibody dependent cellular viral inhibition

ADNKA: Antibody dependent natural killer cell activation

ADNP: Antibody dependent neutrophil phagocytosis

Ag: Antigen

AGM: African green monkeys

AIDS: Acquired immunodeficiency syndrome

AMP: Antibody mediated protection

AP1: Activator protein 1

AP3: Activator protein 3

APOBEC3G: Apolipoprotein B mRNA editing enzyme, catalytic subunit 3G

APOBEC3H: Apolipoprotein B mRNA editing enzyme, catalytic subunit 3H

ART: Antiretroviral therapy

ATI: Antiretroviral therapy interruption

AU: Arbitrary units

AUC: Area under the curve

AZT: Azidothymidine

bNAb/BNAb: Broadly neutralizing antibody

BSA: Bovine serum albumin

BST2: Bone marrow stromal protein 2

cART: Combined antiretroviral therapy

CA: Capsid

CCHSP: Canadian cohort of HIV slow progressors

CCL3: Chemokine ligand 3

CCL4: Chemokine ligand 4

CCL5: Chemokine ligand 5

CCR5: C-C chemokine receptor 5

CD: Cluster of differentiation

CD4bs: CD4 binding site

CD4m: CD4 mimetic

CDC: Centers for Disease Control

CDK: Cyclin dependent kinase

CDS: Complement deposition score

CFSE: Carboxyfluorescein succinimidyl ester

CH: Constant heavy chain

CL: Constant light chain

CMI: Cell-mediated immunity

CMV: Cytomegalovirus

CoRBS: Coreceptor binding site

COVID: Coronavirus disease

CPSF-6: Cleavage-and-polyadenylation-specificity-factor-6

CPZ: Chimpanzee

CRF: Circulating recombinant form

CTL: Cytotoxic T lymphocytes

CTN: Canadian HIV trials network

CXCR4: C-X-C chemokine receptor 4

CycT1: Cyclin T1

CypA: Cyclophylin A

DIS: Dimerization initiation site

DNA: Deoxyribose nucleic acid

dsDNA: Double-stranded deoxyribonucleic acid

EDTA: Ethylenediaminetetraacetic acid

EI: Entry inhibitors

ELISA: Enzyme-linked immunosorbent assay

Env: Envelope

ER: Endoplasmic reticulum

ES: Elite suppressors

ESCRT: Endosomal sorting complexes required for transport

FACS: Fluorescence-activated cell sorting

FBS: Fetal bovine serum

FcγR: Fc gamma receptor

FDA: Food and Drug Administration

FISH: Fluorescent in-situ hybridization

FPPR: Fusion peptide proximal region

FRET: Fluorescence resonance energy transfer

GC: Germinal center

GFP: Green fluorescent protein

GlcNAc: N-acetylglucosamine

GOR: Gorilla

Gp120/gp120: Glycoprotein 120

GRID: Gay-related immunodeficiency

gRNA: Genomic ribose nucleic acid

GTL: GranToxiLux

HAART: Highly active antiretroviral therapy

HDACI: Histone deacetylase inhibitor

HIC: HIV controllers

HIV: Human immunodeficiency virus

HIVIG: Human immunodeficiency virus immunoglobulin

HLA: Human leukocyte antigen

HR1: Heptad repeat 1

HR2: Heptad repeat 2

HSA: Heat stable antigen

HTLV: Human T lymphotrophic virus

HTS: High-throughput system

HVTN: HIV vaccine trials network

ICEM: Infected CEM cells

IFN: Interferon

Ig: Immunoglobulin

IgG: Immunoglobulin G

IgA: Immunoglobulin A

IN: Integrase

INSTI: Integrase nuclear strand transfer inhibitors

IPDA: Intact proviral DNA assay

IQR: Inter-quartile range

IRES: Internal ribosome entry site

IU: Infectious units

kb: Kilobase

KS: Kaposi's sarcoma

LAMP: Lysosome-associated membrane protein

LEDGF: Lens epithelium-derived growth factor

LRA: Latency reversing agent

LTNP: Long term non-progressor

LTR: Long terminal repeat

LTS: Long term survivor

mAb: Monoclonal antibody

MA: Matrix

MAC: Membrane attack complex

MERS: Middle eastern respiratory syndrome

MFI: Mean fluorescence intensity

MHC: Major histocompatibility complex

MPER: Membrane proximal region

mRNA: Messenger ribose nucleic acid

MSM: Men who have sex with men

MVB: Multivesicular bodies

MX2: Myxovirus resistance protein B

nAb/NAb: Neutralizing antibody

NC: Nucleocapsid

NCs: Non-controllers

NCI: National Cancer Institute

NES: Nuclear export signal

NF-κB: nuclear factor kappa-light-chain-enhancer of activated B cells

NFAT: Nuclear factor of activated T cells

NHP: Non-human primate

NK cell: Natural killer cell

NLS: Nuclear localization signal

NnAb/nnAb: Non-neutralizing antibody

NNRTI: Non-nucleoside reverse transcriptase-inhibitors

NP: Non-progressors

NRTI: Nucleoside reverse transcriptase inhibitor

NtRTI: Nucleotide reverse transcriptase inhibitor

OI: Opportunistic infections

PBE: Plate-based enzyme linked immunosorbent assay

PBMC: Peripheral blood mononuclear cells

PBS: Primer binding site

PBST: Phosphate buffer saline; tween 20

PCP: Pneumocystis carinii pneumonia

PCR: Polymerase chain reaction

PEP: Post-exposure prophylaxis

PFA: Paraformaldehyde

PHI: Primary HIV infection

PI: Protease inhibitor

PIC: Pre-integration complex

PJP: Pneumocystis jiroveci pneumonia

PKC: Protein kinase C

PLWH: People living with HIV

PM: Plasma membrane

PMA: Phorbol myristate acetate

PPE: PSI packaging element

PPT: Polypurine tract

PR: Protease

PrEP: Pre-exoposure prophylaxis

PS: Phagocytic score

PTC: Post-treatment controllers

pTfh: Peripheral T follicular helper

PTM: Post-translational modification

QVOA: Quantitative viral outgrowth assay

RFADCC: Rapid fluorometric antibody dependent cellular cytotoxicity

rgp120: Recombinant glycoprotein 120

RNA: Ribosenucleic acid

RRE: Rev-responding element

RSV: Respiratory syncytial virus

RT: Reverse transcriptase

RTI: Reverse transcriptase inhibitors

SAMHD1: SAM domain and HD domain-containing protein 1

SARS: Severe acute respiratory syndrome

sCD4: soluble form of CD4 containing domains 1 and 2

SERINC3: Serine incorporator 3

SERINC5: Serine incorporator 5

SIV: Simian immunodeficiency virus

SLFN11: Schlafen family member 11

Smac: Second mitochondrial-derived activator of caspases

SMM: Sooty mangabey

smFRET: Single-molecule fluorescence resonance energy transfer

siCEM: Sorted, infected CEM

SP: Slow progressor

SP1: Specificity protein 1

ssRNA: Single stranded ribose nucleic acid

TAR: Tat-activating region

TBP: TATA box binding protein

TILDA: Tat/Rev induced limiting dilution assay

TM: Transmembrane

TNF: Tumor necrosis factor

TP: Treated progressor

TRIM5: Tripartite-motif-containing 5α

U3': Unique 3' region

U5': Unique 5' region

USA: United States of America

UTP: Untreated progressor

VC: Viremic controllers

VL: Viral load

VLP: Virus-like particles

WT: Wild type

List of figures

Chapter 1. Introduction and Literature review.

1. History of infectious diseases in humans.

The quest for power, wealth, and resources have led man to discover new lands with consequences affecting human life positively and negatively. Slavery, colonisation, and war brought about human conflict while simultaneously opening new trade routes and markets. This led to increased contact with other humans and with nature, which afforded infectious pathogens in animals with increased opportunities to infect human hosts and to spread among humans. The frequency of zoonotic spillovers has appeared to increase in the past 100 years. Some recent examples include, the 1989-1990 Malaysian outbreak of Nipah virus from pigs [1], the 2002-2004 Severe Acute Respiratory Syndrome (SARS) outbreak caused by coronavirus (CoV) in China [2, 3], the 2009 outbreak of swine influenza in the United States and subsequently the world [4], the 2012 outbreak of Middle Eastern Respiratory Syndrome (MERS) in Saudi Arabia [5], the 2013 outbreak of avian influenza in China [6] the 2014 Ebola outbreak in West Africa [7], and the current COVID-19 pandemic caused by SARS-CoV-2 infection thought to have originated from a reservoir in bats [8]. These outbreaks have often been self- limited. The human immunodeficiency virus (HIV) has a zoonotic origin thought to be simian immunodeficiency virus (SIV) in chimpanzees [9, 10]. While causing a mild disease in chimpanzees, the jump to humans has led to a deadly infection that has spread worldwide. The jump is thought to have occurred between 1884 and 1924 in sub-Saharan Africa [11]. HIV has spread like wildfire since its discovery in 1983 [12, 13]. As of 2020, it is estimated that 38 million people currently live with HIV. Even though 73% of infected individuals have access to antiretroviral therapy (ART), approximately 1 million infected individuals died in 2020 and new infections continue to occur [14]. Therefore, HIV infection remains a major human pathogen to this day.

2. HIV and acquired immunodeficiency syndrome (AIDS)

I. History/Discovery of HIV

Between October 1980 and May 1981, five healthy, homosexual men or men who have sex with men (MSM) in Los Angeles, United States of America (USA) were diagnosed with Pneumocystis carinii pneumonia (PCP), now known as pneumocystis jiroveci pneumonia (PJP), Until then, this condition was exclusively observed in severely immunocompromised individuals [15]. Simultaneously, the cases of homosexual men suffering from a rare form of skin cancer, Kaposi's sarcoma (KS), also associated with individuals with immunodeficiency were rising [16, 17]. It was also discovered that MSM with these diseases were displaying lowered immune cell numbers [18-20]. CD4 T lymphocyte numbers and the ratio of T helper (CD4) to T cytotoxic (CD8) cells was inversed in MSM with KS compared to healthy individuals [19]. Compared to MSM without KS and healthy controls, MSM with KS and MSM with lymphadenopathy demonstrated a generalised elevation of plasma immunoglobulin G (IgG) and A (IgA) along with abnormalities in T cell functions [21]. T cells, specifically OKT-4-positive cells (now known as the cluster of differentiation-4, [CD4]), were markedly reduced in one case of an MSM with KS [22]. Teams across the globe reported an increased number of MSM suffering from cytomegalovirus (CMV) infections, KS, lymphadenopathy, along with other opportunistic infections (OI) associated with immunodeficiency [23-38]. Given that early cases were reported predominantly in MSM, the Centers for Disease Control (CDC), USA, coined this new condition, gay-related immunodeficiency disease (GRID) [39]. Further investigations identified injection drug use and unprotected (condomless) sexual activity as risk factors linked with immunodeficiency and spread of OI associated with GRID [30, 35, 40]. Accumulating evidence indicated that blood transfusion could also lead to a horizontal transfer of immunodeficiency [41, 42]. This prompted the CDC to

adopt a change in the name of the disease to acquired immunodeficiency syndrome (AIDS) as the number of immunodeficiency cases and immunodeficiency-related OIs in heterosexual men and women increased in 1983 [43-46]. However, the agent causing this syndrome was not known.

Dr. Robert Gallo's team at National Cancer Institute (NCI) in the USA, determined that retroviruses belonging to human T-lymphotropic virus (HTLV) family may be involved in causing AIDS [47]. In 1982, a lymph node biopsy from an asymptomatic and otherwise healthy 33-year-old homosexual man with multiple lymphadenopathies was obtained by a team of virologists at the Pasteur Institute, in Paris, France that included Dr. Luc Montagnier and Dr. Françoise Barré-Sinoussi [12]. Isolated from the biopsy was a virus having reverse transcriptase (RT) activity able to cause cells to form syncytia [13]. More investigation revealed that sera from AIDS patients from all age groups was reactive with HTLV-III infected cell lysates [48-50]. Thus, HTLV-III was determined to be the pathogen behind AIDS. The virus was officially renamed HIV in lieu of HTLV-III in 1986 [51]. Since HIV was now being detected in AIDS-inflicted individuals across the Americas and Europe, retrospective samples were tested. In 1986, sera samples from two individuals in West Africa reacted poorly with HTLV-III/HIV from AIDS patients but more strongly with proteins from simian T-lymphotropic virus III from an African macaque (STLV-III_{mac}). The viral extracts from these two infected individuals also demonstrated distinct antigenicity compared to HIV and it was promptly called HTLV-IV [52, 53]. Thus, it was established that HIV had at least two circulating strains – HTLV-III called HIV type 1 (HIV-1) and HTLV-IV now called HIV type 2 (HIV-2) [54].

II. Origin of HIV

A fundamental question remained unanswered – from where did HIV infected humans originate? It was reported that the rhesus macaques (*Macaca mulatta*) in research centers in the USA

displayed clinical manifestations of a simian acquired immunodeficiency syndrome reminiscent of AIDS [55, 56]. A simian immunodeficiency virus (SIV) that was antigenically and virologically similar to HIV-1 was isolated from these monkeys [57] [58]. Simultaneous research with other monkey species revealed that African green monkeys (AGM) were infected with SIV (SIV_{AGM}) [59] as were sooty mangabeys (SMM) infected with SIV_{SMM} [60]. It was notable that SIV infected AGM and SMM monkeys showed no clinical manifestations characteristic of human AIDS or simian acquired immunodeficiency syndrome seen in SIV infected rhesus macaques. Sequencing data clustered HIV-2, compared to HIV-1, more closely with SIV_{AGM} and SIV_{SMM} [61, 62]. Scientific endeavours in Central and Western Africa found evidence of SIV infection in chimpanzees (CPZ; SIV_{CPZ}) and gorillas (GOR, SIV_{GOR}). $SIV_{CPZ/GOR}$ was more antigenically/phylogenetically related to HIV-1 than HIV-2 [9, 10, 63-66]. This fueled speculation that HIV originated from zoonotic transmissions when $SIV_{CPZ/GOR}$, SIV_{AGM} and SIV_{SMM} jumped from their simian hosts to humans. It is now well accepted that these zoonotic transmissions are the origin of the HIV/AIDS pandemic in man. Several teams globally were studying retroviruses like HTLV. It is well known that pig-tailed monkeys, cats, and cows could also harbor immunodeficiency viruses [67-69]. Thus, animal models could be developed to study the kinetics and virology of these immunodeficiency causing viruses.

Currently, a large majority of infected individuals across the globe have access to ART. However, before the advent of ART, infection and replication of this retrovirus went unchecked. The error-prone HIV-1 (hereafter referred to as HIV) reverse transcriptase supported high mutations rates and rapid evolution. Worldwide, based on sequence divergence HIV isolates are divided into four groups: Major or Main (M), Outlier (O), non-O and non-M (N), and a relatively new group, P [70, 71]. Group M HIV dominates most global infections and is further subdivided into clades/subtypes

designated as A, B, C, D, F, G, H, J, K, and L and circulatory recombinant forms (CRFs), designated with a combination of letters for sequences that match partially with two clades, such as CRF01_AE and CRF02_AG [72]. *Figure 1* shows the distribution of HIV clades across the globe.

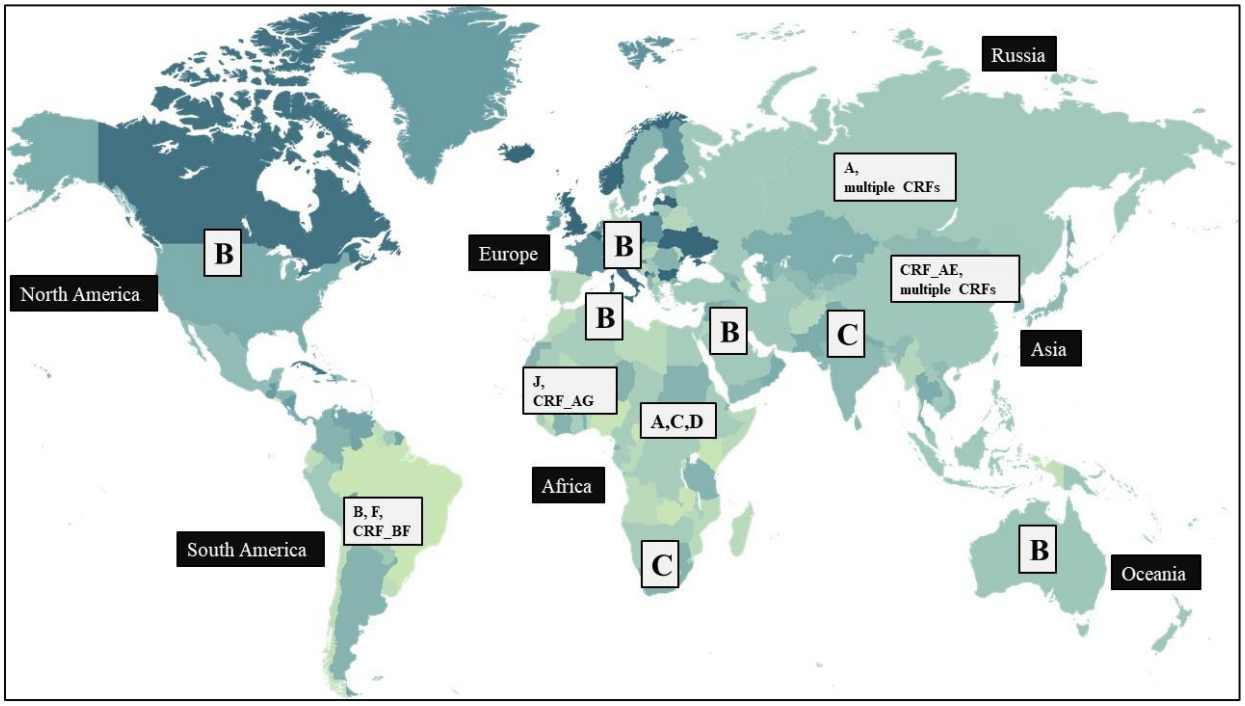

Figure 1: Global HIV subtype distribution. Under group M, subtype C leads global infection numbers due to its spread in heavily populated regions of Asia (China and India) and South Africa. Subtype B dominates infections in the Americas, Europe, the Middle East, North Africa, and Australia. Certain CRFs account for a large majority of infections in regions of East and South-east Asia, South America, and West Africa.

III. HIV disease progression

HIV can be spread parenterally by contaminated blood transfusions, sharing needles with infected injection drug users or accidental occupational exposures to contaminated needle sticks. Mother

to child transmission can occur prenatally, perinatally or postnatally by breast feeding. However sexual transmission remains the most common route of exposure [14, 73]. Irrespective of the subtype or clade, HIV infection follows similar disease progression trends. The approximate timeline of HIV infection is demonstrated in *Figure 2*. First, HIV infects $CD4^+$ T cells [74-76]. The earliest events post-viral contact with an uninfected host have been studied in female rhesus macaques exposed to SIV through an atraumatic intravaginal route [77]. This infection phase before the appearance of viremia is known as the eclipse phase. Thus, information available on the eclipse phase of HIV disease progression mostly arises from SIV infection in rhesus macaques. One of the earliest animal models studying transmission of HIV via sexual routes demonstrated that by a small number of cells were already infected between day 3 and 7 post infection, and HIV could be detected in lymph tissues by day 12 [78]. Starting ART as early as day 3 post infection does not prevent viral rebound thereby suggesting that the viral reservoir, as defined by quiescent infected cells, is established as early as day 3 post-infection [79]. However, initiating ART within 3 days post-infection prevents establishment of infection [80]. Retrospective longitudinal studies in humans have showed that HIV viral products can be detected in blood as early as between 5 to 10 days after a suspected post-infection event [81, 82]. This phase marks the beginning of acute phase. At this stage HIV is rapidly replicating, spreads throughout the host and CD4 counts rapidly drop [83]. At a certain point in acute infection, around 4-6 weeks post infection, viremia reaches a set point determined by the ability of the host's immune system to partially control the infection [84]. In untreated persons, the virus continues to replicate, and CD4 T cell numbers decline. After reaching the viral set point, the level of viral RNA remains constant. It has been shown that a higher VL can acts as a prognostic marker for faster disease progression [84, 85]. The chronic phase lasts a median of 10 years, and the AIDS phase is defined when CD4 T cell numbers fall

below 200 cells/mm^3. While ART controls the viral replication, it does not provide a functional cure, as its interruption leads to viral rebound. Additionally, ART does not prevent CD4 decline which may indicate that subtle, background HIV replication continues in long-term ART-treated individuals [86-90]. This marks the chronic, latent phase of HIV infection. There are certain rare, ART-naïve HIV-infected individuals that can spontaneously control their infection [91, 92]. These individuals, known as elite controllers (ECs), can durably control their viremia below clinically detectable levels, however there is evidence of background replication in these individuals as well [93, 94]. Although ECs often maintain stable CD4 counts, a few individuals exhibit loss of CD4 over many years [95, 96]. Thus, irrespective of ART-treatment or spontaneous elite control, there is a progressive loss of CD4 T cells that occurs over many years that eventually lead to immune dysregulation and AIDS-associated comorbidities.

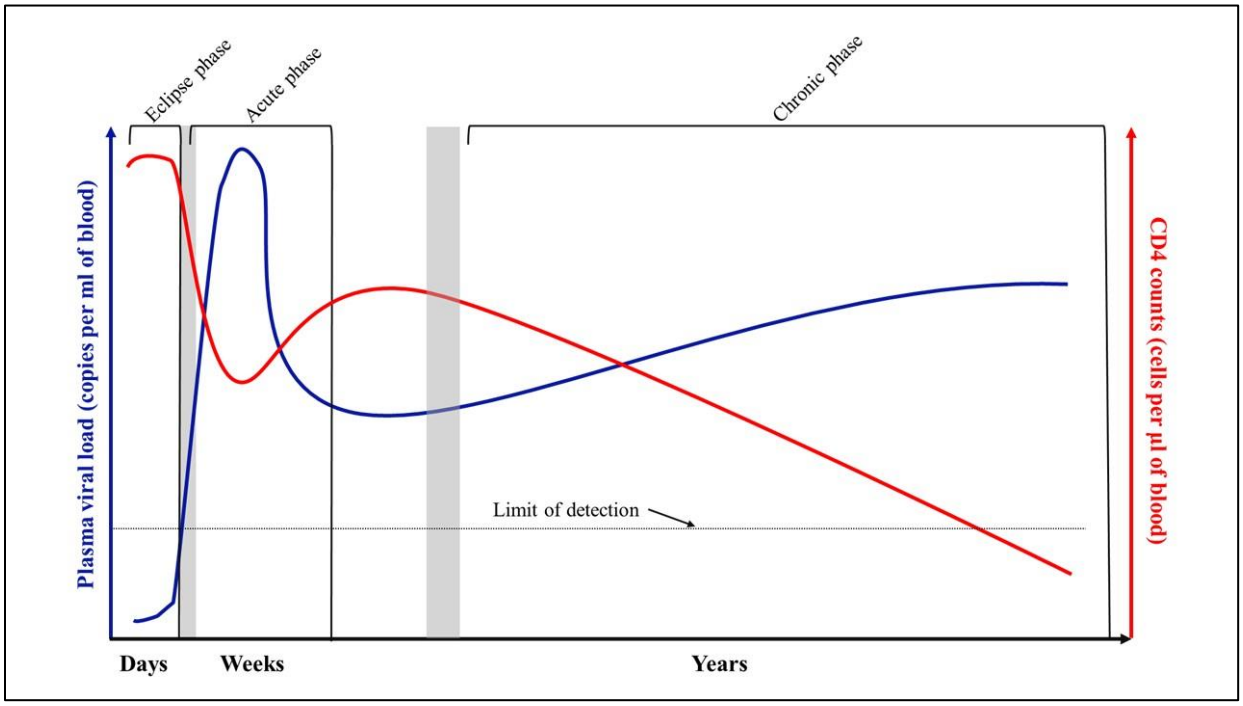

Figure 2: HIV disease progression. When left untreated, the plasma VL (indicated in blue) increases rapidly during the acute phase. This coincides with a large loss of CD4$^+$ cells (indicated

in red). The immune system takes over in the next few weeks post-infection and tries to control viral replication, however HIV manages to escape immune pressure over time. The chronic phase lasts a median of 10 years after which the person develops AIDS.

IV. Viral classification

HIV belongs to the genus Lentivirus, a subgroup of retroviruses (family: retroviridae) and is classified in group VI of the Baltimore classification. HIV carries two copies of positive-sense, single-stranded ribonucleic acid (ssRNA) and carries a reverse transcriptase (RT) enzyme that can reverse transcribe the viral ssRNA to double-stranded deoxyribonucleic acid (dsDNA). Lentiviruses typically cause chronic diseases preceded by long incubation periods [97]. As is typical of human retroviruses, apart from the viral RNA, the essential virion components are lipid-based envelope (Env) and enzymatic proteins such as RT, integrase (IN), and protease (PR), and group-specific antigen (Gag).

V. Viral genome and structure

Once the 10 kilobase (kb) viral single-stranded RNA (ssRNA) is reverse transcribed to viral double-stranded DNA (dsDNA) and integrated in the host genome, its nine viral genes encode fifteen proteins *Figure 3*. Spanning the genes on either end of the dsDNA are identical long terminal repeats (LTRs) that contain regions for reverse transcription and viral packaging. Each LTR contains a R (repeat), U5 (unique, 5') region, and U3 (unique, 3') region [98, 99]. The 5' LTR binds to host nuclear factor kappa-light-chain-enhancer of activated B cells (NF-κB), which promotes transcription [100, 101]. The 3' LTR region contains sequences for viral messenger RNA (mRNA) polyadenylation [102]. HIV encodes three classes of proteins: structural proteins (Gag, Pol, and Env), essential regulatory proteins (Tat and Rev), and accessory regulatory proteins (Nef, Vpu, Vpr, and Vif). Matrix (MA), capsid (CA), and nucleocapsid (NC) and the enzymes protease

(PR), reverse transcriptase (RT), RNAse H, and integrase (IN) are cleavage products of the Gag and Pol polyproteins respectively [103, 104].

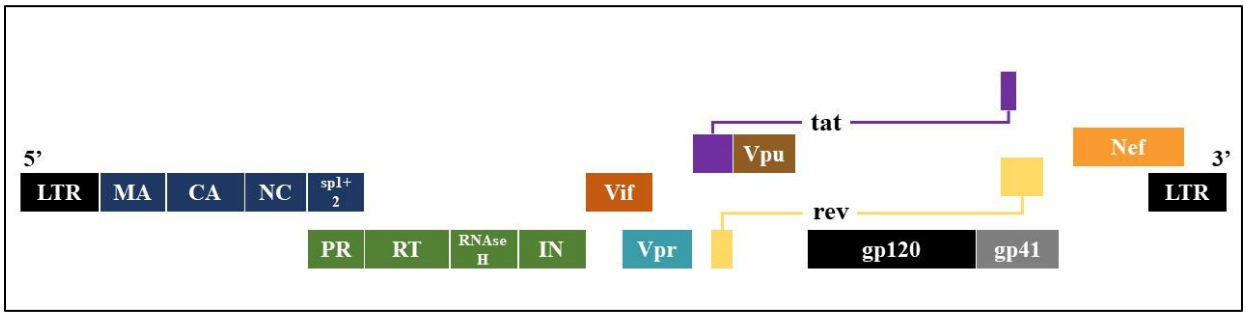

Figure 3: HIV viral genome. The HIV genome is 9719 base pairs in size and consists of nine genes that encode fifteen proteins.

Env encodes envelope (gp160) that is further cleaved into gp120 and gp41 by the host protease, furin [105]. Resulting trimers of gp120 and gp41 are non-covalently linked and used for virion entry into host $CD4^+$ T cells [106-108]. Env is the only viral antigen exposed on the surface of virions and it is thus a major target for antibodies and vaccine design *Figure 4*. The large polyprotein, Gag (p55) is cleaved by viral protease into p17 MA, p24 CA and p7 NC proteins and two small spacer peptides (p1 and p2). Gag proteins are essential for HIV viral assembly [109]. MA proteins are attached to the cytoplasmic tail of Env and are involved in viral assembly and ensuring Env is incorporated into mature virions [110]. MA also plays a key role in the pre-integration complex (PIC) of viral dsDNA transport from the cytoplasm to the nucleus [111]. CA monomers form stable pentameric or hexameric subunits with adjacent monomers to form a protective shell around the viral RNA [112]. The NC protein plays different roles in the viral life cycle. After cell entry, NC localises to the nucleus via its the nucleus localisation signal (NLS) [113]. During reverse transcription, NC forms a complex with the host tRNALys3 and primer binding site (PBS) on viral RNA to initiate reverse transcription [114]. NC also plays a role in the

assembly of virions [103]. Two strands of viral RNA, each 5' capped and 3' polyadenylated, are encapsulated by CA into each virion [99, 115].

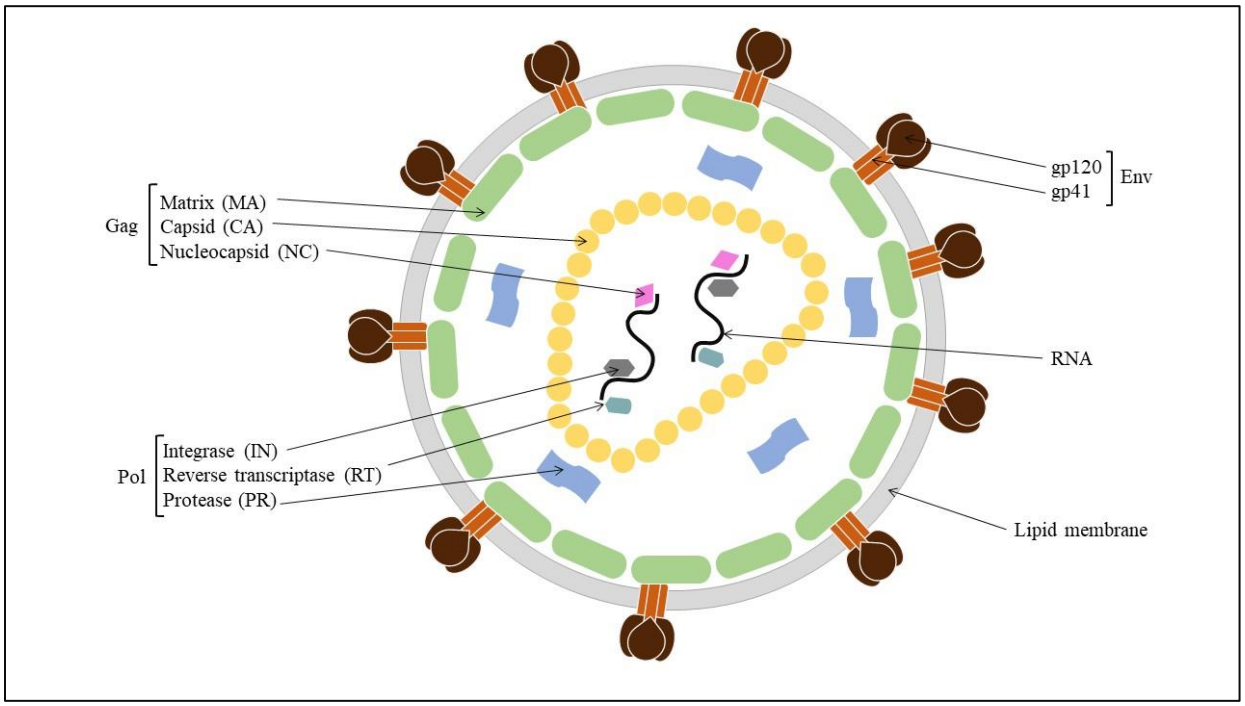

Figure 4:Structure of an HIV virion.

VI. Viral life cycle and replication

The HIV life cycle occurs in three major steps, starting with virus entry, replication (early and late), and budding of new virions from host cell as shown in *Figure 5.*

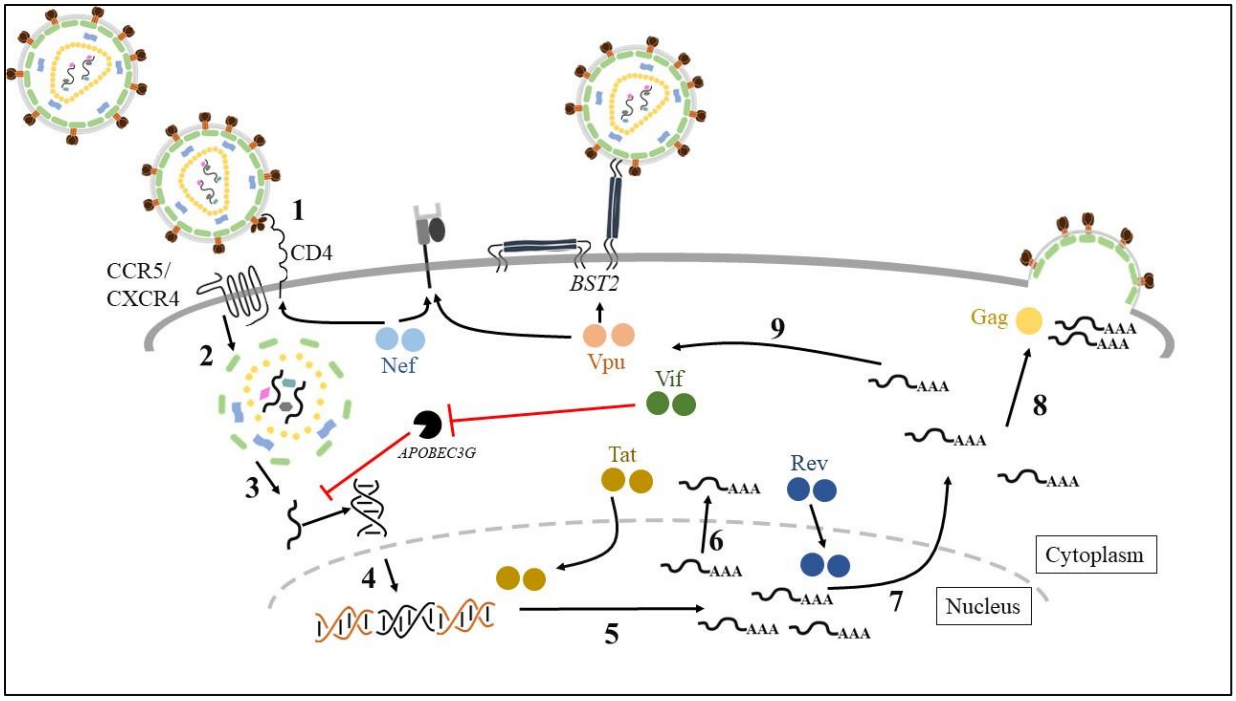

Figure 5: HIV replication cycle. HIV replication occurs in the following sequence: 1) binding of Env to the CD4 receptor on target cells followed by coreceptor (CCR5/CXCR4) binding, 2) entry and uncoating, 3) reverse transcription, 4) transport to the nucleus and integration, 5) synthesis of early and late viral mRNA and genomic RNA, 6) early viral mRNAs produce Tat, Rev, and Nef, 7) Rev-mediated export of late mRNA and genomic RNAs, 8) late mRNAs synthesise the accessory and structural proteins and lastly, 9) genomic RNAs are packaged along with Gag and Gag-Pol and assembly is initiated for nascent viral budding.

a. Viral entry

HIV Env binds to the host CD4 receptor on target cells to facilitate viral entry [106, 116, 117]. Host cells that express CD4 receptors include T-helper cells, monocytes, macrophages, Langerhans cells, brain microglia, and dendritic cells [118-126]. While presence of CD4 permits viral attachment to target cell, alone it is insufficient for permit viral entry [127, 128]. It was later discovered that two additional cell-surface molecules, C-C chemokine receptor (CCR5) and C-X-

C chemokine receptor 4 (CXCR4), serve as coreceptors and are essential in viral fusion and entry [129-133]. The viral fusion and entry occur in a sequential stepwise manner. CD4 binding of gp120 causes conformational changes in gp120 that allow exposure of hidden variable loop 3 (V3) Env structures that bind to bind to coreceptors [134-138]. Cellular tropism, as defined by coreceptor usage, is determined by the amino acid composition of the V3 loop [136, 137, 139]. Viral isolates utilising CCR5 and CXCR4 coreceptors are called R5 and X4 viruses, respectively; dual-tropic strains are denoted as R5X4 viruses. The interaction of Env or the Env V3 loop to coreceptors produces the CD4-gp120-coreceptor complex that allows the exposure of a highly conserved fusion peptide region which penetrates the target cell's bilipid layer [140-146].

b. Viral replication - early

Receptor-mediated endocytosis leads to uncoating of the CA in the target cell cytoplasm close to the nuclear pore releasing the viral contents [147]. RT converts the ssRNA viral genome into dsDNA, which is integrated into the host's genome. RT is like any other DNA polymerase in that it requires a primer and a template. The template is one of the positive senses' ssRNAs. Sequential steps of reverse transcription are shown in *Figure 6*. Step 1: NC recruits host tRNALys3 as a primer and anneals it to the primer binding site (PBS) on 5' end of the viral RNA [148-151]. Step 2: RT generates a short complementary DNA (cDNA) sequence by adding nucleotides from the primer in the 3' to the 5' direction? of the primer. This creates a RNA-DNA duplex, which is a target for the RNase H domain of RT [152]. Step 3: Since the R regions of either LTRs are identical, the short and incomplete cDNA is transferred to the 3' end of the viral RNA. It has been hypothesised that the cDNA hereafter may utilise the second strand of viral RNA as a template which allows recombination [153, 154]. Step 4: The polymerase and endonuclease activity by the RT allows generation of the minus-strand DNA. Step 5: Closer to the middle of the viral genome

lie small fragments of sequences that are rich in purine, called the polypurine tract (PPT), that are resistant to RNAse H activity and serve as primers for positive-strand DNA [155]. Step 6: At this point, one strand of cDNA is generated, cleaving the viral RNA except for the PPT. Step 7: Synthesis of the second strand of DNA starts using PPT as the primer and cDNA as the template. RNAse H cleaves the tRNALys3 primer from the template cDNA strand as it moves along. Step 8: The newly synthesised PBS on the second strand now jumps to the 3' of template cDNA and using the cDNA as the template, generates the second strand of DNA. It is important to note that RT lacks a proofreading domain. The lack of proofreading introduces a high frequency of mutations. This eventually leads to the generation of quasispecies and heterogeneous viral populations within the host during the course of infection [156-159].

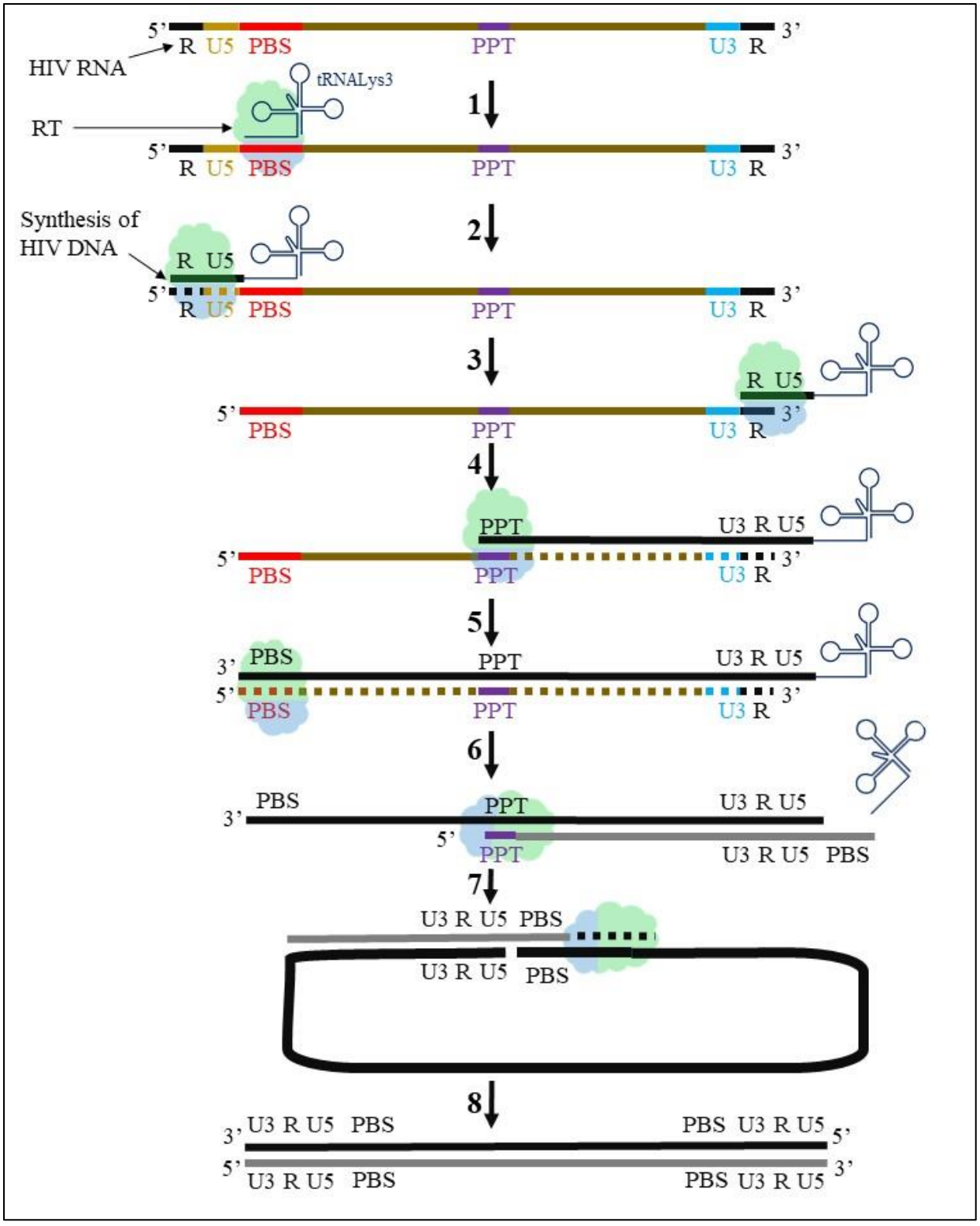

Figure 6: Viral replication by reverse transcription. 1) The RT has a polymerase domain (depicted in green) and a RNAse H domain (depicted in blue). RT and tRNALys3 bind to the PBS of HIV

RNA. 2) The polymerase domain adds nucleotides whereas the RNAse H recognises the RNA:DNA duplex and degrades the RNA template. 3) Since the R region at 5' and 3' regions are identical, the RT complex jumps to the 3' end to continue DNA synthesis. 4) DNA synthesis continues to the central PPT, which is resistant to RNAse H. 5) PPT acts as a primer and RT uses the newly synthesised DNA as the template. 6) A complementary sequence from tRNALys3 is generated, which is identical to the viral RNA PBS. Thereafter tRNALys3 is removed by RT. 7) Since the PBS on these strands are complementary, the new plus-strand makes a jump and RT continues using the cDNA as the template.

c. Viral integration

Without integration, the HIV life cycle remains incomplete. A large nucleoprotein complex, called the pre-integration complex (PIC), consisting of host and viral factors are responsible for viral dsDNA integration into the host genome. In addition to the viral dsDNA, the PIC consists of four viral proteins – MA, RT, Vpr, and IN [111, 160-163]. MA, Vpr, and IN contain a short nuclear localisation signal (NLS) that interacts with importin, a karyopherin that allows the transport of PIC from the cytoplasm through the nuclear pore to the nucleus [160, 161, 163-167]. While CA is absent from the PIC, its contribution to uncoating near the nuclear pore, nuclear transport, and import of PIC into the nucleus is newly found. CA has been shown to interact with several host proteins such as cyclophilin A (CypA), transportin-1, and cleavage-and-polyadenylation-specificity-factor-6 (CPSF-6) that are in proximity to the nuclear pore [168-172]. Other studies have also shown that the interaction of CA with nuclear pore complex proteins called nucleoporins (Nup) is essential for import of viral macromolecules from the cytoplasm to the nucleus [173, 174]. Mutations in CA or silencing of Nups diminishes viral integration and infection.

Once inside the nucleus, IN interact with cellular lens epithelium-derived growth factor (LEDGF/p75) to actively target active genes [175-177]. IN nicks off nucleotides at either ends of 3' termini of the viral dsDNA and 3' ends of the cellular DNA initiating integration. The target cell DNA repair machinery identifies this mismatch as a defect, and thus repairs it, which results in successful integration of viral dsDNA into the host genome [178].

d. Viral replication – late

Once integrated, the viral genome, now called the provirus, forms a permanent part of the host genome. The provirus acts as a template for further viral nuclear and protein production or it can simply slip into dormancy only to reactivate from latency at a later time. This dormant latently infected cell is known as an HIV reservoir [179, 180]). In a transcriptionally active, infected cell, the provirus relies on a combination of already prepared viral proteins and host transcription factors to complete the viral life cycle [181]. The 5' LTR contains four regions important for transcription: the Tat-activating region (TAR) in the R region, the promoter, the enhancer, and the regulatory element [182]. Some of the host transcription factors that participate in viral transcription are specificity protein 1 (SP1), c-Myb, nuclear factor of activated T cells (NFAT), activator proteins 1 and 3 (AP1 and AP3), and NF-κB [183-186]. SP1 and NF-κB are the first general transcription factors to be recruited; the TATA box binding protein (TBP) recruits dormant RNA polymerase II to the enhancer sequence in the U3 region of LTR [187, 188]. Meanwhile, Tat binds to the TAR and recruits cellular protein complex positive transcription elongation factor (p-TEFb) comprised of cyclin-dependent kinase 9 (CDK-9) and cyclin-T1 (CycT1) [189-194]. P-TEFb phosphorylates RNA polymerase II increasing its activity [193]. Absence of, or mutations in, Tat lead to short, non-codable RNA transcripts [195].

Viral transcription occurs in two steps. First, a 2kb viral RNA transcript codes for Tat, Rev, and Nef. The 4kb late transcript codes for viral proteins Env, Vpu, Vif, Vpr, and Tat while the 9kb late transcript codes for precursor protein, Gag-Pol [196]. Early translated proteins play a crucial role in viral replication: Tat is essential to continue viral transcription, Rev is critical for transport of late transcripts to the cytoplasm, and Nef is essential for physiologically modifying the cell for optimum viral transcription, translation, and infection. The NLS of Rev allows its entry into the nucleus and eventually binds to the Rev-responding element (RRE) on the late transcripts and aids in their export to the cytoplasm for either packaging or translation [197-200]. Rev also contains a nuclear export signal (NES) that facilitates Rev trafficking by interacting with exportin-1 [201-203]. Compared to multiply spliced RNA for translation of viral proteins, unspliced genomic RNAs (gRNA) are exported for packaging [204].

e. Viral assembly

The final step of the HIV life cycle is assembly of proteins and nuclear contents to form mature virions. This step occurs at the infected cell's lipid bilayer plasma membrane (PM) [205-207]. Gag drives viral assembly. As mentioned above, post-proteolytic cleavage of Gag results in four distinct proteins – MA, CA, NC, and p6 all of which contribute to viral assembly. Gag is myristoylated at its N-terminus (called the membrane-binding domain or M domain) which allows it to anchor to the PM and interact with phosphatidylinositol (4,5) bisphosphate (PI(4,5)P2) to form a site for viral budding [208, 209]. The protective Gag oligomerization is promoted by NC, via its interacting domain [210]. NC also participates in recruiting two strands of viral unspliced viral RNA to the site of assembly, a necessary step in virion maturation [211, 212]. The two strands of viral RNA are non-covalently conjoined or "dimerized" by the psi (Ψ) packaging element (PPE) or dimerization initiation site (DIS), which is located at the 5' end of the viral RNA, forming a

"kissing loop" structure [213-215]. Env gp160 on the other hand is processed into gp120 and gp41 by the host's furin protease and transported to the cell surface. The exact mechanism by which Env is incorporated into the budding virion is unknown. Once the components of the virus are assembled and incorporated in proximity to the budding site, the Gag protein p6 plays a part in viral release [216]. The late domain of Gag recruits players from the endosomal sorting complexes required for transport (ESCRT) machinery to form multivesicular bodies (MVBs) that aid in the budding and pinching off process of the virus from the target cell [217-220].

3. Anti-retroviral therapy

In 2014, UNAIDS declared the "90-90-90" target for managing and curbing the HIV epidemic. This target had as a goal that by 2020, 90% of infected individuals would know their HIV status, 90% of these PLWH would have access to ART, and 90% of PLWH on ART would have suppressed viral loads (VLs) to below the level of detection of standard VL assays [221]. As of 2020, 81% of infected individuals knew their HIV status, about 67% of PLWH had access to ART, and approximately 59% maintained undetectable VLs [222]. UNAIDS has pushed for accessible diagnosing and ART because four decades of research in anti-HIV therapy has made AIDS manageable. Due to ambitious programs to extend the reach of testing and ART penetration between the period of 2000-2020, global HIV/AIDS-associated deaths have declined by two thirds [223, 224]. This is true in low-income countries as well as in countries where HIV infection was one of the top causes of death in 2019. The life expectancy of PLWH accessing ART has increased [225, 226]. However, compared to uninfected individuals, PLWH accessing ART still have a shorter life expectancy due to comorbidities [226, 227].

The first drug to be approved by the Food and Drug Administration (FDA) in the USA for HIV treatment was azidothymidine (AZT), a nucleoside reverse transcriptase inhibitor (NRTI) in 1987

[228]. Since then, more than 30 drugs targeting different stages of the HIV replication life cycle have been discovered and are available for antiretroviral treatment [229]. Based on the life cycle stage targeted, these molecules/drugs are classified into six classes: 1) Entry inhibitors (EI) targeting the coreceptors to inhibit entry and fusion, RT inhibitors (RTI) – 2) nucleoside transcription inhibitors (NRTI) and 3) nucleotide transcription inhibitors (NtRTI) that introduce chain terminating nucleoside analogues, 4) non-nucleoside RT-inhibitors (NNRTI) that target the active site of RT and block its function, 5) protease inhibitors (PI) that block the viral PR, and 6) IN nuclear strand transfer inhibitors (INSTI) that block integrase function. Since then, combined ART (cART, simply referred to as ART) has been accepted as the standard of care for HIV infection because using a single antiretroviral drug rapidly gives rise to drug resistant viral isolates that become the predominant circulatory form [230, 231]. The standard of care treatment for HIV infection is a cocktail of three drugs – two NRTIs as a backbone with a third agent from the NNRTI class of antiretrovirals. NNRTIs are preferred over PIs as a first line therapy due to considerations of potency and reduced side effects [232]. Recent studies have shown superior viral suppression of cocktails containing INSTIs compared to those containing NNRTIs [233, 234]. Animal studies showed that the seeding of viral reservoir occurs between 1- and 3-days post infection [79, 80]. In humans, it is rarely possible to initiate treatment this early after infection. Most countries including Canada and the USA suggest that ART be initiated as soon as possible after diagnosis [235, 236]. VLs are extremely high during the acute phase of infection increasing the chances of spreading HIV from PLWH to uninfected persons. Initiating ART as early as possible, compared to deferred treatment, ensures that such individuals achieve undetectable VLs much quicker, generally lose fewer CD4 cells, have a higher recovery of CD4 cells, and have fewer AIDS-related outcomes

over time [237-239]. This is also true for HIV-infected infants where infant mortality is reduced by more than 75% by treatment initiation as soon after birth as possible [240].

4. HIV Envelope

The Env spike is the only viral antigen expressed on the surface of the virion and infected cells, which makes it a suitable target for vaccinations inducing prophylactic immunity [241]. The bicistronic *env/vpu* mRNA encodes a gp160 Env polyprotein on rough endoplasmic reticulum (ER). The core protein of gp160 is about 90 kDa and the remaining molecular mass is contributed by predominantly N-linked and, to a much lower extent, by O-linked oligosaccharide side chains [242-244]. The 24 sites available for N-linked glycosylation provide a large variety of oligosaccharides that can contribute to the virus evading host immunity [245-247]. In the ER, gp160 monomers aggregate with other monomers to form dimers, trimers, or oligomers [248, 249]. Here, Env interacts with CD4 in the Golgi, preventing Env release. To counteract this, Vpu initiates CD4 degradation via ubiquitination by interacting with F-box/WD repeat-containing protein 1A (βTrCP1) [250-252]. The immature Env is transported to the Golgi for further processing where it is cleaved into a surface gp120 and a transmembrane gp41 by the host's furin protease [105]. Further oligomerization occurs in the trans-Golgi network after which it is secreted to the plasma membrane. However, the presence of Env on the infected cell's PM is short-lived as it is endocytosed by lysosome-associated membrane protein 1 (LAMP-1) and clathrin adaptor molecules [253, 254]. MA associates with the cytoplasmic tail of gp41 and prevents or slows down Env's internalisation by LAMP-1 thus allowing incorporation of Env into budding virions. Approximately 10 Env trimers are incorporated per virion [255]. The low number of trimers may be attributed to gp120 shedding occurring due to non-covalent interactions with gp41 [256]. Shed gp120 would be expected to leave a gp41 stalk, though these are not visualised by electron

tomography [255]. Exhibiting low levels of Env on the surface on infected cells and viruses thus shields them from host immunity directed to Env. The final cell surface Env consists of non-covalently bonded trimers of gp120 and gp41.

I. Gp120

Comparison of the gp120 sequences of various HIV isolates showed the presence of five variable loops (V1-V5; V1-V4 are surface exposed on the outer domain) distributed amongst five conserved domains (C1-C5) [257, 258]. The V1V2 loop serves two important functions: 1) to shield the bridging sheet that is involved in CD4 binding [259] and 2) to escape host immune responses by evolving throughout the course of disease progression [260, 261]. This bridging sheet contains about 50 amino acids interspersed through the C1, C3, and C4 domains that are critical in efficient CD4 binding [262-264]. Precisely, the phenylalanine residue at position 43 (Phe 43) of CD4 docks with the serine residue at position 375 (Ser 375) of gp120 [265, 266]. CD4 gp120 interactions cause conformational changes in gp120, which exposes hidden residues in the V3 loop that allow for coreceptor binding needed to initiate virion fusion with the target cell membrane [264, 267]. The hydrophobic regions of C1 and C5 interact with gp41 [268, 269].

II. Gp41

Gp41 is a transmembrane unit of the HIV Env that is embedded in the PM of infected cell or the virion. It consists of four domains: 1) the N-terminus ectodomain consisting of fusion peptide, a fusion peptide proximal region (FPPR) and heptad repeat regions 1 and 2 (HR1 and HR2), 2) the membrane proximal region (MPER), 3) the transmembrane (TM) domain and 4) the cytoplasmic domain (C-terminus) [141, 142, 144, 270]. As gp41 contains the machinery to complete the fusion process and inject the viral contents into target cell, it is relatively conserved across HIV isolates thus making it a potential candidate for therapeutics with anti-HIV activity.

III. Env conformations

During viral entry, CD4 interacts with gp120 to induce conformational changes for further binding to coreceptor sites. CD4 binding also exposes the HR1 in gp41; blocking gp41 abolishes viral entry [143]. *Figure 7* is a representative model of the fluid nature of Env sampling. Using single-molecule fluorescence resonance energy transfer (smFRET), it was shown that prefusion Env is visible in a closed conformation (State 1) [271]. Nef and Vpu can reduce cell surface CD4 directly and indirectly, respectively [272-276]. This prevents the interaction of CD4 with gp120 on the PM thereby maintaining cell surface Env in its prefusion State 1. Two types of macromolecules mimicking CD4 have been employed to study CD4-Env interactions and Env conformation: a soluble form of CD4 containing domains 1 and 2 of CD4 (sCD4) [277-279] and CD4 mimetic (CD4m) chemical compounds [279, 280]. SmFRET) studies with sCD4 demonstrated two additional structural rearrangements in Env, which differ from State 1 [271]. A single sCD4 molecule interacting asymmetrically with one gp120 molecule from the trimer resulted in an intermediate State 2 whereas saturating levels of sCD4 interacting with all three gp120 molecules resulted in a completely open Env conformation, known as State 3 [281]. These molecules can present the Env in an open conformation that is ready to bind to the coreceptor and increase infectivity on cells expressing low levels of surface CD4 while expressing the coreceptor [279]. State 2 and 3 conformations of Env reveal previously occluded epitopes, and therefore these epitopes are known as CD4-induced (CD4i) epitopes. These epitopes include the coreceptor binding site (CoRBS) and they can be characterised by CD4i/CoRBS antibodies (Abs) [137, 264, 282-284].

Serine at position 375 (S375) in gp120 creates a cavity that allows for CD4 docking. Mutations encoding residue with large hydrophobic amino acids such as tryptophan (S375W) and histidine

(S375H), resulted in CD4-independent binding and infection of cells expressing only CCR5 [266]. S375W and S375H Env variants open the Env conformation, much like a CD4-bound conformation to which Abs to the CD4i epitope can bind [285]. Such is the importance of S375 for HIV infection and protection against CD4i Abs, that more than 84% of clade M viruses characterised thus far code for a serine at position 375. The only HIV subtypes that have a histidine at position 375 are the HIV belonging to the CRF01_AE isolates. The Env of CRF01_AE isolates have an open conformation to which Abs to the CD4i epitope can bind [285]. This subtype contributes predominantly to the HIV infection in Thailand, and parts of Southeast Asia, and has been identified as the epicentre of CRF01_AE circulation across the globe [286-288]. This will be discussed further in the section on HIV vaccines and its postulated role in the success of RV144 Thai vaccine trial. In addition to these three Env states, an intermediate Env conformation, State 2A, was recently characterised [289]. A combination of sCD4/CD4m + CoRBS Abs (e.g., monoclonal Ab [mAb] 17b) + CD4i mAbs (e.g., A32 or C11) can stabilise the State 2A on infected cells and virions. Thus, the currently defined four conformations of Env demonstrate the fluid nature of the Env conformations and their dependence on interactions with CD4 and other Abs.

Much of the work studying Env conformations involves infecting cells with molecular clones that either lack *nef* and *vpu* genes [290], have a defective *nef* gene [291-293], or use $CD4^+$ target cells coated with recombinant gp120 [294-296]. However, it is important to note that none of these methods provide models of true HIV infection. In none of these situations is cell surface CD4 internalized leaving cell surface CD4 levels stable.

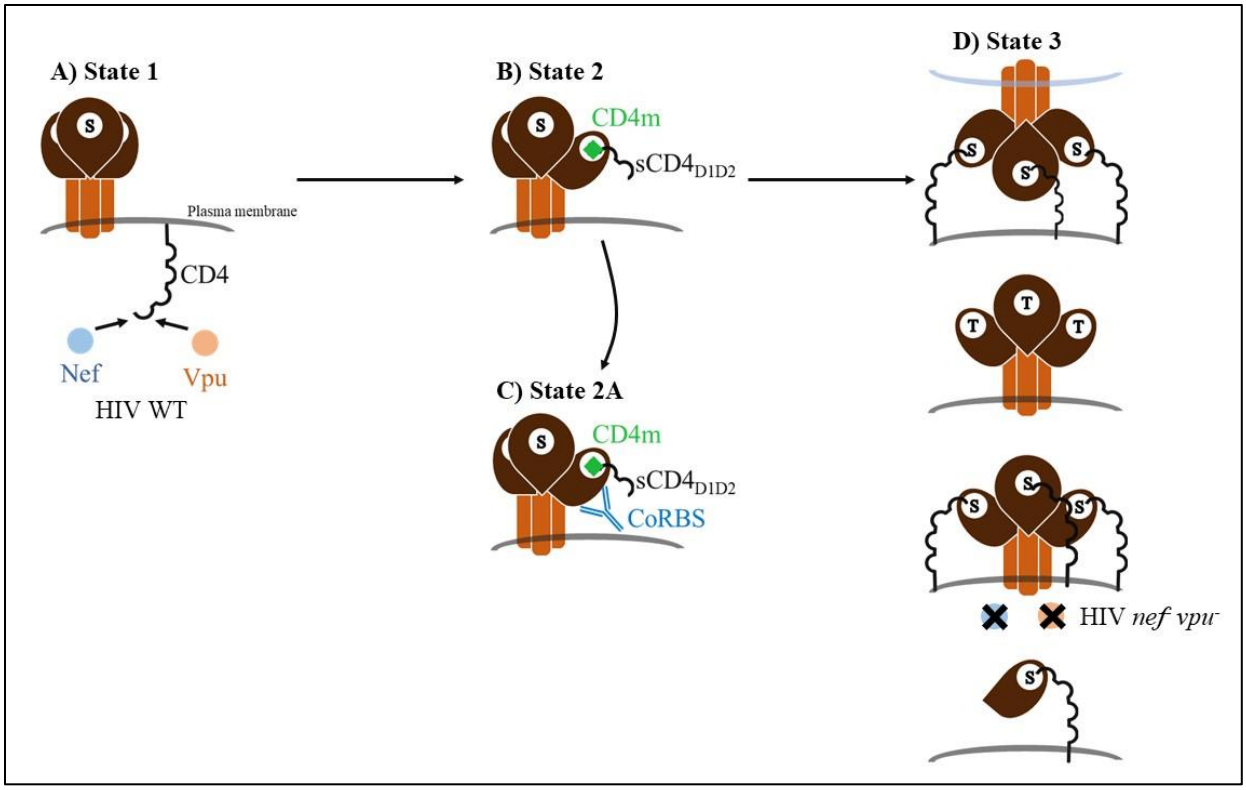

Figure 7: Different conformations of HIV Env. The S375 cavity is denoted by "S". A) In the absence of cell surface CD4, Env samples in State 1 ("closed" conformation). B) Upon binding with either sub-saturating levels of CD4 mimetics (CD4m; green) or domains 1 and 2 of soluble CD4 ($sCD4_{D1D2}$) (black), Env transitions to State 2. C) Further addition of a CoRBS Ab (blue) to the complex of sCD4/CD4m with Env, stabilises Env in State 2A. D) State 3 is defined as a completely "open" conformation of Env that can be achieved when (top to bottom): 1) complete occupancy of 3:3 gp120:CD4 occurs during viral entry, 2) the S375 is replaced by tryptophan (T, shown) or histidine (H, not shown), 3) target cells are infected with molecular clones with defective or deleted nef and vpu, or 4) $CD4^+$ target cells are coated with recombinant gp120 [289, 297, 298]

5. HIV vaccine trials: Targeting the Env

A cure for HIV has been elusive particularly due to the high error rate of RT, Env shedding and glycoshields, and persistence of latent reservoirs amongst other viral escape mechanisms. Nonetheless, efforts to design protective HIV vaccines continue. Env, as the only viral antigenic protein on the surface of infected cells make it a suitable target for HIV vaccines. Vaccines employ various strategies to induce immune responses directed to pathogens. Vaccines designed to induce immunity to SARS-CoV-2 encode viral antigens that induce specific Abs. Vaccines against polio and measles use attenuated forms of these viruses. Other vaccines use viral protein antigens to induce virus specific immune responses. For example, the recent vaccine against SARS-CoV-2 contains mRNA that encodes the viral spike protein [299, 300]. On the other hand, passive infusion of mAbs or polyclonal Abs (pAbs) can be administered for prevention or therapeutic purposes. For example, passive infusion of the mAb, palivizumab against respiratory syncytial virus (RSV) is usually administered to high-risk infants to reduce RSV-induced lower respiratory tract infection [301, 302].

Env is frequently included in vaccine regimens for HIV to elicit anti-Env responses. So far, six human phase 2b or 3 HIV vaccine trials have been completed. All, bar one, have failed to provide protection. The first two phase 3 vaccine trials took place simultaneously in different parts of the world: VAX004 (ClinicalTrials.gov identifier: NCT00002441) was administered to MSMs and heterosexual women in the USA and The Netherlands whereas VAX003 (ClinicalTrials.gov identifier: NCT00006327) was administered to injection drug users in Thailand. Both of these vaccines were formulated with bivalent recombinant gp120 (rgp120) proteins; rgp120 from clade B was used in VAX004 while rgp120 from clades B and E were used in the VAX003 regimens. Neither vaccine provided protection against HIV acquisition over that seen in the placebo arm of the trial [303, 304]. Follow-up studies aimed at understanding the reasons for failure. A

comprehensive comparative Ab analysis revealed that VAX004 participants had significantly lower gp120-, lower total V1V2-, and lower IgG1 and IgG3 V1V2-loop-specific Ab titers compared to VAX003 [305]. Additional work characterizing the Ab functional response elicited by these vaccines showed that Ab-dependent (AD) functions attained a peak in early boosts but waned with subsequent boosts [306]. It is critical to note that the AD functions assessed in these trials employed gp120-coated target cells. As mentioned earlier in this thesis, the conformation of Env plays an extremely important role in determining whether HIV Env CD4i epitopes are exposed for Ab binding (to be discussed later). Since the vaccine-induced humoral immune response failed to exhibit any protective role in HIV acquisition, the possibility that cell-mediated immunity (CMI) was important in protective immunity to HIV was explored in subsequent trials. Two simultaneous trials, the phase 2b Step (HIV Vaccine Trials Network; HVTN 502) and Phambili (HVTN 503) trials enrolled HIV seronegative, at-risk MSM and women with multiple sexual partners across several countries. The objective of these vaccines was to induce anti-viral interferon-γ (IFN-γ) secreting T cells. The Env in both vaccines was derived from a clade B viral isolate and was used in the vaccine formulation administered in South Africa even though clade C is the predominant circulating HIV subtype in this region. Nonetheless, the vaccine was efficacious at inducing cross-reactive (IFN-γ) secreting T cells against clades B and C. Both these trials were halted abruptly before completion because neither trial demonstrated decreased HIV acquisition nor decreased early plasma VL in vaccinees who seroconverted compared to placebo recipients [307, 308]. One of the major drawbacks and criticisms of these studies was pre-existing immunity to adenovirus serotype 5 (Ad5), which was used to deliver HIV gene products to vaccine recipients. Pre-existing immunity to Ad5 may have targeted immune responses to clearing the vector, before responses to HIV gene products could be induced [309].

The focus shifted to finding alternate forms of immunogens for eliciting potent virus-specific responses. Thus newer, DNA-based vaccines began to gain momentum in human HIV vaccine trials. Pre-clinical animal studies showed 50% protective efficacy and a 1 $\log_{10}$ lower VL upon infection when rhesus macaques were administered a DNA prime/rAd5 boost regimen and then challenged with 1 of the two SIV challenge strain delivered as multiple low dose intrarectal challenges. Neither CD8+ T cells responses nor innate immune responses were associated with protection while anti-Env CD4 responses and low-level neutralizing Abs (Nabs) were [310]. Building on this, HVTN 505, a phase 2b DNA/rAd5-based vaccine trial enrolled MSM and transgender women who have sex with men in the US [311]. The objectives of the vaccine were to evaluate immune responses involved in protection against HIV acquisition (if any) and those in vaccinated individuals who seroconverted. The vaccine induced HIV-specific CMI and humoral responses. However, the rates of HIV infection in the vaccine and placebo arms of the study were not significantly different. As a result, the study was halted. The VL set point in infected individuals who received the vaccine was did not differ from [311]. Even though the vaccine failed to provide protection, analysis of CMI results identified that compared to placebo, vaccinees exhibited higher frequencies of polyfunctional $CD8^+$ T cell responses. Also, vaccinated individuals with higher polyfunctional $CD8^+$ T cell responses were at a lower risk of acquiring HIV infection [312]. Humoral immune responses identified IgG3 and AD cellular phagocytosis (ADCP) to be correlated with increased protection [313], however AD cellular cytotoxicity (ADCC) was not associated with protection [314].

I. RV144 HIV vaccine trial & defining immune correlates of protection

RV144 was a phase 3 trial that enrolled over 16,000 heterosexual individuals in Thailand [315]. The vaccine formulation consisted of components from the previously failed vaccine trials.

Enrolled individuals received an attenuated canarypox vector expressing HIV clade B Gag and Pro and Env from the predominant circulating recombinant form of HIV in Thailand, CRF01_AE (ALVAC vCP1521). They also received booster shots of bivalent rgp120 from subtypes B and E (AIDSVAX). The objective of the vaccine was to assess if it provided protection and had an effect on VL if a breakthrough infection occurred. One hundred and twenty-five individuals seroconverted over the duration of the study, of which 74 received placebo and 51 the ALVAC vCP1521/AIDSVAX vaccine regimen. Vaccine efficacy at the end of the study (42 months after the initial vaccination) was at 31.2%. Post hoc analyses revealed that the efficacy peaked at 12 months and then waned over time [316]. The VL set point in infected, vaccinees and placebo recipients did not differ significantly [316]. Thus, the vaccine achieved one of its primary objectives. This led to the question: What then were the correlates of protection?

Correlates of protection (CoP) are defined as the quantifiable immune responses attributed to protection from infection [317]. The RV144 study group assayed six vaccine-induced responses: V1V2-specific IgG, Env-specific IgG avidity, NAbs, Env-specific IgA, ADCC, and Env-specific CD4 function [318]. The only two responses that were significantly associated with protection were V1V2-specific IgG titers and Env-specific IgA. In the vaccine arm, protected vaccine recipients demonstrated higher levels of V1V2-specific IgG and lower levels of Env-specific IgA compared to those who seroconverted during the study. Thus, V1V2-specific IgG titers were positively associated with protection whereas Env-specific IgA responses were negatively correlated with protection. It was imperative to distinguish humoral signatures induced in the RV144 and VAX003/004 trials and to understand the reasons for success in the RV144 trial and the failure in the VAX trials. Comparative analyses between these trials revealed that the AD functions from individuals enrolled in RV144 vaccine trial were significantly correlated with each

other compared to those enrolled in VAX003 [319]. Plasma bulk IgG1 was induced similarly in the three trials, however total IgG3 was significantly higher in RV144 vaccinated individuals compared to those receiving the VAX003 regimen.

Of the 4 IgG subclasses, IgG3 has the longest hinge region, which offers more flexibility and greater reach [320]. The importance of IgG3 in infectious diseases has been well established in the literature [321]. In non-HIV infectious diseases, IgG3 appears the earliest after dengue infection [322], provides long-term protective immunity in malaria [323], in fetuses, it provides anti-malarial immunity [324], in SARS-CoV-2, it performs a strong neutralizing function [325, 326], and is negatively associated with SARS-CoV-2 VL [327]. With regards to functions, IgG3 is the most potent of the subclasses to elicit complement activation and binding to Fc gamma receptors (FcγR) [328, 329]. With regards to HIV, IgG3 peaks during acute infection and wanes quickly thereafter [330]. As such, it was demonstrated that AD cellular viral inhibition (ADCVI) correlated strongly with IgG3 and the loss of IgG3 paralleled the loss of ADCVI [331]. A longitudinal comparison between IgG subclasses distinguished ECs from untreated progressors (UTPs) also known as non-controllers (NCs) [332]. Specifically, it was not only the maintenance of gp120-specific IgG3 but also lower titers of gp120-specific IgG2 and 4 in ECs compared to NCs that may have contributed to some effect in spontaneous control of infection.

When comparing IgG subclass distribution in plasma from the participants of the RV144 and VAX003/004 vaccine trials, non-specific total IgG2 and 4 concentrations in VAX003 recipients were significantly higher than those from RV144 vaccinees [319]. The proportion of gp120-specific IgG that was IgG3 was higher in RV144 than VAX003 recipients while the proportion of these Abs that were IgG2 and IgG4 was lower in RV144 than in VAX003 vaccinees. Over time, individuals vaccinated with the RV144 compared to the VAX003 vaccine regimens also

maintained significantly higher proportions of gp120-specific IgG3 and lower proportions of gp120-specific IgG2 and IgG4 amongst total gp120-specific IgG concentrations. A similar distribution of IgG subclasses was observed for Abs specific for gp120 V1V2 peptides in recipients of the RV144 and VAX003 vaccines [333]. Not surprisingly, vaccinated individuals in the VAX004 trial also had significantly lower proportions of gp120- and V1V2-specific IgG1 and IgG3 and significantly higher proportions that were IgG4 compared to the level of these antibodies present in the RV144 trial participants [305]. From the RV144 trial, it was deduced that gp120-specific IgA was directly correlated with risk of infection. Thus, when gp120-specific IgA concentrations were compared between these vaccine trials, VAX003 and VAX004 vaccinees had significantly higher concentrations of these IgA Abs than RV144 vaccinees, suggesting that IgA might indeed mitigate the protective benefits conferred by IgG Abs [305]. It is unsurprising that IgG3 takes the podium when analysing the gp120-specific IgG levels as a CoP in these HIV vaccine trials.

To further study the protective mechanism of action, a comprehensive systems serology approach was undertaken [334]. This approach consisted of two steps. The first step was to obtain information on Fc functions and biophysical characteristics of vaccine induced Abs such as Ab subclass and glycosylation patterns. The second step employed a mathematical/bioinformatics approach to condense and identify humoral signatures that identified a vaccine-induced "fingerprint". This methodology was fielded to compare immune signatures identified in the successful phase 3 RV144 with the unsuccessful phase 3 VAX003 and VAX004 vaccine trials, and with a novel phase 1 vaccine trial that used an adenovirus 26 (Ad26) vector encoding clade A Env (IPCAVD001) [334, 335]. This approach was able to distinguish vaccine groups based on differences in vaccine induced Abs based on their AD functions and biophysical characteristics.

These mathematical models found that plasma from RV144, compared to VAX003/004 trial recipients, differed from each other not only based on gp120-specific IgG3 distribution, but also by an associated network that included multiple AD functions. Such networks were absent in plasma from VAX003/004 recipients. These results were interpreted as evidence that the RV144 vaccine regimen tuned Ab features such as Ig class and/or subclass switching in a manner that may have led to the success of the RV144 vaccine trial.

Some RV144 vaccinated individuals seroconverted during the course of the trial. The sequences of the breakthrough viruses in these individuals were compared with seroconverters in the placebo arm of the trial. This sieve analysis found evidence that vaccine induced humoral immune responses exerted immune pressure upon the HIV Env V2 region, which led to viral escape. The approach was able to identify two amino acid sites (K169 and I181), which conferred immune escape without losing viral fitness [336].

Caution should be taken when interpreting and comparing the results of the RV144 and VAX003/004 trials. Participants enrolled in RV144 trial were primed with a canarypox vector encoding Gag and Pro from clade B and Env from clade CRF01_AE whereas the VAX003 and VAX004 regimens included bivalent rgp120 protein vaccines (B/B and B/E, respectively). Participants enrolled in these 3 vaccine trials were boosted with rgp120, however the boosting schedules differed in these three vaccine trials. How these differences affected vaccine induced immune responses is unknown. Lastly, plasma used for CoP analyses was collected at different times post-vaccination, which may have influenced features of the vaccine-specific Abs that were generated in these three vaccine trials. Nonetheless, it is crucial to know what is at the root of the RV144 vaccine trial's success so that this can be replicated and built upon in other vaccine trials and to fine tune CoP analyses. So too, it is important to understand the reason(s) underlying the

failures of the VAX003/004 trials to avoid proceeding down the pathway of these failed trial approaches. To confirm the CoP identified in RV144 trial, it was important to replicate this trial.

II. HVTN 702 – RV144 in South Africa

HVTN 097 was a phase 1 clinical trial conducted in South Africa. The objective of this trial was to evaluate the circulating Ab specificities induced by the vaccine regimen used in the RV144 trial that were identified as CoP this trial [337]. Initial results were highly encouraging with regards to the induction of similar immune responses by the HVTN 097 and RV144 regimens [338]. Compared to vaccinated individuals in the RV144 trial, participants in HVTN 097 exhibited a lower frequency of Env-specific $CD4^+$ cells but the overall functionality of these cells was significantly higher. Further, the CoP identified in the RV144 vaccine trial were compared with the immune responses generated by the HVTN 097 trial. All together, HVTN 097 vaccination induced cross-clade reactive gp120- and V1V2-specific IgG, with titers that were significantly higher than those seen in the RV144 trial. Over time, participants from HVTN 097 had a slower decline in V1V2 Ab titres compared to those seen in the RV144 trial, although the difference in the rate of decay was not significant ($p=0.069$). Explorative analysis of results from the RV144 trial identified the importance of the IgG3 Ab subclass that may have contributed to the success of the RV144 trial. When compared with results from the RV144 trial, HVTN 097 participants had significantly higher values of total, gp120-, and V1V2-specific IgG3 titres and these values were significantly higher over several time points post vaccination. Moreover, gp120-specific Abs induced by the HVTN 097 regimen had similar ADCC functionality to that induced in the RV144 trial [338]. These data motivated HIV investigators to push for a phase 3, RV144-like clinical trial in South Africa.

HVTN 702 (NCT02968849) was initiated in 2016 and enrolled more than 5,000 healthy, HIV negative, sexually active men, and women [339, 340]. The vaccine formulation was based on that used in the RV144 trial – a canarypox vector expressing clade B Gag and Pro and clade C Env gp120 linked to clade B gp41. Vaccinated participants received booster doses of clade C rgp120, since clade C is the predominant circulating clade in South Africa. The primary outcome of the study was to investigate vaccine efficacy in preventing HIV acquisition. The study was halted in early 2020 when the vaccine failed to demonstrate efficacy [341]. The rates of HIV acquisition in the vaccine and placebo arms were similar (138/2704 and 133/2700, respectively) [340]. Investigation is underway to identify what factor(s) could have led to the failure of HVTN 702.

a. Postulates on failures of HVTN 702

There are several lines of thought postulating the reasons behind the failure of the HVTN 702 trial. In the RV144 trial, Env-specific IgA levels were a significant variable, which was directly correlated with rate of infection. It was suggested that Env-specific IgA could mitigate the potential benefits of Env-specific IgG Abs. However, preliminary analysis performed on samples from the HVTN 097 or HVTN 702 vaccine trials quantified neither total nor Env-specific IgA Abs. Therefore, a hypothetical negative role for IgA, if any, is currently unknown. The ADCC assay used in the CoP analyses performed on samples from the HVTN 097 trial employed gp120-coated target cells. As mentioned above, gp120-coated target cells display CD4i epitopes also exposed when HIV Env is in its State 3 open conformation. This conformation is not found on productively HIV-infected cells. Such gp120-coated target cells probe for the presence of Abs to CD4i epitopes and the open HIV Env conformation. Such Abs preferentially bind uninfected bystander cells that have taken up gp120 shed from HIV-infected cells [342]. There were differences in the vaccine formulations of the RV144 and HVTN 702 trials. The canarypox vectors used encoded clade C

Env and CRF01_AE Env in for the HVTN 702 and RV144 trial, respectively. The adjuvant used in these trials differed as well, with alum being used in the RV144 and HVTN 097 trials, and MF59 in the HVTN 702 trial. In animal models, it was reported that monkeys injected with Env in MF59 had a significantly higher amount of Env-specific Abs compared to those injected with Env in alum [343]. The number of booster shots administered in these two trials was also different (2 in the RV144 and 4 in the HVTN 702 trials). However, one of the most interesting hypotheses for why the HVTN 702 vaccine trial failed to protect from HIV infection is differences in the predominant circulating HIV strains in Thailand and South Africa. As mentioned earlier in this thesis, the serine at position 375 of gp120 is highly conserved across all known HIV isolates and clades with the exception of the CRF01_AE strain, which predominates in Thailand [344]. The CRF01_AE has a histidine at this position which partially opens the Env conformation on infected cells that usually sample a State 1 closed conformation. This exposes the hidden, CD4i epitope. Thus, the anti-gp120-specific Abs induced by the RV144 vaccine regimen included a high concentration of Abs specific for CD4i epitopes that were able to bind the partially open Env conformation on HIV-infected cells, which could then be eliminated by ADCC. In contrast, Abs to CD4i epitopes induced in the HVTN 702 trial were unable to bind the closed Env conformation on HIV-infected cells and were thus unable to clear these cells by ADCC. Whether this actually underlies the success of the RV144 and the failure of the HVTN 702 trials is currently unknown, but worth investigating.

III. Other vaccine trials in progress

Thus far five out of six vaccine trials have failed to provide protection. Replicating the one modestly successful vaccine trial has failed as well. This has not deterred investigators from investigating alternate immunogens and vaccine strategies. Three pivotal clinical trials are

underway: HVTN 705 [345], HVTN 706 [346], and antibody-mediated prevention (AMP) trials (HVTN 703 [347] and HVTN 704 [348]).

HVTN 705 (NCT03060629) was a "proof-of-concept" phase 2b trial initiated in sub-Saharan African countries, enrolling women. The vaccine used "mosaic" antigens as the immunogen, i.e., sequences covering most of the antigenic regions targeted by $CD4^+$ and $CD8^+$ T cells. This strategy, as opposed to the ones using single clade- or strain-specific sequences, induced a greater breadth of cellular immune responses in rhesus macaques [349]. Sixty-six percent of the monkeys were protected even after 6 low dose intrarectal challenges [350]. This encouraged the investigators of this mosaic vaccine approach to test this strategy in human trials. However, the phase 2b/3 trial was halted as preliminary results determined that the vaccine did not provide adequate protection against HIV acquisition [351]. HVTN 706 (NCT03964415) is an ongoing phase 3 trial based on the same strategy as HVTN 705, the only difference being the demographic make-up of the participants, which are cis-gender men and transgender persons who engage in sexual activities with men or transgender persons. Both these vaccines encoded four mosaic antigens: two each for Gag-Pol and Env. The results of the HVTN 706 trial are expected in 2024.

As opposed to the vaccine trials described thus far, the phase 2 AMP trials are designed to provide passive immunity by administering broadly neutralizing Abs (bNAbs). HVTN 703 (NCT02568215) enrolled women from sub-Saharan Africa whereas HVTN 704 (NCT02716675) enrolled MSM and transgender MSM from the Americas and Europe. Participants received infusions of varied concentrations of the bNAb VRC01, which targets the Env CD4 binding site (CD4bs). As the rates of infection in the vaccine and placebo arms were similar, preliminary data concluded that VRC01 was unable to protect against infection in both trials and they were discontinued [352]. While VRC01 did not prevent HIV acquisition, breakthrough virus sequences

showed that fewer VRC01-sensitive strains circulated in infected individuals. Significantly, the VLs in vaccinated infected individuals was lower than in infected individuals in the placebo arm. Even though these trials failed, they were key to indicating that passive infusion of bNAbs could offer selective immune pressure and could potentially contribute to controlling *in vivo* viral replication. As such, clinical trials employing a cocktail of bNAbs are underway (NCT04173819 [353], NCT04212091 [354], and NCT03928821 [355] amongst others). By targeting different Env epitopes, these cocktails aim to apply critical immune pressure to HIV that affects its fitness.

IV. SOSIP – a new class of immunogen for HIV vaccine strategies

Induction of immune responses by engineering vectors to encode HIV proteins has failed to provide any protection against infection. None of the vaccine trials have induced bNAbs, which may be able to prevent infection. Several groups conceived of the idea of producing trimeric Env with the goal of employing it as an immunogen to induce bNAbs [356]. Making a trimeric Env in itself has been difficult. However, after two decades of intense research, Sanders and Moore generated SOSIP.gp140, a molecule that most closely resembles trimeric Env. This SOSIP molecule contains two key modifications; introduction of two cysteines, one each in gp120 and gp41 to create a disulfide bond (S-O-S, SOS) and an isoleucine to proline substitution at position 559 (I559P) [357, 358]. BNAbs such as b12 (CD4bs) and 2G12 (an N-linked carbohydrate specific mAb) bound equally to gp120 monomers and SOSIP.gp140 trimers [359]. Soluble CD4 could open the closed conformation of SOSIP [359, 360]. Mice, rabbits, and macaques were immunized with SOSIP trimers, and these animals generated potent bNAbs that bound to different sites on the Env – no single class of bNAbs dominated in two or more animal species [361-364]. The concentrations of rabbit serum bNAbs were significantly and strongly correlated with the neutralising titers. Animals also generated cross-clade bNAbs. These pilot studies showed the

strengths of SOSIP in inducing bNAbs that target multiple sites of Env bypassing the clade sequence barrier. To test whether SOSIP-generated bNAbs provide protection against acquisition, Pauthner et al. immunised 78 macaques with SOSIP trimers [365]. Only 6 out of the 78 (7.69%) immunized animals generated high titers of bNAbs. To assess if the titers of these bNAbs played a role in protection, they challenged animals and compared the high titer and low titer bNAb groups of 6 animals. More than 25% of the macaques in the high bNAb titer group consistently remained uninfected 24 weeks post-first challenge. The VL of infected macaques in the high bNAb titer group was significantly lower than those in the low bNAb titer group. No AD functional activity was detected in either group, thus it was concluded that protection from HIV acquisition was attributed to the neutralising function of the bNAbs only. The probability of protection from infection was directly correlated with and predicted by bNAb titers. This was the first-of-its-kind study where a protein immunogen elicited bNAbs that were associated with protection [365]. From the initial 6 animals in the high bNAb titer group, only 1 remained uninfected at the end of the study. All 6 low bNAb titer macaques were infected within the first 6 challenges suggesting that while high titers of bNAbs could offer some degree protection, the amount of protection was somewhat up to chance. This has not deterred investigators from initiating safety and efficacy studies using SOSIP trimers [366, 367].

V. mRNA vaccines

Interest in messenger RNA (mRNA) strategies for immunisations has received increased attention of late due to the recent success of SARS-CoV-2 vaccines [368]. In mice, mosaic Gag-Pol mRNA induced and maintained potent IFN-γ secreting T cells specific for the immunogen 22 weeks post-immunisation [369]. In conjunction, mRNA vaccine formulations aimed at generating humoral immunity are being developed. Rabbits and monkeys immunised with Env-encoding mRNA

produced high levels of gp120-specific Abs by 6 weeks post-immunisation and maintained peak Ab titers for an additional 32 weeks [370]. These Abs efficiently neutralised and performed non-neutralising ADCC function at the study endpoint (i.e., 38 weeks post-immunisation for rabbits and 52 weeks post-immunisation for rhesus macaques) confirming that functional Abs were maintained for several months after a single immunisation. Building on this, Saunders et al. demonstrated that Env-encoding mRNAs combined with rgp120 protein immunisation could elicit neutralising and non-neutralising Abs in rhesus macaques [371]. ADCC and AD cellular phagocytosis (ADCP) activities were observed 8 weeks post-immunisation. Whether the mRNA induced Abs have any role in protection has yet to be assessed. To investigate this, Zhang et al. immunised mice and macaques with virus-like particles (VLP) consisting of mRNA that encoded Env and Gag and challenged them intrarectally with SHIV [372]. Vaccinated animals remained uninfected until challenge 5, after which the probability of remaining uninfected declined with each subsequent challenge. Env-specific Ab titers and ADCC function were significantly correlated with protection, whereas Gag-specific CD4 and CD8 cell responses were not. Infected, vaccinated rhesus macaques had VLs similar to that seen in infected, unvaccinated controls, which suggested that while the mRNA vaccine conferred some degree of protection from infection, it failed to control or reduce viremia after infection. This further strengthened the idea that Abs, and specifically non-neutralising Abs (nnAbs) could indeed play a role in protection from HIV acquisition [372]. This has prompted the International AIDS Vaccine Initiative and Moderna to initiate phase 1 safety clinical trials in humans (IAVI G002) [373, 374].

6. Natural control of HIV: Model for a functional cure

I. Historical background

Early reports of AIDS in North America and Europe were predominantly observed among MSM. Some of the earliest reports from longitudinally followed MSMs followed for more than 10 years included a few MSMs who were HIV seropositive, remained asymptomatic and exhibited stable and "healthy" levels of CD4 counts [375, 376]. Initial studies showed that "non-progressors (NPs)", as compared to non-controllers (NCs), had more stable CD4 counts and often had elevated CD8 T cell counts. Long term non-progressors (LTNP) are individuals who maintain healthy CD4 counts (above 400 to 500 CD4 cells per mm^3) for 7 or more years irrespective of VL since the means of quantifying VL as a marker of HIV disease did not become available until the mid-1990s. Once the VL technology became available, it was shown that a subset of LTNPs had stable VLs with declining CD4 [85, 377-379]. These individuals were known as slow progressors (SPs) as they were slowly progressing towards AIDS [380]. Thus, arose ambiguity in the literature with regards to nomenclature for NPs; over time, they have been interchangeably named "long term survivors (LTS)", "LTNPs", "SPs", "HIV controllers (HIC)", "elite controllers (EC)", "elite suppressors (ES)" and "viral/viremic controllers (VC)" along with the original NP. With the advancement of technology, new assays measuring VLs reduced the limit of detection to 20 to 75 copies/ml plasma (c/ml) depending on the instrument and assay employed. This led to a more standardised nomenclature for NP [381-386]. As such, individuals who could maintain undetectable VLs ($\leq$ 20, 50, or at most 75 c/ml, based on the design and setup of the cohort and the instrument used) were now termed ECs. ECs overlapped with the LTNP subset who maintained VLs below the limits of detection mentioned above, whereas CD4 counts were exclusively used to define LTNPs. The duration of undetectable VLs used to define ECs can range from a few months to decades depending on the design of the cohort (reviewed extensively in [387, 388]). The International HIV Controller Consortium defined ECs as ART-free PLWH with undetectable VLs

by clinical assays (most often in the range of 20 to 75 c/ml) for at least 12 months [387]. Viral controllers (VCs) were defined using the same criteria as ECs, except that the VL cut off used for VC is <2000 c/ml. However, recent longitudinal follow-up studies for ECs for over 20-25 years have observed that some ECs lose the ability to control HIV VL and can lose their classification as ECs as per the definition setup by the Consortium [389-392]. Due to the different ambiguous terms used by each study, moving ahead, HICs, ES, NPs, and LTS will be referred to as controllers, whereas the terms LTNPs, ECs, and VCs will be referred to as described above.

The current standard of care for HIV infection is to treat PLWH as soon as they are diagnosed as being HIV infected. Therefore, it is no longer possible to identify or recruit new ECs. Additionally, the sensitivity of VL assays has increased over time which has compromised the possibility of collating or defining ECs across cohorts over time. A French cohort of treatment-naïve PLWH (SEROCO) found that 12 out of 330 (4%) of enrolled participants had VL <200 c/ml, and only 1 individual (0.3%) had a VL <20 c/ml [393]. When the SEROCO cohort was followed longitudinally, the frequency of ECs 5 years post-seroconversion was 6.7%, however they were categorised as such only if 2 consecutive VL measurements were ≤500 c/ml [394]. Thus, varying VL cut-offs from the same cohort did not provide an accurate representation of frequency of ECs amongst PLWH. Elsewhere, an international cohort of 2176 seroconverters in the pre-ART era also found that 145 (6.7%) of enrolled participants had a VL of <400 or 500 c/ml [395]. In another cohort of 46,880 PLWH in France, 0.15% and 0.4% of enrolled participants were ECs and LTNPs, respectively [396]. ECs accounted for 0.5% of the 4,586 American military personnel living with HIV [397]. In Canada, Dr. Cecile Tremblay and Dr. Nicole Flore Bernard established the Canadian Cohort of HIV^+ Slow Progressors (CCHSP; Canadian HIV Trials Network (CTN) 247) to identify SPs amongst Canadian PLWH and characterize immune mechanisms underlying spontaneous HIV

control [398, 399]. The CCHSP used CD4 counts and VLs to categorise subjects. ECs were defined as PLWH with CD4 counts >400 cells/mm^3 and VL ≤50 c/ml, VCs as PLWH with CD4 counts >400 cells/mm^3 and having VLs of between 51 and 3000 c/ml. In summary, it is estimated ECs account for less than 1% of PLWH. The EC and VC samples included in the research chapters of my thesis were drawn from the CCHSP. The non controller samples were drawn from the Montreal Primary HIV Infection (PHI) cohort. They included samples from untreated progressors (UTP) with CD4 counts <500 cells/mm^3 and VL >3000 c/ml. More than 99% of untreated PLWH will proceed to AIDS, if left untreated. For this reason, the standard of care is to treat PLWH with ART as soon as possible after diagnosis, especially before CD4 counts drop below 400-500 cells/mm^3. Treated progressor (TP) samples also drawn from the Montreal PHI cohort are included in the research chapters of my thesis [400].

The mechanisms underlying spontaneous HIV control are an intense area of investigation. The rationale for studying ECs is to uncover what factors play a role in the natural control of HIV infection. This information may be useful for developing therapeutic strategies aimed at converting NC into controllers. Figure 8 illustrates some of the viral and immunological factors that may be important in spontaneous HIV control.

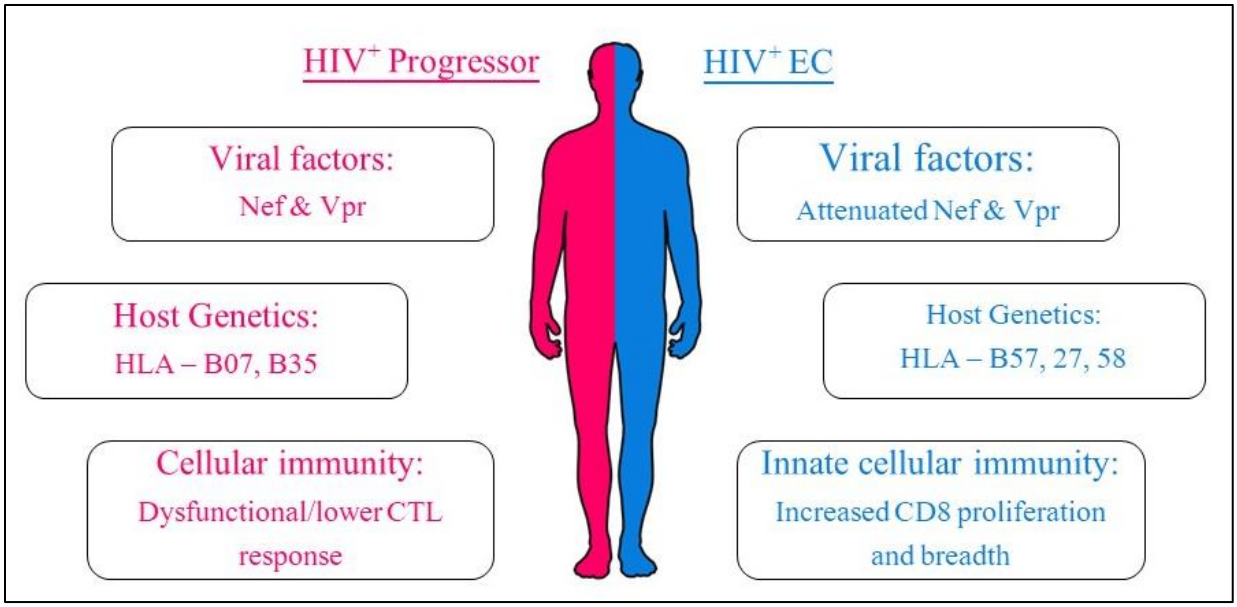

*Figure 8: Immune differences between HIV$^+$ progressors/NCs and ECs. Studies conducted over the past few decades have discovered that a variety of factors can contribute to spontaneous control of HIV. EC, compared to NCs, can harbor viruses containing attenuated viral proteins. There is a higher prevalence of HLA-B*57, *27, or *58 amongst ECs than NC and a higher prevalence of HLA-B*07 or B*35 amongst NCs than ECs. Some ECs have HIV-specific T cells that are more effective at proliferating and suppressing HIV replication than those from NCs.*

II. Viral factors

In a transfusion-acquired HIV cohort from Australia, a group of individuals remained asymptomatic and maintained normal healthy CD4 counts for more than 7 years post-transfusion [401]. The infecting HIV strain had deleterious mutations in the *nef*-LTR region which hampered the virus' replicative capacity [402, 403]. This Sydney Blood Bank Cohort was one of the earliest studies to propose that HIV mutations affecting replicative fitness could account for slow HIV disease progression [401-405]. Simultaneous studies showed that mutations hampering Nef's functions were also observed in a small subset of NPs [406-408]. Some of these functions included

defective ability to downmodulate CD4, major histocompatibility class I (MHC I) antigens, and ligands for activating NK cell receptor, NKG2D [409-411]. Mutations in other HIV proteins such as Vpr, Vpu, Rev, and Env were also implicated in HIV controller status [412-416]. In contrast, viruses isolated from 10 LTNPs did not harbor *nef* deletions or mutations [417]. Overall, none of the cohorts or the studies published to date identified a common viral factor, which could explain HIV controller status, suggesting that viral factors accounted for only a subset of controllers.

III. Host factors

Host immunological responses to HIV have been studied extensively. Early studies found that CD4 cells from a subset of high risk, HIV exposed individuals were resistant to infection. These individuals were homozygous for a 32-base deletion in the CCR5 gene. This deletion mutation prevented cell surface expression of the CCR5 co-receptor for HIV entry, thus conferring resistance to infection [418-420].

a. Host genetics and cellular responses

The *MHC* encodes three classes of molecules: MHC class I antigens include classical (or class Ia) antigens HLA-A, -B, and -C and non-classical (class Ib) HLA-E, -F, and -G antigens, MHC class II molecules include HLA-DP, -DQ, and -DR antigens and MHC class III molecules include a group, which mainly consists of heat shock proteins. MHC class I antigens are the most polymorphic antigenic system in man. These antigens provide an extensive array of molecules restricting epitope recognition by $CD8^+$ T cells. The Amsterdam cohort of controllers found that these individuals were enriched in HLA-B*57 [421]. Simultaneous work in 2 seroconverter cohorts in the USA found that PLWH expressing HLA-B*57, -B*27, or -B*51 had a slower progression to AIDS, compared to PLWH expressing HLA-B*18, -B*58 or -A*25 [422]. Two pivotal studies linked the presence of certain alleles with slower HIV disease progression. First,

Goulder et al. showed HLA-B*57 restricted HIV epitope responses dominated the cytotoxic T cell (CTL) response in controllers expressing this allotype [423-425]. However, presence of HLA-B*57 alone did not confer slower progression to AIDS as it was observed in the same cohort that a subset of HLA-B*57 progressors could also display an immune response against a broad array of HLA-B*57 restricted antigen epitopes [424]. A survey of the number of HIV epitopes recognized and the HLA antigens they were restricted by in a cohort of 375 individuals from South Africa showed that HLA-B restricted T cell responses dominated those restricted by HLA-A by a factor of 2.5-fold [426]. Furthermore, the HLA-B, but not the HLA-A, restricted $CD8^+$ T cell responses were strongly associated with VL set point, CD4 count and rate of HIV disease progression [426]. One of the largest genome-wide association studies found a significant association between an endogenous retroviral element associated with HLA-B*57 and a second locus near HLA-C with VL control [427, 428].

Genetic association studies cannot prove a causative link between enrichment of specific alleles with rates of HIV disease progression. Migueles et al. demonstrated that CD8 cells from EC had significantly higher proliferation and perforin expression and concentration compared to those from progressors when stimulated with HLA-B*57-restricted HIV peptides [429]. Betts et al. showed that a hallmark of HIV controllers was an HIV-specific $CD8^+$ T cell response that was more polyfunctional than that of NC. This was independent of the response's MHC I restriction and the T cell memory phenotype [430]. Proviruses cultured from HLA-$B*57^+$ controllers harbored escape mutations in *gag*, however the presence of strong CTL responses against mutated Gag demonstrated evolution of host immune response and the virus [431]. This could potentially explain that despite significant immune pressure exerted by CTL in controllers that controls viremia to below detectable levels, virus is not cleared and continues to replicate at very low levels

[432]. It should be noted that not all controllers express protective HLA allotypes. Migueles et al. showed that while ECs may have fewer CTLs, they are functionally potent with respect to HIV lytic activity targeting autologous HIV-infected cells. These data collectively suggest an interesting hypothesis: The CTL response plays a crucial role in viral replication leading to eradication of the most fit viruses. CTL mediated immune pressure allows selection of less fit viruses, i.e., those harboring mutations that reduce fitness. Thus, it could be argued that other host immune responses also participate in viral control.

Along with cellular immunity, host cell intrinsic immune factors, known as restriction factors, also play a significant role in HIV control by intervening at different stages of the retroviral life cycle, thereby controlling HIV spread. Some of these restriction factors are: 1) the apolipoprotein B messenger RNA (mRNA)-editing enzyme catalytic polypeptide-like 3 (APOBEC3) family of proteins; specifically APOBEC3G and APOBEC3H, 2) tripartite-motif-containing 5α (TRIM5α), 3) BST2 also known as tetherin, 4) SAM domain and HD domain-containing protein 1 (SAMHD1), 5) serine incorporator 3 (SERINC3) and SERINC5 and 6) schlafen family member 11 (SLFN11), amongst others [433-435]. APOBEC3G catalyses the conversion of cytidine to uridine thereby introducing lethal mutations in the viral DNA rendering progeny viruses less fit [436, 437]. Viral Vif counteracts the effects of APOBEC3G. It was recently shown that the viral Vif was more highly active in progressors than in ECs [438]. TRIM5α targets HIV capsid and interferes with viral uncoating. It was shown that capsid from virus isolated from HLA-B*57/B*27^{+} ECs was more sensitive to TRIM5α-induced degradation compared to capsid from other, non-HLA-B*57/B*27^{+} ECs [439]. A comprehensive investigation comparing the activities of different restriction factors showed that compared to progressors, LTNPs had similar mRNA levels of TRIM5α, SLFN11, SAMHD1, and myxovirus resistance protein B (MX2) RNA, but

higher levels of BST2 mRNA. [440]. Overall, HIV controllers and LTNPs represent a heterogenous group of which a subset have potent cellular responses able to control HIV.

b. Humoral immunity

There is great interest in identifying humoral host responses in natural control of HIV. Data obtained from the RV144 vaccine trial showed that anti-V1V2-specific Abs and ADCC competent Abs were associated with protection. This, combined with the failures of STEP and PHAMBILI trials, made the field reassess whether humoral responses could be important either in HIV protection or control. Before I delve into the literature on Ab-mediated HIV protection or control, it is important to first discuss Abs and their participation in anti-HIV responses.

i. Antibodies

Abs are a part of the immunoglobulin (Ig) family. They are produced by B cells that can recognize and opsonise non-self objects such as bacteria, fungi, viruses, and other foreign molecules. An Ab consists of two regions: the antigen binding fragment called the Fab portion, and the fragment crystallizable region termed the Fc portion that binds to Fc gamma receptors (FcγR) on immune cells such as NK cells and monocytes, among other cell types and early components in the complement cascade. The Fab segment contains a region known as the paratope that recognises an epitope on an antigen (Ag). The non-covalent interactions between an Ab and an Ag are highly specific. Ab forms a bridge between Ag on target cells and FcRs on innate immune cells that activates the later to induce their effector functions. Ab bound to Ags on the surface of cells, bacteria or other pathogens initiate the complement cascade, which generates molecules that contribute to cell, pathogen or Ag clearance. In the context of HIV such Abs can be nnAbs or neutralizing Abs (nAbs). NAbs also bind Ags in a manner that prevents them from entering new

target cells. In general, there are five classes of human Igs, and in descending order based on the amount of each class in blood, they are: IgG, IgA, IgM, IgE, and IgD.

The structure of an IgG Ab is depicted in *Figure 9*.

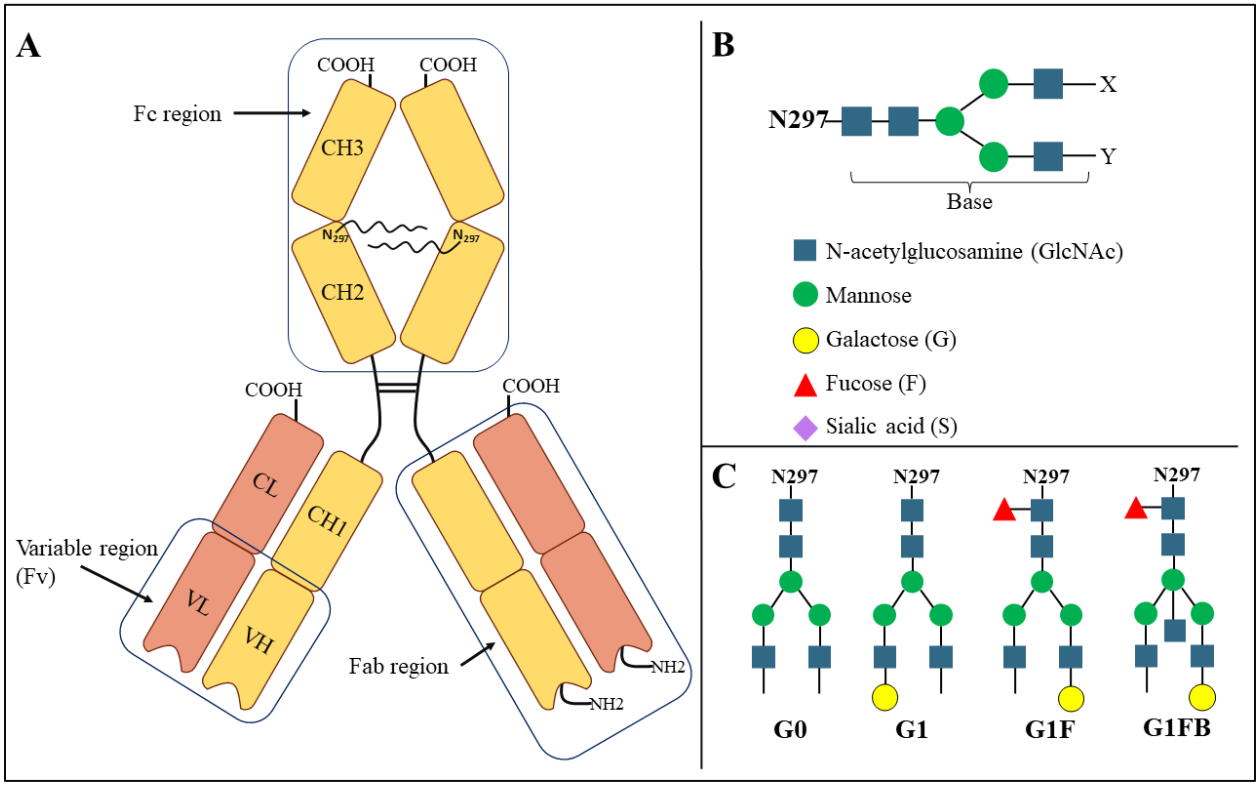

Figure 9: Structure of an IgG Ab. A. Abs consist of two parts, the Fc region that binds to FcR on innate cells or to early components in the complement cascade, and the Fab region that recognises the Ag via the paratope as shown in the curvature on N-terminus. Each Ab is made of 2 identical heavy chains and each chain consist of 3 constant regions (C) and 1 variable region (V) and 2 identical light (L) chains consisting of 1 C and 1 V region. The Fab and Fc portions are joined by a hinge region. The two H chains are linked by disulfide bonds at the hinge region. Abs undergo N-linked glycosylation at asparagine 297 (N297) in the CH2 domain of the Fc portion. B. More than 20 sugar combinations can bind at aa N297. The base glycosylation consists of two N-acetylglucosamine (GlcNAc) followed by a branch created by a mannose. Each branch consists of

mannose followed by a molecule of GlcNAc. Sugar moieties such as galactose (G), fucose (F), and sialic acid (S) and additional GlcNAc and, mannose can be added to the base at various positions. X and Y indicates the terminal positions at which G and S can be added. C. Some examples of these combinations are shown here. G0 is the base structure to which no other sugars are added. Addition of G or S at either X or Y is referred to as G1 (shown) or G0S (not shown). It is important to note that F is the only sugar to be added to the first GlcNAc closest to N297. G1F Abs consist of 1 G and F added to the base. In addition, the central mannose can be further branched to add another molecule of GlcNAc. This structure is known as bisected (B). Addition of G and F to a bisected Ab is labelled as G1FB.

IgG is a Y-shaped monomeric glycoprotein that contains two Fab regions and can either neutralize or perform extra-neutralizing functions [441, 442]. All IgG Abs are composed of 2 identical chains, and each chain consists of 3 constant (C) and 1 variable (V) domains (Figure 9A). These identical chains are linked to each other via disulfide bonds in the hinge region of the Ab. The hinge region links the Fab and Fc portions. Each Fab region is made up of heavy (H) and light (L) chains. All together, the Fab region consists of 2 variable (V) and 2 constant (C) domains making up variable heavy (VH), variable light (VL), constant heavy (CH), and constant light (CL) domains. The V domain, as the name suggests, is highly variable and imparts specificity to the Ab-Ag interaction, and thus, it is responsible for binding to the Ag. Abs from a single B cell clone will all recognise the same specific epitope on an Ag. HIV Env is the only Ag present on the free virions and expressed on the surface of infected cells to which various Abs can bind [443]. As mentioned earlier, the Fc portion binds to the FcR expressed on innate immune cells. The Fc region consists of only CH domains. All IgG Abs undergo post-translational modification (PTM) at the asparagine amino acid at position 297 (N297), located in the CH2 domain of the Fc region. The N-linked

glycosylation at N297 is crucial for Ab Fc-mediated function [441, 442]. PTM of N297 is highly complex and the base PTM consists of 2 GlcNAc, followed by 3 mannose residues, of which branching occurs at the first mannose residue (Figure 9B, [444]). Additional sugar moieties can be added at each terminal end of the last GlcNAc (indicated by X and Y in Figure 9b). These sugar molecules can be either galactose (G) or sialic acid (S) or a combination of the two. In addition, the central mannose can accommodate another GlcNAc, which bisects the entire quaternary structure. Thus, more than 30 combinations of PTM are theoretically possible at a single amino acid residue. Each chain of the Fc region can have different PTMs, which adds further complexity to the Ab structure [444]. Combinations of these sugar molecules affects the interaction and affinity of the Fc region to FcRs. Extensive studies have been performed on glycosylation patterns and Ab-dependent (AD) functions. These have shown that the absence of fucose increases Ab Fc-FcR binding avidity, which supports significantly higher ADCC functionality than their fucosylated counterparts [445-449]. This has also been shown for anti-HIV mAbs. Afucosylated b12, a CD4bs-specific bNAb and PGT121, a V3 loop N332-specific bNAb outperformed their respective wild type (WT) counterparts when tested for ADCC function [450, 451]. Similar observations have been reported for Abs to SARS-CoV-2 and dengue virus [452, 453]. Such studies demonstrate that glycosylation plays a key role in influencing the functions of Abs.

There are four IgG subclasses, IgG1-4, with decreasing plasma abundance. Each subclass has unique characteristics and functions in infectious diseases and specifically, in anti-HIV responses. For example, of the IgG subclasses in healthy individuals, IgG3 and IgG1 have the highest binding affinities for FcRs and are best at initiating the complement cascade [454, 455]. In the context of anti-HIV responses, V1V2-specific IgG3 levels were associated with a reduced risk of HIV infection [333]. As mentioned above, RV144 vaccine trial participants had significantly higher

concentrations of HIV-specific IgG3 compared to those in VAX003 and VAX004 trials [319, 333]. In contrast, the VAX trials induced significantly higher quantities of HIV-specific IgG2 and IgG4 Abs [319, 333]. Gp120-specific IgG3 and IgG1 concentrations also strongly correlated with AD functions in the RV144 trial but not in the VAX trials suggesting that quantities of IgG3/IgG1 drive AD responses. This could be due to the structure of IgG3, which has the longest hinge region of the four IgG subclasses. This confers greater flexibility allowing for more avid interaction with FcRs, which upon binding generate intracellular signals that drive AD functions [442, 456, 457].

In general, Abs can be classified as nAbs or nnAbs. Both play a significant role in the anti-HIV responses.

NAbs are generated in 10 to 30% of HIV-infected individuals [458]. When present nAbs do not neutralize contemporaneous HIV isolates. Most primary HIV isolates are more resistant to neutralization than lab-adapted viruses [459]. Even fewer PLWH (< 10%) develop bNAbs [460]. Since HIV can rapidly escape the immune pressure exerted by nAbs, it was imperative to find these key "pressure points" that HIV Env mutates to avoid recognition by nAbs. Longitudinal studies in untreated PLWH found a constant stream of evolving viral isolates that would easily escape nAb responses over several months [461]. Viral escape was most often observed in untreated acute infection (<6 months post-infection) compared to in chronic phase of infection (>6 months post-infection) [462]. Further, compared to untreated PLWH, PLWH on-ART had lower nAb levels. Importantly, Deeks et al. showed that ECs had significantly lower nAb potency compared to untreated progressors. Early reports on nAb responses in ECs/LTNPs were conflicting. While some studies found that most controllers demonstrated potent and broad nAbs [91, 463, 464], others reported the absence of nAbs [465-467]. Where nAbs were shown to be abundant in controller, there was a strong and positive correlation between the amount of nAbs

with VLs [94]. The discordant results could be due to 1) different criteria used to define "controllers" and/or 2) persistent low level viral replication driving an Ab response in controllers with different VLs (e.g., VLs < 50 c/ml vs VL < 2000 c/ml).

It takes at least 2 years post-infection for < 20% of untreated PLWH to achieve some degree of neutralisation [468, 469]. This suggests that there exists a paradoxical yet dynamic relationship between the behavior of the pathogen and host response. It would appear that the virus drives nAb generation and evolution while they simultaneously exert pressure on HIV to evolve and escape this immune pressure [470-473]. This did not deter investigators from isolating and characterising bNAbs from PLWH, because nAbs still offered hope that 1) they could be used as a passive mode of protection and 2) understanding the biology of B cell germinal center evolution was important. The earliest bNAbs to be characterised were CD4bs-specific b12 [474], and glycan shield-specific 2G12 [475]. Characteristically, b12 was shown to be a potent bNAb that can bind to FcRs and trigger AD functions whereas 2G12 lacked this property [296, 476]. More than 20 bNAbs recognising various epitopes on Env were discovered and characterised in the 3 decades that followed [477]. Most of these bNAbs performed extra-neutralizing functions while some could not. Some of the most intensively investigated bNAbs and the epitopes they target are: b12, VRC01, and 3BNC117 (all specific for CD4bs epitopes), 2G12 (glycan specific), PGT121 and 10-1074 (V3 glycan on N332 specific), 4E10 (MPER specific), and others as shown in *Figure 10*.

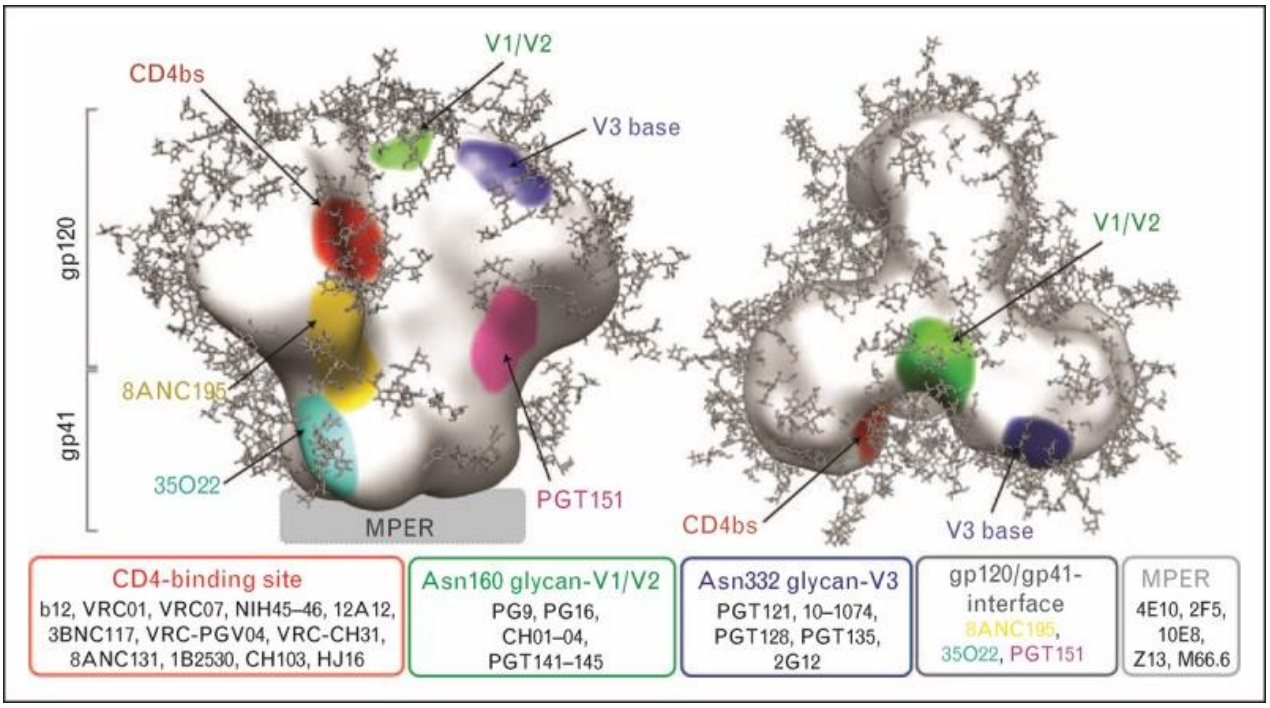

Figure 10: Epitopes on Env targeted by bNAbs. The different epitopes on trimeric Env are color coded. The respective bNAbs targeting these epitopes are shown in the boxes below. This figure is reused with permission [478].

This led investigators to question if passively infused bNAbs could prevent HIV acquisition or suppress infection in animal models. To understand if bNAb could prevent HIV infection, Hessell et al., passively infused four sets of monkeys with WT b12, b12-LALA which abrogates binding to FcRγIIIA on NK cells and prevents ADCC function, b12 KA which abrogates complement activation, and an isotype control Ab [479]. They reported that 1) passive infusion of WT b12 Ab protected monkeys from HIV acquisition and suppressed plasma VLs for 5 months post-challenge and 2) along with neutralization, extra-neutralizing functions such as ADCC but not complement activation played a key role in preventing of HIV acquisition. A follow-up study by the same investigators reported that it took 40 low dose intrarectal viral challenges to infect all the monkeys receiving WT b12 [480]. Comparatively, all b12-LALA-infused monkeys were infected by

challenge #25. A drawback of these 2 studies was that the viral isolates infecting the monkeys was not assessed. Therefore, it was unknown whether the infecting viruses has escaped immune recognition by b12. These pilot studies were expanded to include other bNAbs and cocktails of bNAbs. Moldt et al. reported the protective benefits of VRC01 (CD4bs) and PGT121 (N332 glycan on V3) infusions in NHPs [481]. Pegu and colleagues demonstrated that by passively infusing VRC01, PG9 (V1V2 glycans), and 10e8 (MPER) Abs in 3 separate groups of NHPs, offered a substantial amount of protection against SHIV challenge [482]. It was also shown that the protective activity offered by VRC01, PGT121, and 10-1074 (N332 glycan on V3) was dose-dependent [481, 483]. Yet again, viruses were not isolated from monkeys that became infected in these studies precluding an analysis of whether emergence of specific Ab escape mutations accounted for seroconversion. Another drawback of most of these studies was the quick clearance of Abs from the plasma, which indicated that if bNAbs were to be used in a setting of pre-exposure prophylaxis (PrEP), then the timing of Ab infusions would be extremely crucial relative to high-risk activity for HIV acquisition. Nonetheless, the data from animal models were highly encouraging and clearly demonstrated that protection was possible following administration of bNAb. These investigations collectively set the groundwork for conducting AMP clinical trials in humans. Unfortunately, the passive infusion of bNAbs into HIV-infected individuals failed to provide sterilizing immunity and the data generated in the AMP trials quickly halted pursuing this objective [484].

If bNAbs do not to prevent infection, can they control pre-existing HIV infection? SIV/SHIV infection in rhesus macaques progresses rapidly and is detected in lymph nodes by day-3 post-challenge [80]. So, to test the effects, if any, of bNAbs in animal models of post-exposure prophylaxis (PEP), Hessell et al. challenged NHPs with SHIV and administered animals, with

either PGT121 or VRC07 (CD4bs) within 24 hours of challenge [485]. They detected no virus in the blood, or any other tissue tested for up to 6 months post-challenge, concluding that all challenged animals were virus-free. To prove that bNAbs were responsible for preventing the establishment of infection and possibly providing the first evidence that Abs could confer of a sterilizing cure to these challenged rhesus macaques, CD8 cells were depleted from the challenged monkeys on the last month of the 6-month study without seeing VL rebound [485]. To replicate a mother-to-child mode of transmission, Shapiro et al. orally challenged infant macaques with SHIV and employed the same Abs utilised by Hessell et al. in the previously described study, though in this instance, providing both Abs in combination [486]. If the Ab infusion was administered within 30 hours of challenge, the animals remained aviremic for up to 6 months post-challenge. In contrast, if the infusion was administered within 48 hours of challenge, 50% of challenged animals became viremic but suppressed viremia sooner than did control animals receiving no Ab infusion. CD8 depletion had no effect on either VL suppression or remaining aviremic, strongly suggesting that infused bNAbs, not CD8 T cell responses were responsible for virus control [486]. To further test if nAbs played a role in viral control, PLWH on ART underwent a supervised analytical treatment interruption (ATI) and were infused with 3BNC117 or 10-1074, both together or neither [487]. Viral suppression mediated by these Abs was transient. The individuals receiving bNAbs experienced a slower time to viral rebound compared to those in the control arm. In individuals receiving the bNAb cocktail, the rebounding viral isolates remained sensitive to both bNAbs reducing concerns that Ab-mediated viral escape was the cause of rebounding virus.

Could the bNAbs themselves be modified in such a way that they can perform extra-neutralizing functions? As mentioned above, abrogating the ADCC-potential, but not the complement activating potential, of b12 diminished the effects of its protective mechanism [479]. As for b12,

1913 the Fc region of bNAbs 3BNC117 and PGT121 and their FcR mediated effector functions also
1914 played a role in the ability of these Abs to block viral entry, control VL and confer therapeutic
1915 activity [488]. HIV-infected humanised mice injected with bNAbs with mutations conferring
1916 enhanced binding to FcRγIIA on monocytes and to FcRγIIIA on NK cells demonstrated lower VLs
1917 compared to those injected with WT bNAbs. Viral suppression in mice injected with these Fc-
1918 mutated Abs was maintained over a period of two months, which illustrated the strengths of FcR-
1919 mediated functions of bNAbs [488]. The study by Bournazos et al. described here was the first to
1920 show the *in vivo* importance of AD cellular phagocytosis (ADCP) performed by monocytes in the
1921 presence of immune complexes. The importance of ADCP was also shown when HIV-infected
1922 humanised mice were injected with WT and abrogated AD functional variants of VRC07 [489].
1923 Viral decay was quicker in mice injected with WT VRC07 compared to those injected with variants
1924 with no extra-neutralizing functions. However, Parsons et al. recently showed that in virus
1925 challenged-monkeys, WT PGT121 and PGT121-LALA had the same effect on viral decay,
1926 demonstrating that Fc-mediated functions may not provide additional benefits to certain bNAbs
1927 [490]. In addition to broad Fc-functions, Anand et al. showed that by modulating the N-linked
1928 glycosylation at N297 in the Fc region, afucosylated PGT121, compared to WT PGT121,
1929 performed superior ADCC functions *in vitro* [491]. Addition or removal of galactose on PGT121
1930 did not have any effect on ADCC function. Whether such fine-tuned, modified PGT121 or other
1931 bNAbs could be employed *in vivo* to confer effects on prevention or control of HIV remains to be
1932 seen. Nonetheless, the choice of bNAbs to be employed is crucial. *In vitro* binding experiments
1933 using PGT121 and PGT151 that recognise glycan epitopes, but not 3BNC117, 10-1074, and PG9,
1934 bound non-specifically to lymphocytes from uninfected and infected individuals [492]. Non-
1935 specific binding of PGT151 led to spontaneous NK cell degranulation and eventually NK cell

death [492]. Thus, infusing PGT151 or other glycan-dependent bNAbs could lead to offsite binding and disastrous side-effects such as bystander and non-specific killing of immune cells. This study warrants further research into the selection of bNAbs for passive infusion mediated protection or control of HIV.

001. Non-neutralizing Abs

It takes many years for a small percentage of untreated PLWH to generate potent bNAbs. This timeline is out of sync with the rapid evolution of HIV viral dynamics. Data obtained for HIV controllers and ECs are conflicting in terms of the role of nAb functions in the VL control seen in these individuals. Failure of AMP trials in humans has underlined the failure to protect against HIV acquisition via passive infusion of bNAbs. On the other hand, bNAbs exert some degree of protection and control via its Fc region. Additionally, in the only modestly successful RV144 vaccine trial, V1V2-specific IgG Abs and ADCC were identified as correlates of protection. Thus, there is significant need to study if AD functions play a role in anti-HIV response. ECs naturally and spontaneously control viremia, thus representing a model of functional cure. This prompted us to characterize anti-Env Ab in ECs and compare them to those in VCs, UTPs and TPs.

NnAbs recognise the antigen-bearing entity via its Fab portion. The Fc portion of Abs binds to FcγRs on innate immune cells [493]. The Fc region also has the capability of binding to complement component protein, C1q [494, 495]. An overview of anti-Env Ab functions is depicted in *Figure 11*.

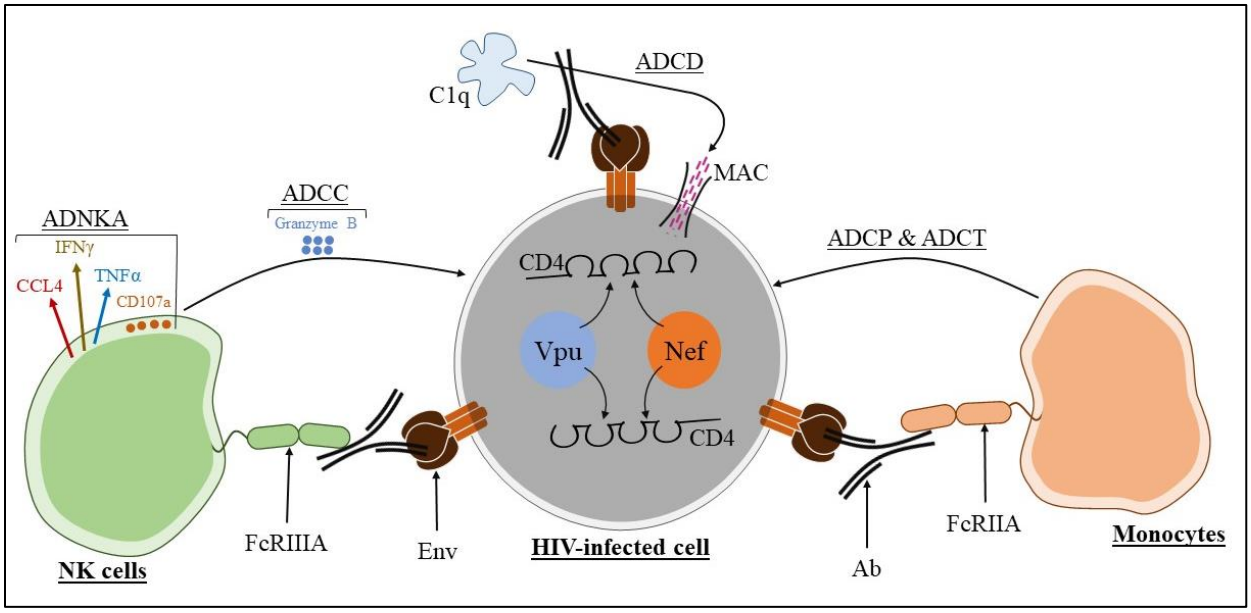

Figure 11: Overview of anti-Env nnAb functions. The closed conformation of Env is expressed on the surface of HIV-infected cell when HIV proteins Nef and Vpu downregulate cell surface CD4. The Fc region of Env-specific Abs can activate NK cells via FcγRIIIA, monocytes via FcγRIIA, and bind to complement component C1q. Activated NK cells release chemokines CCL3, CCL4 and CCL5 (shown here is CCL4 only), the cytokine TNF-α, and antiviral factor IFN-γ (collectively known as ADNKA) but can also directly lyse the infected cell by releasing granzyme B (ADCC). Monocytes can phagocytose (ADCP) or trogocytose (ADCT) the infected cell. Complement activation leads to formation of a membrane attack complex (MAC) that leads to infected cell lysis. The readout of this phenomenon is AD complement deposition (ADCD).

In the literature, several studies have investigated different anti-Env/gp120 specific Ab Fc-mediated responses. Abs can bind to CD16/FcγRIIIA on NK cells triggering an immune reaction. Activated NK cells release several antiviral factors such as TNF-α, IFN-γ, and CCL3, CCL4, and CCL5 [496, 497]. Tumor necrosis factor α (TNF-α) is a proinflammatory cytokine that recruits other innate immune cells such as neutrophils which further phagocytose and lyse infected cells

[498]. Interferon γ (IFN-γ) is also a proinflammatory cytokine that has a broad and polyfunctional effect on the host immune system; it can upregulate MHC I and II antigen on the surface of presenting cells, recruit neutrophils, induce class switching in B cells, regulate T cell immunity, and activate surrounding NK cells [499]. The CCL3, CCL4 and CCL5 chemokines binds to HIV entry co-receptor CCR5, thereby blocking HIV entry into new target cells [500]. Upon recognising an Ag-Ab immune complexes, NK cells can also upregulate a cytosolic protein known as lysosomal-associated membrane protein 1 (LAMP-1)/CD107a [501]. Since CD107a expression was significantly correlated with cytokine secretion and target cell lysis, it is used as a surrogate marker for NK cell activation. CD107a is a marker of functional NK cell activity in activated effectors that do not readily secrete antiviral factors [501]. Collectively, methodologies and assays that quantify the Ab-mediated effect of effector NK cells measure the frequency of NK cells expressing CD107a or secreting TNF-α, IFN-γ, and CCL4. These assays are collectively referred to as AD NK cell activation (ADNKA) [496, 502] (Figure 11). ADNKA readouts are measured at the level of NK cells and often were used because of their simplicity. In comparison, first generation ADCC assays were adopted from the field of mAb therapeutics in cancer and utilised radioactive chromium 51 (Cr^{51})release as a functional readout [503, 504]. However, newer ADCC methods were quick to replace Cr^{51} release to limit using and disposing of radioactive material. Broadly, AD function by NK cells can be classified based on the readouts of the intended cell population; it is widely accepted that readouts focussed on quantifying or measuring NK cell/effector cell activity are called as ADNKA assays and assays focused on cell death of the target cells (gp120-coated or HIV-infected cells) are called as ADCC assays. While ADNKA remains a popular choice for measuring the AD function of NK cells, it has been shown that the binding of Ab to target cells correlates poorly with ADNKA but correlates significantly with some

ADCC assays (luciferase assays and flow cytometry based ADCC). Thus, newer investigations are moving toward developing, optimising, and employing ADCC assays in favor of ADNKA assays. However, compared to ADNKA assays, there is significant controversy with respect to the materials and methodologies employed for assessing ADCC activity. To begin with, all ADCC assays require a target cell, Ab/source of Ab, and effector cells. There is disagreement among those investigating AD functions regarding each of the components of ADCC assays, including the advantages and disadvantages of the assays employed. Issues with regards to target cells has been described in depth in section 4.III, Env conformations, page 59 of the Introduction to my thesis. To summarize, gp120-coated $CD4^+$ cells expose the open conformation of gp120 [295-298, 505]. The coated target cells reveal Env epitopes also found on bystander cells in HIV-infected cultures in which uninfected $CD4^+$ cells have taken up gp120 shed from infected cells in the culture. ADCC assays performed on HIV-infected co-cultures preferentially kill uninfected bystander cells rather than infected cells [296, 342]. Additionally, gp120 binds to the CD4 receptor, occluding the CD4bs on the gp120, which may further compete with or block CD4bs Abs in plasma or mAbs having this specificity from binding this epitope [506]. Thus, the focus shifted toward utilising infected cells. To overcome problems inherent in using HIV-infected cells as target cells where both infected and uninfected bystander cells are present, most newer assays focus on identifying and distinguishing genuinely infected target cells from uninfected bystander cells by staining for p24 or modified infectious viral molecular sequences encoding green fluorescent protein (GFP), or luciferase. Utilising luciferase activity to mark HIV-infected target cells and their disappearance as a surrogate for target cell lysis as an ADCC readout allowed using HIV-infected cell cultures as ADCC target cells. In general, the viral clone used to infect potential ADCC target cells encoded luciferase linked to *nef* via a ribosome skipping molecule, T2A, which are referred to as Luc-T2A

molecular clones [507]. Such infectious molecular clones proved to be extremely useful for developing and optimising novel ADCC assays. These assays showed that the mAb A32, which recognizes an occluded epitope in the closed conformation of HIV Env that is exposed when Env is in an open conformation, supported ADCC activity [293, 508]. It was later shown that cells infected with these Luc-T2A molecular clones of HIV were defective in Nef, and thus failed to modulate cell surface CD4, leaving it free to interact with Env to open its conformation [290, 292, 293, 508-511]. In other words, these infectious molecular clones generated target cells exposing Env in an open conformation, which is not representative of the Env conformation present on genuinely HIV-infected cells. In the first research chapter of this thesis, I describe and characterise a novel ADCC target cell line that is close to 100% HIV-infected (i.e., sorted, infected CEM.NKr.CCR5 [siCEM] cells). In siCEM cells HIV Nef and Vpu are intact and participate in downregulating cell surface CD4, thereby exposing HIV Env in its closed conformation.

Early studies utilised whole peripheral blood mononuclear cells (PBMCs) from HIV negative individuals as effector cells. NK cells account for 5 to 15% of PBMC, whereas monocytes account for approximately 5 to 10% of PBMCs. Using whole PBMCs, dilutes the actual effect of NK cell-mediated cytolysis. Abs can bind to FcRs on monocytes leading to phagocytosis of targets. Early ADCC studies using PBMC as effector cells showed that monocytes were engaged due to the formation of Ag-Ab immune complexes [512, 513]. ADCC methods such as the rapid fluorometric ADCC (RFADCC, [514]) and GranToxiLux (GTL) [515, 516]) assays use PBMCs as effector cells. The RFADCC assay has been conclusively shown to mediate target cell loss via monocytes [512].

Apart from target and effector cells, the choice of the assay used to measure ADCC activity has led to controversies. ADNKA measures the Ab-mediated effects at the level of effector cells, It

quantifies NK cell activation rather than measuring cytolysis of target cells [502]. However, Ab-binding to the target cell did not correlate with ADNKA readouts [342]. Early forms of the GTL assay employed gp120-coated target cells, a topic that has been discussed extensively in the introduction to this thesis [515, 516]. Briefly, the GTL assay measures the delivery of the granzyme B from the NK cell to target cells. The assay readout is based on a fluorescent reaction that is activated once granzyme B is delivered to the target cell. Infected cells have been employed in GTL assays however a limitation of this assay is that it assesses the frequency of granzyme B positive cells among all PBMC target cells including uncoated, uninfected, and bystander cells [342]. The original principle of RFADCC was to measure target cell elimination based on the loss of cells positive for the cytoplasmic fluorescent dye, carboxyfluorescein succinimidyl ester (CFSE) from target cells. The target cells were also labelled with a fluorescent membrane dye (PKH26), which distinguished them from effector cells that were PBMCs. It was eventually shown that monocytes among the PBMC effector cells up took PKH26 through a process known as trogocytosis [512, 517]. Overall, the RFADCC and GTL assays cannot distinguish true target cells from bystander cells and thus these assays are being replaced by second generation ADCC assays. Another type of luciferase-based assay utilised HIV encoding firefly luciferase under the expression of Tat [518]. In this scenario, luciferase was expressed in productively infected cells. Loss of luciferase occurs when target cells are eliminated, and this was the principle behind the Luc-ADCC assay. Alternatively, target cells can be infected with modified viruses expressing green fluorescent protein (GFP, [511]) or WT viruses expressing p24 [519]. Thus, productively infected target cells can be detected by either GFP or p24 expression and ADCC-mediated target cell elimination is based on the decrease of the frequency of either GFP^+ or $p24^+$ cells in the presence of Abs. The second chapter of this thesis addresses ADCC assay selection by describing

the advantages of a novel ADCC assay based on the use of siCEM cells as ADCC target cells [296]. This ADCC assay measures the frequency of apoptotic siCEM cells in the presence of plasma Abs and isolated NK cells as effector cells.

002. AD functions in ECs

Results from the RV144 vaccine trial associated ADCC with protection from HIV infection. Whether ADCC activity and other AD functions participate in spontaneous control of HIV is still unclear. As previously mentioned, there is a great deal of variation in the literature with regards to terms used to identify PLWH who control their infection without ART. Not withstanding, ECs are untreated PLWH with undetectable VLs as per standard clinical assays. To study mechanisms of Ab-mediated slow progression to AIDS, Baum et al. compared ADCC functions in untreated PLWH who were either controllers or NC [520]. They showed that controllers usually displayed higher ADCC activity than NCs. Lambotte et al. were the first to evaluate AD functions in controllers (VL <400 c/ml) [521]. Compared to NCs (VL >4000 c/ml), they showed that controllers had significantly lower nAb levels but exhibited significantly higher plasma ADCC function. Interestingly, the amount of Abs binding to gp160 and gp120 were similar in both groups, suggesting that on a per-Ab basis, controllers had significantly more potent Abs. Both these studies used gp120-coated CEM cells as target cells, which meant that the assay readout was based on CD4i Abs binding to open conformation of Env. Additionally, they used Cr^{51} release assays, which are compromised in their quantitative ability and do not allow the identification of the dying cell type releasing Cr^{51}. Nonetheless, they paved the way for the field to evaluate if AD activity were associated with spontaneous HIV control. Wren et al. demonstrated that controllers (VL <9000 c/ml, with CD4 >500 cells/mm^3 for 8+ years) compared to NCs demonstrated ADNKA responses to several HIV antigens and peptides [522]. While the frequency of functional NK cells stimulated

by ADNKA in both the groups was similar, controllers demonstrated an ADNKA response to a broader range of antigens and antigen derived peptides. In this study they used markers of NK cell activation as surrogates for ADCC activity. A follow-up study investigated if controllers could mount ADNKA/ADCC function against gp120 from a variety of HIV clades (A, B, C, and E) [523]. All enrolled controllers had broad ADNKA responses against gp120 from the different HIV clades tested in the study. The RFADCC assay was also employed to assess the level of target cell cytolysis. Plasma from controllers supported a significantly higher RFADCC readout than plasma from NCs. As this study used gp120-coated target cells, the Abs supporting RFADCC were specific for the open Env conformation, and the activity measured was monocyte-mediated trogocytosis rather than NK cell mediated ADCC. A further follow-up study showed similar results in that compared to non-controllers, controllers (VL < 400 c/ml) had significantly higher gp120-specific ADNKA and ADCC activity measured by the GTL assay irrespective of whether, or not, they carried protective *HLA* alleles [524]. However, the RFADCC activity was similar in both study groups, which was the first study to subtly hint that the choice of the AD assay had a significant impact on the conclusions. At this stage it can also be appreciated that the handful of studies described thus far used disparate definitions for controllers. A study investigating AD cellular viral inhibition (ADCVI) and ADNKA in ECs (VL < 50c/ml), UTPs, and TPs showed that plasma from ECs supported significantly higher levels of ADCVI and ADNKA functions compared to the other study groups [525].

In one of the most comprehensive and insightful investigations conducted thus far, Ackerman et al. compared 1) five AD functions (ADCP, AD neutrophil phagocytosis [ADNP], ADCD, ADCC, and ADNKA), and 2) quantified gp120-specific IgG subclasses in ECs, UTPs, TPs, and VCs (ART-naïve, VL < 2000 c/ml) [526]. They found few significant differences among the study

groups. However, ECs differed from the other groups in terms of their strongly correlated polyfunctional AD responses. Potential limitations of this study included the use of gp120-coated CEM cells as target cells and gp120-coated beads to measure anti-gp120-specific IgG subclass Ab titers. Ackerman et al. tested the plasma from ECs, UTPs, and TPs in different ADCC assays (GTL, RFADCC, and Luc.ADCC). No single assay distinguished ECs from the other study groups [527].

In addition to the AD functional responses, ECs compared to TPs, had higher frequencies of gp140-specific B cells and Ab-secreting B cells [528]. A higher frequency of memory B cells were also observed in ECs versus TPs. B cell response levels were significantly correlated with the frequency of nAb responses tested against different HIV strains. There were no significant differences amongst ECs carrying, versus not, the protective *HLA-B*57* allele [529].

IV. Unique cases of HIV control and cure

As seen above, rare PLWH demonstrate superior immune responses and ability to control HIV below detectable levels. ART also controls viremia below detectable levels, though its interruption generally leads to viral rebound. Nonetheless, there are a few instances where ART treated individuals have demonstrated natural control of viremia after ATI. These individuals are known as post-treatment controllers (PTCs). Investigators of the French VISCONTI cohort studied 14 PTCs after ATI [530]. These PTCs maintained undetectable VLs (<400 c/ml) for at least 4 years, and in some individuals more than 7 years. Early initiation of ART (<10 weeks after primary infection) was suggested as a possible reason responsible for viral control, which may in turn limit viral diversity. The CHAMP study conducted in the USA and Canada identified a second group of PTCs [531]. They found that 13% of individuals starting ART soon after infection went on to become PTCs (VLs <400 c/ml) as compared to 4% of individuals starting ART during the chronic phase of infection. The frequency of individuals achieving post-treatment control is extremely low

and thus, ATI is unwise. The Mississippi child was another instance of control after treatment was stopped, albeit for a short period of time, as 30 months later, the virus rebounded [532, 533].

A handful of cases have been reported as examples of HIV "cures". It is well known that post-infection, some infected cells enter a stage of quiescence where they harbor the intact, replication-competent proviral DNA but do not generate virions. These cells are known as latent reservoirs. Resting cells containing intact proviruses can restart viral transcription and virion production when cell latency is reversed. To achieve a sterilizing cure, the intended curative agent should eliminate all infected cells including reservoir cells. Reservoirs, their detection, and mechanisms to target them will be discussed below. The first case of a successful HIV cure was the late Mr. Timothy Ray Brown, who received a stem-cell transplant from an individual who was homozygous for the *CCR5Δ32* allele [534, 535]. A second individual, Mr. Adam Castillejo underwent a similar procedure and is also supposedly free of HIV 30 months post-ATI [536]. In 2022, a third case of an unnamed individual "cured" of HIV was presented at the Conference on Retroviruses and Opportunistic Infection, in Denver, CO, USA [537]. The female patient received cord blood and a stem-cell transplant from an individual homozygous for the *CCRΔ32/Δ32* mutation and no virus was detected 14 months post-ATI. Virus was detected in neither cells nor tissues and viral rebound was not observed in any of these individuals. These cases offer a proof of concept that a cure for HIV in possible. But given the rarity of finding a stem-cell match and the risk associated with stem cell transplantation, it is not the feasible that such an approach can be deployed widely to cure HIV.

V. Reservoirs

An HIV reservoir is defined as a resting cell that harbors replication-competent, intact proviral DNA integrated in the host genome. The reservoir in its latent and quiescent state does not produce

any virus [538]. Animal models have shown the reservoir is seeded as early as 3 days post-infection [79]. Studies longitudinally following ECs show persistent, low-level HIV replication [539-542]. This is also the case in TPs [543-546]. This could be due to division of infected cell(s) that allow for the reservoir to expand without infecting new cells. This can occur in cells in the blood or other tissues such as brain, kidney, lymph nodes, and the gut amongst others [547]. Reservoir cells do not express HIV gene products making them invisible to the immune system. Therefore, detection and eradication of HIV reservoir is challenging. Further, obtaining tissue specimens and biopsies is laborious and not always feasible. Thus, most of HIV reservoir research is performed on blood samples from PLWH.

a. Detection of HIV reservoir

$CD4^+$ cells remain the largest and most often, the sole HIV reservoir. Recently, urethral macrophages were shown to harbor replication-competent proviral genomes, thus representing a new source of HIV reservoir cells [548]. Other myeloid cells such as circulating monocytes and tissue-resident macrophages also express HIV receptor CD4 and coreceptor CCR5, which suggests that they can be infected and be an HIV reservoir [549]. Anatomical sites further complicate detecting reservoir cells containing replication-competent HIV. There are several techniques that detect and quantify viral reservoir cells. The earliest method to evaluate the size of the HIV reservoir was by culturing CD4 cells under limiting dilution conditions with HIV susceptible cells and CD4 T cell activating signals and measuring the p24 levels in each well [550, 551]. But not all reservoir cells are inducible. Thus, quantitative viral outgrowth assays (QVOA) underestimate the HIV reservoir size. The most widely used technique is based on measuring the viral DNA in various forms in the cell using polymerase chain reaction (PCR) methods to measure integrated HIV DNA, 2-LTR circles, and total HIV DNA [552]. Compared to QVOA, PCR-based techniques

require fewer host cells, no external stimulation of the reservoir, and measure the proviral DNA content. It is estimated that approximately 98% of proviruses detected by regular PCR techniques are in fact defective, which confounds the detection of a full-length, intact provirus [553, 554]. Thus, PCR techniques overestimate the HIV reservoir size. RNA-based detection methods lie somewhere between the size of the reservoir obtained by QVOA and quantification of viral DNA by PCR assays. The most commonly used RNA technique is the Tat/Rev Induced Limiting Dilution Assay (TILDA) which detects *tat/rev* HIV RNA. This technique can be used with or without exogenous stimulation [555]. Compared to PCR, TILDA detects a semi-functional reservoir, i.e., latently infected cells that may have the ability to produce infectious virions. Similar to viral DNA-PCR methodology, TILDA requires $<10^6$ CD4 cells as starting material and can be used to detect viral nucleic acid content in individuals with undetectable VLs (TPs and ECs). However, results generated in TILDA assays correlate poorly with other reservoir quantification methods [555]. Additionally, not all *tat/rev* mRNA producing cells harbor replication-competent, intact viral genomes. Therefore, TILDA most likely overestimates the size of the HIV reservoir. Due to their sensitivity and specificity, flow cytometry-based techniques have garnered interest in the past 5 years. A unique technique developed by Baxter et al. detected viral *Gag* mRNA and Gag protein by flow cytometry [556]. The flow cytometry-fluorescent *in situ* hybridisation (FISH) methodology (Flow-FISH) detects translation-competent reservoirs at the single-cell level by using distinct fluorescent probes recognising the *Gag* mRNA and Gag protein, respectively. Staining for p24 at two distinct regions greatly reduces background detected by Ab against each epitope individually and thus improves the sensitivity of detecting a true $p24^+$ cells [557]. This HIV-Flow methodology can detect p24 in TPs as well, however the reservoir cells positive for p24 using Abs of two distinct specificities may not all harbor a replication-competent, intact viral

genome. Similar to the Flow-FISH assay, the HIV-Flow assay can be complemented with additional cell surface markers to differentiate between various CD4 cell subsets such as naïve and memory subsets. Results using the HIV-Flow assay strongly correlated with DNA-PCR, TILDA, and QVOA assays; HIV-Flow is thought to get closer to quantifying the replication competent HIV reservoir than nucleic acid-based and protein-quantification based methods [557]. The Flow-FISH and HIV-Flow assays are similar in many regards; both methodologies offer sensitivity and specificity on a single-cell level and they can be combined with other cell surface markers to identify the CD4 subsets harboring proviruses [558]. However, they both require external stimulation to reactivate the reservoir, which lead to the death of infected cells. Additionally, they both rely on measuring p24, which may be detectable in cells that do not harbor intact replication competent viral genomes. Both techniques correlate strongly with other methodologies discussed thus far and with each other, which shows that the flow cytometry-based quantification protocols can be used as surrogates for reservoir quantification. A recently characterised nucleic acid-based detection methodology, termed the intact proviral DNA assay (IPDA) utilises two distinct probes against the 3' and 5' terminal ends of the integrated viral genome [553]. Droplet digital PCR (ddPCR) can then be used to determine the size of the intact proviral DNA reservoir, with an accuracy of 97% compared to full-length sequencing, on a single-cell level even in individuals with undetectable VLs. However, this method requires a fairly large number of cells (>$5x10^6$ CD4 cells). Recent studies employing the revolutionary IPDA have shown that due to HIV diversity, probe-target sequence mismatch can falsely attribute the identified reservoir as defective, i.e. cells harboring replication-incompetent viral DNA [559, 560].

b. Eradication of HIV reservoir

The HIV reservoir is stable, with a half-life of approximately 44 months for individuals on long-term ART [561]. ART can control viral spread by targeting productively infected cells and virions but offers nothing to eliminate HIV reservoir cells, stressing the need for detecting and eradicating these *in vivo* latently infected cells. However, latently HIV-infected reservoir cells do not express HIV gene products making them undetectable by the immune system and ART. There are two strategies being employed for HIV cure: "shock-and-kill", which reverses latency and induces anti-HIV immune response able to target HIV-infected cells and "block-and-lock", which aims to induce irreversible latency. Exogenous stimulants such as phorbol myristate acetate (PMA)/ionomycin are known as latency reversing agents (LRAs) can reverse the latency *in vitro*. Some of the well characterised LRAs are histone deacetylase inhibitors (HDACIs) and protein kinase C (PKC) stimulants such as PMA. Vorinostat, a potent HDACI, was the first LRA to be employed in clinical trials to reverse viral latency [562]. While it successfully restimulated HIV transcription, it failed to decrease plasma VL or total HIV DNA [563, 564]. The latency reversal effect of vorinostat was not consistent in infected individuals. Romidepsin, another HDACI showed a transient increase in viremia *in vivo* without disrupting the T cell immune response [565]. Disulfiram targets the Akt signalling pathway and reactivates the reservoir cells via the NK-κB pathway [566]. Clinical trials demonstrated the failure of disulfiram at different doses to reactivate the HIV reservoir [567, 568]. A combined disulfiram and romidepsin administration did not reactivate the reservoir *ex vivo* suggesting that other combinations of LRAs need to be tested [569]. Bryostatin-1, a PKC agonist, failed to increase cell associated DNA or plasma VL [570]. Maraviroc, a CCR5 agonist that reverses latency by activating the NK-κB pathway, has shown great promise in reversing latency *in vitro* either alone or in combination with bryostatin-1 [571]. Overall, *in vitro* research on LRAs has translated poorly to clinical trials. Thus far, LRAs have

shown very little promise in reversing HIV latency *in vivo*. It should be noted that different LRAs target different CD4 cell subsets suggesting that a combination of LRAs would be the way forward should these combinations have acceptable side effects [572]. The "kill" in "shock-and-kill" has been a challenging issue to solve due to the extremely low number of latent reservoir and the various anatomical compartments in which they reside. Since latent reservoirs are long lived, cell death can be induced by utilising pro-apoptotic compounds such as activating second mitochondrial-derived activator of caspases (Smac) [573]. A combination of LRA and Smac mimetics was recently shown to selectively eliminate reactivated HIV-infected cells *in vitro* [574]. Allogeneic NK cells showed promise by providing the "kill" component following latency reversal in HIV-infected humanized mice [575].

The other strategy to limit the spread of the HIV reservoir is by inducing latency in transcriptionally active, infected cells. Tat binds to TAR and initiates HIV transcription. Thus, HIV transcription can be blocked by antagonising Tat or TAR. Mousseau et al. showed that didehydro-Cortistatin A (dCA) selectively binds to the TAR-binding domain of Tat and blocks transcription [576]. To further elaborate the strength of dCA, subsequent study by the same group demonstrated that dCA induced strong latency in cells even in the presence of different LRAs (HDACI and PKC agonists) [577].

Reducing the latent reservoir holds the key to preventing viral rebound. While both strategies of targeting the latent reservoir have their own merits and demerits, a common theme is that they are in their infancy and require further work. For example, new molecules either reversing or inducing latency need to be identified and tested in clinical trials. The appropriate safe and effective dosage with specificities of intervals also need to be known because the effectiveness of these drugs would only be successful when participants undergo an ATI without experiencing a VL rebound. Even

then, targeting the deep seeded reservoirs in various anatomical sites remains a challenge. Lastly, it is important to understand and respect that PLWH undergoing ATI might be hesitant as viral rebound might lead to reseeding of the HIV reservoir and worsen their quality of life. Overall, reactivating and reducing the HIV reservoir size, or locking the reservoir into a permanent state of latency, are excellent strategies to preventing rebound, allowing PLWH to live ART-free.

Bridge paragraph to Chapter 2.

Understanding the immunological mechanisms behind spontaneous HIV control in ECs is an area of great interest. The RV144 trial identified nnAbs and ADCC as a correlate of protection. Additionally, studies in animals suggested that AD functions can play a role in viral control. However, in many cases, accurate interpretation results generated by AD function assays is compromised by methodological considerations, including the nature of the target cells and assays used to measure these functions. Therefore, we decided to first, generate a cell line that expresses Env in a closed conformation and second, to investigate if nnAbs and their functions or their biophysical characteristics have a role in viral control in ECs.

To address limitations relating to the use of gp120-coated CEM cells as target cells in AD function assays, I and my colleagues developed siCEM cells that express viral Env in a closed conformation. Using these target cells, I quantified HIV Env-specific Ab titers in the plasma of four study groups, UTPs, TPs, ECs, and VCs. Next, I tested and compared the ability of plasma Ab to support four AD functions – ADCP, ADCD, ADCC, and ADCT. Amongst the two groups of controllers (ECs + VCs), I detected the cell-associated reservoir using a PCR assay that measured the size of the integrated HIV DNA reservoir to determine whether AD functions were associated with the size of the reservoir. Using the same plasma sample set, gp120-specific IgG subclass and gp120-specific Ab glycosylation patterns were measured by the team of Dr. Galit Alter, Ragon Institute, Massachusetts General Hospital, Boston, MA (USA). I analysed whether the biophysical characteristics of these Abs participated in AD functions and whether they distinguish the different study groups. With this dataset, we investigated if AD functions and/or Ab biophysical characteristics are associated with the HIV reservoir.

Chapter 2: Quantifying Anti-HIV Envelope-Specific Antibodies in Plasma from HIV Infected Individuals

Published in Viruses 2019, 11(6), 487; https://doi.org/10.3390/v11060487

Sanket Kant[1,2,3], Ningyu Zhang[1,3], Jean-Pierre Routy[1,3,4,5], Cécile Tremblay[6,7], Réjean Thomas[8], Jason Szabo[8], Pierre Côté[9], Benoit Trottier[9], Roger LeBlanc[10], Danielle Rouleau[11], Marianne Harris[12], Franck P. Dupuy[1,3,†] and Nicole F. Bernard[1,2,3,5,†,*]

[1] Research Institute of the McGill University Health Centre (RI-MUHC), Montreal, QC H3A 3J1, Canada; sanket.kant@mail.mcgill.ca (S.K.); crystal.zhang.1995@hotmail.com (N.Z.); jean-pierre.routy@mcgill.ca (J.-P.R.); dura007@hotmail.fr (F.P.D.)

[2] Division of Experimental Medicine, McGill University, Montreal QC H4A 3J1, Canada.

[3] Infectious Diseases, Immunology and Global Health Program, Research Institute of the McGill University Health Centre, Montreal, QC H4A 3J1, Canada

[4] Division of Hematology, McGill University Health Centre, Montreal, QC H4A 3J1, Canada

[5] Chronic Viral Illness Service, McGill University Health Centre, Montreal, QC H4A 3J1, Canada

[6] Centre de Recherche du Centre Hospitalier de l'Université de Montréal (CRCHUM), Montreal, QC H2X 3H8, Canada; c.tremblay@umontreal.ca

[7] Department of Microbiology Infectiology and Immunology, University of Montreal, Montreal, QC H3C 3J7, Canada

[8] Clinique médicale l'Actuel, Montréal, QC H2L 4P9, Canada; rejean.thomas@lactuel.ca (R.T.); jason.szabo@lactuel.ca (J.S.)

[9] Clinique Médicale Quartier Latin, Montréal, QC H2L 4E9, Canada; dufresne.cote@sympatico.ca (P.C.); bentrotte@gmail.com (B.T.)

[10] Clinique Médicale Opus, Montréal, QC H3A 1T1, Canada; rogerpleblanc@me.com (R.L.)

[11] Département de microbiologie, infectiologie et immunologie, Faculté de médecine, Université de Montréal, Montréal, QC H2L 4M1, Canada; danielle.rouleau@umontreal.ca (D.R.)

[12] St. Paul's Hospital, Vancouver, BC V6Z 1Y6, Canada; mharris@cfenet.ubc.ca (M.H.)

† These authors contributed equally to the work.

* Correspondence: nicole.bernard@mcgill.ca; Tel.: +1-(514)-934-1934 x-44584; Fax: +1-(514)-933-1562

1. Abstract

Quantifying HIV Envelope (Env)-specific antibodies in HIV^+ plasma is useful for interpreting antibody dependent cellular cytotoxicity assay results. HIV Env, the only viral protein expressed on the surface of infected cells, has a native trimeric closed conformation on cells infected with wild-type HIV. However, $CD4^+$ uninfected bystander cells in HIV^+ cell cultures bind gp120 shed from HIV^+ cells exposing CD4-induced epitopes normally hidden in native Env. We used flow-cytometry based assays to quantify antibodies in HIV^+ plasma specific for native trimeric Env or gp120/CD4 conjugates using CEM.NKr.CCR5 (CEM) cells infected with HIV (iCEM) or coated with recombinant gp120 (cCEM), as a surrogate for $gp120^+$ HIV^- bystander cells. Results from both assays were compared to those of a plate-based ELISA to monomeric gp120. The levels of Env-specific antibodies to cCEM and iCEM, measured by flow cytometry, and to gp120 by ELISA were positively correlated. More antibodies in HIV^+ plasma recognized the gp120 conformation exposed on cCEM than on iCEM. Comparisons of plasma from untreated progressors, treated

progressors, and elite controllers revealed that antibodies to Env epitopes were the lowest in treated progressors. Plasma from elite controllers and untreated progressors had similarly high levels of Env-specific antibodies, despite elite controllers having undetectable HIV viral loads, while untreated progressors maintained high viral loads.

Keywords: HIV; HIV envelope; antibodies; flow cytometry; ELISA; CEM.NKr.CCR5

2. Introduction

The RV144 or Thai HIV vaccine trial was the first to show a significant, though modest (31.2%), efficacy in protecting against HIV infection [1]. In this trial, broadly neutralizing antibodies (BnAbs) and cytotoxic T lymphocyte responses were not implicated in HIV protection. The presence of human immunoglobulin G (IgG) antibodies (Abs) specific for the V1/V2 loop of HIV Envelope (Env) was associated with protection, provided that human immunoglobulin A Abs with overlapping specificity were absent [2–4]. Secondary analyses of the results of the RV144 trial and the earlier VAX004 vaccine trial found an inverse correlation between Fc mediated effector functions, such as antibody dependent cellular cytotoxicity (ADCC) and risk of HIV infection [2,5]. The possibility that non-neutralizing ADCC competent Abs may be implicated in preventing HIV infection provides a rationale for quantifying non-neutralizing Abs (NnAbs) endowed with Fc mediated effector functions in HIV-infected individuals [6,7].

HIV Env glycoprotein is the HIV gene product targeted by ADCC since it is the only viral protein expressed on the surface of infected cells [8]. HIV Env exposed on HIV virions and on the surface of infected cells are highly glycosylated spikes, composed of a heterotrimer of the surface glycoprotein gp120 non-covalently associated with the transmembrane glycoprotein gp41 [9–14]. Native Env is present in a “closed” conformation on the surface of infected cells [15]. This native conformation can be recognized by BnAbs and some NnAbs to mediate Fc-dependent effector

functions such as ADCC. Env interactions with CD4 drive the transition of the closed Env conformation to a CD4 bound "open" conformation [15,16]. The HIV Env open conformation is normally absent from the surface of productively infected cells since CD4 is downregulated by HIV Nef and/or Vpu [17–19]. However, gp120/CD4 conjugates can transiently occur during viral entry, when the virion binds to $CD4^+$ cells during infection, but also on the surface of uninfected $CD4^+$ bystander cells [20]. Indeed, Env trimers are not stable. Consequently, productively infected cells shed gp120, which is taken up by the cell surface CD4 on uninfected bystander cells exposing CD4 induced epitopes normally hidden inside Env trimers [20]. These epitopes are recognized by monoclonal Abs such as A32 and C11 specific for a highly-conserved cluster A region, making uninfected bystander cells susceptible to ADCC mediated by these Abs [20,21]. BnAbs bind to epitopes other than those in the cluster A region and can mediate ADCC, but are rare in plasma from HIV-infected individuals [22–24].

The amount and specificity of anti-Env Abs to the open or closed Env conformation in plasma samples are critical parameters, which most likely impact directly on their ADCC competence. Several assays have been used to quantify ADCC activity to target cells expressing HIV Env [20]. Among these are the ADCC-GranToxiLux assay, which measures the delivery of granzyme B to target cells, an early step in the pathway leading to target cell apoptosis [25], diverse assays that measure the elimination of target cells [26,27], and the Rapid Fluorescence ADCC assay [28], which does not measure ADCC activity, but rather trogocytosis, as defined by the transfer of target cell membranes to effector cells [29]. The target cells used in these assays are either recombinant gp120 (rgp120) coated CEM.NKr.CCR5 (CEM) cells [25,30–34], HIV-infected CEM or primary $CD4^+$ T cells [20,22–24]. The rgp120 used to coat CEM cells, like gp120 shed by infected cells, has a conformation that is distinct from native trimeric Env on target cells infected with wild type

HIV. The use of rgp120 coated or HIV-infected cells as ADCC target cells using assays that do not distinguish infected from uninfected bystander cells has led to the widely held view that the only ADCC-competent Abs present in plasma from HIV^+ individuals are specific for cluster A CD4 induced Env epitopes [17,18,20,30].

Here, we developed two new flow cytometry-based methods to quantify the levels of Env-specific Abs in HIV^+ plasma. One method used rgp120 coated CEM (cCEM) cells and the other used HIV-infected CEM cells selected for being HIV^+ (iCEMs). Quantification of Env-specific Abs in HIV^+ plasma using these two methods were compared to results generated using a previously described rgp120 coated enzyme linked immunosorbent assay (ELISA) [35]. The rgp120 used to coat ELISA plates and on cCEM was present in an open conformation exposing CD4 induced epitopes. ICEMs expressed Env in a closed conformation and had downmodulated their cell surface CD4 expression. Using iCEM cells allowed us probe HIV^+ plasma for the presence of Abs to closed conformation Env exposing no CD4 induced epitopes. We quantified the levels of anti-gp120/HIV Env Abs in plasma from 78 HIV-infected individuals, including untreated progressors, individuals successfully treated with anti-retroviral therapy, and elite controllers using these three methods. We showed that Env-specific Abs in HIV^+ plasma samples preferentially recognized monomeric-linear epitopes, including CD4 induced epitopes. However, because HIV^+ plasma also bound iCEM cells, we showed that HIV^+ plasma also contains Abs to native Env epitopes. There was a positive correlation between the amount of Env-specific Abs measured in plasma samples using these three methods. By comparing subject groups, we showed that plasma from treated progressors with undetectable viral loads (VL) had lower Env-specific Ab levels than untreated progressors and elite controllers did. Untreated progressor and elite controller plasma had similar levels of Env-specific Abs despite elite controllers having undetectable VLs.

3. Materials and Methods

I. Ethics Statement

This study was approved by the Institutional Review Boards of the Comité d'Éthique de la Recherche du Centre Hospitalier de l'Université de Montréal, project identification code, 17-096, July 2018 and of the McGill University Health Centre, project identification code (2018-4505) July 2018. Informed consent was obtained from all study participants.

II. Study Subjects

For this study, we used plasma samples from 3 groups of HIV-infected individuals in the chronic phase of HIV infection. Untreated progressors (n = 18) had CD4 counts <400 cells/mL and a VL of >10,000 HIV RNA copies/mL of plasma, treated progressors (n = 24) had CD4 counts <400 cells/mL and a VL of <50 copies/mL of plasma and elite controllers (n = 37) had CD4 counts >400 cells/mL and an HIV VL of <50 copies/mL of plasma. The untreated and treated progressors were drawn from subjects enrolled in the Montreal Primary Infection Cohort. These samples were from time points collected at least 1 year post infection. Those from treated progressors were from persons receiving antiretroviral therapy that controlled HIV VL for at least 1 year. The elite controller samples were drawn from participants in the Canadian Cohort of HIV-Infected Slow Progressors [36].

III. Gp120 Capture Plate-Based ELISA

The gp120-capture plate-based ELISA has been described elsewhere [35]. Briefly, ELISA plates (Nunc MaxisSorp, Thermo Fisher Scientific, Whitby, ON, Canada) were coated with 2.5 µg/mL D7324, a sheep anti-gp120-specific capture Ab (Aalto Bio Reagents, Dublin, Ireland) in 0.037 M Na2CO3 buffer, pH 9.5 (coating buffer) overnight at 4 °C. Plates were washed 3 times with

phosphate buffered saline (PBS, Wisent Bio Products, St-Jean-Baptist, QC, Canada); 0.05% Tween 20 (Sigma-Aldrich, St. Louis, MO, USA) (PBST, wash buffer) and blocked with PBS; 0.05% Tween 20; 1% bovine serum albumin (Sigma-Aldrich) (blocking buffer) for 30 min at 37 °C in a humidified, 5% CO_2 incubator. One hundred μL of HIV-1 rgp120 (from the NIH Reagent Bank, HIV-1 BaL gp120 recombinant protein from DAIDS, NIAID) at 100 ng/mL in PBST was added to each well of a 96-well plate for 3 h at room temperature (RT). The following additions were made to the ELISA plates, washing 3 times with wash buffer between steps. 100 μL/well of diluted plasma, positive and negative controls were added to each well in duplicate for 1 h at 37 °C in a humidified 5% CO_2 incubator. Plasma from each study subject was serially two-fold diluted in blocking buffer starting at a dilution of 1:100. The positive control was anti-HIV Immunoglobulin (HIVIG, a pool of polyclonal IgG isolated from HIV-infected donors from the NIH Reagent Bank, NABI and NHLBI). HIVIG was serially three-fold diluted starting at 150 μg/mL. Wells with no rgp120 served as a negative control. Binding of anti-gp120 specific Abs to rgp120 was detected by adding 100 μL per well of horseradish peroxidase conjugated-goat anti-human IgG Fc secondary Ab diluted 1:7500 in blocking buffer (Invitrogen, Frederick, MD, USA) for 30 min at RT. Binding of the secondary Ab was detected by adding 100 μL/well of 3,3',5,5'-tetramethylbenzidine (TMB) substrate (Thermo Fisher Scientific) until the desired color development was achieved. The reaction was stopped by adding 100 μL of 1M phosphoric acid (H_3PO_4, Thermo Fisher Scientific). Plates were read at an optical density of 450 nm on an ELISA microplate reader (Infinite 2000 PRO, Tecan Group Ltd., Männedorf, Switzerland). The concentrations of the anti-gp120 specific Abs in each plasma sample were obtained by interpolating from the HIVIG standard curve using GraphPad Prism version 7.00 (GraphPad

Software, La Jolla, CA, USA). Only values that fell within the linear range of the standard curve were used to calculate anti-gp120 specific IgG plasma concentrations in µg/mL relative to HIVIG.

IV. Flow Cytometry-Based Env-Specific Ab Quantification Assay Using rgp120 Coated CEM (cCEM) Cells

In this assay, cCEM cells were used as target cells. They were prepared by incubating 1×10^6 CEM cells with 0.6 µg of the same rgp120 as the one used to coat ELISA plates in Section 2.3, in 100 µL of RPMI 1640; 10% fetal bovine serum (FBS); 2 mM L-glutamine; 100 IU/mL penicillin; 100 mg/mL streptomycin (R10) (all from Wisent) at 37 °C in a 5% CO_2 humidified incubator for 75 min. Cells were washed twice and resuspended to 4×10^6 CEM cells per ml in PBS: 4% FBS. Uncoated CEM cells served as an internal negative control. They were distinguished from target cells by staining with carboxyfluorescein succinimidyl ester (CFSE, Life Technologies, Burlington, ON, Canada). Briefly, CEM cells, at 2×10^6 cells/mL of PBS, were mixed with 1 mL of 0.32 µM CFSE and incubated for 8 to 10 min at RT. The reaction was stopped by adding 1 mL of FBS at RT for 8 to 10 min. The cells were washed and resuspended at 4×10^6 cells/mL in PBS; 4% FBS. CCEM and CFSE+ CEM cells were mixed at a ratio of 1:1 and 25 µL containing 5×10^4 rgp120-coated CEM cells and 5×10^4 CEM cells were plated into each well of a V-bottomed 96-well plate in duplicate (Sarstedt Inc., Montreal, QC, Canada). Serial 3-fold dilutions of HIVIG, starting at a concentration 150 µg/mL, was used to generate a standard curve. Twenty-five µL of diluted plasma or HIVIG were added to wells containing cCEM and CEM cells and incubated for 20 min at RT in the dark. Cells were washed twice with 100 µL of PBS: 4% FBS. Bound Abs were detected by adding 50 µL of a 1:50 dilution of an APC-conjugated anti-human IgG Fc (huIgGFc, BioLegend, Burlington, ON, Canada) to each well for 20 min at 4 °C in the dark. Plates were washed twice with PBS; 4% FBS and fixed with 2% paraformaldehyde (Santa Cruz

Biotechnology, Dallas, TX, USA). At least 30,000 cells were acquired from each well of the 96-well plates using an LSR Fortessa X20 instrument (BD Biosciences, Mississauga, ON, Canada) and a high-throughput system. The results were analyzed using FlowJo software version 10 (Tree Star, Inc. Ashland, OR, USA). Negative controls included binding to $CFSE^+$ CEM cells present in the same well as the unlabelled cCEM cells and a no Ab control included in the same plate.

V. Preparation of HIV-Infected CEM (iCEM) Cells

ICEM cells were generated by infecting CEM cells with the replication competent NL4-3-Bal-IRES-HSA construct and sorting for cells expressing heat stable antigen (HSA) also known as murine CD24. The NL4-3-Bal-IRES-HSA viral construct was a kind gift from Dr. Michel Tremblay (Laval University, Quebec, QC, Canada) [37]. CEM cells were HIV-infected by adding supernatant from NL4-3-Bal-IRES-HSA transfected 293T cells to 10^6 CEM cells followed by spinoculation at 2000× g for 90 min. Cells were then incubated for 30 min at 37 °C in a humidified 5% CO_2 incubator before washing twice with R10. Cell surface expression of HSA was used to identify HIV-infected cells. On average 52% were HSA^+ (range 45 to 73%) four days post infection. To isolate the iCEM from uninfected CEM cells, we stained them with PECy7-conjugated rat anti-mouse CD24 specific monoclonal Ab (Clone M1/69, BD Biosciences) and sorted for cells expressing HSA using a FACSAria instrument (BD Biosciences). To confirm that cells were HIV-infected, sorted, expanded iCEM cells were stained for cell surface CD4 with BV421-conjugated anti-human CD4 mAb (Clone OKT4, BioLegend), cell surface HSA expression with PECy7-conjugated anti-mouse CD24 and intracellularly for HIV p24 using FITC-conjugated anti-p24 (Clone KC57, Beckman Coulter, Mississauga, ON, Canada). To confirm cell surface HIV Env expression, we stained sorted iCEM cells with the BnAb 2G12 monoclonal Ab (from the NIH AIDS Reagent Program, Division of AIDS, NIAID, NIH: Anti-HIV-1 gp120

monoclonal Ab 2G12 from Dr. Hermann Katinger [38–42]) and the NnAb A32 monoclonal Ab (from the NIH AIDS Reagent Program, Division of AIDS, NIAID, NIH: HIV-1 gp120 monoclonal Ab A32 from Dr. James E. Robinson [43,44]) for 20 min at RT. 2G12 binds both closed and open conformation Env at a CD4 independent outer domain epitope [39]. A32 is specific for a CD4 induced epitope on open conformation Env. Cells were washed with 100 µL of PBS; 4% FBS and stained with APC-conjugated anti-huIgGFc, (BioLegend). Stained cells were fixed in 2% paraformaldehyde (Santa Cruz). At least 30,000 cells were acquired using an LSR Fortessa X20 flow cytometer instrument. CEM cells were also stained and acquired in parallel to quantify non-specific background binding.

VI. Flow Cytometry-Based Env-Specific Ab Quantification Assay Using iCEM

In this assay, iCEM were used as target cells. Non-specific binding to CEM cells was measured simultaneously in the same wells. CEM cells were distinguished from iCEM cells by staining them with CFSE as described above. iCEM and $CFSE^{+}$ CEM cells were mixed at a ratio of 1:1 and plated by adding 25 µL of cells to each well of V-bottomed 96-well plates in duplicate (Sarstedt Inc.). Plasma samples were serially 3-fold diluted starting at dilutions of either 1:10 for treated progressors or 1:100 for untreated progressors and elite controllers in cold PBS; 4% FBS. Serial 3-fold dilutions of HIVIG, starting at a concentration 150 µg/mL, was used to generate a standard curve. Twenty-five µL of plasma or HIVIG dilutions were added to the cells for 20 min at RT in the dark. Each plate had an internal no Ab negative control. After the Ab incubation step, plates were washed twice with 100 µL/well of PBS; 4% FBS. Ab binding was detected by adding 50 µL of 1:50 dilution of APC-conjugated anti-huIgGFc (BioLegend) to each well for 20 min at 4 °C in the dark. Plates were then washed twice with PBS; 4% FBS and fixed with 2% paraformaldehyde (Santa Cruz). At least 30,000 cells were acquired from each well of the 96-well plates using an

LSR Fortessa X20 instrument and a high throughput system. The results were analyzed using FlowJo software version 10 (Tree Star, Inc.). Negative controls included binding to $CFSE^+$ CEM cells in the same well and a no Ab control in the same plate.

VII. Data Analysis

Abs from study subjects binding to rgp120 on ELISA plates and to cCEM as well as to Env on iCEM cells were quantified by interpolating from the HIVIG standard curve present in the same 96-well plates as the test samples. Values that lay within the linear range of the standard curve were selected to calculate Ab concentrations. When values for 2 or more sample dilutions were within the standard curve's linear range, the mean of these results was used to assign the anti-Env Ab concentration for that sample. In the rgp120 plate-based ELISA assay, values generated by Ab binding were background subtracted by the values generated when no Ab was present. For the flow cytometry-based assays, each 96-well plate included a no Ab negative control that evaluated binding generated by the anti-huIgGFc secondary Ab. Values generated in these wells were subtracted from those of the test wells. $CFSE^+$ CEM served as a within-well internal negative control measuring non-HIV Env-specific binding. Binding levels to CEM were subtracted from results generated by the same Ab dilution used to assess binding to cCEM and iCEM cells. HIVIG is a 50 mg/mL protein solution of purified Ab. The same HIVIG preparations was used for all assays permitting comparison between assays. However, the amount of anti-gp120 specific Abs in the polyclonal HIVIG solution is unknown. For this reason, the quantity of the Abs measured for all subjects were reported as arbitrary units (AU) per mL of plasma.

The average intra-assay coefficient of variation and (95% confidence intervals) for the HIV^+ plasma samples tested in duplicate in the plate-based ELISA was 4.03% (3.77, 4.92). The average inter-assay coefficient of variation for HIVIG standard curves run 8 times in the plate-based ELISA

was 15.18% (12.81, 17.55). The average intra-assay coefficient of variation for HIV^+ plasma sample duplicates was 2.87% (0.77, 4.97) for flow cytometry quantification experiments using cCEM and 4.57% (3.07, 6.07) for those using iCEM cells. The average intra-assay coefficient of variation for 5 HIVIG standard curves using cCEM as target cells was 7.96% (5.86, 10.06) and for the 8 HIVIG standard curves using iCEM at target cells was 7.74% (5.74, 9.74). Plasma from 7 individuals were tested on two occasion. The average inter-assay coefficient of variation for experiments using cCEM and iCEM target cells was 15.9% (13.8, 18) and 11.5% (9.4, 13.6) respectively.

VIII. Statistical Analysis

GraphPad Prism version 7.00 or 8.00 for Windows, (GraphPad Software, Inc., La Jolla, CA, USA) was used for statistical analyses and graphical presentation. The significance of between-group differences in monoclonal Ab binding to CEM, cCEM and iCEM as well as for AU results for untreated progressors, treated progressors, and elite controllers was assessed using Kruskal-Wallis tests with Dunn's post tests. The significance of within-individual differences in AUs generated using the three methods were assessed using Friedman tests with Dunn's post tests. The significance of the correlation between results obtained using the plate-based ELISA assay, and the two flow cytometry based binding assays was assessed using Spearman's correlation tests.

4. Results

I. Characterization of iCEM Cells

Plate-based ELISA methods that quantify gp120 specific Abs in plasma from HIV-infected persons detect Abs to linear gp120 epitopes including CD4 induced epitopes that are normally hidden in native trimeric Env expressed on the surface of cells infected with wild type HIV. HIV-

infected cell cultures include not only infected cells but also uninfected $CD4^+$ bystander cells [20]. The CD4 on bystander cells interacts with gp120 shed from infected cells and/or HIV virions originating from the infecting inoculum [20,45]. Consequently, anti-gp120 Abs in HIV^+ plasma preferentially bind CD4 induced epitopes on uninfected bystander cells. This situation precludes identifying the contribution of Abs to native closed Env on HIV-infected cells versus Abs to open Env on bystander cells in plasma from HIV^+ subjects. Therefore, to measure the binding of Env-specific Abs in plasma from HIV^+ individuals to a closed conformation of trimeric Env expressed on HIV-infected cells, we generated iCEM cells expressing native trimeric Env.

Figure 1 shows the results of staining live singlet CEM, cCEM and iCEM with monoclonal Abs to CD4, HSA, intracellular p24, 2G12 and A32. Figure 1a shows the strategy for gating on live singlet cells. Figure 1b–f show examples of staining CEM, cCEM, and iCEM cells with these five monoclonal Abs. Figure 1g–j show the results generated for staining six replicates of CEM, cCEM and iCEM cells with these monoclonal Abs. CD4 was expressed on a mean ± standard deviation of 99.5 ± 0.24%, 97.9 ± 0.41% and 0.47 ± 0.01% of CEM, cCEM, and iCEM cells, respectively. HSA was detected on 0.32 ± 0.3%, 0.54 ± 0.21% and 99.6 ± 0.2% of CEM, cCEM, and iCEM cells. Intracellular p24 was present in 0.52 ± 0.16, 0.53 ± 0.17% and 95.66 ± 0.6% of CEM, cCEM, and iCEM. Thus, CD4 was downmodulated on iCEM, likely due to the actions of HIV Nef and Vpu making CD4 unavailable to interact with Env on these cells. HIV infection of iCEM cells was confirmed by the expression of the HSA selection marker encoded by the HIV viral isolate they were infected with and the presence of intracellular p24.

Monoclonal Abs 2G12 and A32 bound CEM cells at background levels. 2G12 and A32 bound 0.91 ± 0.8% and 0.27 ± 0.3%, of CEM cells with a mean fluorescence intensity of 272 ± 5 and 119 ± 1.6, respectively. 2G12 bound 96.07 ± 0.34% and 80.42 ± 0.86% of cCEM and iCEM cells with

a lower mean fluorescence intensity for cCEM than for iCEM recognition (2105 ± 92 versus 7049 ± 141 for cCEM and iCEM cells) though these differences did not achieve statistical significance (Kruskall-Wallis test with Dunn's post test. A32 bound a higher frequency of cCEM than iCEM cells (97.85 ± 0.77% versus 2.3 ± 0.3% $p < 0.001$, Dunn's post test). The mean fluorescence intensity of A32 binding to cCEM cells was also higher than that to iCEM cells (3209 ± 257 versus 89.2 ± 21, $p < 0.001$, Dunn's post test). The mean fluorescence intensity of A32 binding to iCEM was as low as that to CEM cells ($p > 0.05$, Dunn's post test). In summary, 2G12 detected a non-conformation dependent HIV Env epitope present on both cCEM and iCEM cells. Monoclonal Ab A32 detected a CD4 induced epitope only on cCEM cells. The low level of A32 binding to iCEM is consistent with CD4 induced epitopes not being exposed on Env expressed on iCEM cells, supporting the conclusion that Env is in a closed conformation on these cells.

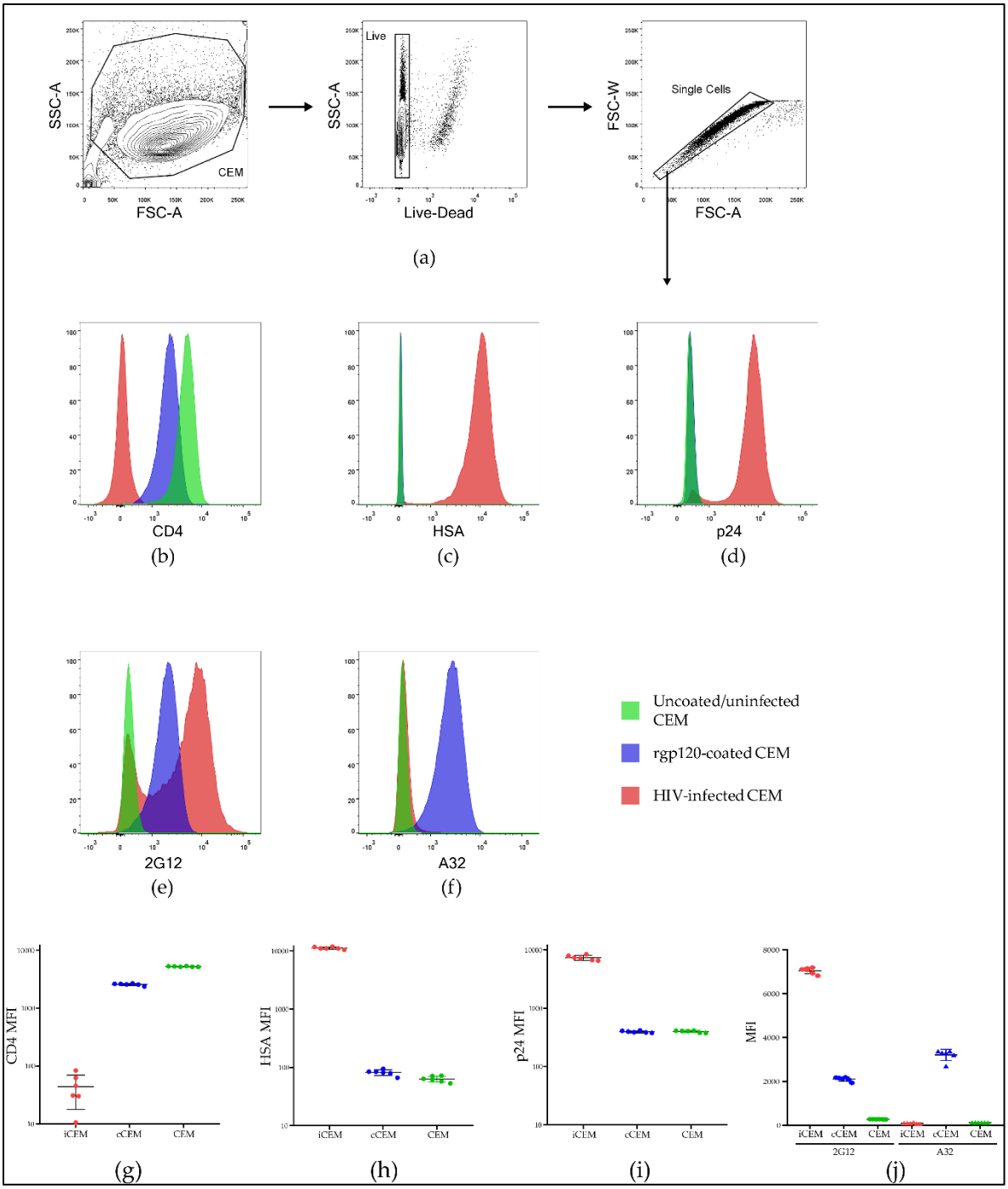

2598

2599 *Figure 12 (Figure 1 in article): Characterization of HIV-infected CEM (iCEM) cells. ICEM and*

2600 *CFSE^{+} CEM cells were stained with a panel of monoclonal antibodies to cell surface CD4, HSA,*

2601 *intracellular p24, and cell surface 2G12 and A32. Live singlet cells were gated on (a). Histograms*

2602 *show expression of (b) CD4, (c) HSA, (d) intracellular p24, (e) the HIV Envelope epitope detected*

by 2G12 and (f) the CD4 induced epitope detected by A32 on CEM cells (in green) cCEM cells (in blue) and iCEM (in pink). The MFI of $CD4^+$ (g), HSA^+ (h) and $p24^+$ (i) CEM, cCEM, and iCEM cells. The mean fluorescence intensity of 2G12 and A32 staining to CEM, cCEM, and iCEM cells (j). FSC-A = forward scatter-area; SSC-A = side scatter-area; FSC-W forward scatter width; HSA = heat stable antigen, also known as murine CD24; MFI = mean fluorescence intensity.

II. Flow Cytometry-Based Env-Specific Ab Quantification Assay

In order to quantify and compare the relative amounts of HIV Env-specific Abs in plasma from HIV^+ subjects, we developed two flow cytometry-based Ab binding assays using either cCEM or iCEM as target cells. After gating on $cCEM^+$ CEM (Figure 2a) cells and $iCEM^+$ CEM (Figure 2b, left-hand panels), cCEM, and iCEM cells were distinguished from $CFSE^+$ CEM by flow cytometry (Figure 2, middle panels). Figure 2, right hand panels show from the top to the bottom rows the binding of secondary Ab to $CFSE^+$ CEM and CFSE- cCEM and binding of HIVIG to $CFSE^+$ CEM and CFSE- cCEM cells (a) and the same for binding of secondary Ab and HIVIG to $CFSE^+$ CEM and CFSE- iCEM cells (b). HIVIG bound to both cCEM and iCEM cells with a higher mean fluorescence intensity than to their internal negative controls. Secondary Ab recognized CFSE- cCEM and iCEM and $CFSE^+$ CEM with equivalent, low mean fluorescence intensities.

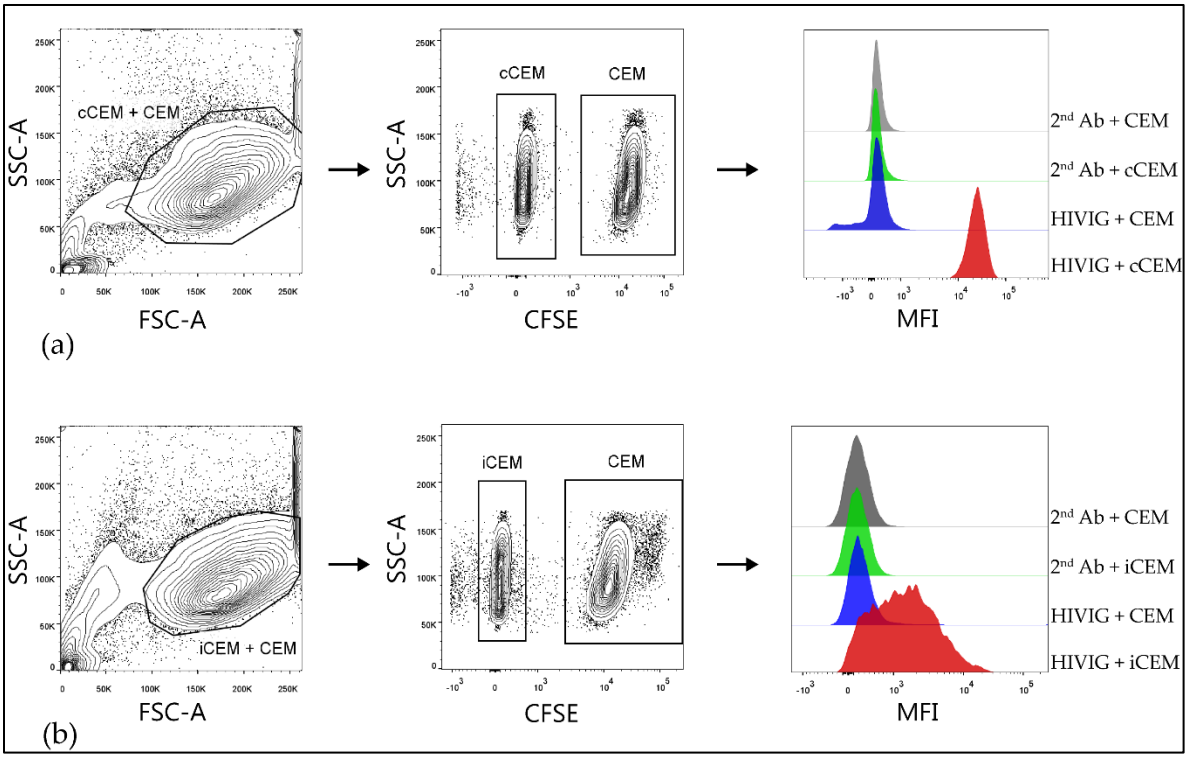

Figure 13 (Figure 2 in article): Gating strategy used to detect HIVIG binding to cCEM and iCEM cells. Both cCEM and CFSE$^+$ CEM (left panel of (a)) or iCEM and CFSE$^+$ CEM cells (left panel of (b)) were gated on. From these, cCEM and iCEM were distinguished from CFSE$^+$ CEM cells (middle panels of (a) and (b) respectively). Binding of secondary antibody specific for human IgG Fc to CEM and cCEM (1st and 2nd rows of right panel of (a)) or CEM and iCEM (1st and 2nd rows of right panels of (b)). Binding of HIVIG primary antibody at 150 µg/mL to CEM and cCEM (3rd and 4th rows of right panel of (a)) and CEM and iCEM (3rd and 4th rows of right panel of (b)) was detected by using a fluorochrome conjugated secondary Ab. FCS-A = forward scatter-area; SSC-A = side scatter-area; CFSE = carboxyfluorescein succinimidyl ester; CEM = CEM.NKr.CCR5; cCEM = recombinant gp120 coated CEM cells; iCEM = HIV-infected CEM cells; MFI = mean fluorescence intensity. 2nd Ab = anti-human immunoglobulin G Fc specific secondary antibody; Fc = the fragment crystallizable portion of immunoglobulin G.

Figure 3 shows the standard curves generated by HIVIG binding to rgp120 coated ELISA plates (a), cCEM and CFSE$^+$ CEM (b) and to iCEM and CFSE$^+$ CEM cells (c). HIVIG recognized cCEM and iCEM cells with a higher mean fluorescence intensity than CEM cells. These results show that the mean fluorescence intensity of HIVIG binding to cCEM was higher than to iCEM cells.

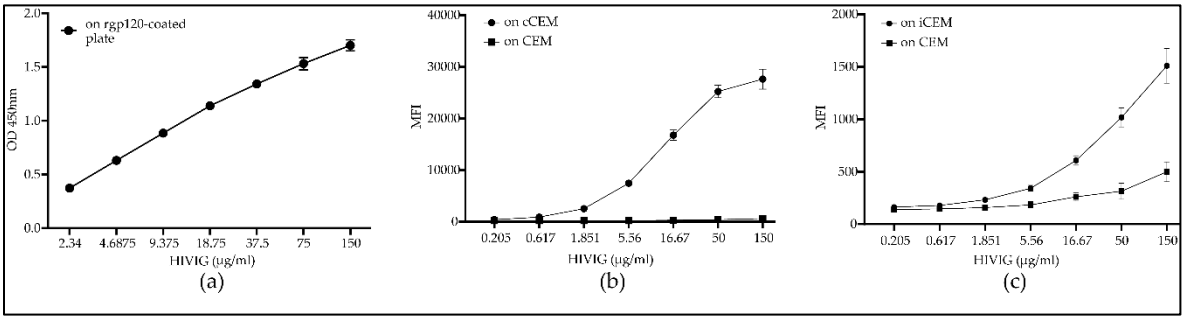

Figure 14 (Figure 3 in article): Standard curves generated by binding HIVIG to plates coated with recombinant gp120, recombinant gp120 coated CEM (cCEM) cells and to HIV-infected CEM (iCEM) cells. Binding of a 2-fold serial dilution of HIVIG to ELISA plates coated with rgp120 (a). Binding of a 3-fold serial dilution of HIVIG to cCEM (b) and iCEM (c) and their CFSE$^+$ CEM cell internal controls. The y-axis shows the optical density measured at 450 nm (OD450nm) generated by HIVIG binding to rgp120 coated plates (a). In (b) and (c), the y-axes show the mean fluorescence intensity (MFI) generated by HIVIG binding to (b) cCEM (closed circles) and CEM (closed squares) and (c) to iCEM (closed circles) and CEM (closed squares). The standard curve in (b) shows average values for 5 replicates; the curve in (c) is shows average values for 8 replicates. Each point and its error bars represent averages and standard deviations for these values. OD450nm = optical density at a wave length of 450 nanometers; MFI = mean fluorescence intensity; CEM = CEM.NKr.CCR5 cell line

III. HIV Env-Specific Ab Quantification in Plasma Samples from HIV$^+$ Subjects

We questioned whether Abs in plasma from untreated progressors, treated progressors and elite controllers differed in their ability to bind plate-bound rgp120, cCEM, and iCEM cells. Our results showed that plasma from treated progressors, as compared to those from untreated progressors and elite controllers, contained significantly lower levels of Abs to plate-bound rgp120, cCEM and iCEM cells (Figure 4a–c, Kruskal-Wallis test with Dunn's post-tests). Plasma from 1 untreated progressor, 4 treated progressors, and 1 elite controller bound iCEM at levels below the detection limit (Figure 4c). Since, we did not detect any Ab binding to iCEM cells by plasma from these subjects, they were excluded from further analyses. Plasma from untreated progressors had higher levels of Env-specific Abs than plasma from elite controllers, but this difference only achieved statistical significance for Abs recognizing cCEM cells (Kruskal-Wallis tests with Dunn's post-tests (Figure 4 a–c).

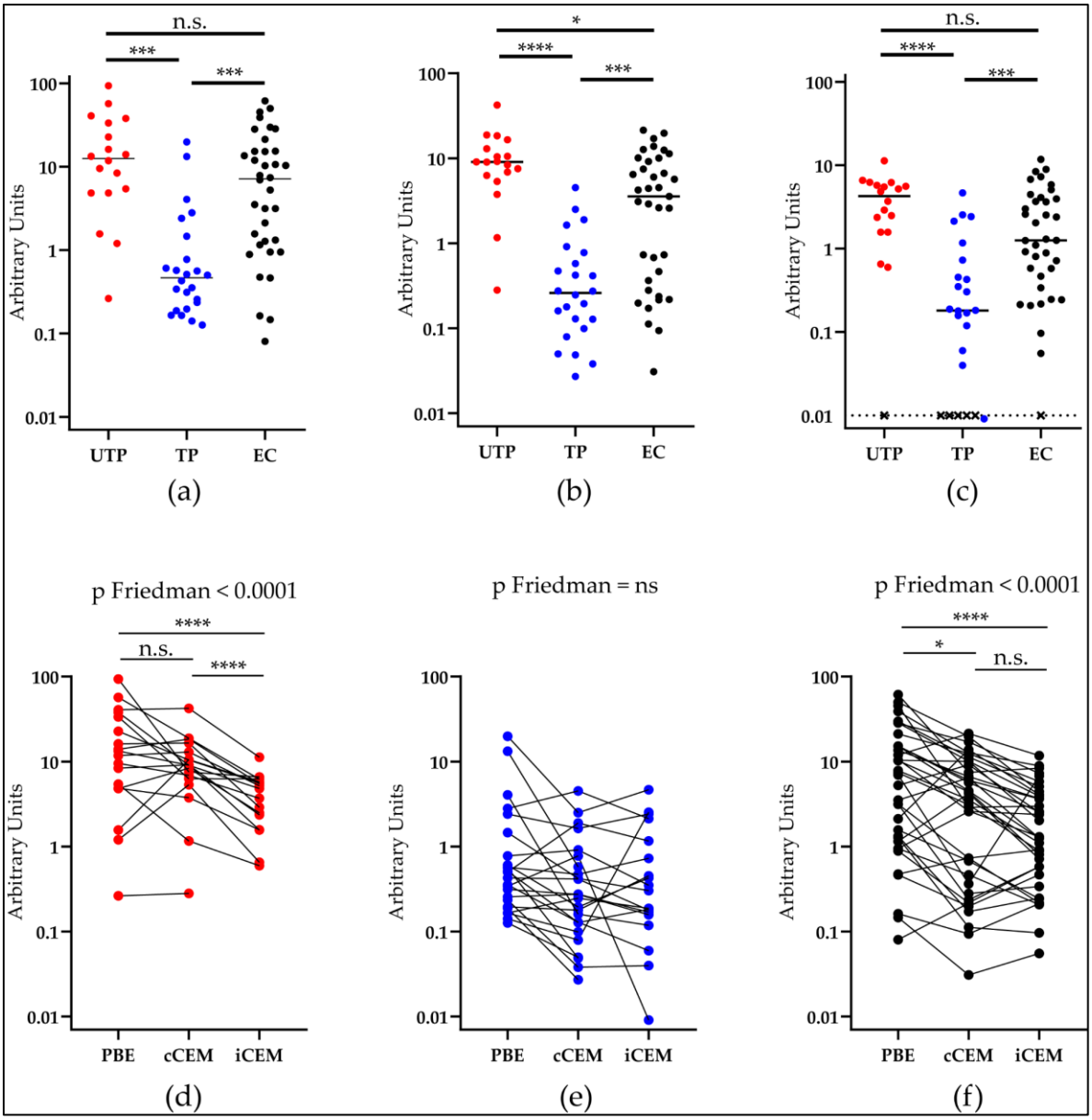

Figure 15 (Figure 4 in article): Quantification of antibodies to rgp120/HIV Envelope-using three methods. The y-axis shows the relative amount of recombinant gp120 or HIV Envelope-specific antibody measured in plasma from three HIV$^+$ subject groups using (a) a plate-based ELISA assay, or by flow cytometry-based assays using (b) cCEM and (c) iCEM cells as target cells. The subject groups being compared are indicated by lines joining two groups and the significance of between-group differences is indicated by "" symbols over the lines joining the two groups being*

compared. Anti-rgp120/HIV Envelope-specific antibody levels in 1 untreated progressor, 4 treated progressors and 1 elite controller were below the limit of quantitation when iCEM cells were used as target cells and are represented by an "×" (c). Plasma from (d) untreated progressors, (e) treated progressors, and (f) elite controllers were tested for their capacity to bind rgp120 coated wells in the plate-based ELISA assay to cCEM and to iCEM cells. PBE = plate-based ELISA; UTP = untreated progressors; TP = treated progressors; EC = elite controllers; "" = $p < 0.05$; "***" = $p < 0.0005$, "****" = $p < 0.0001$, ns = not significant.*

The binding results were re-analyzed by examining how plasma from each study subject bound Env in the three Ab quantification assays. We found that within-subject differences in the ability of plasma Abs from treated progressors to recognize rgp120 coated ELISA plates, cCEM and iCEM cells did not differ significantly (Figure 4e, $p > 0.05$, Friedman test). Plasma from untreated progressors bound the linear rgp120 on coated plates and on cCEM at levels that were not significantly different from each other, but were at higher levels than to iCEM (Figure 4d, $p < 0.0001$ for both, Dunn's post tests). Plasma from elite controllers bound rgp120 coated plates at a higher level than they bound cCEM and iCEM cells (Figure 4f, $p < 0.05$ and $p < 0.0001$, respectively, Dunn's post tests). The binding levels of plasma from elite controllers to cCEM and iCEM did not differ significantly.

The 3 methods generated results that were correlated with each other when all study subjects were considered, (Figure 5a–c, $r > 0.70$, $p < 0.0001$, Spearman correlation tests). Results generated by the three assays were significantly positively correlated for untreated progressors and elite controllers (Figure 5d). For treated progressors, the only significant positive correlation was between results generated by the rgp120 plate-based ELISA assay and binding to cCEM cells (Figure 5d).

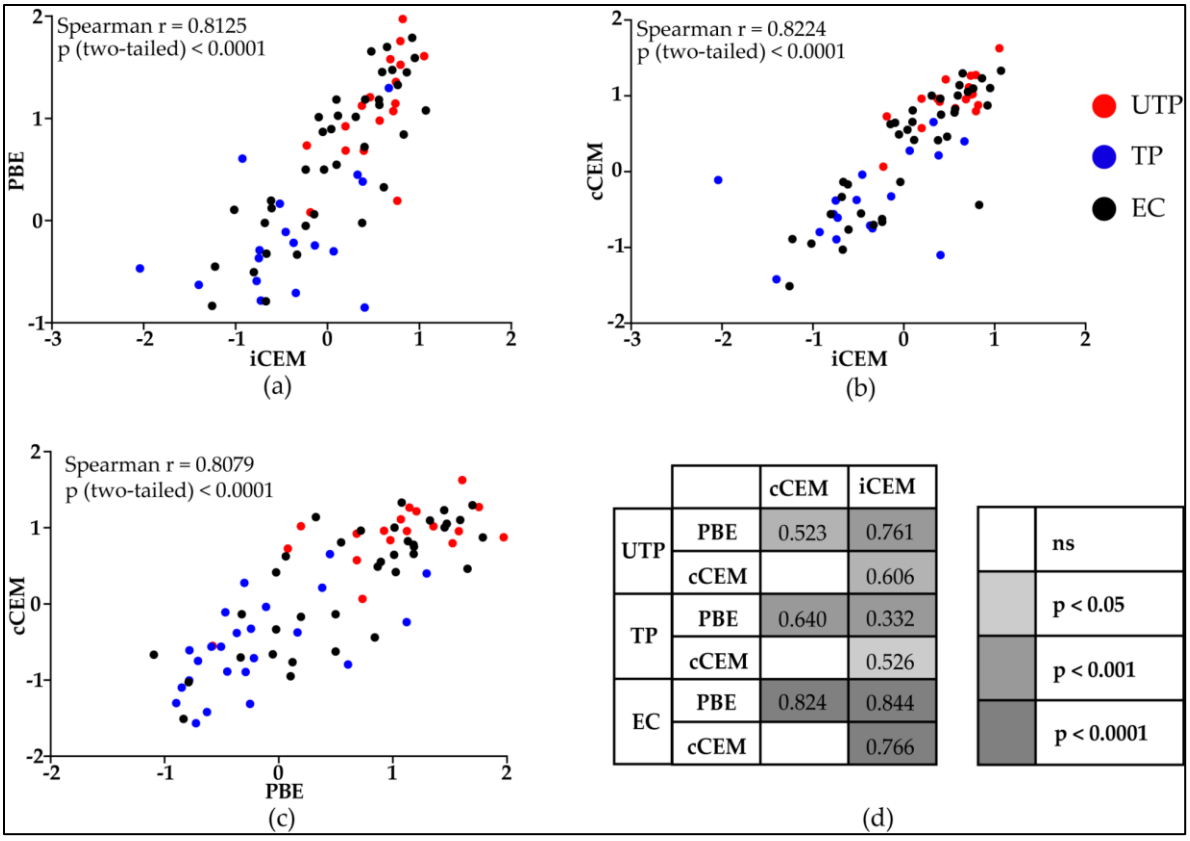

Figure 16 (Figure 5 in article): Correlations between rgp120/HIV Envelope-specific antibody levels quantified by a plate-based ELISA and two flow-cytometry based assays. Spearman correlation tests were used to evaluate the significance of the correlation between results generated by the (a) plate-based ELISA and flow cytometry-based quantification assays using iCEM as target cells, (b) the two flow cytometry-based quantification assays using iCEM and cCEM cells as target cells, and (c) the plate-based ELISA assay and the flow cytometry-based quantification assays using cCEM as target cells for all HIV-infected subjects (a–c) or for untreated progressors, treated progressors and elite controllers separately (d). Values in (d) indicate the correlation coefficient "r" for each comparison. The color scale indicates the "p" values for each correlation. PBE = plate-based ELISA; cCEM = recombinant gp120 coated CEM

cells; iCEM = HIV-infected CEM cells; UTP = untreated progressors; TP = treated progressors; EC = elite controllers.

In summary, these results indicate that Env-specific Abs in HIV^+ plasma samples preferentially targeted the CD4 induced epitope exposed on the open Env conformation, which is exposed on the linear rgp120 used to coat ELISA plates and on cCEM cells. However, there exists a subset of Env-specific Abs in HIV^+ plasma that recognize Env in its closed conformation as shown by their ability to bind iCEM cells. Untreated progressors have higher levels of anti-Env-specific Abs than do treated progressors. This suggests that antigenemia, which in HIV^+ persons is represented by detectable HIV VL, drives and maintains high levels of Env-specific Abs. High levels of Env-specific Abs without detectable VL is a distinctive characteristic of elite controllers possibly associated with the maintenance of a strong memory B cells compartment in these individuals [46,47].

5. Discussion

In this report, we describe two new flow cytometry-based assays that quantitate Abs specific for HIV Env by interpolation from an HIVIG standard curve. One method recognizes cCEM as a target cell and the other iCEM cells. Anti-HIV Env-specific Abs in plasma from HIV-infected untreated progressors, treated progressors and elite controllers were compared for their ability to recognize Env in the two flow-cytometry based assays and in a plate-based ELISA assay in which wells were coated with rgp120. Plasma from untreated progressors and elite controllers had higher levels of anti-gp120-specific Abs in all three assays compared to plasma from treated progressors. The concentration of plasma IgG in μg/mL from each study subject binding HIV Env in these three assays was significantly correlated for untreated progressors and elite controllers. For treated

progressors, only the results generated by the two assays measuring monomeric gp120 were significantly correlated.

Native Env is a trimer assembled of heterodimers made up of gp120 and gp41 glycoproteins. While gp120 forms the outer part of the trimer, gp41 is mostly buried at the trimer interface and anchors Env into the plasma membrane [9–12]. Env interactions with CD4 drive the transition from a closed Env conformation to a CD4 bound open conformation [15,16]. CD4 is downregulated from the surface of productively infected cells by Nef and Vpu [17–19]. Unliganded Env is normally present in a closed conformation on HIV-infected cells [15]. Advancements in electron microscopy and cryo-tomography have shown that highly conserved epitopes are hidden in the native Env trimer [13,48–51].

The iCEM cells, used as anti-HIV Env binding targets, were 99.6 ± 0.2% HSA^+, and 95.66 ± 0.6% intracellular $p24^+$. Less than 1% expressed CD4 at a low mean fluorescence intensity. Staining with monoclonal Ab 2G12 confirmed that 80.42 ± 0.86% expressed HIV Env at a mean fluorescence intensity of 7049 ± 141, which was 26-fold over that to CEM cells. The low frequency and intensity of staining by monoclonal Ab A32 to iCEM cells indicated that Env on these cells maintains a closed conformation. On the other hand, rgp120 used to coat ELISA plates and Env present on the surface of cCEM is monomeric, linear and recognized by the NnAb A32 specific for a CD4 induced epitope only exposed on Env in an open conformation. Plasma from HIV^+ subjects readily recognized epitopes on rgp120 coated plates and on cCEM cells. On the other hand, iCEM cells are highly enriched for the presentation of closed conformation HIV Env, the conformation which is present on wild type HIV-infected cells. They thus have a superior capacity than do HIV-infected and bystander cells present in recently HIV-infected cultures to bind Abs in HIV^+ plasma to closed conformation Env [20,45]. Using iCEM cells as target cells overcomes

problems inherent in interpreting results of anti-Env Ab binding using recently infected CD4 cells to probe HIV+ plasma for the presence of Abs specific for Env on productively infected cells. Using iCEM cells, we were able to confirm that HIV+ plasma contains Abs recognizing closed conformation HIV Env. These iCEM cells will be useful as target cells for ADCC assays. They can be used to assess whether Abs to closed conformation Env can indeed target and kill productively HIV-infected cells and not just bystander cells

Others have also described methods to detect gp120- or Env-specific Abs in HIV^+ plasma [35,52,53]. Two of these methods were used to detect Abs in HIV^+ plasma specific for monomeric linear HIV gp120 [35,52]. Veillette et al. reported detecting Env in a 3-dimensional conformation on the surface of transfected cells [53]. However, the method used provided a relative quantification since it did not use a standard curve with a known source of Env-specific Abs to interpolate results from plasma samples. Furthermore, the preparation of target cells for this assay relied on antigen availability, which was associated with transfection efficiency. In other words, not all the target cells used to probe for Env-specific Abs expressed Env. Furthermore, between-preparations differences in transfection efficiency may compromise the ability to compare results generated using different batches of transfected Env expressing cells. The use of iCEMs, which are essentially all positive for cell surface Env overcomes the limitations of these assays by only expressing Env in a closed conformation and by eliminating concerns relating to inter-batch variability due to transfection efficiency.

We observed that plasma from treated progressors had lower concentrations of Env-specific Abs in all three assays. This is probably due to antiretroviral therapy dependent reduction in HIV VL. Presence of antigen is likely needed to maintain HIV Env-specific Ab responses. HIV-specific T cell responses also decline drastically after the initiation of antiretroviral therapy [54]. When

results generated by the three assays using plasma from treated progressors were correlated, we only observed a significant correlation between responses generated by the rgp120 coated plate-based assay and the flow cytometry-based assay using cCEM cells as target cells. The positive correlation between the results of these two assays likely reflects the similar structure of the rgp120 detected by the plate-based ELISA assay and on cCEM cells and the difference of this structure from that detected on iCEM cells. By contrast, untreated progressors have an uncontrolled HIV VL, which drives persistent anti-HIV Env Ab responses. Interestingly, elite controllers, who have undetectable HIV VLs maintain robust anti-Env specific Ab responses. The reason for this is unclear. One possibility is that elite controllers maintain a strong memory B-cell response, which may also be involved in VL control [46,47]. Even though elite controllers have VLs < 50 copies/mL of plasma, there is evidence they have HIV VLs below this detection limit and low-level viral replication [55–57]. This could potentially explain the maintenance of high anti-Env-specific Ab levels in the setting of the VL suppression seen in elite controllers.

Polyclonal IgG from HIV^+ individuals, was used to generate a standard curve for all three assays used to quantify anti-Env specific Abs. By interpolating results from the three assays with the same range of HIVIG concentrations it was possible to compare results from all three assays and to confirm that plasma from HIV^+ individuals include Abs to both linear and 3-dimensional Env epitopes. The use of internal negative controls in the form of CEM cells permitted detection of Abs to these target cells that were not Env-specific. The exact amount of anti-gp120 or anti-Env specific Abs in HIVIG is not precisely known, though we have estimated that anti-gp120 specific Abs represent approximately 5% of the total IgG pool. This is the reason that quantification of results in relation to HIVIG concentrations were defined as AUs rather than concentrations of anti-gp120-specific Abs.

Generation of Abs that bind and neutralize a broad range of HIV isolates is one of the major goals of current HIV vaccine strategies. But there are significant obstacles to achieving this goal [58–62]. Results from the RV144 HIV vaccine trial, simian immunodeficiency virus infected (SIV) rhesus macaque studies, and in HIV elite controller studies have shown that there is a significant proportion of Env-specific Abs in plasma from vaccinees, rhesus macaques and elite controllers that mediate non-neutralizing functions such as ADCC [2,63–65]. These Abs have been implicated in HIV/SIV protection and control [64]. HIV elite controllers represent a unique example of a functional cure as they control HIV without antiretroviral therapy. While cellular immunity is certainly important in elite controller HIV suppression, elite controllers also generate Abs with unique signatures that perform non-neutralizing functions [65,66]. Whether the amount of Abs generated by elite controllers plays a role in HIV control is currently unknown, but warrants further investigation.

6. Conclusions

In summary, we demonstrate here that we can detect and quantify anti-gp120- and anti-HIV Env-specific Abs in untreated progressors, treated progressors and elite controllers. The amount of Ab binding to native trimeric Env is significantly lower than that binding to gp120-coated plates and cCEM. Abs specific to native trimeric Env on HIV-infected cells and open conformation Env on uninfected bystander cells support both ADCC activity. Whether the impact of the Abs to closed conformation HIV Env on HIV control is greater than that of Abs to open conformation Env merits further investigation that will rely on the availability of tools and methods such as those we have described in this report.

Author Contributions: N.F.B., F.P.D. and S.K. conceived the study; S.K., N.Z. and F.P.D. were responsible for methodology, validation, formal analysis and investigation; N.F.B., J.-P.R., C.T.,

R.T., J.S., P.C., B.T., R.L., D.R. and M.H. provided material from study subjects used in the study; Data was curated by S.K. and F.P.D.; S.K. and N.F.B. wrote the original draft; N.F.B., S.K., J.-P.R., C.T., R.T., J.S., P.C., B.T., R.L., D.R., M.H. and F.P.D. reviewed and edited the manuscript; S.K. and F.D.P. prepared the figures (visualization); N.F.B. supervised the project, provided project administration oversight and obtained funding for the project.

7. Acknowledgments

This study received support from the Canadian Institutes for Health Research [grant PJT-148491] and the Fonds de Recherche du Quebec-Santé (FRQ-S). SK, FPD, J-PR and NFB are members of the Research Institute of the McGill University Health Centre (RI-MUHC), an institution funded in part by the FRQ-S. We wish to acknowledge. Tsoarello Mabanga, Xiaoyan Ni, Cindy Xu Zhang, Alexa Del Corpo and Olfa Debbeche for sample processing and expert technical assistance. Mario Legault provided administrative support and coordination for the Montreal Primary Infection Cohort. Stéphanie Matte was responsible for coordinating the Canadian Cohort of HIV-Infected Slow Progressors. We also thank Oussama Meziane for his insightful comments on this project and for technical and analytical advice. The following physicians recruited and followed subjects providing samples for this study: Louise Charest, Sylvie Vézina, Jean-Guy Baril, Marc-André Charon, Serge Dufresne, Stéphane Lavoie, Claude Fortin, Marie Munoz, Benoit Deligne, Danièle Longpré, Bernard Lessard, Bertrand Lebouché, Norbert Gilmore, Marina Klein, Hélène Senay, Noël Grégoire, Julian Falutz, Dominique Tessier, Danielle Legault, Jonathan Angel, Colin Kovacs, Ken Logue, Brian Conway and Bill Thompson. We thank the Immunophenotyping Technology Platform of the RI-MUHC and staff for their contribution to this publication. We acknowledge the contribution of the study subjects, without whose donation of blood samples this project would not have been possible.

8. Conflicts of Interest

The authors declare no conflict of interests. The funding sponsors had no role in the design of the study; in the collection, analyses, or interpretation of data; in the writing of the manuscript, and in the decision to publish the results.

9. References

1. Rerks-Ngarm, S.; Pitisuttithum, P.; Nitayaphan, S.; Kaewkungwal, J.; Chiu, J.; Paris, R.; Premsri, N.; Namwat, C.; de, S.M.; Adams, E.; et al. Vaccination with alvac and aidsvax to prevent HIV-1 infection in thailand. N. Engl. J. Med. 2009, 361, 2209–2220.

2. Haynes, B.F.; Gilbert, P.B.; McElrath, M.J.; Zolla-Pazner, S.; Tomaras, G.D.; Alam, S.M.; Evans, D.T.; Montefiori, D.C.; Karnasuta, C.; Sutthent, R.; et al. Immune-correlates analysis of an HIV-1 vaccine efficacy trial. N. Engl. J. Med. 2012, 366, 1275–1286.

3. Liao, H.X.; Bonsignori, M.; Alam, S.M.; McLellan, J.S.; Tomaras, G.D.; Moody, M.A.; Kozink, D.M.; Hwang, K.K.; Chen, X.; Tsao, C.Y.; et al. Vaccine induction of antibodies against a structurally heterogeneous site of immune pressure within HIV-1 envelope protein variable regions 1 and 2. Immunity 2013, 38, 176–186.

4. Tomaras, G.D.; Ferrari, G.; Shen, X.; Alam, S.M.; Liao, H.X.; Pollara, J.; Bonsignori, M.; Moody, M.A.; Fong, Y.; Chen, X.; et al. Vaccine-induced plasma iga specific for the c1 region of the hiv-1 envelope blocks binding and effector function of igg. Proc. Natl. Acad. Sci. USA 2013, 110, 9019–9024.

5. Forthal, D.N.; Gilbert, P.B.; Landucci, G.; Phan, T. Recombinant gp120 vaccine-induced antibodies inhibit clinical strains of hiv-1 in the presence of fc receptor-bearing effector cells and correlate inversely with HIV infection rate. J. Immunol. 2007, 178, 6596–6603.

6. Chung, A.A.-O.; Alter, G. Systems serology: Profiling vaccine induced humoral immunity against HIV. Retrovirology, 2017, 14, 57.

7. Mayr, L.M.; Su, B.; Moog, C. Non-neutralizing antibodies directed against HIV and their functions. Front. Immunol. 2017, doi: 10.3389/fimmu.2017.01590

8. Checkley, M.A.; Luttge, B.G.; Freed, E.O. Hiv-1 envelope glycoprotein biosynthesis, trafficking, and incorporation. J. Mol. Biol. 2011, 410, 582–608.

9. Merk, A.; Subramaniam, S. Hiv-1 envelope glycoprotein structure. Curr. Opin. Struct. Biol. 2013, 23, 268–276.

10. Wyatt, R.; Kwong, P.D.; Desjardins, E.; Sweet, R.W.; Robinson, J.; Hendrickson, W.A.; Sodroski, J.G. The antigenic structure of the HIV gp120 envelope glycoprotein. Nature 1998, 393, 705–711.

11. Allan, J.S.; Coligan, J.E.; Barin, F.; McLane, M.F.; Sodroski, J.G.; Rosen, C.A.; Haseltine, W.A.; Lee, T.H.; Essex, M. Major glycoprotein antigens that induce antibodies in aids patients are encoded by HTLV-III. Science 1985, 228, 1091–1094.

12. Robey, W.G.; Safai, B.; Oroszlan, S.; Arthur, L.O.; Gonda, M.A.; Gallo, R.C.; Fischinger, P.J. Characterization of envelope and core structural gene products of HTLV-III with sera from aids patients. Science 1985, 228, 593–595.

13. Liu, J.; Bartesaghi, A.; Borgnia, M.J.; Sapiro, G.; Subramaniam, S. Molecular architecture of native HIV-1 gp120 trimers. Nature 2008, 455, 109–113.

14. Zhu, P.; Chertova, E.; Bess, J., Jr.; Lifson, J.D.; Arthur, L.O.; Liu, J.; Taylor, K.A.; Roux, K.H. Electron tomography analysis of envelope glycoprotein trimers on hiv and simian immunodeficiency virus virions. Proc. Natl. Acad. Sci. USA 2003, 100, 15812–15817.

15. Munro, J.B.; Gorman, J.; Ma, X.; Zhou, Z.; Arthos, J.; Burton, D.R.; Koff, W.C.; Courter, J.R.; Smith, A.B., 3rd; Kwong, P.D.; et al. Conformational dynamics of single HIV-1 envelope trimers on the surface of native virions. Science 2014, 346, 759–763.

16. Herschhorn, A.; Ma, X.; Gu, C.; Ventura, J.D.; Castillo-Menendez, L.; Melillo, B.; Terry, D.S.; Smith, A.B., 3rd; Blanchard, S.C.; Munro, J.B.; et al. Release of gp120 restraints leads to an entry-competent intermediate state of the HIV-1 envelope glycoproteins. MBio 2016, 7.

17. Veillette, M.; Coutu, M.; Richard, J.; Batraville, L.A.; Dagher, O.; Bernard, N.; Tremblay, C.; Kaufmann, D.E.; Roger, M.; Finzi, A. The HIV-1 gp120 CD4-bound conformation is preferentially targeted by antibody-dependent cellular cytotoxicity-mediating antibodies in sera from HIV-1-infected individuals. J. Virol. 2015, 89, 545–551.

18. Veillette, M.; Desormeaux, A.; Medjahed, H.; Gharsallah, N.E.; Coutu, M.; Baalwa, J.; Guan, Y.; Lewis, G.; Ferrari, G.; Hahn, B.H.; et al. Interaction with cellular CD4 exposes HIV-1 envelope epitopes targeted by antibody-dependent cell-mediated cytotoxicity. J. Virol. 2014, 88, 2633–2644.

19. Moore, J.P.; McKeating, J.A.; Weiss, R.A.; Sattentau, Q.J. Dissociation of gp120 from HIV-1 virions induced by soluble CD4. Science 1990, 250, 1139–1142.

20. Richard, J.; Prevost, J.; Baxter, A.E.; von Bredow, B.; Ding, S.; Medjahed, H.; Delgado, G.G.; Brassard, N.; Sturzel, C.M.; Kirchhoff, F.; et al. Uninfected bystander cells impact the measurement of HIV-specific antibody-dependent cellular cytotoxicity responses. MBio 2018, 9.

21. Guan, Y.; Pazgier, M.; Sajadi, M.M.; Kamin-Lewis, R.; Al-Darmarki, S.; Flinko, R.; Lovo, E.; Wu, X.; Robinson, J.E.; Seaman, M.S.; et al. Diverse specificity and effector function among

human antibodies to HIV-1 envelope glycoprotein epitopes exposed by CD4 binding. Proc. Natl. Acad. Sci. USA 2013, 110, E69–E78.

22. Von Bredow, B.; Arias, J.F.; Heyer, L.N.; Moldt, B.; Le, K.; Robinson, J.E.; Zolla-Pazner, S.; Burton, D.R.; Evans, D.T. Comparison of antibody-dependent cell-mediated cytotoxicity and virus neutralization by HIV-1 env-specific monoclonal antibodies. J. Virol. 2016, 90, 6127–6139.

23. Bruel, T.; Guivel-Benhassine, F.; Amraoui, S.; Malbec, M.; Richard, L.; Bourdic, K.; Donahue, D.A.; Lorin, V.; Casartelli, N.; Noel, N.; et al. Elimination of HIV-1-infected cells by broadly neutralizing antibodies. Nat. Commun. 2016, 7, 10844.

24. Bruel, T.; Guivel-Benhassine, F.; Lorin, V.; Lortat-Jacob, H.; Baleux, F.; Bourdic, K.; Noel, N.; Lambotte, O.; Mouquet, H.; Schwartz, O. Lack of adcc breadth of human nonneutralizing anti-HIV-1 antibodies. J. Virol. 2017, 91, e02440-16.

25. Pollara, J.; Hart, L.; Brewer, F.; Pickeral, J.; Packard, B.Z.; Hoxie, J.A.; Komoriya, A.; Ochsenbauer, C.; Kappes, J.C.; Roederer, M.; et al. High-throughput quantitative analysis of HIV-1 and SIV-specific adcc-mediating antibody responses. Cytom. A 2011, 79, 603–612.

26. Richard, J.; Veillette, M.; Batraville, L.A.; Coutu, M.; Chapleau, J.P.; Bonsignori, M.; Bernard, N.; Tremblay, C.; Roger, M.; Kaufmann, D.E.; et al. Flow cytometry-based assay to study HIV-1 gp120 specific antibody-dependent cellular cytotoxicity responses. J. Virol. Methods 2014, 208, 107–114.

27. Smalls-Mantey, A.; Doria-Rose, N.; Klein, R.; Patamawenu, A.; Migueles, S.A.; Ko, S.Y.; Hallahan, C.W.; Wong, H.; Liu, B.; You, L.; et al. Antibody-dependent cellular cytotoxicity against primary HIV-infected CD4+ T cells is directly associated with the magnitude of surface igg binding. J. Virol. 2012, 86, 8672–8680.

28. Gomez-Roman, V.R.; Florese, R.H.; Patterson, L.J.; Peng, B.; Venzon, D.; Aldrich, K.; Robert-Guroff, M. A simplified method for the rapid fluorometric assessment of antibody-dependent cell-mediated cytotoxicity. J. Immunol. Methods 2006, 308, 53–67.

29. Kramski, M.; Schorcht, A.; Johnston, A.P.; Lichtfuss, G.F.; Jegaskanda, S.; De, R.R.; Stratov, I.; Kelleher, A.D.; French, M.A.; Center, R.J.; et al. Role of monocytes in mediating HIV-specific antibody-dependent cellular cytotoxicity. J. Immunol. Methods 2012, 384, 51–61.

30. Ferrari, G.; Pollara, J.; Kozink, D.; Harms, T.; Drinker, M.; Freel, S.; Moody, A.M.; Alam, M.S.; Tomaras, G.D.; Ochsenbauer, C.; et al. An HIV-1 gp120 envelope human monoclonal antibody that recognizes a C1 conformational epitope mediates potent antibody-dependent cellular cytotoxicity (adcc) activity and defines a common adcc epitope in human HIV-1 serum. J. Virol. 2011, 85, 7029–7036.

31. Konstantinus, I.N.; Gamieldien, H.; Mkhize, N.N.; Kriek, J.-M.; Passmore, J.-A.S. Comparing high-throughput methods to measure nk cell-mediated antibody dependent cellular cytotoxicity during HIV-infection. J. Immunol. Methods 2016, 434, 46–52.

32. Ackerman, M.E.; Mikhailova, A.; Brown, E.P.; Dowell, K.G.; Walker, B.D.; Bailey-Kellogg, C.; Suscovich, T.J.; Alter, G. Polyfunctional HIV-specific antibody responses are associated with spontaneous HIV control. PLOS Pathog. 2016, 12, e1005315.

33. Gooneratne, S.L.; Richard, J.; Lee, W.S.; Finzi, A.; Kent, S.J.; Parsons, M.S. Slaying the trojan horse: Natural killer cells exhibit robust anti-HIV-1 antibody-dependent activation and cytolysis against allogeneic T cells. J. Virol. 2015, 89, 97–109.

34. Parsons, M.S.; Wren, L.; Isitman, G.; Navis, M.; Stratov, I.; Bernard, N.F.; Kent, S.J. Hiv infection abrogates the functional advantage of natural killer cells educated through kir3dl1/hla-

bw4 interactions to mediate anti-HIV antibody-dependent cellular cytotoxicity. J. Virol. 2012, 86, 4488–4495.

35. Banerjee, K.; Klasse, P.J.; Sanders, R.W.; Pereyra, F.; Michael, E.; Lu, M.; Walker, B.D.; Moore, J.P. Igg subclass profiles in infected HIV type 1 controllers and chronic progressors and in uninfected recipients of env vaccines. AIDS Res. Hum. Retroviruses 2010, 26, 445–458.

36. El-Far, M.; Kouassi, P.; Sylla, M.; Zhang, Y.; Fouda, A.; Fabre, T.; Goulet, J.-P.; van Grevenynghe, J.; Lee, T.; Singer, J.; et al. Proinflammatory isoforms of il-32 as novel and robust biomarkers for control failure in HIV-infected slow progressors. Sci. Rep. 2016, 6, 22902.

37. Imbeault, M.; Lodge, R.; Ouellet, M.; Tremblay, M.J. Efficient magnetic bead-based separation of HIV-1-infected cells using an improved reporter virus system reveals that p53 up-regulation occurs exclusively in the virus-expressing cell population. Virology 2009, 393, 160–167.

38. Buchacher, A.; Predl, R.; Strutzenberger, K.; Steinfellner, W.; Trkola, A.; Purtscher, M.; Gruber, G.; Tauer, C.; Steindl, F.; Jungbauer, A.; et al. Generation of human monoclonal antibodies against HIV-1 proteins; electrofusion and epstein-barr virus transformation for peripheral blood lymphocyte immortalization. AIDS Res. Hum. Retroviruses 1994, 10, 359–369.

39. Trkola, A.; Purtscher, M.; Muster, T.; Ballaun, C.; Buchacher, A.; Sullivan, N.; Srinivasan, K.; Sodroski, J.; Moore, J.P.; Katinger, H. Human monoclonal antibody 2g12 defines a distinctive neutralization epitope on the gp120 glycoprotein of human immunodeficiency virus type 1. J. Virol. 1996, 70, 1100–1108.

40. Mascola, J.R.; Lewis, M.G.; Stiegler, G.; Harris, D.; VanCott, T.C.; Hayes, D.; Louder, M.K.; Brown, C.R.; Sapan, C.V.; Frankel, S.S.; et al. Protection of macaques against pathogenic

2970 simian/human immunodeficiency virus 89.6pd by passive transfer of neutralizing antibodies. J.
2971 Virol. 1999, 73, 4009–4018.

2972 41. Etemad-Moghadam, B.; Sun, Y.; Nicholson, E.K.; Karlsson, G.B.; Schenten, D.; Sodroski,
2973 J. Determinants of neutralization resistance in the envelope glycoproteins of a simian-human
2974 immunodeficiency virus passaged in vivo. J. Virol. 1999, 73, 8873–8879.

2975 42. Crawford, J.M.; Earl, P.L.; Moss, B.; Reimann, K.A.; Wyand, M.S.; Manson, K.H.; Bilska,
2976 M.; Zhou, J.T.; Pauza, C.D.; Parren, P.W.H.I.; et al. Characterization of primary isolate-like
2977 variants of simian-human immunodeficiency virus. J. Virol. 1999, 73, 10199.

2978 43. Wyatt, R.; Moore, J.; Accola, M.; Desjardin, E.; Robinson, J.; Sodroski, J. Involvement of
2979 the v1/v2 variable loop structure in the exposure of human immunodeficiency virus type 1 gp120
2980 epitopes induced by receptor binding. J. Virol. 1995, 69, 5723–5733.

2981 44. Moore, J.P.; Thali, M.; Jameson, B.; Vignaux, F.; Lewis, G.; Poon, S.-W.; MacArthur, C.;
2982 Fung, M.; Sun, B.; Durda, P.J.; et al. Immunochemical analysis of the gpl20 surface glycoprotein
2983 of human immunodeficiency virus type 1: Probing the structure of the C4 and V4 domains and the
2984 interaction of the C4 domain with the v3 loop. J. Virol. 1993, 67, 12.

2985 45. Lee, W.S.; Prevost, J.; Richard, J.; van der Sluis, R.M.; Lewin, S.R.; Pazgier, M.; Finzi,
2986 A.; Parsons, M.S.; Kent, S.J. CD4- and time-dependent susceptibility of HIV-1-infected cells to
2987 ADCC. J. Virol. 2019. 93, doi: 10.1128/JVI.01901-18.

2988 46. Buckner, C.M.; Kardava, L.; Zhang, X.; Gittens, K.; Justement, J.S.; Kovacs, C.;
2989 McDermott, A.B.; Li, Y.; Sajadi, M.M.; Chun, T.W.; et al. Maintenance of HIV-specific memory
2990 b-cell responses in elite controllers despite low viral burdens. J. Infect. Dis. 2016, 214, 390–398.

47. Brocca-Cofano, E.; McKinnon, K.; Demberg, T.; Venzon, D.; Hidajat, R.; Xiao, P.; Daltabuit-Test, M.; Patterson, L.J.; Robert-Guroff, M. Vaccine-elicited siv and HIV envelope-specific iga and igg memory b cells in rhesus macaque peripheral blood correlate with functional antibody responses and reduced viremia. Vaccine 2011, 29, 3310–3319.

48. Lee, J.H.; Ozorowski, G.; Ward, A.B. Cryo-em structure of a native, fully glycosylated, cleaved HIV-1 envelope trimer. Science 2016, 351, 1043–1048.

49. Hu, G.; Liu, J.; Taylor, K.A.; Roux, K.H. Structural comparison of HIV-1 envelope spikes with and without the V1/V2 loop. J. Virol. 2011, 85, 2741–2750.

50. Bartesaghi, A.; Merk, A.; Borgnia, M.J.; Milne, J.L.S.; Subramaniam, S. Prefusion structure of trimeric HIV-1 envelope glycoprotein determined by cryo-electron microscopy. Nat. Struct. Mol. Boil. 2013, 20, 1352–1357.

51. Guzzo, C.; Zhang, P.; Liu, Q.; Kwon, A.L.; Uddin, F.; Wells, A.I.; Schmeisser, H.; Cimbro, R.; Huang, J.; Doria-Rose, N.; et al. Structural constraints at the trimer apex stabilize the HIV-1 envelope in a closed, antibody-protected conformation. mBio 2018, 9, e00955-00918.

52. Brown, E.P.; Licht, A.F.; Dugast, A.-S.; Choi, I.; Bailey-Kellogg, C.; Alter, G.; Ackerman, M.E. High-throughput, multiplexed igg subclassing of antigen-specific antibodies from clinical samples. J. Immunol. Methods 2012, 386, 117–123.

53. Veillette, M.; Coutu, M.; Richard, J.; Batraville, L.-A.; Désormeaux, A.; Roger, M.; Finzi, A. Conformational evaluation of HIV-1 trimeric envelope glycoproteins using a cell-based elisa assay. J. Vis. Exp. 2014, 14, 51995.

54. Casazza, J.P.; Betts, M.R.; Picker, L.J.; Koup, R.A. Decay kinetics of human immunodeficiency virus-specific CD8+ T cells in peripheral blood after initiation of highly active antiretroviral therapy. J. Virol. 2001, 75, 6508–6516.

55. Lamine, A.; Caumont-Sarcos, A.; Chaix, M.-L.; Saez-Cirion, A.; Rouzioux, C.; Delfraissy, J.-F.; Pancino, G.; Lambotte, O. Replication-competent HIV strains infect HIV controllers despite undetectable viremia (ANRS EP36 study). AIDS 2007, 21, 3.

56. Hatano, H.; Delwart, E.L.; Norris, P.J.; Lee, T.-H.; Dunn-Williams, J.; Hunt, P.W.; Hoh, R.; Stramer, S.L.; Linnen, J.M.; McCune, J.M.; et al. Evidence for persistent low-level viremia in individuals who control human immunodeficiency virus in the absence of antiretroviral therapy. J. Virol. 2009, 83, 329–335.

57. Pereyra, F.; Palmer, S.; Miura, T.; Block, B.L.; Wiegand, A.; Rothchild, A.C.; Baker, B.; Rosenberg, R.; Cutrell, E.; Seaman, M.S.; et al. Persistent low-level viremia in HIV-1 elite controllers and relationship to immunologic parameters. J. Infect. Dis. 2009, 200, 984–990.

58. Burton, D.R.; Hangartner, L. Broadly neutralizing antibodies to HIV and their role in vaccine design. Annu. Rev. Immunol. 2016, 34, 635–659.

59. West, A.P., Jr.; Scharf, L.; Scheid, J.F.; Klein, F.; Bjorkman, P.J.; Nussenzweig, M.C. Structural insights on the role of antibodies in HIV-1 vaccine and therapy. Cell 2014, 156, 633–648.

60. Rusert, P.; Kouyos, R.D.; Kadelka, C.; Ebner, H.; Schanz, M.; Huber, M.; Braun, D.L.; Hoze, N.; Scherrer, A.; Magnus, C.; et al. Determinants of HIV-1 broadly neutralizing antibody induction. Nat. Med. 2016, 22, 1260–1267.

61. Mouquet, H. Antibody b cell responses in HIV-1 infection. Trends Immunol. 2014, 35, 549–561.

62. Klein, F.; Diskin, R.; Scheid, J.F.; Gaebler, C.; Mouquet, H.; Georgiev, I.S.; Pancera, M.; Zhou, T.; Incesu, R.B.; Fu, B.Z.; et al. Somatic mutations of the immunoglobulin framework are generally required for broad and potent HIV-1 neutralization. Cell 2013, 153, 126–138.

63. Chung, A.W.; Kumar, M.P.; Arnold, K.B.; Yu, W.H.; Schoen, M.K.; Dunphy, L.J.; Suscovich, T.J.; Frahm, N.; Linde, C.; Mahan, A.E.; et al. Dissecting polyclonal vaccine-induced humoral immunity against HIV using systems serology. Cell 2015, 163, 988–998.

64. Lewis, G.K. Role of fc-mediated antibody function in protective immunity against HIV-1. Immunology 2014, 142, 46–57.

65. Lambotte, O.; Ferrari, G.; Moog, C.; Yates, N.L.; Liao, H.X.; Parks, R.J.; Hicks, C.B.; Owzar, K.; Tomaras, G.D.; Montefiori, D.C.; et al. Heterogeneous neutralizing antibody and antibody-dependent cell cytotoxicity responses in HIV-1 elite controllers. AIDS 2009, 23, 897–906.

66. Migueles, S.A.; Connors, M. Success and failure of the cellular immune response against HIV-1. Nat. Immunol. 2015, 16, 563–570.

Bridge from Chapter 2 to Chapter 3

In Chapter 2, we generated and characterised a novel HIV-infected cell line, sorted and infected CEM cells (siCEM cells; [296]). We demonstrated that the siCEM cell line completely downregulates cell surface CD4 receptors and expresses the trimeric Env in a closed conformation. Using siCEM cells and flow cytometry, we designed a novel Env-specific Ab-quantification technique and I quantified Env-specific Abs from UTP, TP, and ECs. Because I observed that compared to UTPs, ECs had similar levels of Abs binding to gp120-coated wells, gp120-coated CEM cells and trimeric Env on siCEM cells, in Chapter 3, I sought to investigate Env-specific AD functions using siCEM cells. Studies from Dr. Galit Alter's and Dr. Margaret Ackerman's teams showed that even though VCs are controllers with detectable but controlled viremia, they do not exhibit the same polyfunctional AD response as compared to ECs [525, 526]. In chapter 2 I used siCEM cells to measure the Env-specific Abs in VCs and measured the AD functions of plasma from my study population. To investigate the role of extra-neutralising Abs and AD functions in HIV control, I quantified the HIV reservoir size among controllers (ECs + VCs) and compared the AD function levels in controllers with detectable versus undetectable HIV reservoir sizes.

Chapter 3: Polyfunctional Fc dependent activity of antibodies to native trimeric envelope in HIV Elite controllers

Published in Frontiers in Immunology, 2020; 11: 583820. doi: 10.3389/fimmu.2020.583820

Sanket Kant[1,2,3], Ningyu Zhang[1,3], Alexandre Barbé[1,4,5], Jean-Pierre Routy[1,3,6,7], Cécile Tremblay[8,9], Réjean Thomas[10], Jason Szabo[3,7,10], Pierre Côté[11], Benoit Trottier[11], Roger LeBlanc[12], Danielle Rouleau[9], Marianne Harris[13], Franck P. Dupuy[1,3*], Nicole F. Bernard[1,2,3,7,14,*,**]

[1]Research Institute of the McGill University Health Centre (RI-MUHC), Montreal, QC, Canada.

[2]Division of Experimental Medicine, McGill University, Montreal, QC, Canada.

[3]Infectious Diseases, Immunology and Global Health Program, Research Institute of the McGill University Health Centre, Montreal, QC, Canada.

[4]Faculté de Médecine de l'Université de Lille Henri Warembourg, Lille, France

[5]Lille University Hospital, Ophthalmology Department, Lille, France

[6]Division of Hematology, McGill University Health Centre, Montreal, QC, Canada.

[7]Chronic Viral Illness Service, McGill University Health Centre, Montreal, QC, Canada.

[8]Centre de Recherche du Centre Hospitalier de l'Université de Montréal (CRCHUM), Montreal, QC, Canada.

[9]Department of Microbiology Infectiology and Immunology, University of Montreal, Montreal, QC, Canada.

[10]Clinique Médicale l'Actuel, Montréal, QC, Canada.

[11]Clinique de médecine urbaine du Quartier Latin, Montréal, QC, Canada.

[12]Clinique Médicale Opus, Montréal, QC, Canada.

[13]British Columbia Center for Excellence in HIV/AIDS, Vancouver, BC, Canada.

[14]Division of Clinical Immunology, McGill University Health Centre, Montreal, QC, Canada.

[*]These authors contributed equally to the manuscript

[**]Correspondence:

Nicole F. Bernard, Ph.D.

nicole.bernard@mcgill.ca

Keywords: HIV, Antibody dependent functions, ADCC, HIV envelope conformation, HIV reservoir, Elite controllers, Viral controllers, HIV^+ plasma

Manuscript length

Total number of words: 7037 words

Total number of figures: 5

Total number of supplemental figures: 4

1. Introduction

The HIV vaccines tested thus far have been designed to induce cellular and/or humoral immune responses to HIV (1-4). Although a central goal of HIV vaccines is to generate neutralizing antibodies (nAbs), their induction in vivo has proven to be challenging (5-7). Out of the seven HIV vaccine trials conducted to date, only the RV144 trial showed significant, though moderate, success in protecting against HIV infection (4). Protection was not associated with the induction of vaccine-specific broadly neutralizing antibodies (BnAbs) or cytotoxic $CD8^+$ T-cells (8). Rather, the binding of immunoglobulin G (IgG) antibodies (Abs) to the V1/V2 loop of HIV Envelope

(Env) correlated with protection while the binding of IgA Abs to Env inversely correlated with protection (8, 9). In secondary analyses, high levels of antibody dependent (AD) cellular cytotoxicity (ADCC) also correlated with HIV protection in patients with low levels of plasma anti-Env IgA Abs (8, 10, 11). These findings raised interest in investigating the role of ADCC and other AD function activities in HIV control.

HIV Env is the only viral gene product expressed on the surface of infected cells and therefore represents the main target for HIV-specific Abs able to trigger Fc-dependent functions (12). Most investigations of HIV Env directed AD functions have used target cells coated with monomeric recombinant HIV Env gp120 (rgp120) (13-19). The monomeric rgp120 on these cells exposes gp120 epitopes that are normally hidden inside the native trimeric Env expressed on genuinely HIV-infected cells. These epitopes are called CD4-induced (CD4i) epitopes as they are unveiled by the interaction of trimeric Env with cell surface CD4 on uninfected $CD4^+$ cells. Furthermore, the interaction of rgp120 with the target cell's surface CD4 receptor occludes the CD4-binding site (CD4bs) epitopes on the gp120 molecule (20). The Env CD4bs epitopes are highly conserved and Abs to these epitopes are among the most potent BnAbs (21-23). HIV-infected cells have also been used as target cells for AD function assays (24-27). In HIV-infected cell cultures only a fraction of $CD4^+$ T cells are truly infected (28, 29). The infected cells shed gp120, which binds CD4 on uninfected bystander cells (20, 27). The interaction of shed gp120 with CD4 on bystander cells not only occludes CD4bs epitopes but also opens the Env conformation exposing CD4i epitopes (20, 27). Anti-Env Abs present in HIV^+ plasma bind these bystander cells preferentially leading to the targeting of healthy bystander cells rather than HIV-infected cells by AD functions (30). The potential pathogenicity of Abs to CD4i epitopes is illustrated by the finding that they are positively

associated with mother-to-child HIV transmission and negatively associated with HIV-infected infant survival (31).

In HIV-infected cells, CD4 is downregulated from the cell surface by HIV Nef and Vpu (32, 33). Unliganded HIV Env remains in a closed conformation with hidden CD4i epitopes (34). Upon interaction with cell-surface CD4 or CD4 mimetics, the conserved regions buried in the native Env trimer are exposed and targeted by ADCC- and ADCD-mediating CD4i Abs (34-39). Target cells used for AD function assays should present HIV Env in the conformation it assumes in in vivo infected cells in which Nef and Vpu downregulate CD4 such that Env remains unliganded and in its native trimeric conformation (35).

ADCC-competent Abs from vaccinees enrolled in the RV144 trial were blocked by Env C1 region-specific A32 monoclonal Ab (mAb) Fab fragments. Thus, the epitopes targeted by the ADCC competent Abs induced by the RV144 vaccine regimen were to CD4i epitopes (10, 40). In addition to Abs with ADCC activity, the vaccine used in the RV144 trial induced anti-HIV gp120-specific Abs able to activate the complement cascade and bind to Fc-receptors on monocytes to induce AD cellular phagocytosis (ADCP) and AD cellular trogocytosis (ADCT) (41, 42).

Elite controllers (ECs) are a rare subset (0.3% - 1%) of HIV-infected individuals (43), who spontaneously control HIV viral load (VL) without treatment (44, 45). ECs who maintain VLs below the limit of detection of standard VL assays and high $CD4^+$ T-cell counts represent examples of a functional cure. Studying immune factors responsible for such control in ECs may uncover immune correlates responsible for HIV control that will guide strategies aimed at replicating this EC phenotype in HIV-infected progressors. Some HIV-infected individuals, known as Viral Controllers (VC), maintain VLs at low but detectable levels without treatment (44).

We previously described the generation of a sorted HIV-infected cell line (siCEM) expressing HIV Env in a native, trimeric, closed conformation (27). This cell line was used to quantify the concentration of anti-Env specific Abs in plasma from HIV-infected ECs, untreated progressors (UTPs) and treated subjects (TPs) (46). We showed that HIV^+ plasma contained Abs able to recognize Env on siCEM cells, though at lower concentrations than that of Abs binding to the open conformation of Env exposing CD4i epitopes (27). Here, we used siCEM target cells to determine the relative concentration of Abs specific for the closed conformation of Env that were ADCC-, AD complement deposition (ADCD)-, and ADCT-competent. We report that plasma from UTPs, TPs, ECs and VCs contained Abs recognizing Env on siCEM cells that mediated these three AD functions. We also showed that EC and VC subjects with superior ADCC function achieved an undetectable HIV viral reservoir size while those with inferior AD functions maintained quantifiable HIV reservoirs.

2. Materials and Methods

I. Ethics statement

This research study was approved by the Institutional Review Boards of the Comité d'Éthique de la Recherche du Centre Hospitalier de l'Université de Montréal (Project Identification Code 17-096) and the Research Ethics Committee of the McGill University Health Centre (Project Identification Code 2018-4505). It was conducted according to the principles expressed in the Declaration of Helsinki. Written informed consent for the collection of each individuals' specimens and subsequent analyses using these samples was obtained from all study subjects.

II. Study Subjects

In this study, we used plasma as a source of Abs from 4 groups of HIV^+ individuals in the chronic phase of infection. UTP (n = 18) were treatment-naïve individuals with VLs >10,000 copies of HIV RNA per ml (c/ml) of plasma and CD4+ T-cell counts <400 cells/ml. TP (n= 24) were on combined anti-retroviral therapy (cART) for at least one year with VLs <50 c/ml of plasma and CD4+ T-cell counts >400 cells/ml. UTPs and TPs were enrolled in the Montreal Primary HIV Infection (PHI) Cohort (47, 48). ECs (n = 37) were treatment-naïve persons having VLs <50 c/ml plasma and CD4+ T-cell counts >400 cells/ml. VCs (n = 16) were treatment-naïve individuals with VLs <3000 c/ml of plasma and CD4+ T-cell counts >400 cells/ml. ECs and VCs were enrolled in the Canadian Cohort of HIV Slow Progressors (48).

III. Total IgG ELISA

Total plasma IgG was quantified using a human IgG ELISA quantification kit (Bethyl Laboratories, Montgomery, TX) as per manufacturer's instructions. Total IgG concentrations were tested in duplicate. The mean value of duplicate IgG concentrations in mg/ml was used to determine the volume of each plasma sample to test so that equivalent quantities of IgG were used to measure the concentration of anti-gp120 and anti-Env Abs and the AD functions of these Abs.

IV. SiCEM target cells

SiCEM cells were generated as previously described (27, 46). Briefly, CEM.NKr.CCR5 (CEM), a $CD4^+$ $CCR5^+$ T-cell line was infected with NL4-3-Bal-IRES-HSA, a fully replication-competent HIV-1 virus encoding Env from HIV BaL accession # AY426110 and expressing viral Nef under the influence of an internal ribosome entry site (IRES). The virus also encoded murine heat stable antigen (HSA; mCD24), which was cell-surface expressed and used to sort for infected cells (49). HSA^+ cells were sorted using a BD FACS Aria instrument (BD Biosciences, Mississauga, ON, Canada) (27, 46). Sorted cells were expanded in culture and stained for virus-mediated

downregulation of CD4, expression of HSA and expression of closed conformation HIV Env (27, 46).

V. Gp120- & Env-specific IgG quantification

The quantification of plasma Abs binding to a rgp120-coated ELISA plate (plate-based ELISA [PBE]) and to siCEM cells has been described previously (46, 50). The rgp120 used in the PBE and to coat CEM cells was derived from HIV-1 BaL gp120 (Accession # AAA44191.1 and was obtained through the NIH AIDS Reagent Program, Division of AIDS, NIAID, NIH. All plasma samples were heat inactivated before use. Multiple dilutions of subject plasma were tested in duplicate. Values that fell within the linear range of a standard curve generated by binding a positive control sample of anti-HIV immunoglobulin (HIVIG; a pool of polyclonal IgG isolated from HIV-infected donors obtained through the NIH AIDS Reagent Program, Division of AIDS, NIAID, NIH: from NABI and NHLBI) were used to calculate the relative concentration of anti-gp120 specific Abs in µg/ml relative to HIVIG. We quantified the gp120- and Env- specific Abs for 16 VCs in addition to the values previously reported for UTPs, TPs and ECs (46). IgG concentrations for each group were reported as medians (interquartile ranges [IQR]). Negative controls included no plasma, a pool of plasma from HIV uninfected donors prepared in-house and IgG from HIV uninfected human serum (Sigma-Aldrich, St Louis, MO). Binding results generated by these three negative control conditions were indistinguishable from each other (Supplemental Figure 1).

VI. Antibody-dependent cellular phagocytosis (ADCP)

ADCP activity of HIV^+ plasma Abs from the 4 subject groups was assessed as described elsewhere (13, 51). Briefly, rgp120 was biotinylated using the EZ-Link® Micro Sulfo-NHS-LC-Biotinylation Kit (Thermo Fisher Scientific, Burlington, ON, Canada) as per manufacturer's

instructions. One µg of biotinylated-rgp120 was incubated with 1 µl of 1 µm fluorescent neutravidin beads (Thermo Fisher Scientific) for 2 hrs at 37°C. The beads were washed twice with 1 ml of phosphate buffered saline (PBS, Wisent Inc., St-Jean-Baptiste, QC, Canada); 0.1% bovine serum albumin (BSA, Sigma-Aldrich) to remove any unbound rgp120. Rgp120-conjugated beads were resuspended to a final dilution of 10 µl of beads in 1 ml PBS; 0.1% BSA. For the ADCP assay, 10 µl of total plasma IgG at concentrations of 2 and 100 µg/ml IgG in PBS was added in triplicate to separate wells of a 96-well V-bottomed microtiter plate (Sarstedt Inc., Montreal, QC, Canada) with 10 µl of diluted rgp120-coated beads for 2 hrs at 37°C, in a humidified, 5% CO_2 incubator. After washing twice with PBS, 200 µl of THP-1 cells at 1.25×10^5 /ml RPMI-1640 media; 10% fetal bovine serum (FBS); 2 mM l-glutamine; 100 IU/mL penicillin; 100 µg/mL streptomycin (R10) (all from Wisent Inc.) was added to each well for 3 hrs at 37°C in a humidified, 5% CO_2 incubator. Wells were then fixed with PBS; 2% FBS; 2% paraformaldehyde (PFA; Santa Cruz Biotechnology, Dallas, TX). The positive control in this assay was HIVIG and it was used at the same concentrations as that of the total IgG in subject plasma quantified in Section 2.3. Cells were acquired using a high-throughput system (HTS) with a BD LSR Fortessa X20 (BD Biosciences, Mississauga, ON, Canada) instrument. All the results were analysed using FloJo v10 software (Tree Star, Inc., Ashland, OR). The background phagocytic activity of the THP-1 cells was measured in wells containing PBS alone. Result were calculated as a phagocytic score (PS), where PS = (% of fluorescent THP-1 cells) x (mean fluorescent intensity [MFI] of THP-1 cells). The no plasma background PS was subtracted from each subject's PS. The partial area under the curve (pAUC) was calculated for PS using two concentrations of plasma and HIVIG IgG using the formula [(Y1 + Y2)/2] * (X1 - X2) where X1 and X2 were the concentrations of total IgG that generated the PSs (Y1 and Y2) that were on the linear range of the standard curve of the functional

read out generated by these input IgG concentrations. Each sample's pAUC PS was then divided by the pAUC PS of HIVIG to account for inter-plate and/or inter-assay variability. ADCP values for each group were reported as median (IQR).

VII. Antibody-dependent complement deposition (ADCD)

The ADCD assay was performed as described elsewhere (13, 52, 53) with the following modifications. The target cells used were siCEM cells. 50 µl of siCEM cells at 10^6 cells/ml RPMI were plated in duplicate into the wells of a 96-well V-bottomed microtiter plate with 50 µl of 100 µg/ml and 500 µg/ml of plasma IgG for 20 min at room temperature (RT). Plasma in acid citrate dextrose anticoagulant from an HIV-negative healthy control donor, diluted 1:10 in veronal buffer (Boston BioProducts, Ashland, MA); 0.1% gelatin (Thermo Fisher Scientific) was used as a source of complement. A volume of 50 µls of diluted complement was added to each well for 20 mins at 37°C, in a humidified 5% CO_2 incubator. The reaction was stopped by washing the wells twice with 150 µl of 15 mM EDTA (Thermo Fisher Scientific). Complement deposition was detected by adding 50 µl of FITC-conjugated, mouse anti-human anti-C3b Ab (Cedarlane, Burlington, ON, Canada) diluted 1:50, for 20 mins at 4°C. Cells were fixed, acquired on an LSR Fortessa X20 instrument and results were analyzed as described for the ADCP assay. The same HIVIG concentrations as used for subject plasma were included in each plate as positive controls. Background complement activity was measured in wells with no Abs. The ADCD score was calculated as the (% of $C3b^+$ siCEM cells) x (MFI of $C3b^+$ siCEM cells). The background score was subtracted from the scores generated by test plasma. As for ADCP, the pAUC was calculated for the ADCD score for the two concentrations of plasma and HIVIG IgG. Individual pAUCs for test samples were normalized to the pAUC of HIVIG by dividing the test results by the results for

HIVIG present on the same 96-well plate to account for any inter-plate and/or inter-assay variability. ADCD values for each group were reported as median (IQR).

VIII. Antibody-dependent cellular cytotoxicity (ADCC)

The ADCC assay measures the cytolysis of siCEM target cells (T) by natural killer (NK) cells in the presence of Abs in HIV^+ plasma (27). siCEM cells were labelled with cytosol-staining carboxyfluorescein succinimidyl ester (CFSE; Thermo Fisher Scientific) dye as per manufacturer's instructions (27, 46). Subject plasma and HIVIG was diluted to 50 µg/ml and 500 µg/ml IgG in R10. 50 µl of the diluted plasma IgG was incubated in duplicate with 50 µl of $CFSE^+$ siCEM cells at 2 x 10^6 cells/ml of R10 in the wells of a 96-well V-bottomed microtiter plate for 20 mins at RT in the dark. Peripheral blood mononuclear cells (PBMCs) cells from an HIV seronegative, healthy leukapheresis donor were thawed and rested overnight at 37°C in a humidified, 5% CO_2 incubator. NK effector cells (E) were enriched from these PBMCs by negative selection using magnetic beads (EasySep™ Human NK Cell Enrichment Kit; STEMCELL Technologies, Vancouver, BC, Canada) as per the manufacturer's instructions. After selection, the average purity of NK cells was 93.3%. 100 µl of NK E cells at 5 x 10^5 cells/ml of R10 were added to each well to obtain a final E:T of 5:1. Wells were centrifuged for 1 min at 300 x g and incubated for 1 hr at 37°C in a humidified, 5% CO_2 incubator. After washing with 150 µl of 1x Annexin V (AnV) binding buffer (BD Biosciences), cells were stained with 100 µl of AnV stain (BD Biosciences) diluted 1:100 in in 1x AnV buffer for 10 mins at RT in the dark. Plates were washed once in AnV buffer and resuspended in 100 µl of AnV buffer for acquisition. Results were analyzed as described for the ADCP assay. In each plate, equivalent concentrations of HIVIG IgG as in the plasma test samples and a no Ab negative control were included. ADCC activity was defined as the average of the frequency (%) of T that were AnV^+ after background subtraction. A

pAUC was calculated for the 2 concentrations of plasma and HIVIG IgG. Subject pAUCs were normalized to the pAUC of HIVIG to account for any inter-plate and/or inter-assay variability. ADCC values for each group were reported as median (IQR).

IX. Antibody-dependent cellular trogocytosis (ADCT)

The ADCT assay used in this study was an adaptation of the rapid fluorescence ADCC (RFADCC) assay, which measures the transfer of the cell-surface membrane dye, PKH-26, from target cells to monocyte effector cells (14, 54). SiCEM cells were labelled with PKH-26 as previously described (27, 46). Subject plasma and HIVIG were diluted to 50 µg/ml and 500 µg/ml IgG in R10. Fifty µl of diluted plasma were added in duplicate to the wells of a 96-well V-bottomed microtiter plate containing 50 µl of PKH-26$^+$ siCEM cells at 2 x 10^5 cells per ml of R10 (T) for 20 mins at RT in the dark. Thawed and rested PBMCs from an HIV-negative healthy control donor was used as effector cells (E). 100 µl of E at 3 x 10^6 cells/ml in R10 were added to each well to obtain a final E:T of 30:1. The wells were centrifuged at 300 x g for 1 min and incubated for 1 hr at 37°C in a humidified, 5% CO_2 incubator. After the coculture, cells were washed with PBS; 2% FBS. To measure the ADCT activity of monocytes, each well was stained with 50 µl of Live/Dead stain (Thermo Fisher Scientific) diluted 1:500 and Brilliant Violet (BV) 785-conjugated anti-human CD14 Ab (BioLegend, San Diego, CA) diluted 1:50 in PBS; 2% FBS buffer for 20 mins in a 4ºC. Wells were washed once with PBS; 2% FBS, fixed, acquired and results were analyzed as described for the ADCP assay. Each plate included HIVIG positive control samples at the same IgG concentrations as test plasma and negative control wells with no plasma Abs. ADCT activity was measured as the mean % of live CD14$^+$ PKH-26$^+$ monocytes. The mean % of PKH-26$^+$ monocytes in the no Ab control was used for background subtraction. We calculated the pAUC for the % of live, CD14$^+$ PKH-26$^+$ monocytes for the 2 IgG concentrations for each subject plasma

and HIVIG. Values for test plasma were normalised by dividing these results by the pAUC ADCT of HIVIG to account for inter-plate and/or inter-assay variability. ADCT values for each group were reported as median (IQR). The ImageStream® images in Supplemental Figure 2 show that the % of PKH-26$^+$ monocytes were not due to doublets of PKH-26$^+$ T and CD14$^+$ monocytes but rather to the transfer of PKH-26$^+$ membrane components from siCEM T cells to CD14$^+$ monocytes.

X. Quantification of latent HIV reservoirs

The HIV reservoir size was measured using the integrated HIV DNA PCR assay described elsewhere (55, 56). Cryopreserved subject PBMCs were thawed in R10 before isolating CD4 cells by negative selection (EasySep™ human CD4$^+$ T cell negative enrichment kit, STEMCELL Technologies) as per manufacturer's instructions. Post-isolation, 10^5 enriched cells were stained with Live/Dead stain (Thermo Fisher Scientific), BV-785-conjugated anti-human CD3 (clone: OKT3; BioLegend), VioBlue-conjugated anti-human CD4 (clone: REA623) and PE-Vio770 anti-human CD8 antibody (clone: REA734) (both from Miltenyi Biotec, Auburn, CA) to ascertain the purity of CD4$^+$ T cells, which averaged 96.8%. Enriched CD4 cells were lysed and stored frozen until use. The integrated DNA PCR assays were performed in triplicate and reservoir quantification was calculated as follows:

(copies of integrated HIV DNA/106 CD4 cells) = [(copies of HIV as determined by PCR)/(CD3 copies as determined by PCR)] * 1,000,000 cells.

3. Statistics

Microsoft Excel, GraphPad Prism v7 (GraphPad Software, Inc., San Diego, CA) and RStudio v1.2.5001 (RStudio: Integrated Development for R. RStudio, Inc., Boston, MA) were used for statistical analyses and graphical presentation. The statistical significance of between-group

differences was determined using non-parametric, Kruskal-Wallis tests with Dunn's post tests. P-values <0.05 were considered significant. The statistical significance of correlations and the respective plots between AD function assays and AD function assays with Ab concentrations were assessed using non-parametric Spearman's correlation tests in Rstudio v1.2.5001.

4. Results

I. Plasma from UTPs and HIV controllers have higher HIV-gp120/Env-specific Abs concentration than TPs

Of the four subject groups tested, UTPs had the highest concentration of total plasma IgG with a median (IQR) of 15.41 (12.45, 19.38) mg/ml, which was significantly higher than the 9.93 (8.01, 12.22), 10.24 (8.22, 15.27) and 8.95 (6.46, 13.78) mg/ml of total plasma IgG observed in TPs, ECs and VCs, respectively (Supplemental Figure 3). These results likely reflect hypergammaglobulinemia in this chronically infected, untreated population (57, 58). The AD function assays were performed using equivalent concentrations of plasma IgG. In addition, in this study to determine the relationship between the concentrations of specific anti-gp120- and anti-Env Abs and their individual AD functions, we quantified Abs specific to these antigens using a PBE with wells coated with monomeric gp120 and by flow cytometry using siCEM cells expressing the native trimeric Env, respectively. We previously showed that UTPs and ECs had similar levels of anti-gp120- and anti-Env-specific Abs (46). Figure 1A and 1B display the concentrations of Abs binding to rgp120 using the PBE and closed conformation Env on siCEM cells relative to a standard curve of serial dilutions of known concentrations of pooled IgG isolated from HIV-infected donors (HIVIG). Since the exact amount of Abs binding to rgp120 and trimeric Env in the HIVIG is unknown, our results for subject plasma Abs are reported as "µg/ml normalized to HIVIG". We were unable to quantify anti-gp120 Abs levels for 1 EC in the PBE

assay and for 1 UTP, 5 TP and 1 EC in the siCEM binding assay because these values were below the limit of detection. In addition, we quantified plasma from 16 VCs in this study. VCs had higher levels of both anti-gp120 and anti-Env Abs than did TPs and ECs that did not differ significantly from those measured in UTPs. Overall, TPs had lower levels of anti-gp120- and anti-Env-specific Abs than did UTPs, ECs and VCs.

II. HIV-specific AD functions in UTPs, TPs, ECs and VCs

We performed four AD function assays that measured Fc-dependent functions of plasma HIV gp120/Env-specific Abs. The read outs for the four assays measuring AD function were 1) the pAUCs of the phagocytic scores (PS) for ADCP using biotinylated rgp120 coupled to neutravidin beads, 2) the pAUCs of the complement deposition score (CDS) for ADCD, 3) the pAUCs of the % of AnV^+ siCEM cells for ADCC and 4) the pAUCs of the % of PKH-26^+ monocytes for ADCT. The target cells for ADCD, ADCC and ADCT were siCEM cells. Supplemental Figure 4 shows the non-normalized pAUC results for these 4 assays performed on plasma from the four subject groups as well as the plate to plate variation in the pAUC generated by HIVIG. Figure 2 shows pAUC results for these four AD functions after normalization to the pAUC of the HIVIG standard curve present in the same 96-well plate in which each test was performed. In all four AD function assays, plasma from UTPs, ECs and VCs did not differ significantly from each other in their response score with the exceptions of UTPs having higher ADCD activity than VCs and VCs having higher ADCT activity than ECs (Figure 2 A-D). The ADCP functional score of anti-gp120-specific Abs and the ADCC and ADCT functional score of anti-Env-specific Abs in plasma from the UTP, EC and VC groups were higher than those reported for TPs. So too the ADCD functional score of the anti-Env-specific Abs in plasma from UTPs was higher than that in TPs and VCs (Figure 2 A-D).

Even though gp120-specific and Env-specific Abs from ECs had significantly higher AD functionality levels compared to TPs, with the exception of ADCD activity, that did not differ significantly from those in UTPs and VCs, correlation analyses revealed that these functions were more highly correlated with each other in ECs than in the other study groups (Figure 3). Overall, the functional read outs of ADCC and ADCT activity of anti-Env-specific Abs correlated with each other in all 4 study groups with correlation coefficients (r-values) of 0.61, 0.74, 0.77 and 0.89 for UTPs, TPs, ECs and VCs, respectively ($p<0.01$ for all). In ECs, all AD functions were correlated with each other with r-values > 0.66 ($p < 0.0001$ for all pairs). In contrast, ADCD assay scores correlated with ADCP, ADCC and ADCT results in UTPs with r-values of 0.31, 0.23 and 0.43, respectively ($p < 0.05$ for all comparisons). For VCs, ADCD scores correlated with ADCP, ADCC and ADCT with r-values of 0.45 ($p = 0.08$), 0.64 ($p < 0.01$) and 0.58 ($p < 0.02$), respectively. In VCs, ADCP activity did not correlate significantly with any other AD functional result. Together, these results suggest that while there may not be between-group differences in the AD function of anti-Env Abs relative to HIVIG between UTPs, ECs and VCs (Figure 2 A-D), these functions were more highly correlated in ECs than in UTPs and VCs (Figure 3).

III. AD functional scores are dependent on the concentration of Abs specific to gp120 or Env present in HIV^+ plasma

While previous studies have investigated the underlying relationships between the AD functions with IgG subtypes (13) and with IgG post-translational modifications (59), input IgG concentration has rarely been controlled for, nor has between-subject variation in the concentration of Abs specific for gp120 or Env been accounted for. To address this, we first investigated whether there was a relationship between anti-gp120/Env concentrations and AD functions. Since we used gp120-coated beads in the ADCP assay, results from the ADCP assay were correlated with the

concentration of Abs quantified from the gp120-coated PBE. As the target cells for ADCD, ADCC and ADCT assays were siCEM cells, the results of these assays were correlated with the concentration of anti-Env-specific Abs quantified using siCEM cells (Figure 3). ADCP levels correlated significantly with the concentration of anti-gp120-specific Abs in UTPs, TPs and ECs ($r = 0.68$, 0.78 and 0.91 respectively; $p < 0.01$ for all) but not in VCs ($r = 0.1$; $p > 0.05$). Anti-Env Ab concentrations in HIV^+ plasma correlated with ADCD, ADCC and ADCT activity in UTPs ($r = 0.59$, $p < 0.01$; $r = 0.43$, $p = 0.07$; $r = 0.57$, $p < 0.05$, respectively), in TP ($r > 0.42$; $p < 0.05$ for all) and in ECs ($r = 0.77$, 0.73 and 0.88, respectively; $p < 0.0001$, for all). Anti-Env Ab concentrations did not correlate significantly with any of these 3 AD functions in VCs (Figure 3).

This prompted us to question whether anti-gp120/Env concentrations affected the level of AD functionality. To address this, we normalized each subject's AD functional results by dividing these results by the concentration of their anti-gp120- or anti-Env-specific Abs. After normalization, variation in assay results within groups was reduced with a few exceptions and many of the statistically significant between-group differences in the four AD assays observed before normalization were no longer present. Where between-group differences were obtained post-normalization, they were driven by a few outlier data points. In summary, these results showed that HIV gp120/Env-specific Ab concentrations play an important role in contributing to variation in AD functions (Figure 4 A-D). The loss of between-group difference in AD functionality also suggests that AD functional Ab potency did not differ between groups.

IV. Higher ADCC function is observed in individuals with undetectable reservoir

ECs are untreated individuals with VLs below the limit of detection of standard VL assays, whereas VCs, who are also untreated, have low but detectable VL levels of < 3000 c/ml of plasma. Given that both EC and VC groups have high levels of non-neutralizing AD functions in the range

of those seen in UTP, we questioned whether AD function levels were associated with cell-associated DNA reservoir levels. We therefore quantified the HIV reservoir in ECs and VCs using the integrated HIV DNA PCR assay (55, 56). The minimum detection limit of the standard curve in the integrated HIV DNA PCR assay was 3 HIV copies per 0.1 million ACH2 cells, which carry a singly copy of integrated HIV DNA per cells. Each subject's reservoir quantification was performed in triplicates. We distinguished the reservoir results of the subjects as 'Quantifiable (≥ 2 of the triplicates having ≥ 3 HIV copies per 0.1 million CD4 cells)' and 'Undetectable (< 2 of the triplicates having < 3 HIV copies per 0.1 million CD4 cells)'. Out of the 46 subjects whose HIV reservoir could be evaluated (ECs, n = 30 and VCs, n = 16), the reservoir was quantifiable in 8 subjects (ECs, n = 3 & VCs, n = 5) and the remaining samples had an HIV reservoir size below the limit of detection and were thus categorized as "undetectable". The HIV Env-specific Ab ADCC functional score relative to HIVIG were higher in subjects with an undetectable than a detectable HIV reservoir size (p = 0.0229, Mann Whitney test). We also observed a non-significant trend towards a difference in the Ab normalized ADCT, ADCP and ADCD score results in subjects with quantifiable versus undetectable HIV reservoir sizes of 0.1416 vs 0.3700 (p=0.0544) for ADCT, 0.1607 vs 0.3391 (p=0.1614) for ADCP and 0.3857 vs 0.6493 (p=0.5696) for ADCD.

5. Discussion

In this study, we used siCEM cells rather than rgp120-coated CEM cells as target cells in ADCC, ADCT and ADCD function assays. Using siCEM cells as target cells allowed us to probe for the presence of Abs in HIV^+ plasma to a native, closed conformation of Env exposed on infected cells (27, 46). We show here that plasma from 89 of 96 (92.70%) HIV^+ study subjects had detectable levels of Abs binding to native trimeric HIV Env on siCEM cells. Plasma from UTPs, ECs and VCs had significantly higher concentrations of Abs specific for Env on siCEM that supported these

AD functions than did TPs on ART. This was also the case for ADCP activity, which was measured using gp120-coated fluorescent beads. When ADCC, ADCT and ACCD function results were normalized to the concentration of HIV Env-specific Abs in each subject's plasma, between group differences in AD functions were no longer present. Between group differences in ADCP function were also lost following normalization to the concentration of anti-gp120-specific Abs in subject plasma. This indicated that variation in AD functions was directly dependent on the anti-Env or anti-gp120-specific Ab concentration and was not due to between-group differences in the potency of Abs to support these AD functions. A distinguishing feature of ECs was that their AD responses were more highly and significantly correlated to each other than those of UTPs, TPs and VCs. We also report that individuals who had an HIV reservoir size below the limit of detection had higher AD functional responses than those whose HIV reservoir size was quantifiable, which achieved statistical significance for ADCC activity.

The results reported here for ADCC, ADCT and ADCD function of anti-HIV Env-specific Abs in HIV^+ plasma differ in several aspects from those generated by other groups (13, 18, 19, 60). This is likely due to the target cell we used to measure these functions. Gp120-coated cells have been used extensively as target cells in the investigation of AD functions and in immune monitoring of HIV vaccine trials (3, 10, 13, 14, 17-19, 40, 42, 59-62). Interaction of Env with CD4 exposes conserved residues that are generally hidden in Env on productively infected cells. This exposed inner domain of Env is preferentially bound by Abs to CD4i epitopes. Such epitopes are also accessible on cells infected with HIV Nef and/or Vpu deletion mutants that fail to downmodulate CD4 (35, 36). Some groups have also studied AD functions using HIV-infected cell cultures (25, 26, 63). However, only a fraction of CD4 cells are infected in such cultures. Gp120 is shed from infected cells to be taken up by CD4 on uninfected bystander CD4 cells, also leading to exposure

of CD4i epitopes (20). The consequence of this phenomenon is the preferential targeting by ADCC of uninfected bystander, rather than infected cells opsonized by Abs to CD4i epitopes (20, 27, 30). Thus, studying AD functions using gp120-coated target cells, cells infected with Nef- Vpu- variants of HIV or cultures in which only a fraction of the target cells are HIV-infected, probes for the presence of Abs in HIV^+ plasma that recognize CD4i epitopes of gp120/Env. To overcome this obstacle, we used siCEM cells as a target cell, a productively infected cell line that synthesizes functional Nef and Vpu able to downregulate CD4, tetherin/BST-2 and HLA-C (27, 46). In the absence of cell surface CD4, HIV Env remains in a closed conformation as confirmed by the failure of CD4i-specific Abs such as A32 and C11 to bind Env on siCEM cells (27, 46). In addition to functional viral proteins, the virus used in this model synthesises murine HSA/CD24 (mCD24) which was used to select and sort for infected cells (27, 46, 49). Thus, the use of siCEM target cells provided a unique platform for the assessment of the non-neutralizing functions of anti-Env Abs in plasma from HIV^+ subjects. In this report, we also developed an in-house ADCC assay that measures ADCC as the frequency of apoptotic target cells as a surrogate for target cell cytolysis (27). Apoptosis is a later step in the cascade of events leading to cell death than the expression of granzyme B measured by the GranToxiLux assay (64). It differs from the RFADCC assay, which measures trogocytosis rather than ADCC activity (14, 54, 65). Lastly, our experiments controlled for the input of bulk IgG in plasma. Thus, the between-group differences in AD function assays were a result of the amount of HIV-Env/gp120-specific Abs present in each plasma sample. While the biological properties and subclass distributions of anti-gp120-specific Abs have been shown to have an influence on downstream AD functions, we observe that the amount of Env/gp120-specific Abs played a significant role in the quantification of our AD functional assay readouts.

The phase III RV144 trial was significantly, though modestly, successful in preventing HIV infection (4). This led to significant interest in investigating the role of ADCC activity and other AD functions in protection from HIV infection. Efforts to replicate RV144 vaccine-mediated protection in South Africa using a regimen analogous to the one used in the RV144 trial but with a vaccine regimen based on clade C HIV, the HVTN702 vaccine trial, failed to protect against HIV infection (66, 67). Companion phase II safety and immunogenicity vaccine trials showed that levels of anti-Env Abs induced by the clade C based vaccine regimens were as high if not higher than the levels induced by the RV144 vaccine regimen (3, 62, 68, 69). These Abs responses were tested using cells coated with monomeric gp120 and thus, the immune monitoring strategy preferentially detected Abs to CD4i epitopes. Differences in the protection offered by this vaccine strategy in Thailand versus South Africa may be due to subtle amino acid differences between the predominant HIV strain circulating in Thailand (circulating recombinant form (CRF)01_AE) and clade C HIV in South Africa (70-72). Env from all the phylogenetic M groups possess a serine (S) at amino acid 375, except for the CRF01_AE isolates, which possesses a histidine (H) at this position (71, 72). H375 modifies the HIV Env conformation to a state closer to that of its CD4 bound conformation (71, 73). HIV^+ plasma contains abundant Abs to CD4i epitopes (20, 27, 35-37, 74). The vaccine regimen used in the RV144 trial induced A32-blockable Abs that were specific for the gp120 inner domain. Thus, the reduced risk of infection in RV144 HIV trial recipients may be related to the induction of cluster A-specific Abs able to recognize HIV CRF01_AE-infected cells bearing an Env conformation that is uniquely already partially open. On the other hand, cluster A-specific Abs to an analogous sequence induced by a vaccine regimen that included clade C gp120 may be unable to recognize HIV-infected cells in a South Africa population where clade C Env adopts a more closed conformation on infected cells. In addition, in

the RV144 trial as in companion trials, Ab responses were tested using gp120 coated cells (or HIV CRF01_AE infected target cells) exposing cluster A epitopes usually hidden inside trimeric Env of other HIV clades. This strategy may have been appropriate to detect vaccine induced Abs able to support ADCC of HIV-infected target cells in the Thai population but not in other countries where HIV CRF01_AE is not dominant. In such a setting, ADCC target cells expressing native trimeric Env in a closed conformation would have the potential to be superior to gp120-coated target cells (or HIV CRF01_AE infected target cells) for the purpose of immune monitoring vaccine-induced Abs able to support the ADCC of genuinely HIV-infected cells.

ECs represent a rare population of HIV-infected persons who spontaneously control HIV. There is interest in understanding the mechanisms underlying HIV control without treatment in ECs as this may guide strategies aimed at controlling VL without treatment to effect a functional cure in a broader range of HIV-infected persons. ECs, unlike those in any other study group, had an anti-HIV Env Ab response able to mediate AD functions that were highly correlated with each other. This has been reported by others (13). Although previous studies have not observed any significant differences between TPs, UTPs and ECs in terms of the ability of their anti-gp120 Abs to support AD functions, these studies did report that subclass differences and glycosylation patterns could be key actors in HIV control (13, 59). Additionally, in these studies, AD non-neutralising functions were not normalised to the amounts of HIV-gp120-specific Abs. Here, we demonstrated that the amount of the HIV gp120/Env-specific Abs play a significant role in non-neutralising functions. Unlike UTP, whose Ab responses are likely driven by high VLs, ECs, maintained high levels of Env-specific Abs with AD functionality despite undetectable VL levels. Furthermore, although ECs and successfully treated TPs had VL levels that were < 50 c/ml of plasma, they differed from each other in that ECs maintained high anti-gp120/Env levels while TPs did not. How ECs

maintain high levels of anti-Env/gp120-specific Abs is not well understood. One possibility is that ECs may have a significantly higher HIV antigen-specific memory B cell response than HIV^+ subjects on-ART (75) and untreated persons in chronic phase infection (76). Alternatively, B cells may be stimulated by a low-level of systemic HIV replication that is generally undetectable by currently available VL measuring tools (77-80). Whether ECs display a unique memory B cell phenotype that is different from other groups in our study is worth investigating (75).

A limitation of this study is the choice of HIV BaL Env in the construct used to infect CEM cells and generate siCEM cells. BaL Env is macrophage tropic, has a Tier 1 phenotype and requires little CD4 to support infection. Another limitation is the use of a single Env for these studies. Future experiments should substitute BaL Env with Envs from isolates that more closely resemble circulating viruses, transmitting/founder viruses, Envs from HIV clades other than clade B and Envs being used in vaccine constructs.

In addition to AD functions, we measured the cell-associated reservoir in 53 ECs and VCs by using the integrated HIV PCR assay (55, 56). Of these controllers, only 8 (15.07%) had a reservoir size that was detectable of which 3 individuals were ECs. When ECs and VCs were stratified into 2 groups depending on whether their HIV reservoir size was above or below the limit of detection of this assay, we found that AD function measures were higher in the group with an undetectable HIV reservoir size. This was the case for all AD functions though the differences only achieved statistical significance for ADCC. This finding suggests that AD function, which depends on anti-Env Ab concentration may be associated with HIV control at the level of the HIV reservoir. A limitation of this work is that the measurement of latent HIV reservoirs is challenging, particularly in HIV controllers. The quantitative viral outgrowth assay (QVOA) is considered the gold standard for reservoir quantification. However, this assay is thought to underestimate the HIV reservoir size

because a single round of stimulation does not activate all CD4 cells harboring replication-competent HIV (81). The QVOA requires large numbers of isolated CD4 cells, is time consuming and technically challenging compared to PCR-based assays such as the integrated HIV DNA PCR assay used here. A drawback of the integrated HIV DNA PCR assay is that it overestimates the HIV reservoir size because it also amplifies integrated viral fragments that are not full-length sequences of replication competent HIV. Several assays have been developed to improve the quantification of cells harboring replication competent HIV. The Tat/Rev induced limiting dilution assay (TILDA) measures the frequency of cells with virus isolates able to transcribe multiply-spliced HIV RNA (82). Flow cytometry-based techniques such as RNA flow-FISH (83, 84) simultaneously measures GagPol mRNA and HIV protein double-positive cells. The HIV-Flow assay (85) measures the frequency of cells harboring HIV sequences complete enough to translate HIV p24. The flow cytometry-based assays offer advantages in characterizing the phenotype of cells harboring the reservoir but the starting number of isolated $CD4^+$ cells required for these assays limits the application of these methods to subjects who have undergone leukaphereses. However, the results of the RNA flow-FISH and HIV-Flow assays are significantly correlated with the results generated using the integrated HIV DNA PCR assays (84, 85).

In summary, the study reported here used siCEM cells expressing HIV Env in its native trimeric form to probe plasma from HIV-infected subjects for the presence of Abs recognizing this Env conformation. SiCEM cells were used to quantify Abs of this specificity in different groups of HIV-infected subjects. UTPs, ECs and VCs had similar levels of Env-specific Abs that were higher than those in TPs. These Abs supported Fc-dependent functions, which were dependent on the amount of Env-specific Abs present in the plasma. A unique aspect of Abs from ECs that distinguished them from other study groups was their polyfunctional Fc-dependent activities as

suggested by their highly correlated AD functions (13). A novel feature of this study is that we found that individuals with an undetectable HIV reservoir size tended to have higher AD function levels as compared to individuals with a quantifiable HIV reservoir. Future studies should be directed at characterising the biologic properties and subclass distribution of these Abs and the B cell phenotypes of ECs, which may account for their ability to control HIV without treatment.

6. Conflicts of Interest

The authors declare that the research was conducted in the absence of any commercial or financial relationships that could be construed as a potential conflict of interest.

7. Author Contributions

SK, AB, FD and NB contributed to conception and design of the study. SK, NZ, AB and FD performed experiments and analysed the results. SK performed the statistical analysis and prepared the figures for the manuscript. SK and NB wrote the first draft of the manuscript. J-PR, CT, RT, JS, PC, BT, RL, DR and MH provided samples with linked clinical follow up information from the subjects participating in this study. NB supervised the project, provided administrative oversight and obtained funding for this study. All authors read and contributed to manuscript revisions and approved the submitted version of the manuscript.

8. Acknowledgments

This study received support from the Canadian Institutes for Health Research [grant PJT-148491], the Fonds de Recherche du Quebec-Santé (FRQ-S) and a McGill University Health Centre (MUHC) Ph.D. scholarship to SK. SK, FPD, J-PR and NFB are members of the Research Institute of the MUHC (RI-MUHC), an institution funded in part by the FRQ-S. We wish to acknowledge Tsoarello Mabanga, Xiaoyan Ni, Cindy Xu Zhang, Alexa Del Corpo and Olfa Debbeche for

sample processing and expert technical assistance. Mario Legault provided administrative support and coordination for the Montreal Primary Infection (PI) Cohort. Stéphanie Matte was responsible for coordinating the Canadian Cohort of HIV-Infected Slow Progressors. We also thank Oussama Meziane for his insightful comments on this project and for technical and analytical advice. The following physicians recruited and followed subjects providing samples for this study: Louise Charest, Sylvie Vézina, Jean-Guy Baril, Marc-André Charon, Serge Dufresne, Stéphane Lavoie, Claude Fortin, Marie Munoz, Benoit Deligne, Danièle Longpré, Bernard Lessard, Bertrand Lebouché, Norbert Gilmore, Marina Klein, Hélène Senay, Noël Grégoire, Julian Falutz, Dominique Tessier, Danielle Legault, Jonathan Angel, Colin Kovacs, Ken Logue, Brian Conway, Alain Piché and Bill Thompson. We thank the Immunophenotyping Technology Platform of the RI-MUHC and staff for their contribution to this publication. We acknowledge the contribution of the study subjects without whose donation of blood samples this project would not have been possible.

9. References

1. Buchbinder, S.P., Mehrotra, D.V., Duerr, A., Fitzgerald, D.W., Mogg, R., Li, D., et al., Efficacy assessment of a cell-mediated immunity HIV-1 vaccine (the Step Study): a double-blind, randomised, placebo-controlled, test-of-concept trial. The Lancet, 2008. 372(9653): p. 1881-1893.

2. Gray, G., Buchbinder, S., and Duerr, A., Overview of STEP and Phambili trial results: two phase IIb test-of-concept studies investigating the efficacy of MRK adenovirus type 5 gag/pol/nef subtype B HIV vaccine. Curr Opin HIV AIDS, 2010. 5(5): p. 357-61.

3. Gray, G.E., Huang, Y., Grunenberg, N., Laher, F., Roux, S., Andersen-Nissen, E., et al., Immune correlates of the Thai RV144 HIV vaccine regimen in South Africa. Science Translational Medicine, 2019. 11(510): p. eaax1880.

4. Rerks-Ngarm, S., Pitisuttithum, P., Nitayaphan, S., Kaewkungwal, J., Chiu, J., Paris, R., et al., Vaccination with ALVAC and AIDSVAX to Prevent HIV-1 Infection in Thailand. New England Journal of Medicine, 2009. 361(23): p. 12.

5. McCoy, L.E. and Weiss, R.A., Neutralizing antibodies to HIV-1 induced by immunization. J Exp Med, 2013. 210(2): p. 209-23.

6. Sliepen, K. and Sanders, R.W., HIV-1 envelope glycoprotein immunogens to induce broadly neutralizing antibodies. Expert Rev Vaccines, 2016. 15(3): p. 349-65.

7. Escolano, A., Dosenovic, P., and Nussenzweig, M.C., Progress toward active or passive HIV-1 vaccination. J Exp Med, 2017. 214(1): p. 3-16.

8. Haynes, B.F., Gilbert, P.B., McElrath, M.J., Zolla-Pazner, S., Tomaras, G.D., Alam, S.M., et al., Immune-Correlates Analysis of an HIV-1 Vaccine Efficacy Trial. New England Journal of Medicine, 2012. 366(14): p. 1275-1286.

9. Yates, N.L., Liao, H.X., Fong, Y., deCamp, A., Vandergrift, N.A., Williams, W.T., et al., Vaccine-induced Env V1-V2 IgG3 correlates with lower HIV-1 infection risk and declines soon after vaccination. Sci Transl Med, 2014. 6(228): p. 228ra39.

10. Bonsignori, M., Pollara, J., Moody, M.A., Alpert, M.D., Chen, X., Hwang, K.K., et al., Antibody-dependent cellular cytotoxicity-mediating antibodies from an HIV-1 vaccine efficacy trial target multiple epitopes and preferentially use the VH1 gene family. J Virol, 2012. 86(21): p. 11521-32.

11. Tomaras, G.D., Ferrari, G., Shen, X., Alam, S.M., Liao, H.X., Pollara, J., et al., Vaccine-induced plasma IgA specific for the C1 region of the HIV-1 envelope blocks binding and effector function of IgG. Proc Natl Acad Sci U S A, 2013. 110(22): p. 9019-24.

12. Checkley, M.A., Luttge, B.G., and Freed, E.O., HIV-1 envelope glycoprotein biosynthesis, trafficking, and incorporation. J Mol Biol, 2011. 410(4): p. 582-608.

13. Ackerman, M.E., Mikhailova, A., Brown, E.P., Dowell, K.G., Walker, B.D., Bailey-Kellogg, C., et al., Polyfunctional HIV-Specific Antibody Responses Are Associated with Spontaneous HIV Control. PLoS Pathog, 2016. 12(1): p. e1005315.

14. Gomez-Roman, V.R., Florese, R.H., Patterson, L.J., Peng, B., Venzon, D., Aldrich, K., et al., A simplified method for the rapid fluorometric assessment of antibody-dependent cell-mediated cytotoxicity. J Immunol Methods, 2006. 308(1-2): p. 53-67.

15. Guan, Y., Pazgier, M., Sajadi, M.M., Kamin-Lewis, R., Al-Darmarki, S., Flinko, R., et al., Diverse specificity and effector function among human antibodies to HIV-1 envelope glycoprotein epitopes exposed by CD4 binding. Proc Natl Acad Sci U S A, 2013. 110(1): p. E69-78.

16. Milligan, C., Richardson, B.A., John-Stewart, G., Nduati, R., and Overbaugh, J., Passively acquired antibody-dependent cellular cytotoxicity (ADCC) activity in HIV-infected infants is associated with reduced mortality. Cell Host Microbe, 2015. 17(4): p. 500-6.

17. Williams, K.L., Cortez, V., Dingens, A.S., Gach, J.S., Rainwater, S., Weis, J.F., et al., HIV-specific CD4-induced Antibodies Mediate Broad and Potent Antibody-dependent Cellular Cytotoxicity Activity and Are Commonly Detected in Plasma From HIV-infected humans. EBioMedicine, 2015. 2(10): p. 1464-77.

18. Lambotte, O., Ferrari, G., Moog, C., Yates, N.L., Liao, H.X., Parks, R.J., et al., Heterogeneous neutralizing antibody and antibody-dependent cell cytotoxicity responses in HIV-1 elite controllers. AIDS, 2009. 23(8): p. 897-906.

19. Madhavi, V., Wines, B.D., Amin, J., Emery, S., Group, E.S., Lopez, E., et al., HIV-1 Env- and Vpu-Specific Antibody-Dependent Cellular Cytotoxicity Responses Associated with Elite Control of HIV. J Virol, 2017. 91(18).

20. Richard, J., Prevost, J., Baxter, A.E., von Bredow, B., Ding, S., Medjahed, H., et al., Uninfected Bystander Cells Impact the Measurement of HIV-Specific Antibody-Dependent Cellular Cytotoxicity Responses. mBio, 2018. 9(2).

21. Raja, A., Venturi, M., Kwong, P., and Sodroski, J., CD4 binding site antibodies inhibit human immunodeficiency virus gp120 envelope glycoprotein interaction with CCR5. J Virol, 2003. 77(1): p. 713-8.

22. Scheid, J.F., Mouquet, H., Ueberheide, B., Diskin, R., Klein, F., Oliveira, T.Y., et al., Sequence and structural convergence of broad and potent HIV antibodies that mimic CD4 binding. Science, 2011. 333(6049): p. 1633-7.

23. Wu, X., Yang, Z.Y., Li, Y., Hogerkorp, C.M., Schief, W.R., Seaman, M.S., et al., Rational design of envelope identifies broadly neutralizing human monoclonal antibodies to HIV-1. Science, 2010. 329(5993): p. 856-61.

24. von Bredow, B., Arias, J.F., Heyer, L.N., Moldt, B., Le, K., Robinson, J.E., et al., Comparison of Antibody-Dependent Cell-Mediated Cytotoxicity and Virus Neutralization by HIV-1 Env-Specific Monoclonal Antibodies. J Virol, 2016. 90(13): p. 6127-6139.

25. Bruel, T., Guivel-Benhassine, F., Lorin, V., Lortat-Jacob, H., Baleux, F., Bourdic, K., et al., Lack of ADCC Breadth of Human Nonneutralizing Anti-HIV-1 Antibodies. J Virol, 2017. 91(8).

26. Bruel, T., Guivel-Benhassine, F., Amraoui, S., Malbec, M., Richard, L., Bourdic, K., et al., Elimination of HIV-1-infected cells by broadly neutralizing antibodies. Nat Commun, 2016. 7: p. 10844.

27. Dupuy, F.P., Kant, S., Barbe, A., Routy, J.P., Bruneau, J., Lebouche, B., et al., Antibody-Dependent Cellular Cytotoxicity-Competent Antibodies against HIV-1-Infected Cells in Plasma from HIV-Infected Subjects. mBio, 2019. 10(6).

28. Kiani Z., Bruneau J., Geraghty D. E., and F., B.N., HLA-F on Autologous HIV-Infected Cells Activates Primary NK Cells Expressing the Activating Killer Immunoglobulin-Like Receptor KIR3DS1. J Virol, 2019. 93(18).

29. Kiani, Z., Dupuy, F.P., Bruneau, J., Lebouche, B., Retiere, C., Geraghty, D.E., et al., The Education of NK Cells Determines Their Responsiveness to Autologous HIV-Infected CD4 T Cells. J Virol, 2019. 93(23).

30. Richard, J., Veillette, M., Ding, S., Zoubchenok, D., Alsahafi, N., Coutu, M., et al., Small CD4 Mimetics Prevent HIV-1 Uninfected Bystander CD4 + T Cell Killing Mediated by Antibody-dependent Cell-mediated Cytotoxicity. EBioMedicine, 2016. 3: p. 122-134.

31. Naiman, N.E., Slyker, J., Richardson, B.A., John-Stewart, G., Nduati, R., and Overbaugh, J.M., Antibody-dependent cellular cytotoxicity targeting CD4-inducible epitopes predicts mortality in HIV-infected infants. EBioMedicine, 2019. 47: p. 257-268.

32. Lindwasser, O.W., Chaudhuri, R., and Bonifacino, J.S., Mechanisms of CD4 downregulation by the Nef and Vpu proteins of primate immunodeficiency viruses. Curr Mol Med, 2007. 7(2): p. 171-84.

33. Magadan, J.G., Perez-Victoria, F.J., Sougrat, R., Ye, Y., Strebel, K., and Bonifacino, J.S., Multilayered mechanism of CD4 downregulation by HIV-1 Vpu involving distinct ER retention and ERAD targeting steps. PLoS Pathog, 2010. 6(4): p. e1000869.

34. Munro, J.B., Gorman, J., Ma, X., Zhou, Z., Arthos, J., Burton, D.R., et al., Conformational dynamics of single HIV-1 envelope trimers on the surface of native virions. Science, 2014. 346(6210): p. 759-63.

35. Veillette, M., Coutu, M., Richard, J., Batraville, L.A., Dagher, O., Bernard, N., et al., The HIV-1 gp120 CD4-bound conformation is preferentially targeted by antibody-dependent cellular cytotoxicity-mediating antibodies in sera from HIV-1-infected individuals. J Virol, 2015. 89(1): p. 545-51.

36. Veillette, M., Desormeaux, A., Medjahed, H., Gharsallah, N.E., Coutu, M., Baalwa, J., et al., Interaction with cellular CD4 exposes HIV-1 envelope epitopes targeted by antibody-dependent cell-mediated cytotoxicity. J Virol, 2014. 88(5): p. 2633-44.

37. Prevost, J., Richard, J., Ding, S., Pacheco, B., Charlebois, R., Hahn, B.H., et al., Envelope glycoproteins sampling states 2/3 are susceptible to ADCC by sera from HIV-1-infected individuals. Virology, 2018. 515: p. 38-45.

38. Richard, J., Prevost, J., Alsahafi, N., Ding, S., and Finzi, A., Impact of HIV-1 Envelope Conformation on ADCC Responses. Trends Microbiol, 2018. 26(4): p. 253-265.

39. Dufloo, J., Guivel-Benhassine, F., Buchrieser, J., Lorin, V., Grzelak, L., Dupouy, E., et al., Anti-HIV-1 antibodies trigger non-lytic complement deposition on infected cells. EMBO Rep, 2020. 21(2): p. e49351.

40. Ferrari, G., Pollara, J., Kozink, D., Harms, T., Drinker, M., Freel, S., et al., An HIV-1 gp120 envelope human monoclonal antibody that recognizes a C1 conformational epitope mediates potent antibody-dependent cellular cytotoxicity (ADCC) activity and defines a common ADCC epitope in human HIV-1 serum. J Virol, 2011. 85(14): p. 7029-36.

41. Chung, A.W., Kumar, M.P., Arnold, K.B., Yu, W.H., Schoen, M.K., Dunphy, L.J., et al., Dissecting Polyclonal Vaccine-Induced Humoral Immunity against HIV Using Systems Serology. Cell, 2015. 163(4): p. 988-98.

42. Chung, A.W., Ghebremichael, M., Robinson, H., Brown, E., Choi, I., Lane, S., et al., Polyfunctional Fc-Effector Profiles Mediated by IgG Subclass Selection Distinguish RV144 and VAX003 Vaccines. Science Translational Medicine, 2014. 6(228): p. 228ra38-228ra38.

43. Okulicz, J.F., Marconi, V.C., Landrum, M.L., Wegner, S., Weintrob, A., Ganesan, A., et al., Clinical outcomes of elite controllers, viremic controllers, and long-term nonprogressors in the US Department of Defense HIV natural history study. J Infect Dis, 2009. 200(11): p. 1714-23.

44. Deeks, S.G. and Walker, B.D., Human immunodeficiency virus controllers: mechanisms of durable virus control in the absence of antiretroviral therapy. Immunity, 2007. 27(3): p. 406-16.

45. International, H.I.V.C.S., Pereyra, F., Jia, X., McLaren, P.J., Telenti, A., de Bakker, P.I., et al., The major genetic determinants of HIV-1 control affect HLA class I peptide presentation. Science, 2010. 330(6010): p. 1551-7.

46. Kant, S., Zhang, N., Routy, J.P., Tremblay, C., Thomas, R., Szabo, J., et al., Quantifying Anti-HIV Envelope-Specific Antibodies in Plasma from HIV Infected Individuals. Viruses, 2019. 11(6).

47. Cao, W., Mehraj, V., Trottier, B., Baril, J.G., Leblanc, R., Lebouche, B., et al., Early Initiation Rather Than Prolonged Duration of Antiretroviral Therapy in HIV Infection Contributes to the Normalization of CD8 T-Cell Counts. Clin Infect Dis, 2016. 62(2): p. 250-257.

48. Jenabian, M.A., El-Far, M., Vyboh, K., Kema, I., Costiniuk, C.T., Thomas, R., et al., Immunosuppressive Tryptophan Catabolism and Gut Mucosal Dysfunction Following Early HIV Infection. J Infect Dis, 2015. 212(3): p. 355-66.

49. Imbeault, M., Lodge, R., Ouellet, M., and Tremblay, M.J., Efficient magnetic bead-based separation of HIV-1-infected cells using an improved reporter virus system reveals that p53 up-regulation occurs exclusively in the virus-expressing cell population. Virology, 2009. 393(1): p. 160-7.

50. Banerjee, K., Klasse, P.J., Sanders, R.W., Pereyra, F., Michael, E., Lu, M., et al., IgG Subclass Profiles in Infected HIV Type 1 Controllers and Chronic Progressors and in Uninfected Recipients of Env Vaccines. AIDS and Hum Ret, 2010. 26(4).

51. Ackerman, M.E., Moldt, B., Wyatt, R.T., Dugast, A.S., McAndrew, E., Tsoukas, S., et al., A robust, high-throughput assay to determine the phagocytic activity of clinical antibody samples. J Immunol Methods, 2011. 366(1-2): p. 8-19.

52. Barouch, D.H., Alter, G., Broge, T., Linde, C., Ackerman, M.E., Brown, E.P., et al., Protective efficacy of adenovirus/protein vaccines against SIV challenges in rhesus monkeys. Science, 2015. 349(6245): p. 320-4.

53. Fischinger, S., Fallon, J.K., Michell, A.R., Broge, T., Suscovich, T.J., Streeck, H., et al., A high-throughput, bead-based, antigen-specific assay to assess the ability of antibodies to induce complement activation. J Immunol Methods, 2019. 473: p. 112630.

54. Kramski, M., Schorcht, A., Johnston, A.P., Lichtfuss, G.F., Jegaskanda, S., De Rose, R., et al., Role of monocytes in mediating HIV-specific antibody-dependent cellular cytotoxicity. J Immunol Methods, 2012. 384(1-2): p. 51-61.

55. Chomont, N., El-Far, M., Ancuta, P., Trautmann, L., Procopio, F.A., Yassine-Diab, B., et al., HIV reservoir size and persistence are driven by T cell survival and homeostatic proliferation. Nat Med, 2009. 15(8): p. 893-900.

56. Vandergeeten, C., Fromentin, R., Merlini, E., Lawani, M.B., DaFonseca, S., Bakeman, W., et al., Cross-clade ultrasensitive PCR-based assays to measure HIV persistence in large-cohort studies. J Virol, 2014. 88(21): p. 12385-96.

57. Notermans, D.W., De Jong, J.J., Goudsmit, J., Bakker, M., Roos, M.T.L., Nijholt, L., et al., Potent Antiretroviral Therapy Initiates Normalization of Hypergammaglobulinemia and a Decline in HIV Type 1-Specific Antibody Responses. AIDS Res Hum Retroviruses, 2001. 17: p. 6.

58. Nagase, H., Agematsu, K., Kitano, K., Takamoto, M., Okubo, Y., Komiyama, A., et al., Mechanism of hypergammaglobulinemia by HIV infection: circulating memory B-cell reduction with plasmacytosis. Clin Immunol, 2001. 100(2): p. 250-9.

59. Ackerman, M.E., Crispin, M., Yu, X., Baruah, K., Boesch, A.W., Harvey, D.J., et al., Natural variation in Fc glycosylation of HIV-specific antibodies impacts antiviral activity. J Clin Invest, 2013. 123(5): p. 2183-92.

60. Jia, M., Li, D., He, X., Zhao, Y., Peng, H., Ma, P., et al., Impaired natural killer cell-induced antibody-dependent cell-mediated cytotoxicity is associated with human immunodeficiency virus-1 disease progression. Clin Exp Immunol, 2013. 171(1): p. 107-16.

61. Mabuka, J., Nduati, R., Odem-Davis, K., Peterson, D., and Overbaugh, J., HIV-specific antibodies capable of ADCC are common in breastmilk and are associated with reduced risk of transmission in women with high viral loads. PLoS Pathog, 2012. 8(6): p. e1002739.

62. Fischinger, S., Shin, S., Boudreau, C.M., Ackerman, M., Rerks-Ngarm, S., Pitisuttithum, P., et al., Protein-based, but not viral vector alone, HIV vaccine boosting drives an IgG1-biased polyfunctional humoral immune response. JCI Insight, 2020. 5(12).

63. Lee, W.S., Richard, J., Lichtfuss, M., Smith, A.B., 3rd, Park, J., Courter, J.R., et al., Antibody-Dependent Cellular Cytotoxicity against Reactivated HIV-1-Infected Cells. J Virol, 2016. 90(4): p. 2021-30.

64. Pollara, J., Hart, L., Brewer, F., Pickeral, J., Packard, B.Z., Hoxie, J.A., et al., High-throughput quantitative analysis of HIV-1 and SIV-specific ADCC-mediating antibody responses. Cytometry A, 2011. 79(8): p. 603-12.

65. Richardson, S.I., Crowther, C., Mkhize, N.N., and Morris, L., Measuring the ability of HIV-specific antibodies to mediate trogocytosis. J Immunol Methods, 2018. 463: p. 71-83.

66. [No Authors Listed], Experimental HIV vaccine regimen ineffective in preventing HIV. 2020.

67. [No Authors Listed], HIV vaccine trial failure is a “wake up call” for southern Africa, say researchers.

68. Shen, X., Laher, F., Moodie, Z., McMillan, A.S., Spreng, R.L., Gilbert, P.B., et al., HIV-1 Vaccine Sequences Impact V1V2 Antibody Responses: A Comparison of Two Poxvirus Prime gp120 Boost Vaccine Regimens. Sci Rep, 2020. 10(1): p. 2093.

69. Bekker, L.-G., Moodie, Z., Grunenberg, N., Laher, F., Tomaras, G.D., Cohen, K.W., et al., Subtype C ALVAC-HIV and bivalent subtype C gp120/MF59 HIV-1 vaccine in low-risk, HIV-uninfected, South African adults: a phase 1/2 trial. The Lancet HIV, 2018. 5(7): p. e366-e378.

70. [No Authors Listed]. Available from: http://www.hiv.lanl.gov.

71. Prevost, J., Zoubchenok, D., Richard, J., Veillette, M., Pacheco, B., Coutu, M., et al., Influence of the Envelope gp120 Phe 43 Cavity on HIV-1 Sensitivity to Antibody-Dependent Cell-Mediated Cytotoxicity Responses. J Virol, 2017. 91(7).

72. Zoubchenok, D., Veillette, M., Prevost, J., Sanders-Buell, E., Wagh, K., Korber, B., et al., Histidine 375 Modulates CD4 Binding in HIV-1 CRF01_AE Envelope Glycoproteins. J Virol, 2017. 91(4).

73. Desormeaux, A., Coutu, M., Medjahed, H., Pacheco, B., Herschhorn, A., Gu, C., et al., The highly conserved layer-3 component of the HIV-1 gp120 inner domain is critical for CD4-required conformational transitions. J Virol, 2013. 87(5): p. 2549-62.

74. Alsahafi, N., Ding, S., Richard, J., Markle, T., Brassard, N., Walker, B., et al., Nef Proteins from HIV-1 Elite Controllers Are Inefficient at Preventing Antibody-Dependent Cellular Cytotoxicity. J Virol, 2015. 90(6): p. 2993-3002.

75. Buckner, C.M., Kardava, L., Zhang, X., Gittens, K., Justement, J.S., Kovacs, C., et al., Maintenance of HIV-Specific Memory B-Cell Responses in Elite Controllers Despite Low Viral Burdens. J Infect Dis, 2016. 214(3): p. 390-8.

76. Bussmann, B.M., Reiche, S., Bieniek, B., Krznaric, I., Ackermann, F., and Jassoy, C., Loss of HIV-specific memory B-cells as a potential mechanism for the dysfunction of the humoral immune response against HIV. Virology, 2010. 397(1): p. 7-13.

77. Mens, H., Kearney, M., Wiegand, A., Shao, W., Schonning, K., Gerstoft, J., et al., HIV-1 continues to replicate and evolve in patients with natural control of HIV infection. J Virol, 2010. 84(24): p. 12971-81.

78. Lamine, A., Caumont-Sarcos, A., Chaix, M.-L., Saez-Cirion, A., Rouzioux, C., Delfraissy, J.-F., et al., Replication-competent HIV strains infect HIV controllers despite undetectable viremia (ANRS EP36 study). AIDS, 2007. 21(8).

79. Hatano, H., Delwart, E.L., Norris, P.J., Lee, T.H., Dunn-Williams, J., Hunt, P.W., et al., Evidence for persistent low-level viremia in individuals who control human immunodeficiency virus in the absence of antiretroviral therapy. J Virol, 2009. 83(1): p. 329-35.

80. Pereyra, F., Palmer, S., Miura, T., Block, B.L., Wiegand, A., Rothchild, A.C., et al., Persistent low-level viremia in HIV-1 elite controllers and relationship to immunologic parameters. J Infect Dis, 2009. 200(6): p. 984-90.

81. Ho, Y.C., Shan, L., Hosmane, N.N., Wang, J., Laskey, S.B., Rosenbloom, D.I., et al., Replication-competent noninduced proviruses in the latent reservoir increase barrier to HIV-1 cure. Cell, 2013. 155(3): p. 540-51.

82. Procopio, F.A., Fromentin, R., Kulpa, D.A., Brehm, J.H., Bebin, A.G., Strain, M.C., et al., A Novel Assay to Measure the Magnitude of the Inducible Viral Reservoir in HIV-infected Individuals. EBioMedicine, 2015. 2(8): p. 874-83.

83. Baxter, A.E., Niessl, J., Fromentin, R., Richard, J., Porichis, F., Massanella, M., et al., Multiparametric characterization of rare HIV-infected cells using an RNA-flow FISH technique. Nat Protoc, 2017. 12(10): p. 2029-2049.

84. Baxter, A.E., Niessl, J., Fromentin, R., Richard, J., Porichis, F., Charlebois, R., et al., Single-Cell Characterization of Viral Translation-Competent Reservoirs in HIV-Infected Individuals. Cell Host Microbe, 2016. 20(3): p. 368-380.

85. Pardons, M., Baxter, A.E., Massanella, M., Pagliuzza, A., Fromentin, R., Dufour, C., et al., Single-cell characterization and quantification of translation-competent viral reservoirs in treated and untreated HIV infection. PLoS Pathog, 2019. 15(2): p. e1007619.

10. Figure captions

Figure 1. Quantification of HIV gp120- and Envelope (Env)-specific antibodies (Abs) in plasma from HIV^+ subjects. The concentration of gp120/Env-specific Abs in plasma from four groups of HIV^+ subjects relative to HIVIG was assessed using (A) an ELISA assay in which plates were coated with recombinant gp120 (gp120) and (B) by measuring binding to native, closed conformation Env on sorted HIV-infected CEM.NKr.CCR5 (siCEM) cells by flow cytometry. "x" denotes sample(s) for which Abs concentrations were below the limit of detection. Each point represents results generated by the plasma of a single individual. Lines and error bars though each data set represent medians and inter-quartile ranges (IQRs). Data from 18 UTPs, 24 TPs, 37 ECs and 16 VC are used to prepare panels A and B. Kruskal-Wallis tests with Dunn's multiple comparisons post test were used to assess the significance of between-group differences. * = $p < 0.05$, ** = $p < 0.01$, **** = $p < 0.0001$. HIVIG = a pool of plasma from HIV-infected subjects; gp120-PBE = gp120 plate-based ELISA; UTP = untreated progressors; TP = HIV-infected subjects in chronic phase infection on antiretroviral therapy; EC = Elite Controllers; VC = Viral Controllers.

Figure 2. Quantification of Ab-dependent (AD) functions in HIV^+ plasma. HIV^+ plasma from UTPs, TPs, ECs and VCs were tested for (A) AD cellular phagocytosis (ADCP), (B) AD complement deposition (ADCD), (C) AD cellular cytotoxicity (ADCC) and (D) AD cellular

trogocytosis (ADCT) as described in the methods. Each point represents results generated by the plasma of a single individual. Lines and error bars though each data set represent medians and IQRs. Data from 18 UTPs, 24 TPs, 37 ECs and 16 VC are used to prepare these 4 panels. Kruskal-Wallis tests with Dunn's multiple comparisons post test were used to assess the significance of between-group differences. * = $p < 0.05$, ** = $p < 0.01$, *** = $p < 0.001$, **** = $p < 0.0001$. All results shown were background subtracted and were normalized to the concentrations of internal HIVIG positive controls tested at the same time as test samples. AUC = partial area under the curve; PS = phagocytic score; CDS = complement deposition score; %AnV$^+$ cells = frequency of AnnexinV$^+$ siCEM cells; %PKH-26$^+$ cells = frequency of PKH-26$^+$ cells.

Figure 3. Correlation of AD functions with each other and with anti-HIV-gp120/Env Ab concentrations within HIV-infected subject groups. Correlation matrices for each pairwise combination of AD function and anti-gp120/Env-specific Abs concentrations tested in the four subject groups. Data from 18 UTPs, 24 TPs, 36 ECs and 16 VC were used to generate panel A. Data from 17 UTPs, 19 TPs, 36 ECs and 16 VC were used to generate panels B-C. The increasing strength of positive correlations are illustrated using increasing blue color depth, as depicted in the legend and by the size of each circle. The statistical significance of pairwise correlations is indicated by the number of "*" symbols in each circle (* = $p < 0.05$, ** = $p < 0.01$, *** = $p < 0.001$, **** = $p < 0.0001$). Empty circles represent p-values for correlative relationships that fell below the level of significance ($p > 0.05$). Shown are unadjusted p-values to aid in relative comparisons. Correlation coefficients were calculated using Spearman's correlation tests and they were plotted using Rstudio v1.2.

Figure 4. AD function results normalized to input anti-gp120/Env-specific Ab concentrations present in HIV+ plasma samples. (A) ADCP functional results were normalized to anti-gp120-

specific Ab concentrations in HIV+ plasma quantified using the PBE assay (B) ADCD, (C) ADCC and (D) ADCT functional results were normalized to anti-Env Ab concentrations in HIV+ plasma quantified by binding to siCEM cells. Each point represents a single subject. Lines and error bars though each data set represent medians and IQRs. Data from 18 UTPs, 24 TPs, 37 ECs and 16 VC are used to prepare these 4 panels. Kruskal-Wallis tests with Dunn's multiple comparisons post test were used to assess the significance of between-group differences. * = $p < 0.05$, ** = $p < 0.01$. All results shown were background subtracted and are relative to the concentrations of an internal HIVIG positive control tested at the same time as test samples. "x" symbols represent negative values after background correction. AUC = partial area under the curve; PS = phagocytic score; CDS = complement deposition score; %AnV$^+$ cells = frequency of Annexin V$^+$ siCEM cells; %PKH-26+ cells = frequency of PKH-26$^+$ cells.

Figure 5. Higher ADCC function in HIV controllers is associated an HIV reservoir size below the limit of quantification. The HIV reservoir size in 30 ECs and 16 VCs was measured using the integrated HIV PCR assay. Results were stratified into a group with detectable (n=8, [3 EC and 5 VC]) and undetectable [n=38, 27 EC and 11 VC]) HIV reservoir sizes. (A) The y-axis shows the levels of ADCP function normalized to the anti-gp120-specific Ab concentrations in HIV$^+$ plasma quantified using the PBE assay. (B-D) The y-axes show the levels of ADCD, ADCC and ADCT functions, respectively, normalized to the anti-Env Ab concentration in HIV$^+$ plasma quantified using the siCEM binding assay. Each point represents a single subject. Results for ECs are illustrated in black and those for VCs in red. Lines and error bars though each data set represent medians and IQRs. The significance of between-group differences was assessed using Mann-Whitney tests. P-values are depicted above the lines linking groups being compared.

Supplementary Figure 1. Frequency of AnnexinV$^+$ target cells generated by negative control conditions in an antibody dependent cellular cytotoxicity (ADCC) assay. The y-axis shows the frequency of Annexin V+ target cells generated in an ADCC assay as described in the methods section. Target cells included siCEM cells tested 3 times and HIV uninfected CEM cells (negative control). Target cells were opsonized with 50 or 500 μg/ml of IgG from the positive control HIVIG, a pool of plasma from HIV negative subjects (HIV Ig #1), IgG from HIV negative serum (HIV-Ig #2) and no antibody. Each antibody concentration and the no antibody wells were tested in duplicates and each symbol represents the mean of duplicate determinations.

Supplementary Figure 2. Visualization of antibody dependent cellular trogocytosis (ADCT) using ImageStream®. Single monocytes acquire pieces of membrane from HIVIG opsonized gp120-coated CEM cells labelled with CFSE and PKH-26. (A) Three single gp120-coated CEM cells positive for the fluorochromes FITC (CFSE) and PE (PKH-26) but not for BV786 (CD14). (B) Three single monocytes as shown by the positive signal for the BV786 fluorochrome conjugated to anti-CD14, after a one-hour incubation with CFSE$^+$PKH26$^+$ gp120-coated CEM cells and HIVIG. Membrane (PKH-26) but not cytosolic (CFSE) material was transferred gp120-coated CEM cells by ADCT to single monocytes as demonstrated by the absence of doublets by bright field microscopy.

Supplementary Figure 3. Quantification of total IgG in HIV$^+$ plasma. Plasma samples from 18 UTPs, 24 TPs, 37 ECs and 16 VCs were quantified for total IgG using a plate-based human IgG ELISA quantification kit.

Supplementary Figure 4. Quantification of Ab-dependent (AD) functions in HIV$^+$ plasma. Shown are the results generated by HIV$^+$ plasma from 18 UTPs, 24 TPs, 37 ECs and 16 VCs tested for (A) ADCP, (B) ADCD, (C) ADCC and (D) ADCT as in Figure 2. Results shown were background

subtracted but were not normalized to the concentrations of their internal HIVIG positive controls. Panels A, B, C and D display the results generated by HIVIG present in the 9, 5, 8 and 8 96-well plates, respectively, used to test these AD functions. AUC = partial area under the curve; PS = phagocytic score; CDS = complement deposition score; %AnV$^+$ cells = frequency of Annexin V$^+$ cells; %PKH-26$^+$ cells = frequency of PKH-26$^+$ cells.

11. Figures

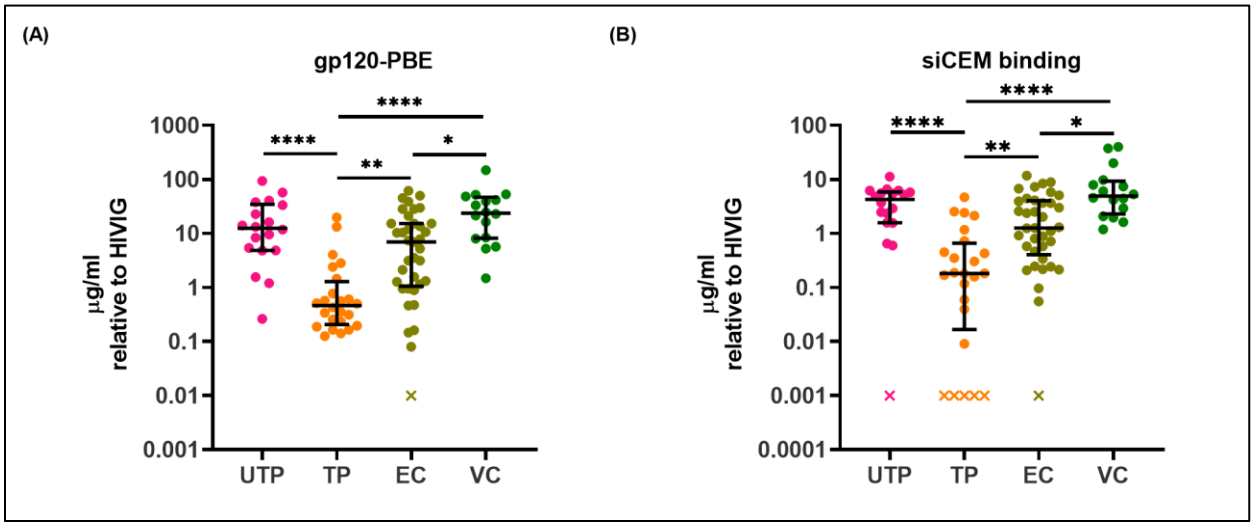

Figure 17 (Figure 1 in article): Quantification of HIV gp120- and Envelope (Env)-specific antibodies (Abs) in plasma from HIV$^+$ subjects.

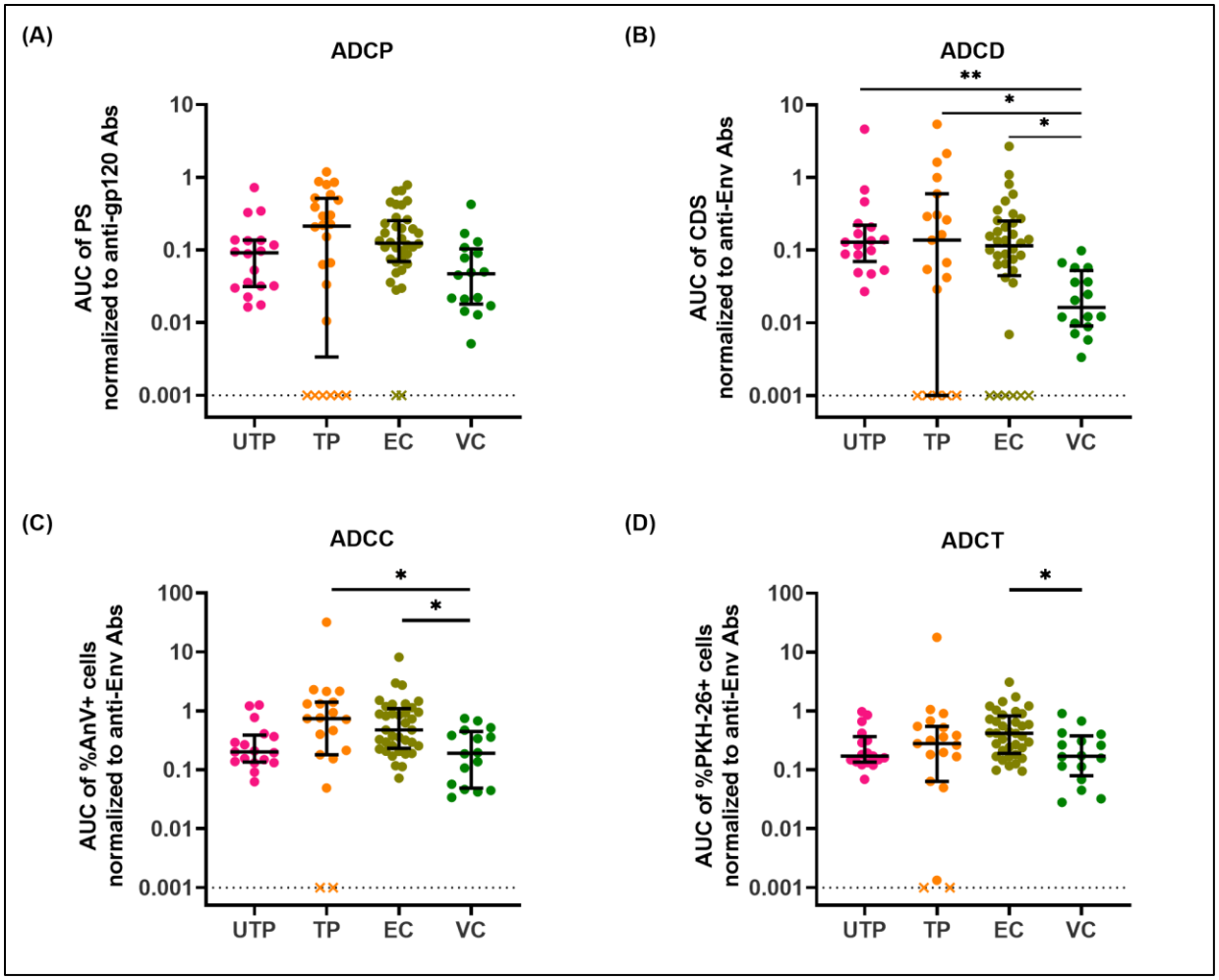

3961

3962 *Figure 18 (Figure 2 in article): Quantification of Ab-dependent (AD) functions in HIV$^+$ plasma.*

3963 *HIV$^+$ plasma from UTPs, TPs, ECs and VCs were tested for (A) AD cellular phagocytosis (ADCP),*

3964 *(B) AD complement deposition (ADCD), (C) AD cellular cytotoxicity (ADCC) and (D) AD cellular*

3965 *trogocytosis (ADCT) as described in the methods.*

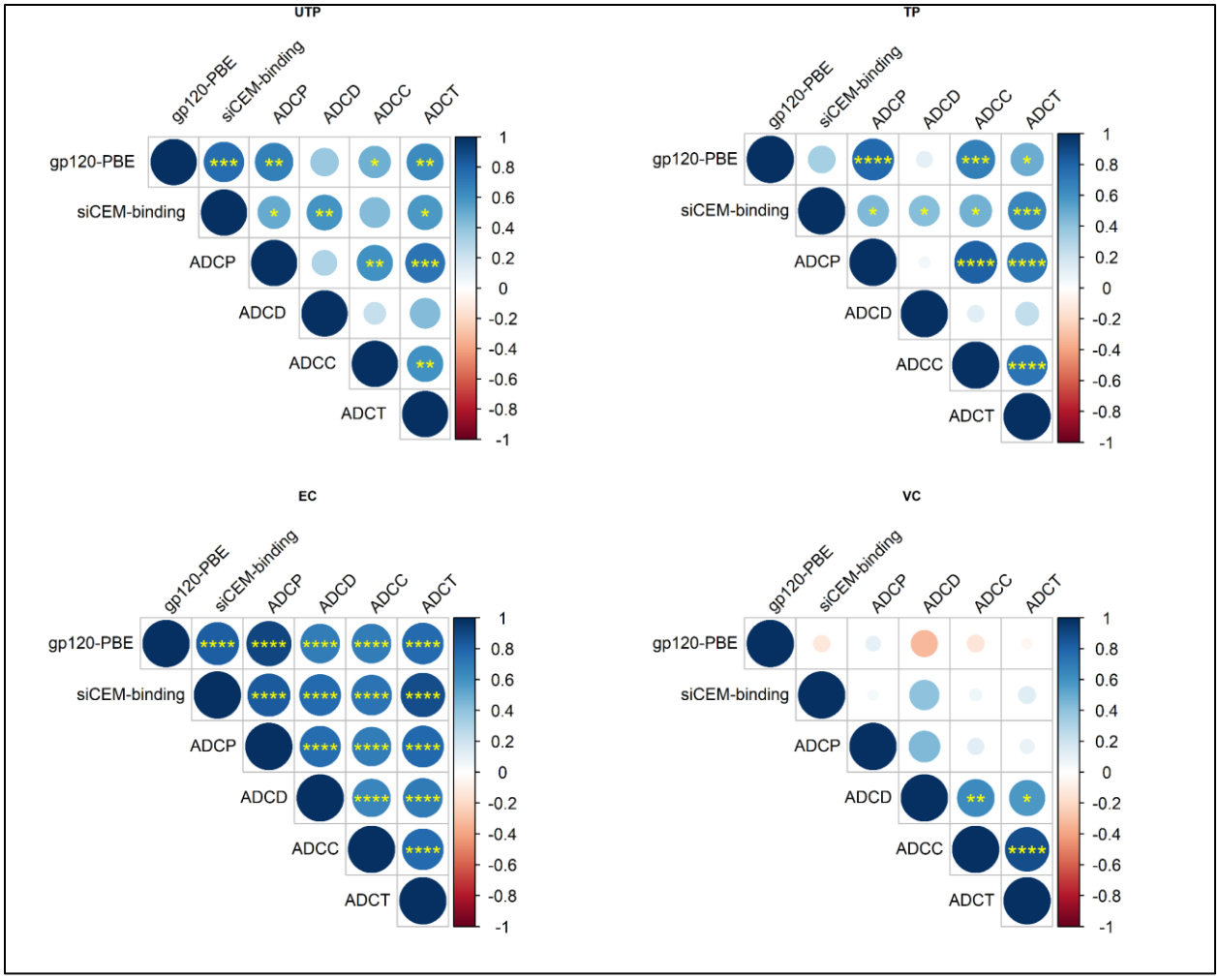

Figure 19 (Figure 3 in article): Correlation of AD functions with each other and with anti-HIV-gp120/Env Ab concentrations within HIV-infected subject groups.

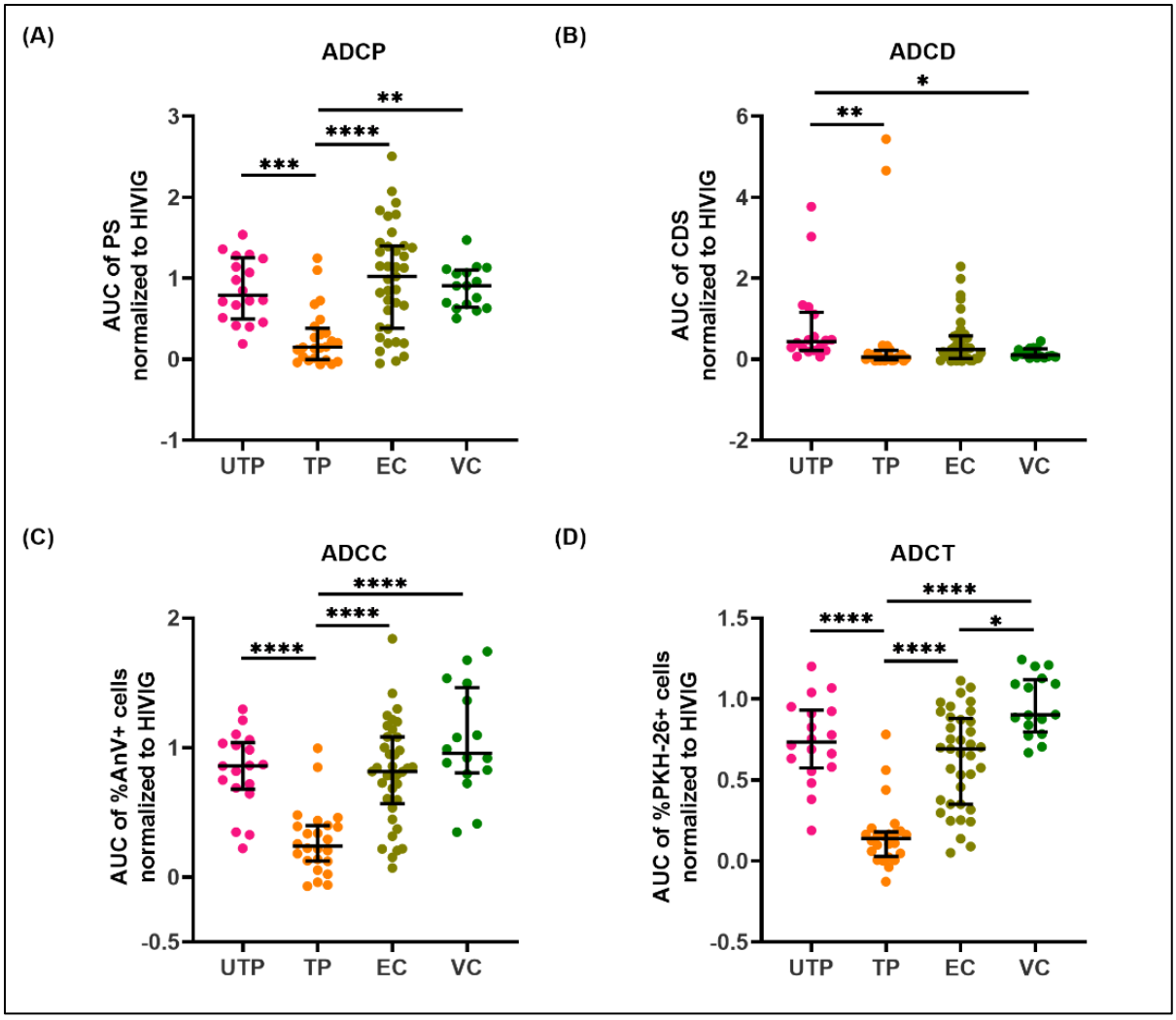

3969

3970 *Figure 20 (Figure 4 in article): AD function results normalized to input anti-gp120/Env-specific*

3971 *Ab concentrations present in HIV^{+} plasma samples.*

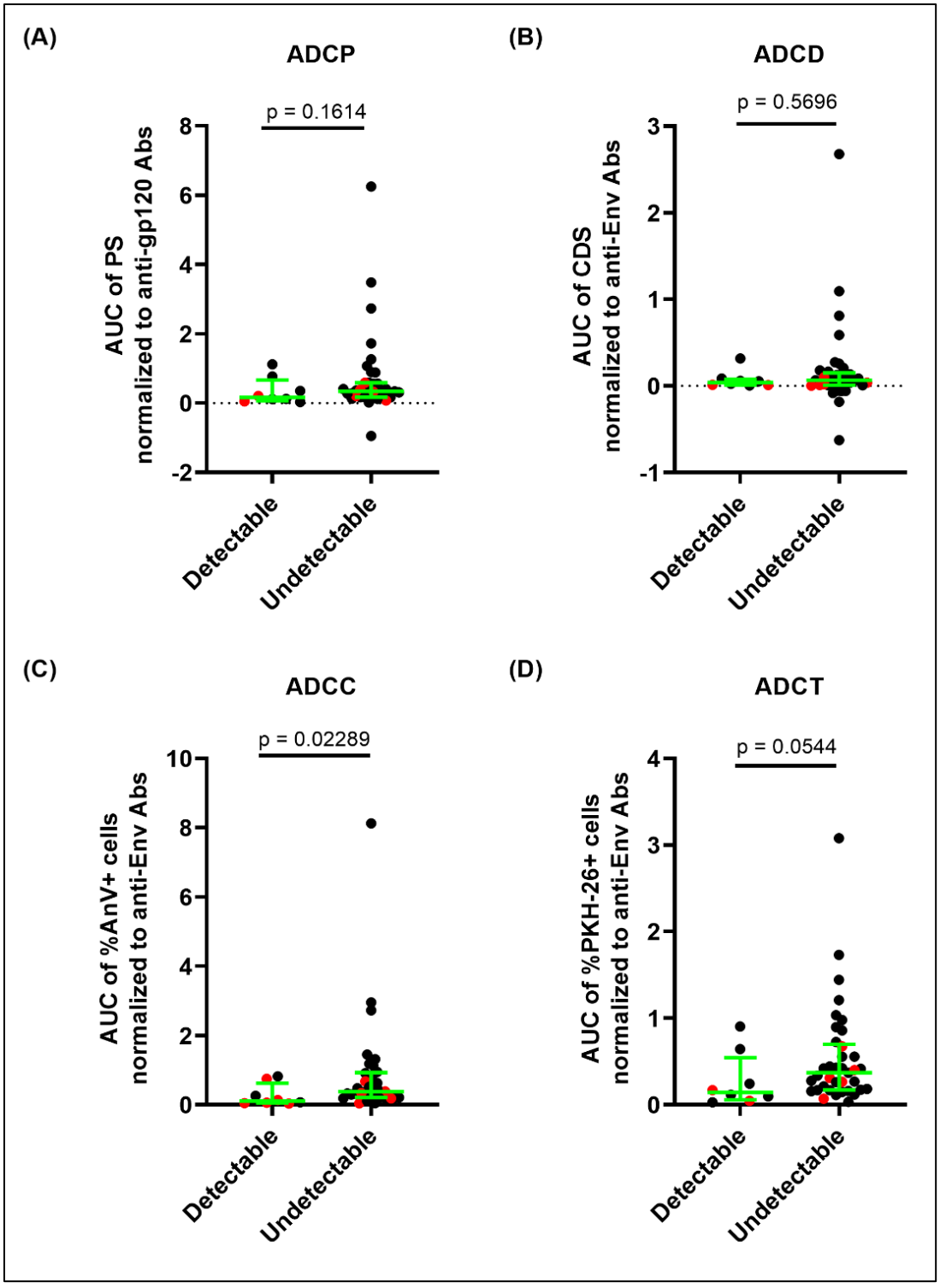

Figure 21 (Figure 5 in article): Higher ADCC function in HIV controllers is associated an HIV reservoir size below the limit of quantification.

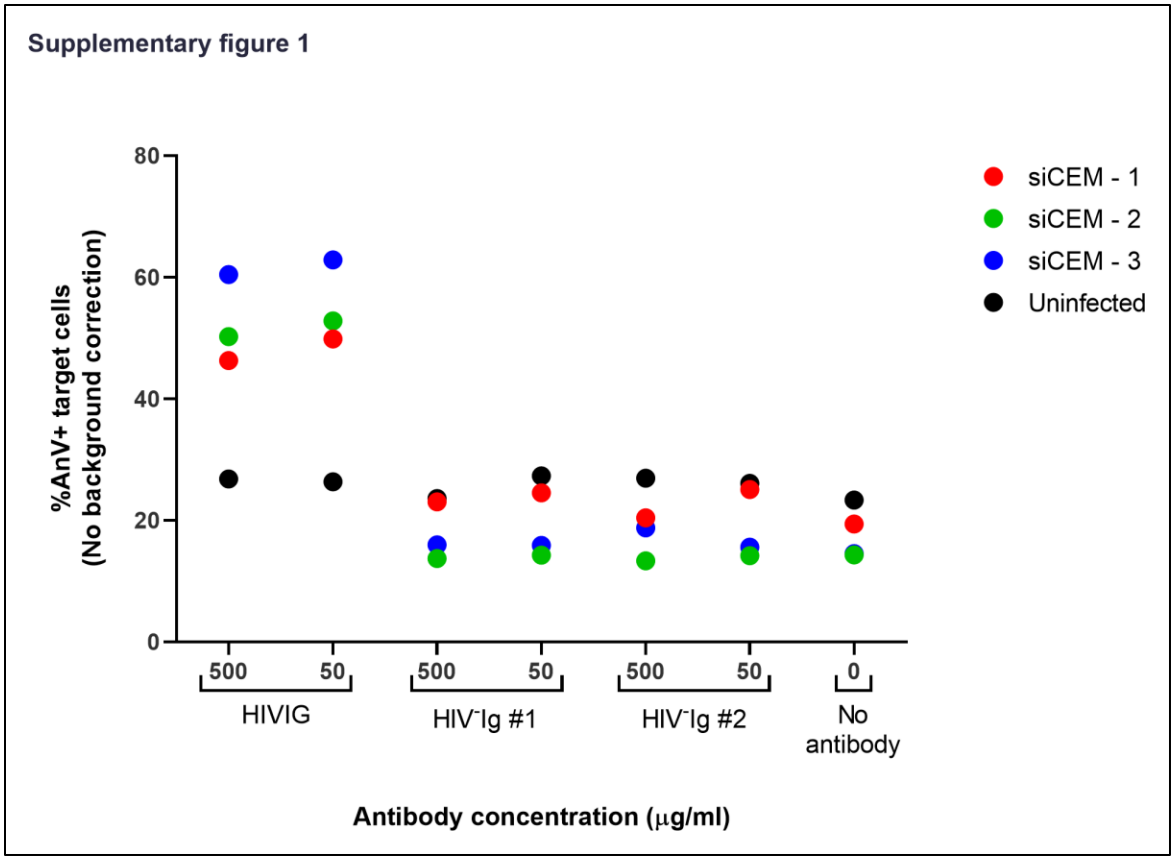

3975

3976 *Figure 22 (Supplemental figure 1 in article): Frequency of AnnexinV^{+} target cells generated by*

3977 *negative control conditions in an antibody dependent cellular cytotoxicity (ADCC) assay.*

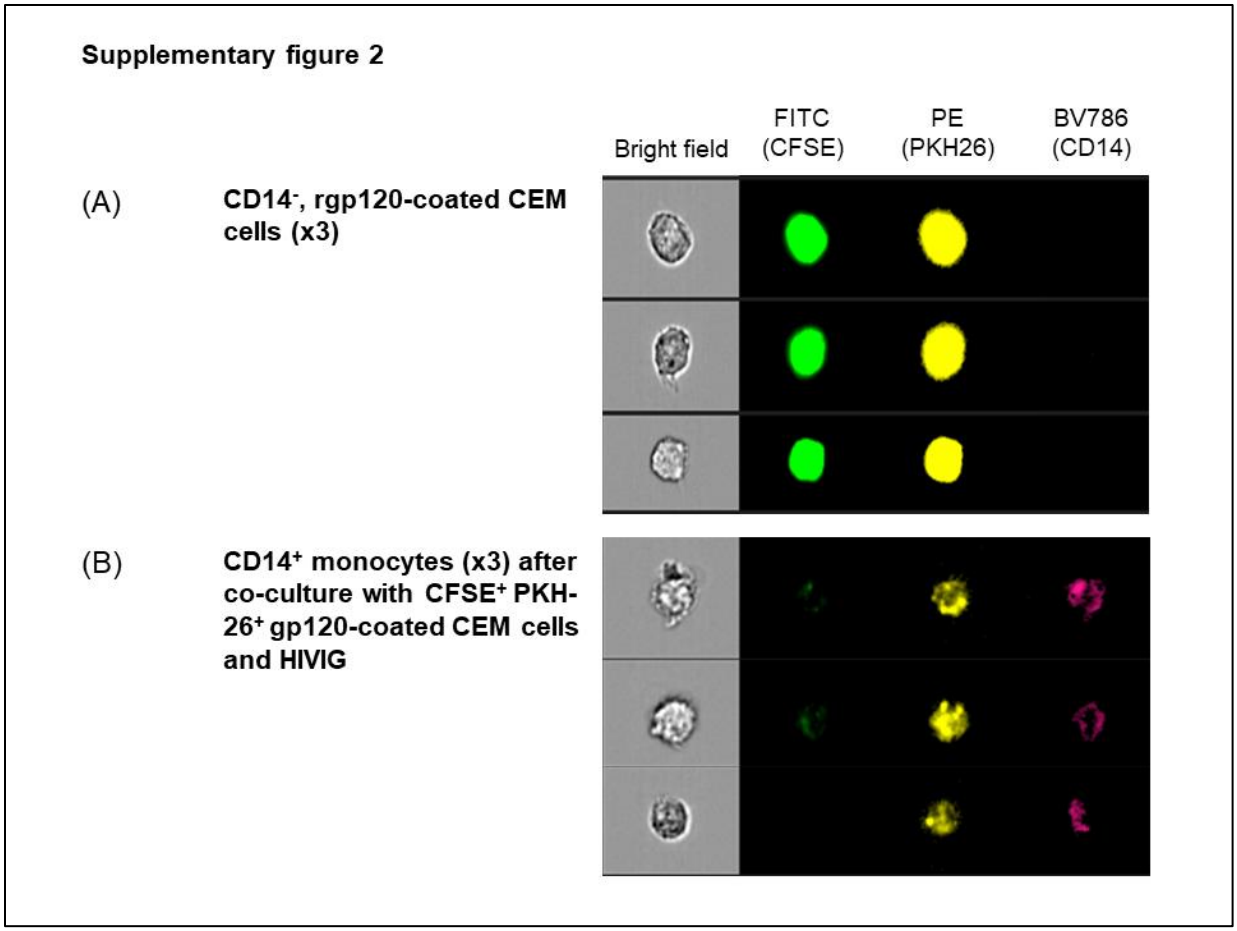

Figure 23 (Supplemental figure 1 in article): Visualization of antibody dependent cellular trogocytosis (ADCT) using ImageStream®.

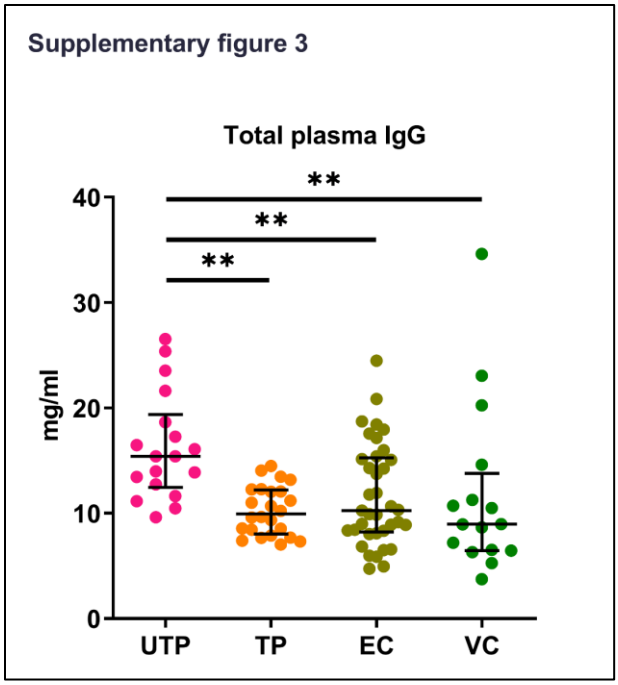

Figure 24 (Supplemental figure 2 in article): Quantification of total IgG in HIV^{+} plasma.

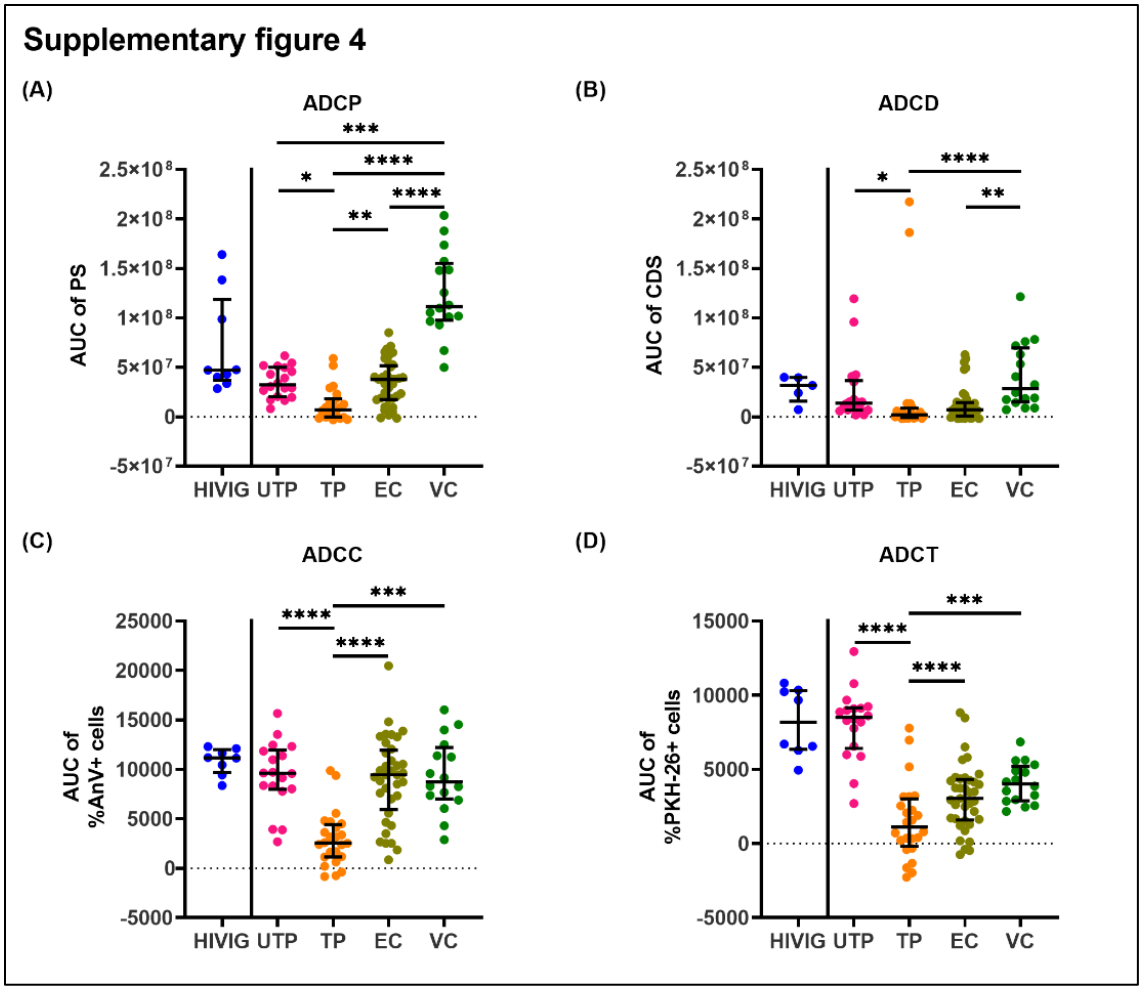

3983

3984 *Figure 25 (Supplemental figure 3 in article): Quantification of Ab-dependent (AD) functions in*

3985 *HIV⁺ plasma.*

3986

Bridge from Chapter 3 to Chapter 4

In Chapter 3, we expanded our study group to include VCs. Using the siCEM cells, we reported that the amount of gp120-specific Abs measured by binding to gp120-coated wells and Env-specific Abs measured by binding to siCEM wells did not differ significantly in plasma from UTPs, ECs, and VCs. Plasma from VCs had significantly higher gp120- and Env-specific Abs levels than plasma from ECs and all three groups had higher gp120/Env-specific Ab levels than TPs. A similar trend for AD functions (ADCP, ADCC, and ADCT) was observed, i.e., plasma from UTPs, ECs, and VCs, supported AD functions that did not differ significantly and were higher than those from TPs. Upon normalizing the AD function levels with the concentration of their anti-gp120/Env specific Abs, between-group differences disappeared. This has not been investigated or reported before. In summary, not one specific or a group of AD functions distinguished ECs from other groups of PLWH. In chapter 4, we investigated whether Abs in ECs had different biophysical characteristics as compared to other groups of PLWH. The two biophysical characteristics we investigated were IgG subclass distribution against 5 groups of Ags (gp120, gp140, gp70V1V2, gp41, and p24) and gp120-specific IgG Ab glycoforms. These experiments were performed in the laboratory of Dr. Galit Alter, Ragon Institute of MGH, MIT, and Harvard, Boston, MA. I analysed this data and compiled the results in chapter 4. The manuscript reporting these results is currently under preparation for submission for publication.

Chapter 4: Biophysical features of gp120-specific Abs in people living with HIV/HIV elite controllers

Manuscript under preparation; in final stages for publication.

Sanket Kant[1, 2, 3], Caitlyn Linde[4], Ningyu Zhang[2, 3], Franck P. Dupuy[1, 3], Vicky Roy[5], Jean-Pierre Routy[1, 3, 6, 7], Cécile Tremblay[8, 9], Réjean Thomas[10], Jason Szabo[10], Pierre Côté[11], Benoit Trottier[11], Roger LeBlanc[12], Danielle Rouleau[8], Marianne Harris[13], Galit Alter[14], Nicole F Bernard[1, 2, 3, 7, 15]

[1] Research Institute of the McGill University Health Centre (RI-MUHC), Montreal, QC H3A 3J1, Canada.

[2] Division of Experimental Medicine, McGill University, Montreal, QC H4A 3J1, Canada.

[3] Infectious Diseases, Immunology and Global Health Program, Research Institute of the McGill University Health Centre, Montreal, QC H4A 3J1, Canada.

[4] SeromYx Systems, Cambridge MA.

[5] Ragon Institute of MGH, MIT and Harvard, Cambridge MA.

[6] Division of Hematology, McGill University Health Centre, Montreal, QC H4A 3J1, Canada.

[7] Chronic Viral Illness Service, McGill University Health Centre, Montreal, QC H4A 3J1, Canada.

[8] Centre de Recherche du Centre Hospitalier de l'Université de Montréal (CRCHUM), Montreal, QC H2X 3H8, Canada.

[9] Department of Microbiology Infectiology and Immunology, University of Montreal, Montreal, QC H3C 3J7, Canada.

[10] Clinique Médicale l'Actuel, Montréal, QC H2L 4P9, Canada.

[11] Clinique Médicale Quartier Latin, Montréal, QC H2L 4E9, Canada.

[12] Clinique Médicale Opus, Montréal, QC H3A 1T1, Canada.

[13] St. Paul's Hospital, Vancouver, BC V6Z 1Y6, Canada.

[14] Ragon Institute of MGH, MIT and Harvard, Cambridge MA.

[15] Division of Clinical Immunology, McGill University Health Centre, Montreal, QC H4A 3J1, Canada.

Correspondence:

Nicole F. Bernard, Ph.D.

nicole.bernard@mcgill.ca

Keywords: Antibodies, ECs, IgG subclass, Glycosylation

1. Introduction

Human immunoglobulin G (IgG) antibodies (Abs) protect the hosts from non-self entities by targeting epitopes on the antigens (Ags) and bridging the Ags with innate immune cells. There are four subclasses of IgG (IgG1-4), and all IgG Abs are N-linked glycosylated, a form of post-translational modification, at asparagine 297 (N297) in the second constant IgG heavy chain domain (CH2) of the fragment crystallizable (Fc) IgG region [1-5]. The IgG subclasses and different forms of glycosylation dictate the binding affinity to the complement component C1q and the Fc gamma receptors (FcγR) on innate immune cells such as natural killer (NK) cells and monocytes, thereby modulating their downstream functions [1, 3, 5, 6]. The affinity for FcγRs for IgG subclasses has the following decreasing hierarchy: IgG3 > IgG1 > IgG2 > IgG4 [6, 7]. Even within an IgG subclass, IgG affinity for various FcγRs on effector cells can be finetuned by virtue of their N-linked glycosylation patterns. NK cells and monocytes express FcγRIIIA/CD16 and

FcγRIIA/CD32, respectively. Presence or absence of sugar moieties such as fucose or galactose can influence which FcγRs the Ab will trigger, thereby determining if the target Ag will be lysed by NK cell or phagocytosed by monocytes. Afucosylated Abs bind strongly to FcγRIIIA on NK cells and support Ab-dependent cellular cytotoxicity (ADCC) [8-11], whereas galactosylated Abs bind strongly to FcγRIIA on monocytes and enhance AD cellular phagocytosis (ADCP) [12]. Thus, a complex yet intricate mechanism behind the different subclasses and glycoforms of IgG Abs regulate the humoral immune response in clearing Ag. Natural infections can skew the amounts of IgG subclass and glycosylation patterns on the Abs. Alternatively, vaccinations can also skew Ab development toward a more favourable response [13-18].

Envelope (Env) is the only human immunodeficiency virus (HIV) protein expressed on the surface of infected cells, which makes it an excellent target for anti-Env Abs induced by vaccines. The RV144 vaccine trial is the only one to date that showed modest, though significant, protection against HIV infection [19]. Correlates of protection analyses showed that non-neutralizing IgG Abs to the Env V1/V2 loop and ADCC activity, and not neutralizing Abs or cytotoxic T cell responses, were associated with protection from HIV infection [19]. However, studying ADCC activity has been challenging. Structural analyses have provided evidence for at least four different Env/gp120 conformations [20, 21]. Recombinant, linear gp120 and gp120-coated $CD4^+$ cells sample gp120 in an open conformation, whereas genuinely infected target cells downregulate cell surface CD4 and express Env in a closed conformation [22-25]. Based on the target system used, there is significant controversy surrounding Ab-dependent (AD) functional assays [22-28].

Although immunological mechanisms underlying protection against HIV infection and HIV control in those already HIV-infected are likely to differ, there is interest in investigating whether the functions and biophysical characteristics of Abs associated with protection from infection are

also associated with HIV control in elite controllers (ECs). ECs are a rare group of people living with HIV (PLWH) who can spontaneously control their viremia without antiretroviral therapy (ART) [29, 30]. AD functions that have been assessed include ADCC, AD NK cell activation (ADNKA), AD cellular phagocytosis (ADCP), AD cellular trogocytosis (ADCT), AD complement deposition (ADCD), and AD neutrophil phagocytosis (ADNP) [26, 31]. Investigations into the AD functions underlying viral control failed to identify a single function that was enriched in ECs compared to other groups of PLWH. However, we and others found that ECs were distinguished from other groups of PLWH by their highly correlated, polyfunctional non-neutralizing Ab (nnAb) responses [26, 31, 32]. We also showed that the amount of gp120-/Env-specific IgG Abs dictate the AD response levels observed in all groups of PLWH studied [31].

Sorted infected CEM.NKr.CCR5 (siCEM) cells were generated in our laboratory [23, 24]. They differ from gp120-coated CEM cells in that virtually all these cells express HIV Env in a closed conformation due to downmodulation of CD4 by full length HIV encoded Nef and Vpu [23]. Gp120-coated CEM cells, gp120-coated wells and beads expose Env epitopes, such as CD4 induced (CD4i) epitopes that are normally hidden in closed conformation Env on genuinely HIV-infected cells. This is also the case for CD4 cells in HIV-infected cell cultures in which only a fraction of the CD4 cells is HIV-infected. In this situation, gp120 is shed from HIV-infected cells and taken up by uninfected, $CD4^+$ bystander cells, thus exposing CD4i epitopes [25]. A comparative analysis of the relationship between the AD functions assayed on siCEM cells and gp120-coated targets has yet to be performed. There is limited information available on IgG subclass distribution and Ab glycoforms amongst different groups of PLWH. In this report, we employed different approaches to investigate if ECs could be distinguished from other groups of

PLWH by specific biosignatures of their anti-Env-specific IgG Abs. Using gp120-functionalized beads, we determined the IgG subclass distribution of IgG Ab specific for various forms of HIV Env and HIV p24 present in the groups of PLWH and correlated these results with AD functions using gp120-coated beads, gp120-coated ELISA wells, gp120-coated CEM cells and siCEM cells. We found no correlation between IgG subclass distribution and AD function levels for any group of PLWH. Next, we sought to investigate if glycosylation patterns could distinguish ECs from other study groups. ECs, compared to UTPs, had significantly lower proportions of fucosylated gp120-specific IgG Abs, higher levels of agalactosylated IgG Abs, and higher concentrations of sialylated gp120-specific Abs. To combine all the data generated so far, we used regression analysis and machine learning for all the Ag-Ab features and AD functional assays. We identified no specific differences or key immune features that distinguished ECs from the other study groups.

2. Methods

I. Study participants

We enrolled four groups of PLWH. Eighteen untreated progressors (UTPs) (CD4 < 400 cells/mL and VL > 10,000 copies of HIV RNA/mL of plasma [c/mL]), 24 treated progressors (TPs; CD4 > 400 cells/mL and VL < 50 c/mL), 37 ECs (CD4 > 400 cells/mL and VL < 50 c/mL), and 16 viremic controllers (VCs; CD4 > 400 cells/mL and VL < 3,000 c/mL). TPs were defined as ART^+ PLWH who had undetectable VLs for at least 1 year prior to being enrolled. UTPs and TPs were enrolled from the Montreal Primary HIV infection cohort [33]. ECs and VCs were selected from the Canadian Cohort of HIV-Infected Slow Progressors [34]. Plasma from these study subjects were assayed for total bulk, gp120- and Env-specific IgG Ab concentrations, AD functions, and the biophysical characteristics of gp120-specific IgG Abs.

II. Ab Quantification

Gp120- and Env-specific Abs in plasma were quantified as previously described [24, 35]. Total plasma IgG Abs were quantified using a human IgG enzyme linked immunosorbent assay (ELISA) quantification kit (Bethyl Laboratories, Montgomery, TX) as per manufacturer's instructions. For quantifying gp120-specific IgG Abs, a plate-based ELISA (gp120-PBE) was used. Briefly, ELISA wells were coated with D7324 (Aalto Bio Reagents, Dublin, Ireland) to capture recombinant gp120 (NIH Reagent Bank, HIV-1 BaL gp120 recombinant protein from DAIDS, NIAID). Different dilutions of subject plasma were incubated with gp120-coated wells. Bound gp120-specific Abs were detected using horseradish peroxidase conjugated-goat anti-human IgG Fc secondary Ab (Invitrogen, Frederick, MD). The colorimetric change due to enzymatic reduction of substrate was read on an optical density (O.D.) of 450nm on a Tecan Plate Reader (Infinite 2000 PRO, Tecan Group Ltd., Männedorf, Switzerland). Wells without gp120 served as the negative control, and the O.D. of negative control wells was subtracted from all samples and the positive control, before further analysis.

Env-specific Abs were quantified on siCEM cells that expressed the closed conformation of Env [22-24]. Briefly, each well contained siCEM cells and carboxyfluorescein succinimidyl ester (CFSE, Life Technologies, Burlington, ON, Canada)-stained uninfected CEM cells at a ratio of 1:1. $CFSE^{+}$ uninfected cells and no Ab wells served as negative controls. Env-specific plasma Abs were detected using APC-conjugated anti-human IgG Fc secondary Ab (huIgGFc, BioLegend, Burlington, ON, Canada) using a BD LSR Fortessa X20 flow cytometer (BD Biosciences, Mississauga, ON, Canada). In both, the gp120-PBE and siCEM-based Ab quantifying technique, the positive control was a pool of polyclonal IgG obtained from PLWH (HIVIG; obtained from NIH Reagent Bank, NABI and NHLBI); known concentrations of HIVIG were used to generate a standard curve. Dilutions of plasma that generated results that lay within the linear range of the

standard curve of HIVIG concentrations were selected and interpolated from the standard curve of HIVIG. Flow cytometry results were analysed using FlowJo v10 software (Tree Star, Inc., Ashland, OR).

III. SiCEM-based AD functional assays

The three AD functions using siCEM target cells have been described in depth elsewhere [22, 23]. For ADCD, we combined siCEM cells and subject plasma or HIVIG. Each subject plasma and HIVIG was used at 2 different total IgG concentrations (500 and 50 μg/mL). HIV-negative plasma served as the source of complement. The deposition of complement component C3b on the surface of siCEM cells was detected using FITC-conjugated, mouse anti-human anti-C3b Ab (Cedarlane, Burlington, ON, Canada) using a BD LSR Fortessa X20 flow cytometer. The complement deposition score (CDS) was calculated as the product of the frequency and mean fluorescence intensity (MFI) of $C3b^+$ target cells. Next, we calculated the area under the curve (AUC) for the CDS for each subject. The AUC for the CDS of each subject plasma was reported following normalization to the AUC of the CDS of HIVIG. The AUC is calculated as [(XA + XB)/2] * (A-B), where X is the CDS resulting from the two concentrations of total plasma Ab IgG, A and B.

The annexin V-based ADCC assay used here detects the frequency of apoptotic target cells in the presence of plasma or control Abs and isolated NK cells from healthy donors. Two concentrations of plasma IgG and HIVIG were used for this assay (500 and 50 μg/mL). The AUC for the frequency of annexin V^+ siCEM cells for each participant plasma was calculated, and the final data used for analysis was normalized to the AUC of HIVIG. The AUC was calculated as mentioned above, where X denotes the frequency of annexin V^+ siCEM cells.

The ADCT assay detected the frequency of monocytes that take up PKH-26 dye-stained membrane from siCEM cells. SiCEM cells were labelled with PKH-26, a lipophilic membrane dye, and

incubated with two concentrations of subject plasma or HIVIG (500 and 50 μg/mL) in separate wells. Whole peripheral blood mononuclear cells (PBMCs) containing monocytes were used as effector cells. Monocytes were detected using fluorescent anti-CD14 Ab (BioLegend, San Diego, CA). The frequency of $CD14^+$ monocytes that had become PKH-26^+ in the presence of Abs was noted and the AUC for each subject plasma and HIVIG was determined. The AUC was calculated as mentioned above, where X represents the frequency of $CFSE^+$ PKH-26^+ monocytes. The AUC for each subject plasma was normalized to the AUC obtained from the HIVIG wells. All AD functional assays using flow cytometry, were analysed using FlowJo v10 software (Tree Star, Inc., Ashland, OR).

IV. Coated-CEM based AD assays

The gp120-coated CEM cell-based assays (ADCD, ADCC, and ADCT) utilized gp120-coated CEM cells as target cells. 1 x 10^6 CEM cells were coated with 0.6 μg of recombinant gp120 in 100 μl of R10 media (RPMI media supplemented with 10% FBS, 2 mM L-glutamine and 100 U/ml penicillin/streptomycin). The AD functional assays for ADCD, ADCC and ADCT were performed using siCEM cell-based AD functional assays.

Gp120-based ADCP

ADCP was the only AD function assay performed using gp120-coated fluorescent neutravidin beads (Thermo Fisher Scientific, Ontario, Canada) and has been described previously by us and others [22, 26]. Two concentrations of plasma IgG and HIVIG (100 and 2 μg/mL) were incubated with Ag-functionalized beads in separate wells. 25,000 THP-1 cells, a monocyte cell line, was added to the Ag-Ab complex for 3 hours at 37oC. The frequency and MFI of fluorescent THP-1 cells was evaluated by flow cytometry using a BD LSR Fortessa X20 flow cytometer. The phagocytosis score (PS) was determined as the product of frequency of THP-1 cells that have

phagocytosed the gp120-fluorescent beads and the MFI of THP-1 cells. The AUC for 2 concentrations of Abs was determined from the formula above, where X represented the PS generated by the respective IgG Ab concentrations. Flow cytometry results were analysed using FlowJo v10 software (Tree Star, Inc., Ashland, OR).

V. ADCP assay #2

The following assays were performed by the laboratory of Dr. Galit Alter (Ragon Institute of Massachusetts General Hospital, Massachusetts Institute of Technology, and Harvard, Boston, MA). This second ADCP assay was adapted from Ackerman et al. 2011 [36]. Briefly, antigen was biotinylated using sulfo-NHS LC-LC biotin, coupled to 1 μm yellow-green fluorescent neutravidin beads (Invitrogen) for 2 hours at 37˚C and washed two times in phosphate buffered saline (PBS); 0.1% BSA. Ten μL/well of coupled beads were added to the wells of 96-well plates with 10 μL/well of diluted plasma sample for 2 hours at 37˚C to allow for the formation of immune complexes. After incubation, the immune complexes were centrifuged, and the supernatant was removed. THP-1 cells were added at a concentration of 2.5 x 10^4 cells/well and incubated for 18 hours at 37˚C. After incubation, the plates were centrifuged, the supernatant was removed, and cells were fixed with 4% paraformaldehyde (PFA) for 10 minutes. Fluorescence was acquired with a Stratedigm 1300EXi cytometer. PS was calculated using the following formula: (percentage of $FITC^+$ cells) x (the geometric MFI (gMFI) of the $FITC^+$ cells)/10,000.

VI. ADNP assay

The ADNP assay was adapted from Karsten et al. 2019 [37]. Recombinant gp120 was coupled to beads and immune complexes were formed as described for ADCP. Neutrophils were isolated from fresh whole blood in acid citrate dextrose anticoagulant using an EasySep Direct Human Neutrophil Isolation kit (Stem Cell Technologies, Cambridge, MA), resuspended in R10 media,

and added to the wells of 96 well plates at a concentration of $5x10^4$ cells/well. The plates were incubated for 30 min at 37˚C. The neutrophil marker CD66b (Pacific Blue conjugated anti-CD66b; BioLegend, San Diego, CA) was used to stain cells. Cells were fixed for 10 minutes in 4% PFA. Fluorescence was acquired using a Stratedigm 1300Exi flow cytometer. PS was calculated as described for ADCP assay #2.

VII. ADCD assay #2

This ADCD assay was adapted from Fischinger et al. 2019 [38]. Gp120 was coupled to 1 μm non-fluorescent neutravidin beads (Invitrogen) as described for ADCP. Immune complexes were formed by incubating 10 μL of coupled beads with 10 μL of diluted plasma sample for 2 hours at 37˚C. Plates were centrifuged and immune complexes in the pellets were washed with PBS. Lyophilized guinea pig complement (Sigma, S1639) was resuspended in cold water, diluted in veronal buffer containing 0.1% gelatin (Boston BioProducts, Millford, MA) and added to the immune complexes. The plates were incubated for 50 minutes at 37˚C and the reaction was stopped by washing the plates twice with 15 mM ethylenediaminetetraacetic acid (EDTA) in PBS. To detect complement deposition, plates were incubated with fluorescein-conjugated goat anti-guinea pig complement C3 (MP Biomedicals, 0855385) for 15 minutes in the dark. Fluorescence was acquired with a Stratedigm 1300Exi flow cytometer.

VIII. Antibody-dependent NK cell activation (ADNKA)

ELISA plates were coated with gp120 at 300 ng/well and incubated for 2 hours at 37˚C. Plates were blocked with 5% bovine serum albumin (BSA) in PBS overnight at 4˚C. The next day, 100 μL of diluted plasma sample were added to the plates. Plates were incubated for 2 hours at 37˚C to allow for formation of immune complexes. During the incubation, human NK cells were isolated from buffy coats using a RosetteSep NK cell enrichment kit (StemCell Technologies) and Ficoll

separation. After the incubation, NK cells were added to the plates at $5x10^4$ cells/well in R10 supplemented with anti-CD107a PE-Cy5, brefeldin A and GolgiStop (BD Biosciences). Plates were incubated for 5 hours at 37˚C. Following the incubation, NK cells were stained for surface markers with anti-CD56 PE-Cy7, anti-CD16 APC-Cy7 and anti-CD3 Pacific Blue (BD Biosciences). NK cells were fixed and permeabilized with Fix-Perm cell permeabilization kit (Invitrogen). Cells were incubated with PE-conjugated anti-CCL4 and FITC-conjugated anti-IFN-γ (BD Biosciences) to stain for intracellular markers. Cells were acquired on a Stratedigm 1300Exi flow cytometer.

IX. Luminex Isotyping and Fc array

Antigen-specific antibody subclass isotypes and FcγR binding were analyzed by Luminex multiplexing. The antigens were coupled to magnetic Luminex beads by carbodiimide-NHS ester coupling with an individual region per antigen. Coupled beads were incubated with different plasma dilutions for 2 hours at room temperature (RT) in 384-well plates (Greiner Bio-One, Monroe, NC). Unbound antibodies were washed away, and subclasses and isotypes were detected with respective PE-conjugated Ab at a 1:100 dilution (Southern Biotech, Birmingham, AL). For the FcγR binding, a respective PE–streptavidin (Agilent Technologies, Santa Clara, CA) coupled recombinant and biotinylated human FcγR protein was used as a secondary probe. After a 1hour incubation, excessive secondary Ab was washed away, and the relative antibody concentration per antigen was determined on an iQue Screener (Intellicyt, Albuquerque, NM).

X. IgG Fc region glycosylation analysis

200 µl of each plasma sample was heat inactivated at 56°C for 1 hour. Samples were incubated with 25 µl of streptavidin coated magnetic beads (New England Biolabs, Ipswich, MA) at RT with rotation. Antigen was biotinylated with LC-LC-biotin (Thermo Fisher Scientific) according to the

manufacturer's protocol. Streptavidin coated magnetic beads were activated with 0.5 M NaCl, 20 mM Tris-HCl [pH 7.5], 1mM EDTA and incubated with biotinylated antigens at RT for 1 hour with rotation. Samples and coupled beads were mixed and incubated at RT for 1 hour in rotation. Adsorbed samples were removed, and antigen-specific IgG bound to the antigen coupled beads was digested with IdeZ (New England Biolabs) at 37°C for 1 hour with rotation. Supernatants that contained cleaved Fc regions were digested with peptide:N-glycosidase F (PNGaseF; New England Biolabs) according to manufacturer specifications. Glycans were purified and labelled with 8-Aminopyrene-1,3,6-trisulfonic acid trisodium salt (APTS) with GlycanAssureTM Kit (Applied Biosystem). Labelled glycans were analyzed by capillary electrophoresis on a 3500XL Genetic Analyzer (Thermo Fisher Scientific)

XI. Statistical analysis

Data was obtained and merged into a Microsoft Excel spreadsheet. Basic statistical analysis and graphical representations were performed in GraphPad Prism v7 (GraphPad Software, Inc., San Diego, CA). Rstudio v1.2.5001 (Rstudio: Integrated Development for R. Rstudio, Inc., Boston, MA) was used to perform and plot the correlation matrix using the library "corrplot". Kruskal-Wallis' one-way ANOVA tests with Dunn's post tests were used to determine the significance of between-group differences. Non-parametric Spearman's correlation tests were used to determine the Spearman rho and p values. P-values < 0.05 were considered significant.

Thirty-three Ags were classified into 5 major groups of Ags (gp120, gp140, gp70V1V2, gp41, and p24) and were used to coat beads that probed for the presence of Abs able to bind these Ags in plasma from PLWH: the gp120 group consisted of gp120 from 15 different sequences, there were 10 variants of gp70V1/V2 Ags and 6 variants of gp140 Ags. The gp41 and p24 Abs corresponded

to the sequences from HxBc2 only. The median for each group for each participant was calculated and used where specified.

The data consisted of 52 covariates measured on 95 patients, segregated into 4 groups including ECs, UTPs, TP, and VCs. We segregated our variables into two subsets: Ab concentrations and functions and glycosylation patterns. Information on only the coated CEM-based AD assays were not available on the 16 VCs. Information on glycosylation patterns was available for all 95 participants. First, we employed principal components analysis (PCA). Linear PCA reduces a multidimensional dataset into a 2-dimensional plot that would account for the largest variation. To reduce the parameters and to increase efficiency of our model, we performed least absolute shrinkage and selection operator (LASSO). After selecting the significant parameters (n=10), we performed a partial least squares-discriminant analysis (PLS-DA). PLS-DA is a multivariate dimensionality-reduction technique. Unlike PCA, PLS-DA performs dimensionality reduction considering the response variable. Sparce PLS-DA (SPLS-DA) is a sparse version of PLS-DA that adds LASSO penalties to select only a subset of variables to achieve better classification. SPLS-DA is useful when the data is high dimensional.

3. Results

I. Relationships between AD functions assayed on different targets

We first investigated the differences between AD functions using gp120-coated beads (ADCD, ADCP, and ADNP) or wells (ADNKA) (Figure 1A). UTPs, ECs, and VCs had ADNKA and ADNP functions that did not differ significantly from each other, and that were significantly higher than those from TPs. There were no significant differences between the groups in terms of ADCD and ADCP function levels when gp120-coated beads were used as targets.

Next, we measured AD function levels using assays performed with different targets opsonized with plasma from the groups of PLWH. The significance of correlations between these methods was assessed. We observed that except for the ADCP assay, the results of all the assays employed in our study, independent of the target used, were significantly correlated with each other (Figure 1B). The correlation coefficients were significantly higher for plasma from ECs compared to the other groups of PLWH (Figure 1C). Specifically, for UTPs and VCs, the Ab concentrations quantified using a PBE weakly correlated with AD functions assayed using gp120-coated beads. In comparison, Ab concentrations quantified using PBE where ELISA plate wells were coated with gp120 and those measured using siCEM cells strongly correlated with all the AD functional assay results, except for ADCP, in ECs. TPs also tended to show moderate correlation coefficients between Ab concentrations and AD function levels, independent of the targets used.

Since neither Ab concentrations nor AD function differentiated ECs from UTPs using simple comparative analyses, we used unsupervised k-means clustering via principal components analysis (PCA) to observe if the dimensional reduction technique differentially clustered the subject groups (Figure 1D). VCs were excluded from this analysis because AD function assays using gp120 coated CEM cells as target cells in these assays were not done for plasma from VCs. This PCA analysis revealed three clusters. After plotting and extracting the subject numbers in each cluster, we observed that the unsupervised PCA did not cluster the groups with the respective group participants. Each cluster housed numbers where each number represents the subject identification number. The blue cluster housed 14 participants (1 UTP, 9 TPs, and 4 ECs), the magenta cluster housed 28 participants (5 UTPs, 13 TPs, and 10 ECs), and the pink cluster contained 35 individuals (9 UTPs, 2 TPs, and 23 ECs). Thus, PCA could not discern PLWH groups based on the AD functions and amount of gp120-/Env-specific Abs.

We used LASSO to select the features which would increase the robustness of our model. VCs were not included in this dataset as we did not have the results for Abs concentrations quantified using gp120-coated CEM cells. The 10 features that provided the lowest coefficients in the LASSO regression analysis were gp120-specific Ab concentrations obtained using PBE, gp120-specific Ab concentrations obtained using gp120-coated CEM target cells, ADCC, ADCD and ADCT assay results using participant plasma opsonized siCEM cells, ADCP results using gp120-functionalized beads, ADNKA assay results measuring IFN-γ secretion, ADCD, ADCP, and ADNP assays results using participant plasma opsonized gp120-coated beads. Data from these features were selected for PCA and PLS-DA for UTPs, TPs, and ECs. Neither PCA nor PLS-DA distinguished the groups of PLWH from each other (Figure 1E).

II. IgG subclass does not correlate with AD functions

The distribution of IgG subclass concentrations specific for each HIV Ag was determined using gp120-coated fluorescent beads. First, we found that UTPs had higher concentrations of gp120-specific IgG4 than ECs and TPs. UTPs had higher concentrations of IgG2 Abs specific for gp70V1V2, gp140, and gp41 than ECs and higher concentrations of IgG2 Abs specific for gp70V1V2, gp41 than TPs (Figure 2A). Next, we generated the correlation plots using medians of individual IgG subclasses 1-4 specific for each group of Ag, present in plasma from each participant and for the gp120-coated bead- and gp120-coated well-based AD functions. We performed correlation analyses only on the results of the functional assays performed using gp120-coated beads since the IgG subclass analyses were performed using gp120-coated beads (ADCP, ADNP, and ADCD) or gp120 coated ELISA plates (ADNKA, measuring the frequency of NK cells producing CD107a, TNF-α, and IFN-γ). All these AD function assays were performed in Dr. Galit Alter's lab. We observed few significantly positive correlations between the relative

concentrations of IgG subclasses specific for the 5 Ag groups with the levels of the AD functions (Figure 2B). For example, gp120-, gp70V1V2-, and gp140-specific IgG1 was significantly and positively correlated with ADNKA, ADCD, and ADNP, when all groups of PLWH were combined. Amongst the individual groups of PLWH, only ECs exhibited significant and positive correlations between IgG1 concentrations specific for gp120, gp140, and gp70V1V2 and the frequency of NK cells producing CD107a, TNF-α, and IFN-γ (Figure 2C). In contrast, IgG1 to gp120, gp140, and gp70V1V2 in TPs correlated negatively and significantly with these ADNKA functions (Figure 2C).

III. Glycosylation patterns in ECs differ from other PLWH groups

Gp120-specific Ab glycoforms were reported as a proportion of the total gp120-specific IgG Ab concentrations in the plasma from each study subject. Out of the 23 glycoforms detected, there were 3 key post-translation glycosylation modification patterns that differentiated ECs from UTPs (Figure 3A-E). ECs and TPs had significantly lower proportions of fucosylated gp120-specific Abs (G0F) compared to UTPs and VCs. ECs had significantly higher proportions of galactosylated (G1) and sialylated (G2S2) gp120-specific Abs compared to UTPs (Figure 3A-E).

To understand if galactosylation, sialylation, fucosylation, or bisected glycans played any role in AD functions, we generated a correlation matrix of AD functions levels with the proportion of these major glycoforms (Figure 3F). Globally, we observed that agalactosylated and sialylated gp120-specific IgG Abs were significantly and positively correlated with all AD function levels except for ADCP. However, these correlations were not present in UTPs, where there were no significant associations between the AD functions and any of the glycoforms. Meanwhile, the proportion of agalactosylated and sialylated gp120-specific IgG Abs in ECs were significantly and positively correlated with all AD functions (Figure 3G).

As done for IgG subclasses, we employed unsupervised PCA and LASSO regression analyses on the 24 glycoforms of gp120-specific IgG Abs. PCA identified 3 clusters, each cluster contained numbers and each number stands for the participant identification number. UTPs, TPs, and ECs were segregated with some certainty in the groups (83.4%, 50%, and 54% respectively). However, VCs were dispersed amongst the clusters and thus could not be distinguished from other groups of PLWH. LASSO regression analysis reduced the 24 glycoforms and identified 12 glycoforms that had the highest influence over differentiation: G2S2, G2S2B, G1S1, G0, G1B, G2B, G2S2F, G1S1F, G2S1F, G0F, G1F, and G1FB/G2. ECs had the largest variability amongst all the groups. Neither PCA nor PLS-DA could discriminate the groups of PLWH with absolute certainty. (Figure 4A and 4B).

4. Discussion

In this report, we characterised the functions and biophysical characteristics of non-neutralizing Abs in four groups of PLWH. We measured AD functions using gp120-coated beads or wells and compared them with previously generated AD function levels obtained using siCEM cells as target cells. We observed that out of the four groups of PLWH tested here, only plasma from ECs demonstrated significant correlations between anti-gp120-specific Ab concentrations and AD function levels, independent of the target system used. Multidimensional reductional techniques (PCA and LASSO-PLSDA) could not distinguish groups of PLWH based on the AD functions these anti-gp120-specific Abs were able to support. We also measured gp120-specific IgG Ab subclass distribution to 33 HIV Ags, which were classified into 5 major specificity groups: 15 Ags corresponded to gp120 glycoproteins from different HIV isolates, 10 corresponded to gp70V1V2 glycoproteins and 6 to gp140 glycoproteins, from various HIV isolates; 1 was a p24 protein, and 1 was a gp41 protein corresponding to a single HIV isolate. ECs had significantly lower

concentrations of IgG2 Abs specific for gp70V1V2, gp140, and gp41 than did UTPs. Only plasma from ECs generated significant correlations between IgG1gp120-, gp140-, and gp70V1V2-specific Ab concentrations and ADNKA function levels. The proportion of each IgG anti gp120-specific Ab glycoform contributing to the total gp120-specific Ab response was measured using gp120-coated beads. ECs had lower proportions of agalactosylated and fucosylated Abs and higher proportions of galactosylated-sialylated gp120-specific Abs (G2S2 and G2S2B) than UTPs. Agalactosylated and sialylated Abs were also correlated with AD functions in ECs, however no specific AD feature distinguished ECs from UTPs. PCA and PLSDA were unable to segregate the groups of PLWH based on glycosylation pattern with absolute certainty.

Our objective was to investigate if ECs would be characterised by a distinct Ab signature that distinguished them from other groups of PLWH. Prior to this report, we had generated data on quantities of Env-specific Abs and AD functions measured on genuinely HIV-infected cells that downregulate CD4 and express Env in a closed conformation [23, 24, 31]. We built upon these results and our knowledge of non-neutralizing Abs by quantifying AD functions on gp120-coated targets as well. To our knowledge, a direct comparison between AD functions performed using different targets, using the same set of samples has never been done before. Our data show that only plasma from ECs contained anti-gp120-/Env-specific IgG Abs with AD polyfunctional response that were highly correlated irrespective of the targets used to assay AD function levels. We and others showed that plasma from ECs, compared to other groups of PLWH, supported AD functions that were significantly correlated with each other [22, 26]. How might the polyfunctionality play a role in HIV control is unclear; perhaps high concentrations of potent Abs that can support several AD functions have a superior ability to control HIV-infected cells. This possibility is supported by our finding that controllers with an undetectable HIV reservoir size had

significantly higher Ab-normalized ADCC function than controllers with a detectable HIV reservoir size [31]. It is important to note, however that these findings are based on associations and cause and effect relationships between AD function levels and HIV reservoir size have not been established.

The structural differences between gp120 on gp120-coated targets versus Env on the surface of infected cells are well characterized [20, 21, 25, 32]. We and others have also shown that in HIV-infected cultures where not all cells are infected, CD4 receptors on uninfected bystander cells take up gp120 shed from HIV-infected cells and present gp120 in a conformation that reveals CD4 induced (CD4i) epitopes also found on open conformation Env that can be detected by monoclonal Abs (mAb) such as A32 and coreceptor binding site-specific 17b [25, 32]. CD4i-specific mAbs A32 and 17b can also recognize the recombinant gp120 on coated wells and beads. We measured the AD functions of effector cells using Ab bound gp120-coated wells and/or gp120-coated CEM cells to investigate if plasma Abs from ECs would differ from those of other groups of PLWH based on the target entities used. Plasma from UTPs, ECs, and VCs supported levels of ADNKA and ADNP functionality, which did not differ significantly from each other, but which was higher than plasma from TPs. This is in line with our previously published data showing that UTPs, ECs, and VCs have similar levels of ADCP, ADCD, ADCC, and ADCT functionality [31]. Additionally, in accordance with our previous study, none of the groups had discernible ADCD functions assayed on gp120-coated beads [31]. The exact role of ADCD in immune responses against HIV is not clear. Ackerman et al. have also shown that the four groups of PLWH had similar levels of ADCD functions [26]. ADCD has been previously shown to be dispensable in protection provided by the anti-Env CD4 binding site specific broadly neutralizing Ab (bNAb) b12 [39]. Abs from only a small subset of HIV-infected children mediate complement deposition

[40]. However, more RV144 vaccinated individuals than VAX003 and VAX004 trial vaccinees, had complement-activating Abs [41]. A recent study by Hessel et al. showed that animals administered mAb 10e8, a gp41-specific bNAb, with enhanced complement activation had lower post-infection viremia compared to animals administered the wild type Ab counterpart [42]. It is important to note that there is a key difference between our results and those reported by Ackerman et al. and the results of the other studies mentioned here. The objective of these studies was to assess the AD functions associated with protection from HIV infection. The mechanisms underlying protection from infection may differ from those associated with HIV control, as occurs in ECs. Thus, more investigations are needed to understand the role of ADCD in protection from HIV infection versus HIV control.

We measured the IgG subclass distribution of Abs specific to 5 groups of Ags in the four groups of PLWH and observed that, ECs, compared to UTPs, had significantly lower concentrations of IgG2 Abs specific for gp140, gp70V1V2, and gp41. Previou work showed that gp120-specific IgG2 subclass was significantly lower in ECs than in UTPs. Banerjee et al. and we as well in our current report did not observe a similar result [26, 35]. Sadanand et al. measured IgG subclass distribution of Abs to gp120, gp140, and gp41 in a longitudinally followed cohort of ECs and UTPs. They found that the IgG subclass levels varied with time during infection [43]. The differences in the titres of these IgG Abs between ECs and UTPs was not assessed. We also observed that ECs, compared to UTPs, had lower amounts of IgG4 Abs specific for gp120, gp140, and gp41. Studies evaluating Ab development in vaccine trials showed that anti-gp120 specific IgG2 and IgG4 Abs were not associated with protective responses in vaccinated individuals enrolled in the VAX003, VAX004 and RV144 vaccine trials [14, 44, 45]. IgG2 and IgG4 bind

more poorly to FcγRs than do IgG1 and IgG3 and thus mediate poor AD functions. In addition, gp120-specific IgG2 also inhibits FcR-mediated ADCP [46].

We investigated between-group differences in the proportion of gp120-specific IgG Ab glycoforms contributing to the total IgG anti-gp120-specific response. This analysis found that UTPs had significantly higher proportions of agalactosylated (G0F) and sialylated (G2S2 and G2S2B) anti-gp120-Abs than ECs. Higher amount of agalactosylated Abs has been associated with higher levels of AD cellular viral inhibition. Addition of fucose to glycosylation decreases FcγRIIIA binding and ADCC function [47-49]. A recent study showed that the G0F form of bNAb PGT121 had equivalent levels of ADCC function as the wild type and G2F forms of PGT121, which was lower than that of G2 glycoform. This suggests that the absence of galactose (G) and presence of fucose (F), i.e., the G0F form, nullify each other in downstream AD function [49]. Interestingly, ECs, compared to UTPs, had significantly higher amounts of G1 and G2 gp120-specific Abs which has been shown to be crucial for NK cell mediated ADCC and ADNKA function [8, 48, 49]. In a recent antiretroviral therapy interruption trial, individuals with a higher proportion of sialylated gp120-specific Abs experience a longer time to viral rebound [50]. The addition of sialic acid occurs only on the terminal galactoses, i.e. the higher number of terminal galactoses (maximum is 2), the higher the number of sialic acids can be added (also maximum is 2). We observed that ECs as compared to UTPs, had a significantly higher proportion of sialylated gp120-specific Abs (i.e. G2S1 and G2S2). We observed a strong and statistically significant positive correlations between the proportion of total gp120-specific sialylated Abs with all AD functions, except for ADCP in ECs and TPs only. In general, ECs had significantly higher concentrations of gp120-specific Abs [24]. While there were key individual differences between certain glycoforms, the proportion of individual glycoforms between the groups of PLWH,

machine learning methodology was unable to discern glycosylation patterns than distinguished one study group from another.

In summary, we assessed the biophysical characteristics of Abs to various linear portions of HIV Env Ags in plasma from different groups of PLWH. We also assessed the AD functions of these anti-gp120/Env specific Abs. We found that AD functionality is largely governed by the concentration of gp120-/Env-specific Abs rather than the potency of these Abs in different groups of PLWH. Minimal changes in the anti-gp120/Env IgG subclass and glycoforms distribution can alter or perhaps contribute to enhancing downstream functions. For the first time, we showed that there are a handful of individual traits that can distinguish ECs from other PLWH groups. A future direction of this work would be to measure the gp120-specific IgG subclass and IgG glycoforms distributions able to bind to trimeric, closed conformation Env expressed on siCEM cells.

5. References

1. Vidarsson, G., G. Dekkers, and T. Rispens, IgG subclasses and allotypes: from structure to effector functions. Frontiers in immunology, 2014. 5: p. 520-520.

2. Irvine, E.B. and G. Alter, Understanding the role of antibody glycosylation through the lens of severe viral and bacterial diseases. Glycobiology, 2020. 30(4): p. 241-253.

3. Jennewein, M.F. and G. Alter, The Immunoregulatory Roles of Antibody Glycosylation. Trends Immunol, 2017. 38(5): p. 358-372.

4. Schroeder, H.W., Jr. and L. Cavacini, Structure and function of immunoglobulins. J Allergy Clin Immunol, 2010. 125(2 Suppl 2): p. S41-52.

5. Lux, A. and F. Nimmerjahn, Impact of differential glycosylation on IgG activity. Adv Exp Med Biol, 2011. 780: p. 113-24.

6. Crowley, A.R. and M.E. Ackerman, Mind the Gap: How Interspecies Variability in IgG and Its Receptors May Complicate Comparisons of Human and Non-human Primate Effector Function. Frontiers in Immunology, 2019. 10.

7. Bruhns, P., et al., Specificity and affinity of human Fcgamma receptors and their polymorphic variants for human IgG subclasses. Blood, 2009. 113(16): p. 3716-25.

8. Karampatzakis, A., et al., Antibody Afucosylation Augments CD16-Mediated Serial Killing and IFNγ Secretion by Human Natural Killer Cells. Frontiers in Immunology, 2021. 12.

9. Bruggeman, C.W., et al., Enhanced Effector Functions Due to Antibody Defucosylation Depend on the Effector Cell Fcγ Receptor Profile. J Immunol, 2017. 199(1): p. 204-211.

10. Peipp, M., et al., Antibody fucosylation differentially impacts cytotoxicity mediated by NK and PMN effector cells. Blood, 2008. 112(6): p. 2390-2399.

11. Moldt, B., et al., A nonfucosylated variant of the anti-HIV-1 monoclonal antibody b12 has enhanced FcγRIIIa-mediated antiviral activity in vitro but does not improve protection against mucosal SHIV challenge in macaques. J Virol, 2012. 86(11): p. 6189-96.

12. Chung, A.W., et al., Identification of antibody glycosylation structures that predict monoclonal antibody Fc-effector function. AIDS (London, England), 2014. 28(17): p. 2523-2530.

13. Balasubramanian, P., et al., Functional Antibody Response Against V1V2 and V3 of HIV gp120 in the VAX003 and VAX004 Vaccine Trials. Sci Rep, 2018. 8(1): p. 542.

14. Karnasuta, C., et al., Comparison of Antibody Responses Induced by RV144, VAX003, and VAX004 Vaccination Regimens. AIDS Res Hum Retroviruses, 2017. 33(5): p. 410-423.

15. Chung, A.W., et al., Dissecting Polyclonal Vaccine-Induced Humoral Immunity against HIV Using Systems Serology. Cell, 2015. 163(4): p. 988-998.

16. Ackerman, M.E., D.H. Barouch, and G. Alter, Systems serology for evaluation of HIV vaccine trials. Immunological reviews, 2017. 275(1): p. 262-270.

17. Chung, A.W. and G. Alter, Systems serology: profiling vaccine induced humoral immunity against HIV. Retrovirology, 2017. 14(1): p. 57.

18. Dobaño, C., et al., Differential Patterns of IgG Subclass Responses to Plasmodium falciparum Antigens in Relation to Malaria Protection and RTS,S Vaccination. Frontiers in Immunology, 2019. 10.

19. Haynes, B.F., et al., Immune-Correlates Analysis of an HIV-1 Vaccine Efficacy Trial. New England Journal of Medicine, 2012. 366(14): p. 1275-1286.

20. Richard, J., et al., Impact of HIV-1 Envelope Conformation on ADCC Responses. Trends Microbiol, 2018. 26(4): p. 253-265.

21. Wang, Q., A. Finzi, and J. Sodroski, The Conformational States of the HIV-1 Envelope Glycoproteins. Trends Microbiol, 2020. 28(8): p. 655-667.

22. Kant, S., et al., Polyfunctional Fc Dependent Activity of Antibodies to Native Trimeric Envelope in HIV Elite Controllers. Front Immunol, 2020. 11: p. 583820.

23. Dupuy, F.P., et al., Antibody-Dependent Cellular Cytotoxicity-Competent Antibodies against HIV-1-Infected Cells in Plasma from HIV-Infected Subjects. mBio, 2019. 10(6).

24. Kant, S., et al., Quantifying Anti-HIV Envelope-Specific Antibodies in Plasma from HIV Infected Individuals. Viruses, 2019. 11(6).

25. Richard, J., et al., Uninfected Bystander Cells Impact the Measurement of HIV-Specific Antibody-Dependent Cellular Cytotoxicity Responses. mBio. 9(2): p. e00358-18.

26. Ackerman, M.E., et al., Polyfunctional HIV-Specific Antibody Responses Are Associated with Spontaneous HIV Control. PLoS Pathog, 2016. 12(1): p. e1005315.

27. Lewis, G.K., et al., Knowns and Unknowns of Assaying Antibody-Dependent Cell-Mediated Cytotoxicity Against HIV-1. Frontiers in Immunology, 2019. 10.

28. Huang, Y., et al., Diversity of Antiviral IgG Effector Activities Observed in HIV-Infected and Vaccinated Subjects. Journal of immunology (Baltimore, Md. : 1950), 2016. 197(12): p. 4603-4612.

29. Saag, M. and S.G. Deeks, How Do HIV Elite Controllers Do What They Do? Clinical Infectious Diseases, 2010. 51(2): p. 239-241.

30. Li, J.Z. and J.N. Blankson, How elite controllers and posttreatment controllers inform our search for an HIV-1 cure. J Clin Invest, 2021. 131(11).

31. Kant, S., et al., Polyfunctional Fc Dependent Activity of Antibodies to Native Trimeric Envelope in HIV Elite Controllers. Frontiers in Immunology, 2020. 11.

32. Dupuy Franck, P., et al., Antibody-Dependent Cellular Cytotoxicity-Competent Antibodies against HIV-1-Infected Cells in Plasma from HIV-Infected Subjects. mBio. 10(6): p. e02690-19.

33. Mehraj, V., et al., Socio-economic status and time trends associated with early ART initiation following primary HIV infection in Montreal, Canada: 1996 to 2015. Journal of the International AIDS Society, 2018. 21(2): p. e25034.

34. El-Far, M., et al., Proinflammatory isoforms of IL-32 as novel and robust biomarkers for control failure in HIV-infected slow progressors. Sci Rep, 2016. 6: p. 22902.

35. Banerjee, K., et al., IgG subclass profiles in infected HIV type 1 controllers and chronic progressors and in uninfected recipients of Env vaccines. AIDS Res Hum Retroviruses, 2010. 26(4): p. 445-58.

36. Ackerman, M.E., et al., A robust, high-throughput assay to determine the phagocytic activity of clinical antibody samples. Journal of immunological methods, 2011. 366(1-2): p. 8-19.

37. Karsten, C.B., et al., A versatile high-throughput assay to characterize antibody-mediated neutrophil phagocytosis. J Immunol Methods, 2019. 471: p. 46-56.

38. Fischinger, S., et al., A high-throughput, bead-based, antigen-specific assay to assess the ability of antibodies to induce complement activation. J Immunol Methods, 2019. 473: p. 112630.

39. Hessell, A.J., et al., Fc receptor but not complement binding is important in antibody protection against HIV. Nature, 2007. 449(7158): p. 101-104.

40. Nduati, E.W., et al., Coordinated Fc-effector and neutralization functions in HIV-infected children define a window of opportunity for HIV vaccination. AIDS (London, England), 2021. 35(12): p. 1895-1905.

41. Perez, L.G., et al., V1V2-specific complement activating serum IgG as a correlate of reduced HIV-1 infection risk in RV144. PLOS ONE, 2017. 12(7): p. e0180720.

42. Spencer, D.A., et al., Phagocytosis by an HIV antibody is associated with reduced viremia irrespective of enhanced complement lysis. Nature Communications, 2022. 13(1): p. 662.

43. Sadanand, S., et al., Temporal variation in HIV-specific IgG subclass antibodies during acute infection differentiates spontaneous controllers from chronic progressors. AIDS (London, England), 2018. 32(4): p. 443-450.

44. Chung, A.W., et al., Polyfunctional Fc-effector profiles mediated by IgG subclass selection distinguish RV144 and VAX003 vaccines. Sci Transl Med, 2014. 6(228): p. 228ra38.

45. Yates, N.L., et al., Vaccine-induced Env V1-V2 IgG3 correlates with lower HIV-1 infection risk and declines soon after vaccination. Science translational medicine, 2014. 6(228): p. 228ra39-228ra39.

46. Forthal, D.N., et al., IgG2 inhibits HIV-1 internalization by monocytes, and IgG subclass binding is affected by gp120 glycosylation. Aids, 2011. 25(17): p. 2099-104.

47. Moldt, B., et al., A Nonfucosylated Variant of the anti-HIV-1 Monoclonal Antibody b12 Has Enhanced FcγRIIIa-Mediated Antiviral Activity In Vitro but Does Not Improve Protection against Mucosal SHIV Challenge in Macaques. Journal of Virology, 2012. 86(11): p. 6189-6196.

48. Ackerman, M.E., et al., Natural variation in Fc glycosylation of HIV-specific antibodies impacts antiviral activity. The Journal of clinical investigation, 2013. 123(5): p. 2183-2192.

49. Anand, S.P., et al., Enhanced Ability of Plant-Derived PGT121 Glycovariants To Eliminate HIV-1-Infected Cells. J Virol, 2021. 95(18): p. e0079621.

50. Offersen, R., et al., HIV Antibody Fc N-Linked Glycosylation Is Associated with Viral Rebound. Cell Reports, 2020. 33(11): p. 108502.

6. Figure legends

Figure 1. A. Shown are the results of antibody dependent (AD) function assays using gp120-coated targets (beads and ELISA plate wells). The y-axes for the upper row graphs show the frequency of $CD56^+$ NK cells positive for CD107a (left), secreting TNF-α (middle) and IFN-γ (right). Equivalent concentrations of IgG in plasma from UTPs, ECs, and VCs supported ADNKA function levels that were not significantly different from each other but that were higher than that in TPs. The bottom row shows results generated using assays measuring AD complement deposition (ADCD, left) AD cellular phagocytosis (ADCP middle) and AD neutrophil phagocytosis (ADNP, right) activity. There were no between group differences in the mean fluorescent intensity (MFI) of cell surface C3b levels in the ADCD assay or phagocytic score (PS) generated in the ADCP assay. Equivalent concentrations of IgG in plasma from UTPs, ECs, and VCs supported ADNP function levels that were not significantly different from each other but that were higher than that in TPs. The significance of between-group differences were assessed using Kruskal-Wallis tests with Dunn's post-tests. $P < 0.05$ were considered significant. * < 0.05, ** < 0.01, *** < 0.001, and **** < 0.0001. B. and C. Correlation matrices for gp120/Env-specific Abs and AD functions performed on different targets using plasma from B. all study participants and C. the 4 groups of PLWH. ADCP (performed in Dr. Galit Alter's lab) did not correlate with any other function for all study participants and for study participants stratified by groups of PLWH. ECs demonstrated significant correlations across all functions independent of the target cell or antigen functionalized beads used. Correlations were calculated using Spearman's correlation. Spearman's rho values are displayed on a gradient scale; negative correlations were displayed in shades of red, whereas positive correlations were plotted in shades of blue. The size and color of the circles reflect the correlation coefficient. $P < 0.05$ were considered significant. * < 0.05, ** < 0.01, *** < 0.001, and **** < 0.0001. D. PCA analysis (k-means=3) for the AD functions and Ab

concentrations assayed on different targets were plotted to observe if groups of PLWH were clustered based on principal components. The two components explain 72.5% of the variability in the data. Each cluster is color coded randomly. The numbers depicted in the plot are individual subject identification numbers. The 3 clusters could not segregate the PLWH into respective groups. Data from UTPs, TPs, and ECs was used to perform PCA. E. PLS-DA for the three groups of PLWH is shown here for the 10 Ab features that were selected from LASSO regression. None of the variation or features in the dataset distinguished the groups of PLWH. The principal components 1 and 2 as well as 1 and 3 together explain 66% of the variation in the data, whereas components 2 and 3 explain 16% of the variation in the data.

Figure 2. A. Shown here is the IgG subclass distribution for Abs specific for the five groups of Ags used to functionalize beads in plasma from the 4 groups of PLWH. As compared to ECs, UTPs have significantly higher amounts of IgG2 Abs specific for gp70V1V2, gp140, and gp41. The y-axis denotes the log10 of medians of MFI. The graphs are depicted as medians with interquartile ranges (IQR). The significance of between-group differences were assessed using one way ANOVA Kruskal-Wallis tests with Dunn's post-tests. P-values < 0.05 were considered significant. * < 0.05, ** < 0.01, *** < 0.001, and **** < 0.0001. B. and C. Correlation matrices for gp120-specific AD functions and Ag-specific IgG subclass distributions for B. all PLWH and C. for each of the 4 groups of PLWH. The IgG subclass was measured on gp120-, gp70V1V2-, and gp140-coated beads. AD functions were performed on gp120-coated beads (ADCP) or gp-120 coated CEM target cells. For all PLWH, all AD functions except ADCP correlated significantly and positively with IgG1 concentrations while there was a significant inverse correlation with gp70V1V2-specific IgG4 levels. Only ECs demonstrated significant correlations between Ag-specific IgG1 and AD function levels. Spearman's correlations were used to calculate the r and

significance levels of the correlations. Spearman's rho values are displayed on a gradient scale; negative correlations were displayed in shades of red, whereas positive correlations were plotted in shades of blue. The size and color of the circles reflect the strength of the rho values. $P < 0.05$ were considered significant. * < 0.05, ** < 0.01, *** < 0.001, and **** < 0.0001.

Figure 3. A-E. The y-axes for panels A-E show the proportion of the total anti-gp120-specific IgG Abs with each of the glycosylation patterns shown above each panel in plasma from the 4 groups of PLWH. Ab levels were measured using gp120-functionalized beads. Compared to UTPs, ECs had significantly lower proportions of agalactosylated (G0F), lower proportion of G1F, and higher proportions of sialylated (G2S2 and G2S2B) anti-gp120-specific IgG Abs. The significance of between-group differences was assessed using Kruskal-Wallis tests with Dunn's post-tests. $P < 0.05$ was considered significant. * < 0.05, ** < 0.01, *** < 0.001, and **** < 0.0001. F. and G. Matrix showing the correlations between gp120-specific IgG glycoforms and AD function levels using plasma from F. all PLWH and G. PLWH stratified into UTPs, TPs, ECs, and VCs. Agalactosylated and Sialylated anti-gp120-Abs were correlated with the majority of AD functions in all PLWH and ECs. Afucosylated Abs were strongly correlated with ADNKA and ADCC. The correlation coefficients (r) and the significance of these correlations were assessed using Spearman's tests. Spearman's r values are displayed on a gradient scale; negative correlations were displayed in shades of red, whereas positive correlations were plotted in shades of blue. The size and color of the circles reflects the strength of r-value. $P < 0.05$ were considered significant. * < 0.05, ** < 0.01, *** < 0.001, and **** < 0.0001.

Figure 4. A. PCA analysis of plasma samples from all four groups of PLWH for their gp120-specific IgG Ab glycoforms. The two principal components collectively explained 52.57% of the variation in the data. PCA clusters contained participants from different groups based on the

principal components. The clusters are color coded, and each cluster contains participants based on their principal component scores. Each number denotes the participant identification number. B. PLSDA analysis was plotted for 12 out of 24 glycoforms that were selected in LASSO regression. Multidimensional reduction techniques could not segregate the different groups of PLWH. Each elipse represents a specific group of PLWH as color coded in the legend, and each symbol represents a participant. Overlapping elipses show that the 12 glycoforms in PLSDA could not discriminate between the groups. ECs (blue elipse and circle symbols) had the highest heterogeneity amongst the variants, as the data was spread across the plot.

7. Figures

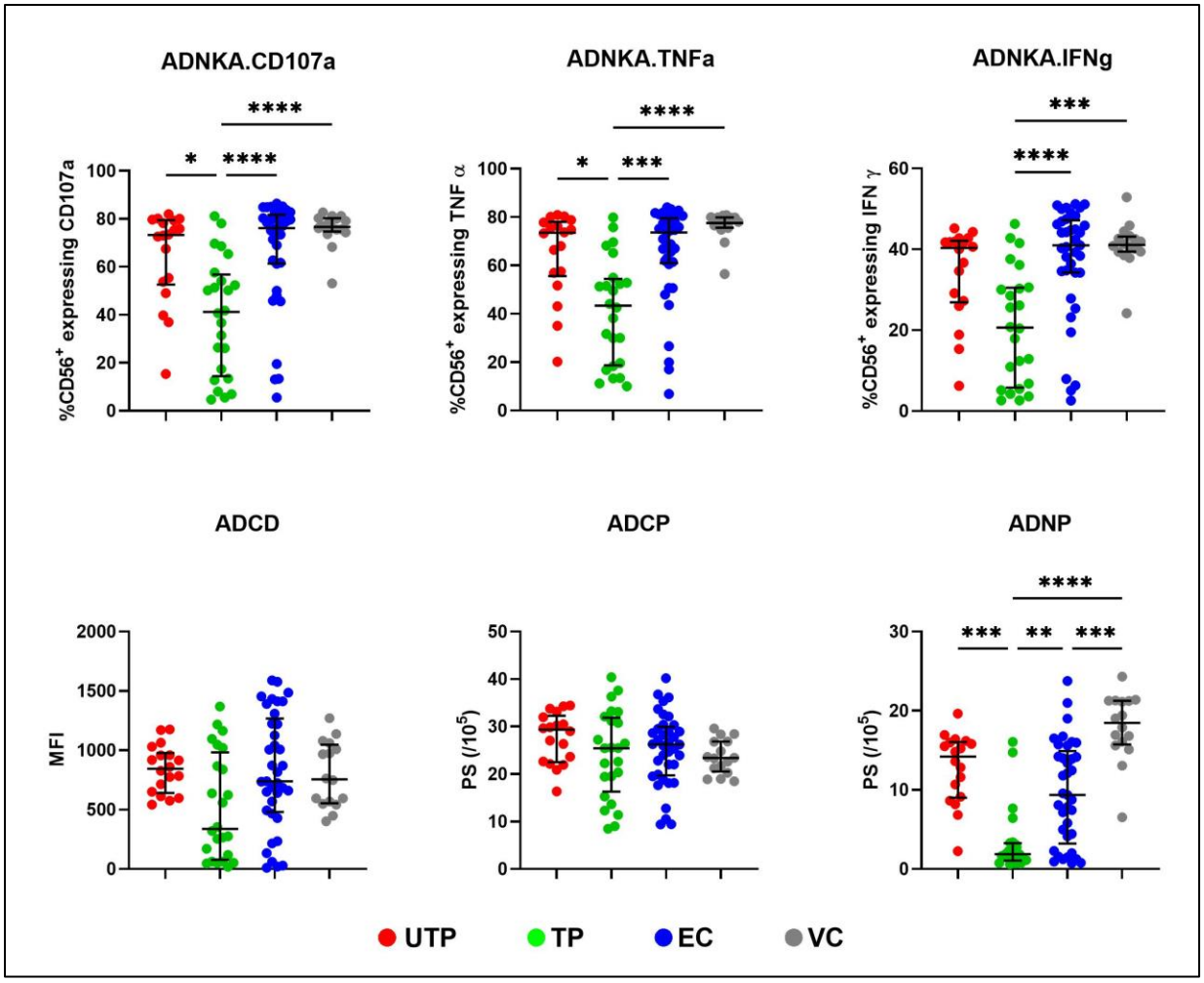

Figure 26 (Figure 1A in article): Shown are the results of antibody dependent (AD) function assays using gp120-coated targets (beads and ELISA plate wells).

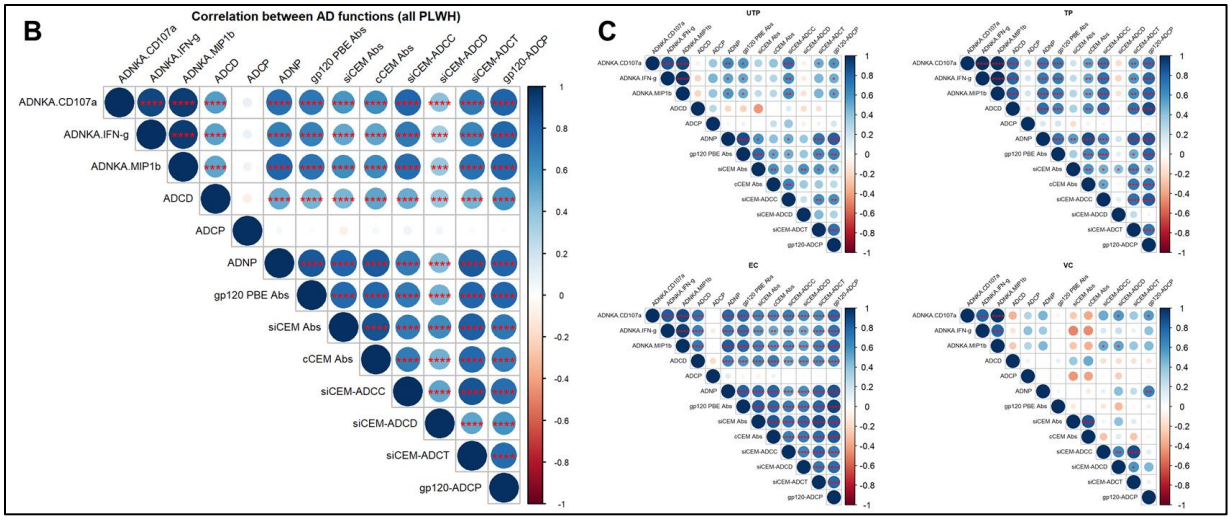

Figure 27 (Figure 1B and 1C in article): Correlation matrices for gp120/Env-specific Abs and AD functions performed on different targets using plasma from B. all study participants and C. the 4 groups of PLWH.

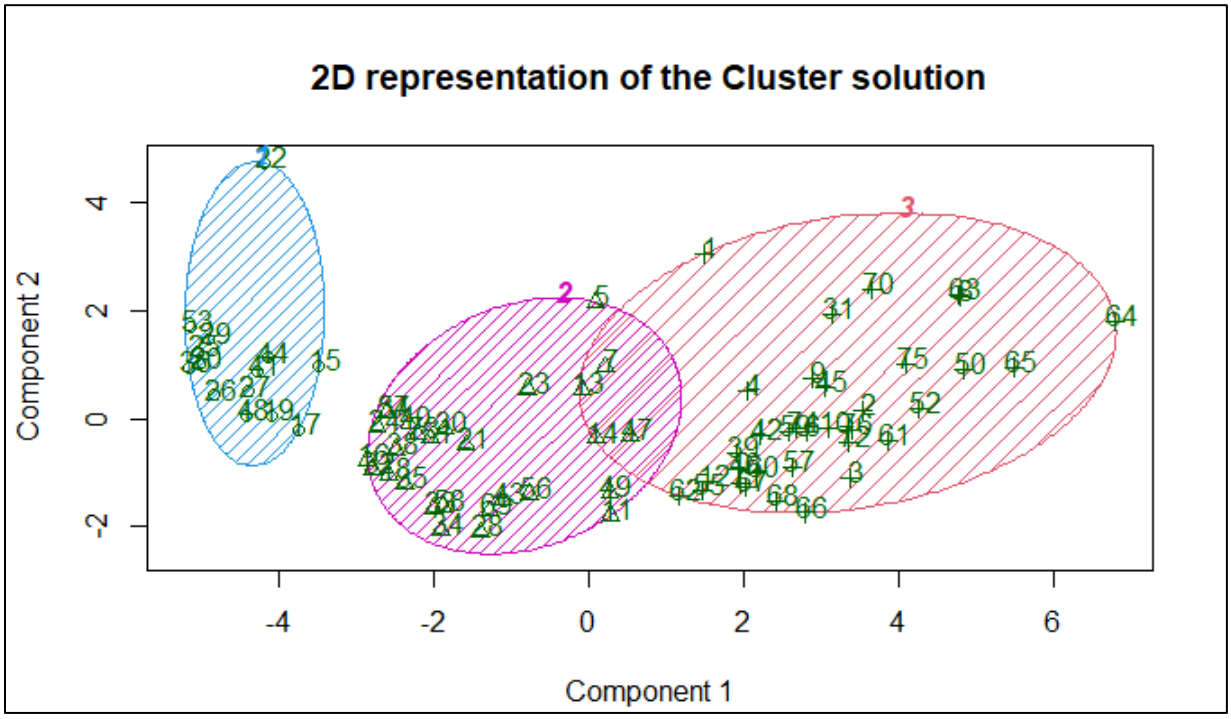

Figure 28 (Figure 1D in article): PCA analysis (k-means=3) for the AD functions and Ab concentrations assayed on different targets were plotted to observe if groups of PLWH were clustered based on principal components.

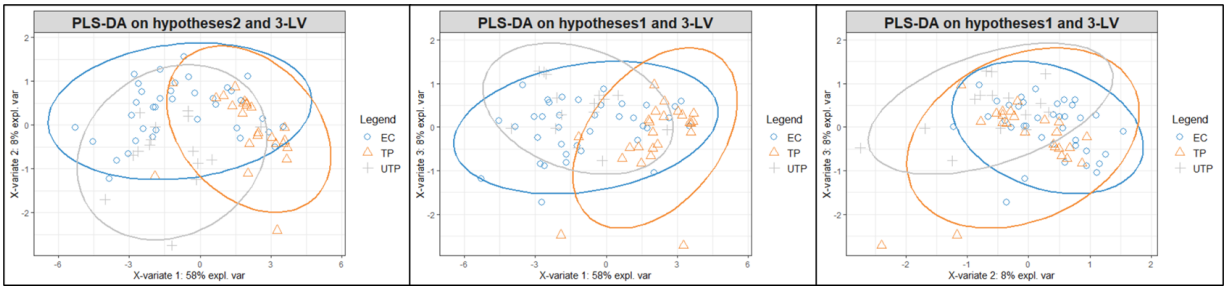

Figure 29 (Figure 1E in article): PLS-DA for the three groups of PLWH is shown here for the 10 Ab features that were selected from LASSO regression.

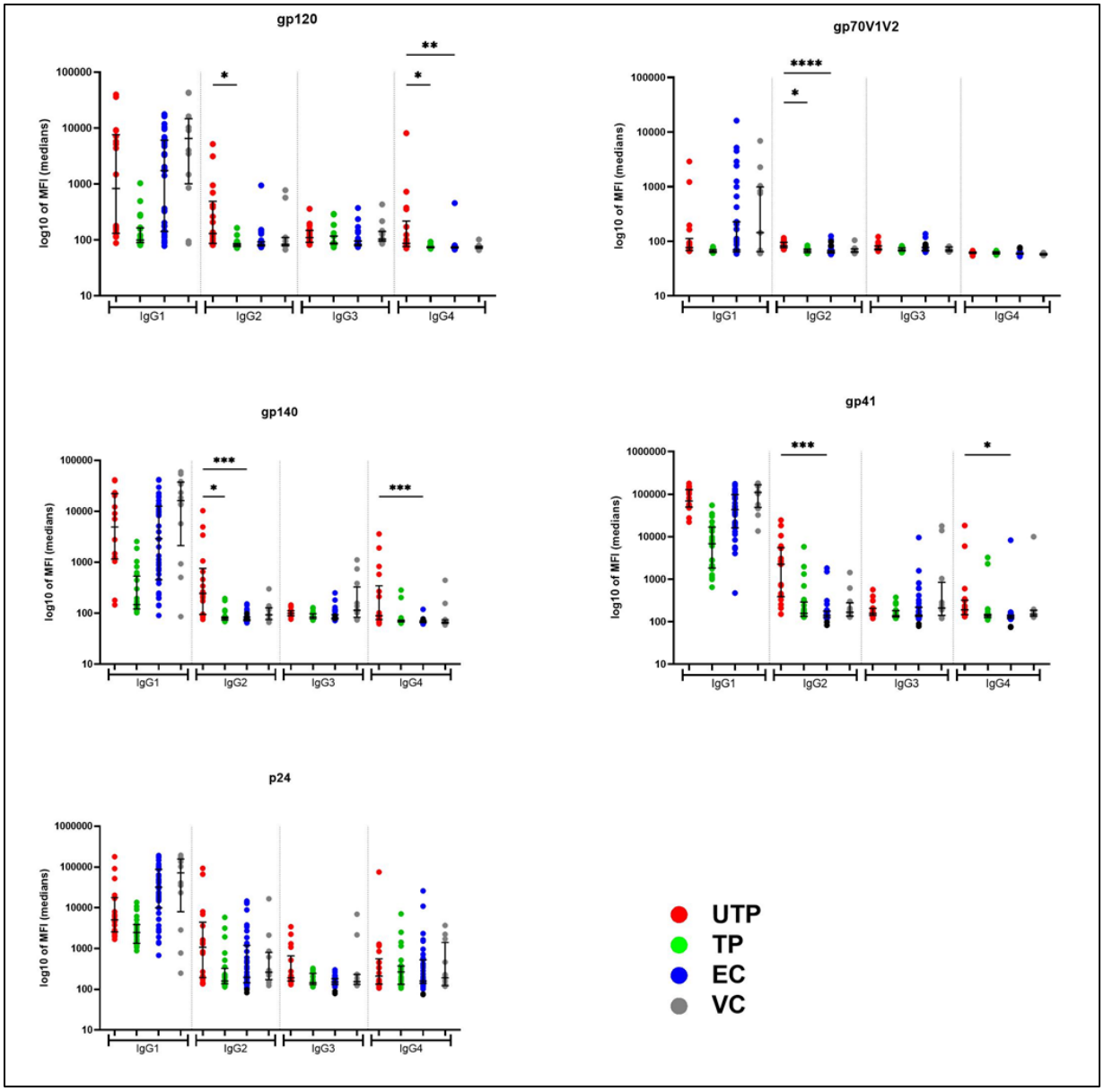

Figure 30 (Figure 2A in article): Shown here is the IgG subclass distribution for Abs specific for the five groups of Ags used to functionalize beads in plasma from the 4 groups of PLWH.

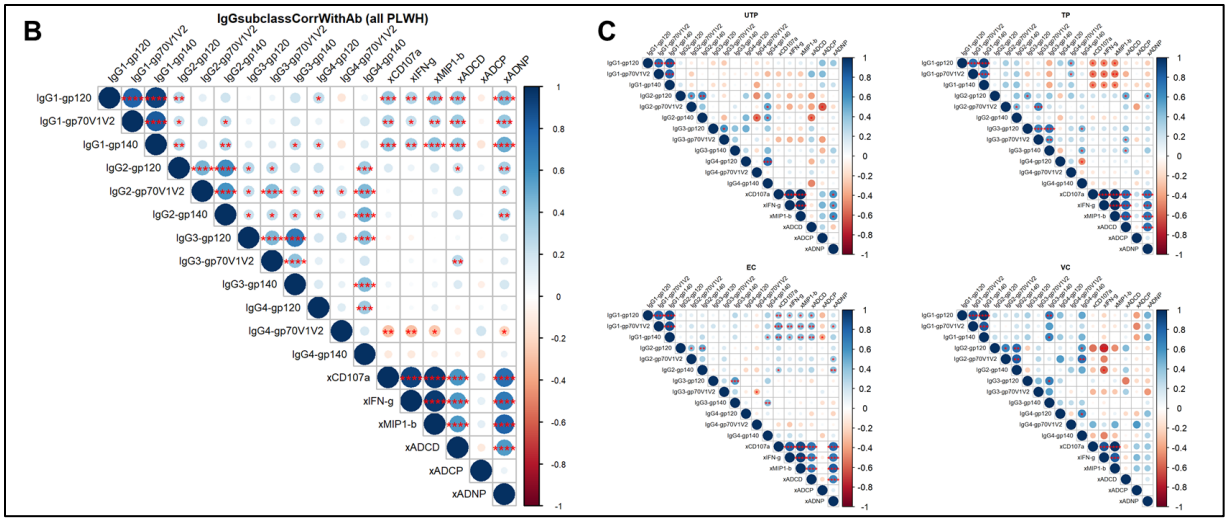

4702

4703 *Figure 31 (Figure 2B and 2C in article): Correlation matrices for gp120-specific AD functions*

4704 *and Ag-specific IgG subclass distributions for B. all PLWH and C. for each of the 4 groups of*

4705 *PLWH.*

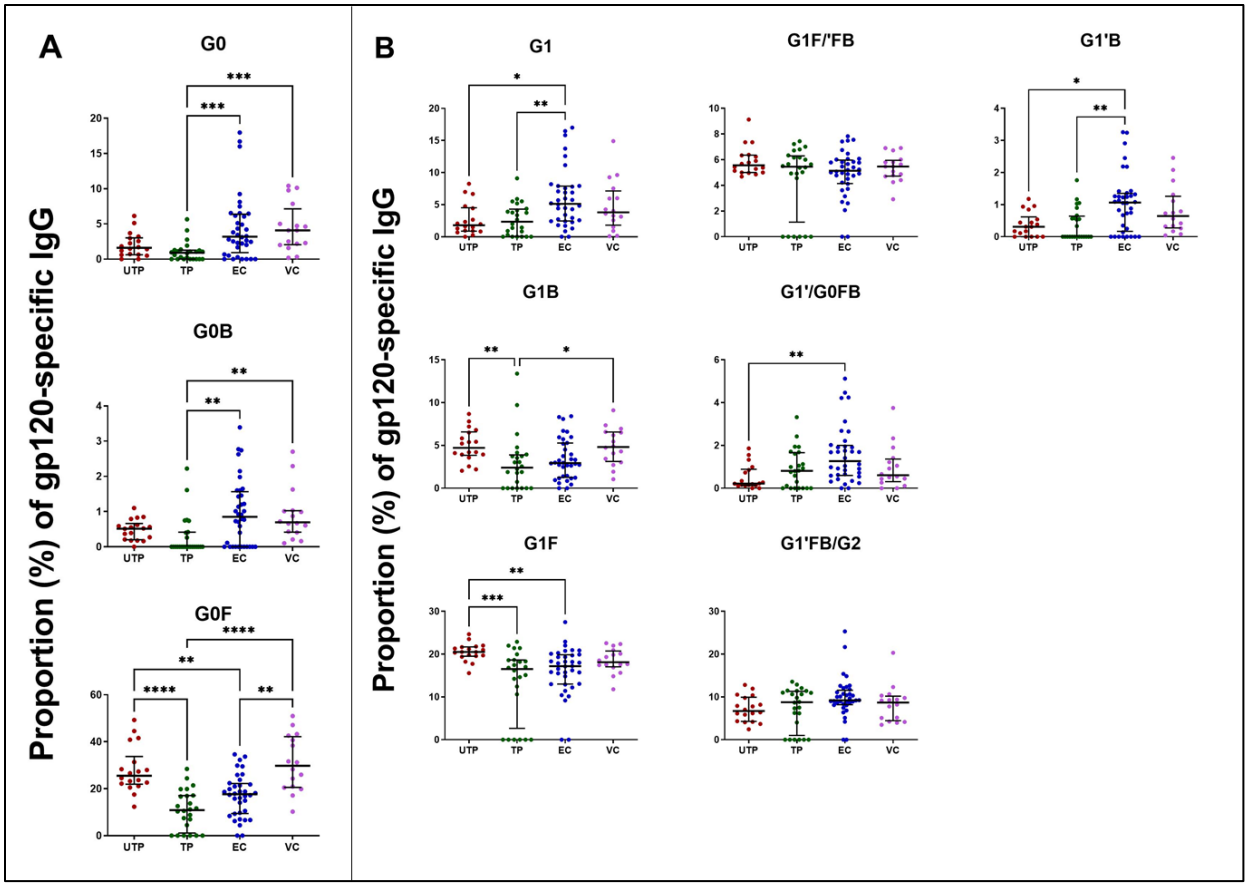

Figure 32 (Figure 3A-E in article): The y-axes for panels A-E show the proportion of the total anti-gp120-specific IgG Abs with each of the glycosylation patterns shown above each panel in plasma from the 4 groups of PLWH.

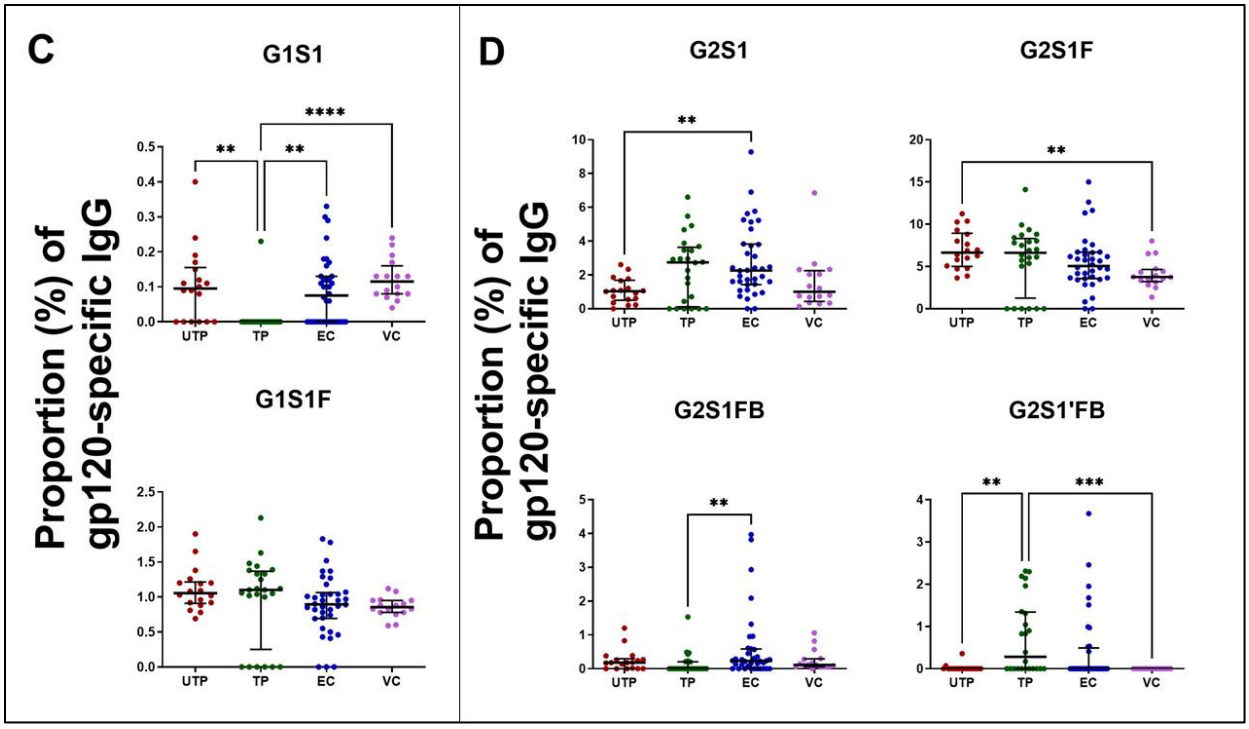
C
G1S1
G1S1F
Proportion (%) of gp120-specific IgG
UTP
TP
EC
VC
D
G2S1
G2S1F
G2S1FB
G2S1'FB
Proportion (%) of gp120-specific IgG

4710

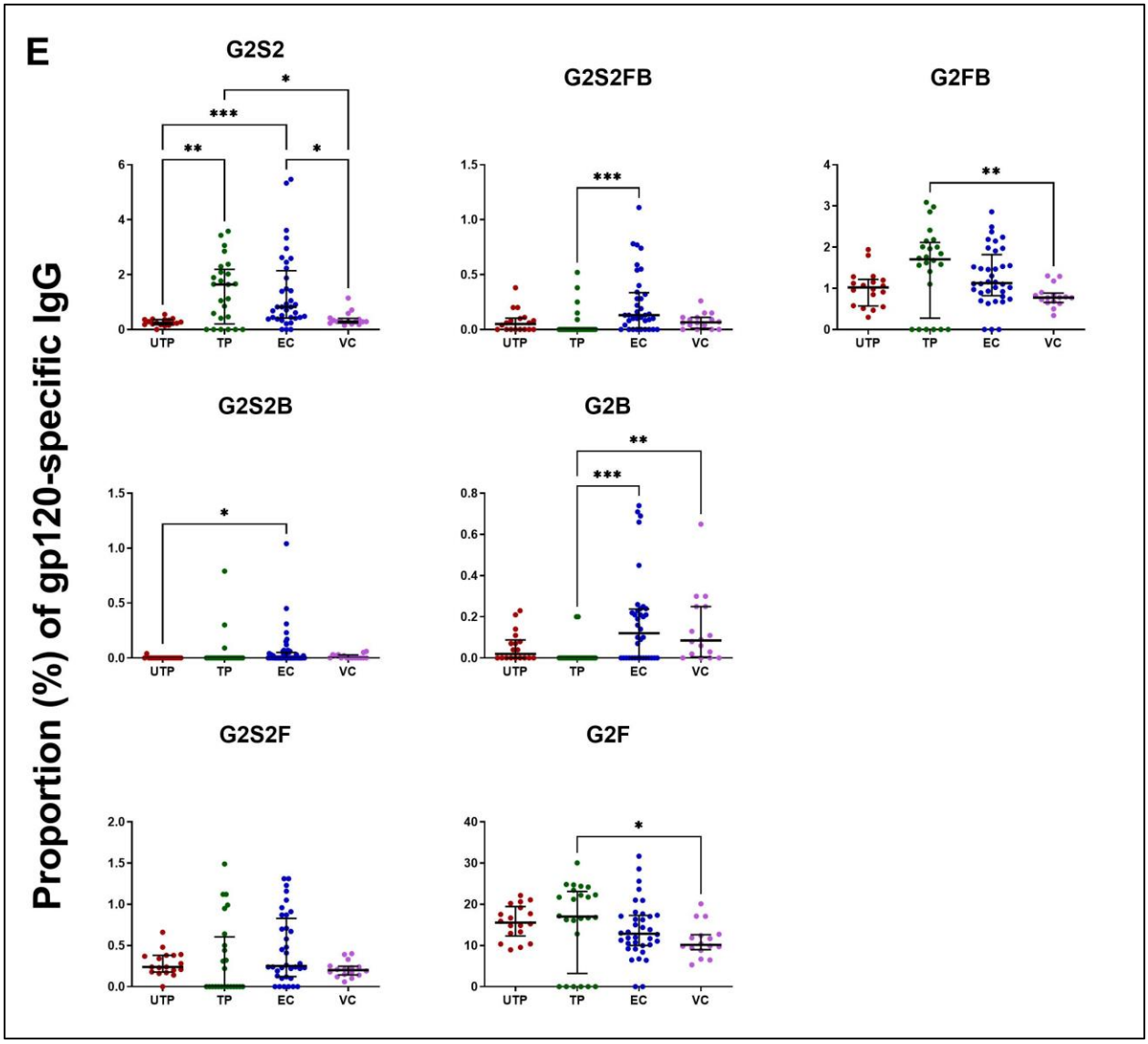
E
Proportion (%) of gp120-specific IgG
G2S2
G2S2FB
G2FB
G2S2B
G2B
G2S2F
G2F
UTP
TP
EC
VC

4711

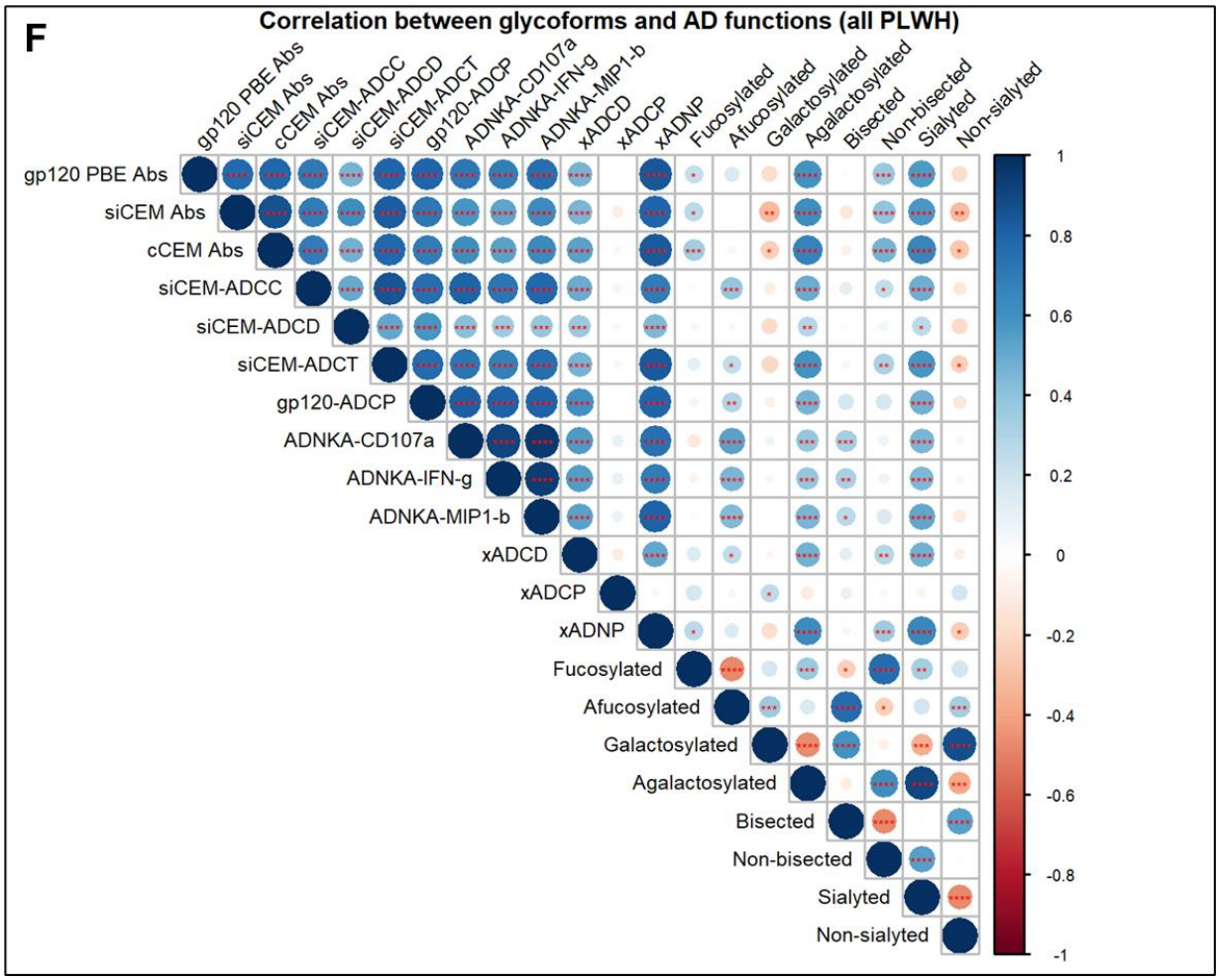

Figure 33 (Figure 3F and 3G in article):Matrix showing the correlations between gp120-specific IgG glycoforms and AD function levels using plasma from F. all PLWH and G. PLWH stratified into UTPs, TPs, ECs, and VCs.

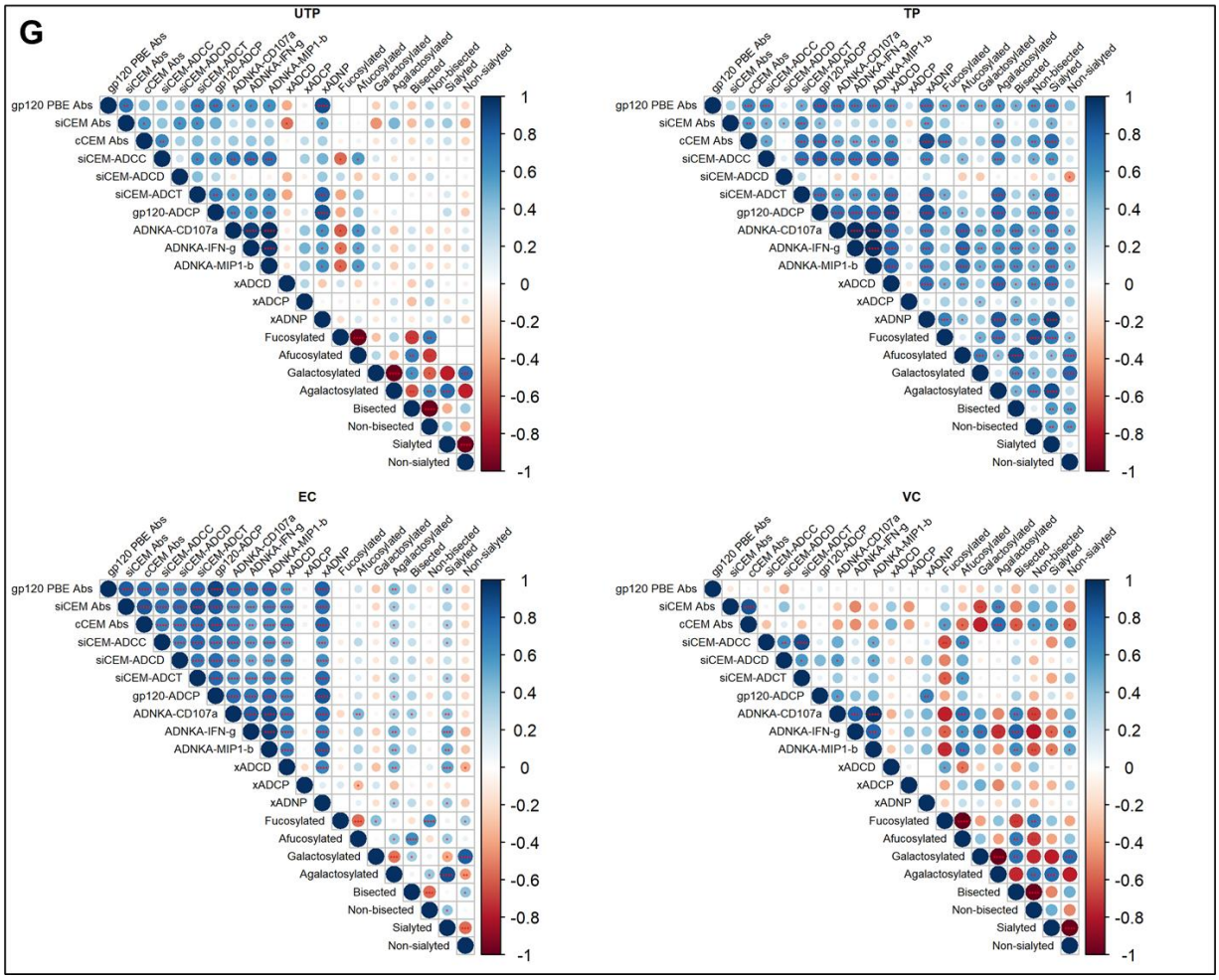
G
UTP
TP
EC
VC
gp120 PBE Abs
siCEM Abs
cCEM Abs
siCEM-ADCC
siCEM-ADCD
siCEM-ADCT
gp120-ADCP
ADNKA-CD107a
ADNKA-IFN-g
ADNKA-MIP1-b
xADCD
xADCP
xADNP
Fucosylated
Afucosylated
Galactosylated
Agalactosylated
Bisected
Non-bisected
Sialyted
Non-sialyted
1
0.8
0.6
0.4
0.2
0
-0.2
-0.4
-0.6
-0.8
-1

4716

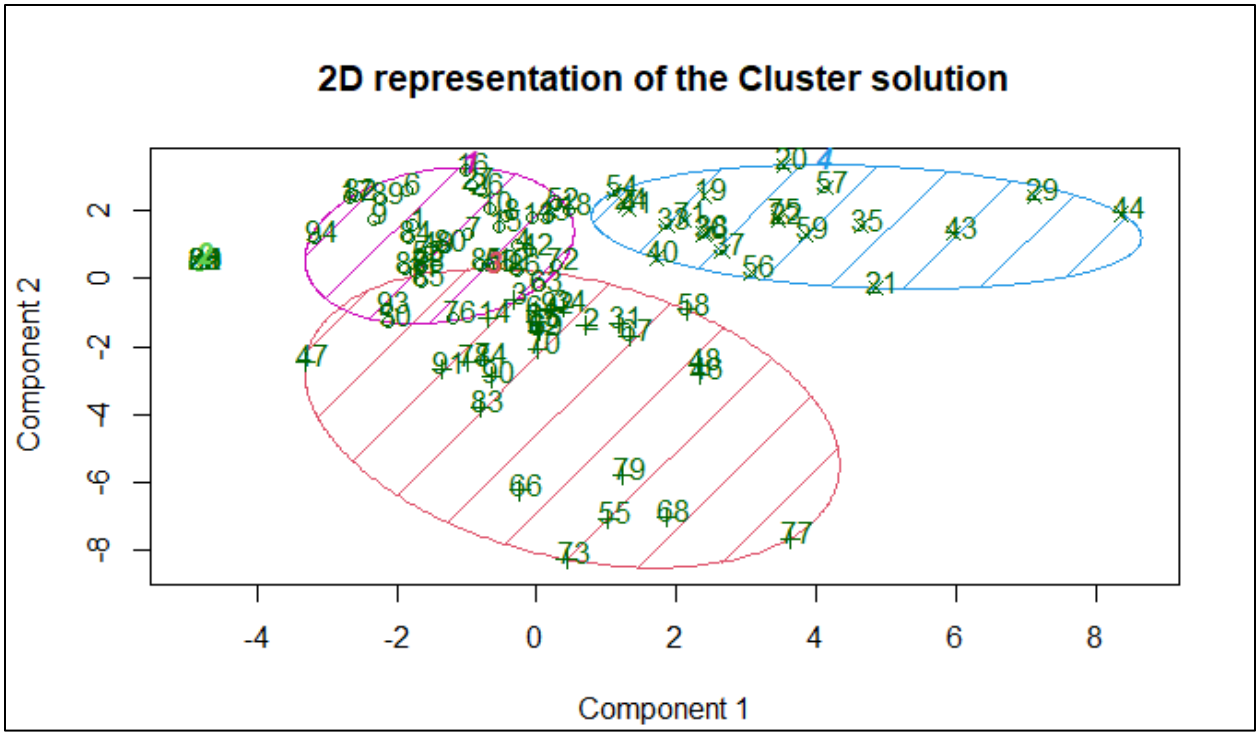

Figure 34 (Figure 4A in article): PCA analysis of plasma samples from all four groups of PLWH for their gp120-specific IgG Ab glycoforms.

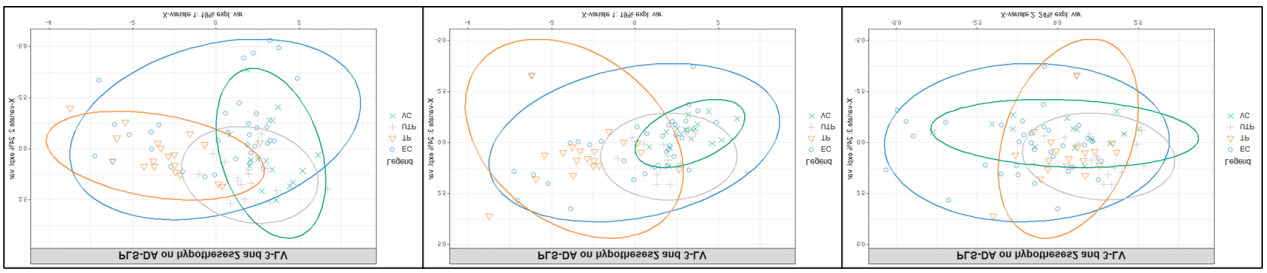

Figure 35 (Figure 4B in article): PLSDA analysis was plotted for 12 out of 24 glycoforms that were selected in LASSO regression. Multidimensional reduction techniques could not segregate the different groups of PLWH.

Discussion

The majority of assays measuring NK cell mediated ADCC and ADNKA activities use HIV Env gp120-coated CEM cells as target/stimulatory cells. The gp120 on these cells differs in important ways from the closed Env conformation exposed on HIV-infected cells and probes for different though possibly overlapping sets of Abs present in HIV plasma. To address this issue, I first characterised a novel, HIV-infected cell line generated in our laboratory. CEM cells were infected with NL4-3-Bal_{Env}-IRES-HSA HIV virions that encoded murine HSA/CD24 (mCD24). After infection, these cells were sorted for expression of HSA as a marker for infected cells. In Chapter 2, I showed that these siCEM cells are productively infected by expression of viral protein p24 and mCD24. These siCEM cells downregulated native cell surface CD4, precluding interactions of CD4 with Env and thus sampling Env in a closed conformation. This was confirmed by the failure of Abs to CD4i and CoRBS Abs such as A32 and 17b to bind to the Env expressed on siCEM cells [295, 296]. In comparison, gp120-coated CEM cells expressed cell surface CD4 and the A32 and 17b mAbs recognized gp120 on these cells. Using these 2 target cells and a gp120-coated PBE, we compared plasma from PLWH for Abs binding to the two target cells and gp120 bound to ELISA plates. We showed that different concentration of IgG bound to gp120 on CEM cells and on ELISA plates versus closed conformation Env. For all groups of PLWH, we observed the following hierarchy for the quantity of Abs binding gp120/Env in the three assays: PBE > gp120-coated cells > siCEM cells. UTPs and ECs had similar quantities of gp120-/Env-specific Abs, that were higher than those in TPs, measured in the three assays. In Chapter 3, we expanded the study population to include VCs and investigated whether plasma from the four groups of PLWH differentially supported AD functions. Using siCEM cells as target cells, we first showed that VCs had similar amounts of gp120-/Env-specific Abs in their plasma as ECs and UTPs that were higher

than in plasma from TPs. We investigated four AD functions – ADCD, ADCT, ADCP, and ADCC. The target cells for ADCD, ADCT, and ADCC were siCEM cells, while the targets for ADCP were gp120-functionalized beads. ADCC activity was assessed using a novel assay that employed annexin V to detect apoptotic target cells as a surrogate marker for NK cell-mediated cytolysis [296]. Plasma from UTPs, ECs, and VCs had similar levels of ADCT, ADCP, and ADCC activity while levels of ADCD activity differed between groups. Upon normalising the functions with the respective anti-gp120 or anti-Env Ab concentrations, the between-group differences disappeared suggesting that the amount of Abs contributed to the functional outputs. Using PCR, we detected the presence of integrated HIV DNA amongst the CD4 cells isolated from ECs and VCs. We observed that in ECs and VCs with undetectable versus detectable HIV reservoir sizes, the Ab-normalised ADCC function level was significantly higher [578].

1. Env conformation and its role in quantification of plasma Abs

ELISA plates coated with, or beads functionalized with gp120 have been employed to measure plasma gp120-specific Abs amongst PLWH or to assess vaccine induced Ab response [305, 318, 319, 333, 525, 529, 579-586]. While this method is simple, gp120 does differ antigenically from the structure of Env on infected cells. Gp120-/Env-specific mAbs bind differentially to gp120, trimeric Env and SOSIP trimers. Specifically, gp120 used to coat plates or CEM cells exposes epitopes (such as CD4i and CoRBS epitopes) found on the open Env conformation [360]. MAbs to these specificities fail to recognize SOSIP trimers or Env on siCEM cells [296, 360]. It has been confirmed that SOSIP and Env sampled on siCEM cells behave like trimers as confirmed by Abs that recognise quaternary structures such as many of the bNAbs [360]. There is a benefit to using target cells that detect and quantify Abs to trimeric Env exposed on genuinely infected cells. Independent of the group of PLWH tested, there is a significantly higher amount of Abs

recognizing gp120 compared to Abs recognizing the trimeric Env on siCEM cells. Therefore, assays utilising gp120-coated wells predominantly measure the amount of CD4i Abs or Abs that recognise the open conformation of Env in plasma and as such, gp120-coated well based methodologies likely overestimate the concentration of Abs able to detect Env on infected cells. Upon coating $CD4^+$ CEM cells with gp120, the CD4 in these cells occludes the CD4bs epitope on gp120 making it unavailable for recognition by bNAbs specific for this epitope [296, 342]. We have shown that CD4bs Abs such as b12, VRC01, and 3BNC117 fail to recognise gp120-coated CEM cells [296]. Further, the gp120 on gp120-coated cells is structurally similar to gp120 shed from infected cells in HIV-infected cell cultures and taken up by uninfected bystander cells in that mAbs to the CD4i epitope bind to bystander cells while bNAbs to the CD4bs epitope do not because these the epitopes are occluded by their interaction with CD4 on bystander cells [342]. Using gp120-coated CEM cells as ADCC target cells probes for the same Abs that target bystander cells in HIV-infected cell cultures, i.e., they target uninfected CD4 cells for lysis. As such, these Abs are likely to contribute to a pathogenic process rather than to HIV control. In Chapter 2, we reported that the amount of Abs recognising gp120-coated targets is lower than the amount detecting gp120-coated ELISA plate wells. The amount of Abs detecting both these forms of gp120 is significantly higher than the amount detecting Env on siCEM cells. Thus, the results presented in chapter 2 provide evidence for the importance of using infected target cells to measure Abs that recognise trimeric Env over Abs recognising open conformation on uninfected bystander cells.

The ADCP assay measured the amount of gp120-functionalized fluorescent beads being phagocytosed by THP-1, a monocyte cell line, in the presence of plasma Abs. Since monomeric gp120 is used to coat the beads, this assay suffers from the same limitations as other gp120-coated

bead- or cell-based Ab functional assays. However, this assay utilizes an effector cell line as opposed to primary cells in ADCC or ADCT assays. This allows for high throughput assessment of Abs and samples using the same standardised effector cell line [587].

2. Env conformation and its role in AD functions

As mentioned in the section above, the conformation of Env/gp120 impacts the class of Abs and the amount of Abs being bound. We compared ADCC functions using both gp120-coated CEM cells and siCEM cells opsonized with plasma from PLWH. We showed that for equivalent amount of total plasma IgG, the ADCC readout was significantly higher when using gp120-coated CEM as compared to when siCEM cells were used as target cells [296]. ADCP, ADCD and ADCT assays, like ADCC assay, have generally been performed using gp120-coated CEM cells as target cells or gp120-functionalised fluorescent beads without a comparison with infected CEM cells [319, 517, 525, 526, 588, 589]. Thus, there is little information available on the impact of Env conformation on ADCD and ADCT assays. Similarly, ADCP has only been performed using gp120-coated beads and thus there is no information on the impact of gp120/Env conformation on ADCP assay results.

3. Confounding ADCC assays

In chapter 3 of the thesis, I used a sensitive ADCC assay that detected the frequency of apoptotic siCEM cells measured by annexin V staining [296]. Dupuy et al. used this assay to show that plasma from PLWH contain Abs that activate NK cells to kill siCEM cells. This methodology was used to test plasma from four groups of PLWH for the concentrations of Abs supporting ADCC activity. I showed that Abs from study participants contained ADCC-competent Abs that specifically recognised trimeric Env on siCEM cells. NK cells release granzyme B and perforin upon CD16 crosslinking by Fc [590]. Released perforin drives the formation of pores in the target

cells through which granzyme B is taken up by target cells, leading to apoptosis and cell lysis [590]. The exposed inner leaflet of the plasma membrane uncovers phosphatidylserine which is detected by annexin V. This method is extremely sensitive as it can detect NK cell-mediated cytolysis for Ab concentrations as low as 0.15 μg/ml of HIVIG. The frequency of target cells positive for annexin V was significantly higher when the 0.15 μg/ml of HIVIG was tested against the GTL assay (19% versus 3%) [296]

A limitation of previously used ADCC assays was the use of gp120-coated target cells rather than HIV-infected target cells [505, 527, 591]. Some investigators measuring NK cell function have used ADNKA assays, which quantifies the activation of NK effector cells by AD mechanisms. Although these assays are often referred to as ADCC assays, in the literature the ADNKA assays measure effector cell activation and not target cell elimination [501, 523, 524]. The frequently used RFADCC assay measures the amount of dye-stained membrane uptake from the target cell by monocytes [512, 514]. Thus, the RFADCC assay does not measure ADCC activity and instead measures trogocytosis [512, 592]. In addition to using gp120-coated cells, the GTL assay has been used to measure the uptake of granzyme B by HIV-infected cell cultures that contain both infected and uninfected bystander cells [342]. Ultimately, the GTL assay does not discriminate between infected and uninfected target cells. There are two types of luciferase-based assays that employ infected target cells: one produces luciferase under the influence of Tat [518] and the other assay uses a virus the contains a ribosome-skipping T2A peptide [292, 507]. Because the T2A virus has impaired Nef protein expression, CD4 remains on the surface of infected cells and interacts with HIV Env to open its conformation [291]. Overall, there are limitations to many of the ADCC assays used to date for testing ADCC activity and vaccine efficacy. In fact, two teams compared plasma samples from their respective study populations and mAbs of a known specificity for HIV

Env epitopes using different AD methodologies. Huang et al. tested plasma from ECs, UTPs, TPs, and vaccinees from the VAX004 vaccine trial in four different ADCC assays and showed that while collectively the assays correlated with each other, the study groups showed disparate results [527]. For example, plasma from the VAX004 trial vaccinees had lower RFADCC and GTL activity than UTPs, TPs, and ECs. It is notable that the significance of between-group differences was not reported, however the same samples showed comparable levels of Luc-ADCC activity. It is important to note that irrespective of the results, the RFADCC and GTL assays used gp120-coated cells as target cells whereas Luc-ADCC used the Luc-T2A virus. Except for ECs, the other groups of PLWH or vaccinees displayed no significant correlations between the different ADCC assays raising the question as to whether one assay was more reliable than another, and if so, which one. [527]. Prévost et al. address this issue from the point of view of different gp120/Env conformations coupled with the different gold standard ADCC assays such as GTL and RFADCC assays, which reflect the Env conformation expressed by uninfected bystander cells [342]. They confirm that the GTL, RFADCC, and Luc-ADCC assays sample the open confirmation of Env/gp120, which is recognised by A32-like CD4i mAbs. We have also shown that the GTL-ADCC using gp120-coated CEM cells can be inhibited by using A32- or 17b-Fab fragments [296]. Employing trimeric, closed conformation Env-expressing siCEM cells as target cells and a sensitive annexin V-ADCC assay overcomes many of the obstacle related to detecting NK cell mediated target cell death. Future work should test the same set of mAbs and plasma samples from PLWH on siCEM based annexin V-ADCC assay and infected cell-based luciferase assays that expresses luciferase under the influence of Tat [518]. A limitation of the annexin V-ADCC assay that I have used in Chapter 3 is that we have infected cells with HIV expressing clade B Env. A future direction of this work would be to generate siCEM cells expressing a panel of Envs from

different clades. One of the biggest advantages of using the annexin V-ADCC assay to detect NK cell-mediated cytolysis is that apoptosis eventually leads to cell death as detected by live-dead staining [296].

4. Other AD function methodologies

In Chapter 3, I used siCEM cells to measure other AD functions from UTPs, TPs, ECs, and VCs. ADCD and ADCT assays, much like ADCC assay, have used gp120-coated CEM cells as target cells [319, 517, 526]. A modified version of an ADCD assay used gp120-functionalised fluorescent beads in lieu of gp120-coated CEM cells [588, 589, 593, 594]. However, two recent publications employed HIV-infected target cells to measure complement activation [595, 596]. It is important to note that to circumvent the unwanted effects by CD4i Abs binding to bystander cells, Dufloo et al. gated on genuinely infected cells. Human plasma Abs mediated complement deposition at levels that were significantly higher when target cells were infected with HIV viruses devoid of *nef* and *vpu* compared to target cells infected with WT viruses [595]. As the former target cells exposed Env in an open conformation while the later exposed Env on a closed conformation, this finding is consistent with Abs targeting CD4i epitopes being present at higher concentrations in HIV plasma than Abs to the closed conformation of Env and that HIV *nef/vpu* deletion mutants cannot downmodulate cell surface CD4, which is then able to interact with Env to open its conformation. Nef and Vpu are also implicated in downregulating CD59, a host cell surface factor known to inhibit complement mediated lysis [595]. This could be an alternate reason for the increased complement deposition and lysis of Δ*nef*Δ*vpu*-infected target cells. While there are several assays measuring ADCD, it is unclear what the importance of complement mediated lysis is in *in vivo* lysis of HIV-infected target cells. CD46, CD55, and CD59 are complement inhibitory host cell surface proteins that prevent non-specific complement mediated lysis of healthy cells

[597]. HIV counteracts complement-mediated lysis by incorporating CD55 and CD59 into its viral membrane during budding from infected cells [598, 599]. Additionally, Hessell et al. showed that Ab-mediated complement activation did not play a biological role in protection against SIV challenge in rhesus macaques passively infused with a bNAb b12 mutant, which abrogates complement activation [479]. Similar to ADCD, ADCT has been measured using gp120-coated target cells [517, 600].

The ADCP assay measured the amount of gp120-functionalized fluorescent beads being phagocytosed by THP-1, a monocyte cell line, in the presence of plasma Abs. Since monomeric gp120 is used to coat the beads, this assay suffers from the same limitations as other gp120-coated bead- or cell-based Ab functional assays. However, this assay utilizes an effector cell line as opposed to primary cells in ADCC or ADCT. This would allow for large throughput assessment of Abs and samples using the same standardised effector cell line [587].

5. AD functions in ECs

In chapter 3, for the first time we showed that plasma Abs from ECs have comparable levels of ADCC-, and ADCT-competent Abs opsonizing siCEM cells, as those from UTPs and VCs, and in concentrations that were higher than those from TPs. Others have compared plasma from controllers and non-controller in ADCC assays finding different results [521]. Lambotte et al. did this using a Cr^{51} release assay and gp120-coated CEM cells. They reported that controllers had significantly higher ADCC activity than non-controllers. However, they defined their controllers as PLWH with VLs <400 c/ml, while the ECs group in our study has a VL <50 c/ml. Ackerman et al. were the first investigate groups of PLWH that were TPs. They showed that plasma from controllers had significantly higher AD viral inhibition and ADNKA activity than UTPs and TPs [525]. While the ADNKA assay they performed used infected $CD4^+$ cells as stimulatory cells, the

opsonizing Abs they used would have bound to both genuinely infected and uninfected bystander cells that had taken up shed gp120. What they measured in their assays was the frequency of the effector cells from controllers and non controllers responding to opsonized HIV-infected cells. To assess ADCC activity targeting HIV-infected cells they would have had to be able to distinguish infected from bystander cells using a method that detected the loss of these cells using a marker such as apoptosis, which is a surrogate for cytolysis [342]. In a follow-up study, a group of VCs were added to the UTP, TP and EC groups, and plasma from these participants were tested on a panel of AD assays that included ADCD, ADCC, ADNKA, and ADCP. They reported that plasma from ECs demonstrated comparable levels of AD functions as plasma from the other groups. What distinguished ECs from the other groups of PLWH was a significant correlation across the different AD functions. In comparison, we used plasma from a similar set of groups of PLWH to opsonize siCEM cells that were virtually all HIV-infected as target cells to assess a similar set of AD functions. The ADCC assay they used was the RFADCC assay, which is actually an ADCT assay. We reported that while plasma from ECs supported similar levels of AD functions as UTPs and VCs, the level of these functions was consistently and significantly higher than those supported by plasma from TPs, when tested on target cells expressing trimeric Env. Much like the results of Ackerman et al., we also found that plasma from ECs supported levels of AD functions with significant inter-assay correlations, which was not observed in any other group of PLWH. Thus, both studies agree that a polyfunctional and correlated AD response distinguished ECs from other groups of PLWH. However, it is important to note that every assay employed by Ackerman et al. used the same plasma dilutions in each assay. In contrast, I used equivalent amounts of plasma IgG in each assay. Quantifying IgG concentrations revealed that there was inter-person variability in this parameter. By using the same range of IgG concentrations in the AD function assays and

comparing these results to the same range of HIVIG concentrations tested together with the test samples, I was able to ensure that the plasma dilutions generating AD function results were within the linear range of the HIVIG results and all results were reported relative to HIVIG. This allowed for the AD function results to be normalized to those of HIVIG.

Ackerman et al. reported that the gp120-specific Ab titers were higher in UTPs than ECs whereas I showed that plasma from UTPs and ECs had similar levels of gp120- and Env-specific Ab concentrations. Whether the gp120-specific Ab titer played a role in AD function in Ackerman et al. is not known. I was able to specifically demonstrate that any between group difference in AD function levels observed in plasma from groups of PLWH were due to differences in the concentration of Env-specific Ab concentrations and not due to between-group differences in per Ab potency. It is important to acknowledge that while Ackerman et al. did not normalize the AD functions to the concentration of gp120-specific Abs in their samples, they did measure gp120-specific IgG subclass titers and demonstrated that ECs and VCs had no gp120-specific IgG4, while UTPs had a significantly higher amount of gp120-specific Abs of this subclass. In summary, there are key differences between our data and those of Ackerman et al. However, a common theme observed in both studies was the ability of ECs to generate polyfunctional, highly coordinated gp120-/Env-specific Abs in the absence of antigenemia. The results presented in Chapter 3 have the advantage of showing that Abs from ECs were able to mediate monocyte-based trogocytosis. Previously, ADCT was mislabelled as RFADCC because both assays rely on monocyte-mediated transfer of membrane from the target cells in the presence of Abs [512, 592, 601]. Trogocytosis has been extensively studied in the field of mAb-based cancer therapeutics and has been suggested to be a reason for the failure of Ab-mediated clearance of cancer cells [602-604]. However, the implications of trogocytosis in the field of HIV are currently unknown. Recently, it was shown

that ADCT eventually leads to target cell lysis [600]. This work was significant because it was also shown that non-Ab targeted cell surface molecules such as CD4 could be transferred from target cells to monocytes. Surprisingly, they did not observe a significant correlation between RFADCC and ADCT, even though both assays are indistinguishable in principle. Yet, they observed a correlation between ADCT and the GTL-ADCC assay, which yet again emphasises the need for standardizing ADCC assays. In contrast, I reported significant correlations between the annexin V-ADCC and ADCT assay using plasma from PLWH enrolled in our study, independent of the study group they belonged to. A major difference between the results reported in Chapter 3 and those reported by Richardson et al. is the use of different target cells. I employed siCEM cells while Richardson et al. used gp120-/SOSIP-coated $CD4^+$ cells. Additional work is needed to understand the relevance of ADCT *in vivo* and in HIV control.

6. Reservoir in ECs

PLWH have proviral DNA integrated into long-lived HIV reservoirs, which are an obstacle to viral clearance and HIV cure [605]. ECs who exhibit the features of a functional HIV cure, are distinguished from successfully treated PLWH by having smaller HIV viral reservoirs [606] . The size of the HIV proviral reservoir is thought to reflect immune mechanisms that contain HIV replication. What these mechanisms are is an active area of investigation. There is some evidence that NK cell subsets play a role in shaping the size of the integrated HIV DNA reservoir. I investigated this by quantifying the size of the HIV reservoir in 53 controllers (37 ECs and 16 VCs) and AD function levels in controllers with a detectable and undetectable reservoir size. Of the 53 controllers, I could not isolate CD4 cells from 7 individuals. I detected integrated HIV DNA in 8 of 46 (17.39%) controllers while the remaining 38 controllers had an undetectable reservoir size. The HIV reservoir size was measured using an integrated HIV DNA PCR because the number

of CD4 cells available for this assay was limiting. However, the integrated HIV DNA PCR assay overestimates the HIV reservoir size as 98-99% of the HIV DNA in CD4 cells is not replication competent due to deletions, insertions, and mutations [553, 554]. With this proviso in mind, I observed that in controllers with a detectable HIV reservoir size, the level of Ab-normalized ADCC function was lower than in controllers with an undetectable HIV reservoir size. While there were similar trends for other Ab-normalized AD functions, between-group differences did not achieve statistical significance.

HIV reservoir size and AD functions have not been explored using more accurate methods for measuring the size of HIV reservoirs. The reason for this is partly due to the small size of the HIV reservoir detected in ECs and controversies regarding the assays used to measure AD functions as mentioned in section 5 “AD functions in ECs”. It was recently shown that activated functional NK cells were negatively but significantly correlated with HIV reservoir size in controllers [606]. Whether the NK functions *in vivo* were being driven via Ab-Fc interactions were not investigated. Nonetheless, it is known that ECs have a low level of HIV viral replication [93, 540, 541, 546]. This would suggest that there is either a silent reseeding of reservoir or clonal expansion of latently infected cells [607-609].

7. Role of B cells in ECs

T follicular helper (Tfh) cells are a subset of memory CD4 T cells that are key participants in HIV replication in untreated infection and latency in TPs and ECs, the two groups of PLWH who have low or undetectable VLs [610-614]. Tfh cells typically reside in lymph nodes, anatomical sanctuaries that are inaccessible to some anti-retroviral drugs, allowing these sites to be permissive for HIV replication [613-615]. Tfh cells influences activation of, class switching of, and generation of Abs in B cells in the germinal centers (GC) of lymph nodes [616]. Could there be a relationship

between latently infected Tfh cells and B cells in the GC that could result in the selection or enrichment of potent and polyfunctional Ab producing B cells in ECs? To answer this question, Yamamoto et al. found a significant correlation between the development of bNAbs later in infection and frequencies of Env-specific-Tfh and Env-specific B cells, both in the GC of lymph nodes of untreated SHIV-infected NHP early in infection [617]. Particularly, the breadth of bNAb was significantly correlated with the degree of somatic hypermutation in Env-specific B cells. This suggested that Tfh in the periphery may transport HIV Env to prime, enrich, and increase the breadth of bNAb-secreting B cells in the GC. However whether the Tfh cells themselves were infected was not assessed in this study [617]. In humans, it has been reported that the frequency of gp120-specific Tfh cells was significantly correlated with the frequency of gp120-specific B cells [618]. In particular, when ECs were compared with UTPs, *ex vivo* stimulation of B cells with autologous Tfh cells led to enhanced class-switching from IgM to IgG and increased IgG expression in ECs [618].

8. Biophysical characteristics of Abs in PLWH

In chapter 4, we characterised the biophysical characteristics of the anti-gp120/Env IgG Abs in the four groups of PLWH. We quantified the IgG subclass distribution of Abs specific for 5 groups of Ags (gp120, gp140, gp70V1V2, gp41, and p24) and observed that UTPs had significantly higher amounts of IgG2 gp70V1V2-, gp140-, and gp41-specific and gp120- and gp41-specific IgG4 Abs. Neither of these subclasses as compared to IgG3 and IgG1, would be expected to bind strongly to FcγRs to support AD functions nor to initiate the complement cascade [619, 620]. Correlates of protection analyses performed on samples obtained from the VAX003/004 and the RV144 vaccine trials showed that the unsuccessful VAX003/004 vaccines preferentially induced IgG2 and IgG4 anti-gp120-specific Abs while the regimen used in the RV144 vaccine trial preferentially induced

IgG1 and IgG3 anti-ag120-specific Abs [305, 319, 333]. Moreover, it was shown that the gp120- and gp140-specific IgG1 and IgG3 Abs were significantly and positively correlated with ADNKA functions [319]. In our ECs, we did not observe any significant correlations for gp120-, gp70V1V2-, or gp140- specific IgG3 subclass with AD functions, however we report here that IgG1 subclass for gp120, gp70V1V2, and gp140 were significantly correlated with AD functions in our enrolled ECs. This association was not observed in any other group of PLWH in our study. Apart from this, we did not observe any specific correlations between any Ag specific IgG subclass amount with the different AD functions which distinguished ECs from other groups of PLWH. We also quantified the different glycoforms of gp120-specific IgG Abs and observed that UTPs, compared to ECs, had significantly lower amount of galactosylated and sialylated forms of gp120-specific IgGs. Agalactosylated (G0) and digalactosylated-sialylated (G2S1) Abs were positively and significantly correlated with AD functions in ECs only. Galactosylated Abs have stronger FcγRIIIA/CD16 affinity on NK cells, which can impact downstream function [451, 621, 622]. G2S1 gp120-specific Abs were also recently observed in controllers with a smaller HIV reservoir size [623]. We and others have also observed ECs have significantly lower gp120-specific agalactosylated, fucosylated (G0F) Abs [525]. Fucosylated Abs have been shown to have reduced FcγRIIIA binding on NK cells and therefore reduced ADCC function [450, 451]. Additionally, it was also shown that individuals with a delayed viral rebound, compared to individuals with a rapid viral rebound after starting ART, had higher proportion of sialylated gp120-specific Abs amongst total gp120-specific Abs, however differences in the timing of viral rebound did not achieve statistical significance [624].

9. Should ECs be treated?

ECs have a low but detectable HIV reservoir size. Replication-competent viruses can be isolated from ECs and there is low level persistent viral replication in ECs. These are reasons for treating ECs. It is important to note that some ECs lose the ability to control HIV [390, 392, 625]. Follow-up studies with ECs have shown that they suffer from AIDS-related comorbidities such as increased coronary plaque and dysregulated immune activation compared to healthy, uninfected individuals [626]. Moreover, cancers are being increasingly observed in ECs which could suggest dysregulated immune functions [627, 628]. In one of the largest longitudinal follow-up studies of ECs, it was observed that ECs, compared to TPs, had higher rates of cardiovascular disorders, such as coronary disease and heart failure, and were more prone to hospitalisation [629]. Thus, it may be necessary to treat ECs to prevent AIDS-related comorbidities.

Some studies have investigated the effects of ART on ECs. Chun et al. treated 4 ECs with ART and observed that the number of cells harboring replication-competent viral genomes decreased on treatment, compared to pre- and post-treatment levels [630]. Treatment also reduced the frequency of HIV-specific CD8 responses and reduced immune activation. Compared to pre-treatment, ECs on-ART had significantly lower plasma HIV RNA levels [90]. However, ART did not have a clear effect on CD4 counts [90, 631, 632]. Whether to treat ECs has become moot as the current standard of care is to treat all PLWH upon diagnosis of HIV infection. Therefore, treatment naïve PLWH are not followed long enough to determine who would become an EC.

10. Avenues for assessing vaccine efficacy

In this thesis, I have assessed the concentration and function of anti-Env specific Abs in ECs. The results described in the thesis raise an important question with regard to the target cells used in ADCC assays to analyse the ADCC function of HIV Env-specific Abs. The plasma Abs collected from the prevention trials (RV144, VAX003, and VAX004) were assessed using gp120-coated

target cells [305, 306, 319]. The relevance of different conformations of Env targeted by AD function assays have been discussed [296-298, 505]. In Chapter 2, I showed that plasma from all groups of PLWH contain significantly higher amount of Abs binding to open conformation Env on gp120-coated cells than the concentrations of Abs binding to closed conformation Env on siCEM cells [295]. CD4i Abs such as A32 and 17b recognise gp120-coated CEM cells and uninfected bystander cells but not genuinely infected cells [295, 296, 342]. Thus, gp120-coated target cells probe for Abs that recognise bystander cells, which are likely to be pathogenic as they kill healthy cells. Thus, using these coated cells to measure vaccine-induced Abs should be used with caution. In order to identify anti-Env Abs and their functions that have the potential to target HIV-infected cells, future vaccine trials should consider using HIV-infected target cells that are virtually 100% infected as is the case for siCEM cells when performing correlates of protection analyses.

11. Contribution to current knowledge

The results presented in this thesis contribute to knowledge on host responses to HIV infection. I have quantified and characterised the anti-gp120/Env specific Abs in plasma from PLWH who exhibit spontaneous HIV control (ECs and VCs), who are untreated progressors (UTPs) or who are treated non-controllers (TPs). Quantification of these Abs was done using binding assay such as binding to gp120 coated onto ELISA plates, binding to CEM cells coated with gp120 and binding to siCEM cells expressing Env in a native trimeric conformation that mimics that found on HIV-infected cells. The ability of Abs to gp120/Env in plasma from these four groups of PLWH to support AD functions was assessed using four AD function assays. In Chapter 4, we have also seen that as compared to ECs, UTPs had significantly higher amounts of gp70-, gp140-, & gp41-

specific IgG2 and gp120- and gp41-specific IgG4. They also exhibited lower amounts of galactosylated and sialylated gp120-specific Abs as compared to ECs.

By infecting CEM.NKr.CCR5, a $CD4^+$ T cell line, with a virus that encodes HIV gene products and murine HSA, we were the first to generate an HIV-infected cell line that downmodulated cell surface CD4 and expressed Env in its closed conformation. This cell line is referred to as siCEM.

In Chapter 2, using siCEM cells, I demonstrated that plasma from PLWH have Env-specific Abs. We developed a novel flow cytometry-based assay to quantify Env-specific Abs from plasma of PLWH. I quantified Abs specific for gp120 using gp120-coated CEM cells and by ELISA using gp120-coated onto the wells of 96-well plates and Abs specific for Env using siCEM cells. All the gp120-/Env-specific Ab quantification experiments were controlled for input dilutions of IgG and were calculated by interpolating from a standard curve of known input quantity of HIVIG, which is a pool of plasma from PLWH. This allowed for a rigorous comparison of Ab concentrations specific for gp120 and Env. I found that the quantity of anti-gp120-specific Ab in plasma from PLWH detected by the flow cytometry-based assay and by ELISA was similar and higher than the quantity obtained using the flow cytometry-based assay to quantify Abs in plasma from PLWH binding to Env on siCEM. To my knowledge this work is the first to show that HIV plasma contains Abs to genuinely HIV-infected CD4 cells, which may play a role in HIV control by opsonizing HIV-infected target cells. Irrespective of method used to quantify Abs specific for gp120/Env, ECs had similar levels of these Abs as UTPs, which were higher than those in plasma from TPs. These results showed that despite undetectable antigemia, ECs maintain high levels of anti-gp120/Env-Abs.

In Chapter 3, we advanced these findings by investigating the AD functions of anti-gp120/Env-specific Abs. We show that the polyfunctional AD response in PLWH are driven by concentrations

of anti-Env specific Abs. Not a specific AD function distinguished ECs from other groups of PLWH, however ECs were the only group to demonstrate a polyfunctional and highly correlated Ab response. This has also been shown in the Ackerman study [526]. When comparing these studies, it is important to note the use of different target cells in the two studies. We also showed that controllers with detectable reservoir had a significantly lower Ab-normalized ADCC response as compared to controllers with undetectable reservoir. As per our knowledge, our study was the first to identify and report this observation.

In chapter 4, we characterised the biophysical characteristics of Abs in four groups of PLWH. We quantified their gp120-, gp70V1V2-, gp140-, gp41, and p24-specific IgG subclass distribution, and assessed the gp120-specific IgG glycoforms. As compared to UTPs, ECs had lower amounts of gp70-, gp140-, & gp41-specific IgG2 and gp120- and gp41-specific IgG4. Amongst the glycoforms, we report that ECs had higher proportions of G1 and G2S1 gp120-specific Abs. Additionally, sialylated gp120-specific Abs were shown to be significantly correlated with AD functions in ECs. Thus, there were subtle differences between the subclass distribution and glycoforms of Abs. We performed unsupervised and supervised clustering methods which included the AD functions, subclass distribution, and proportions of the different glycoforms as variables. We could not distinguish ECs from other groups of PLWH, which suggested to us, that the amounts of Abs rather than the biophysical characteristics of Abs played a role in spontaneous control of HIV. An effort to characterise the nnAbs in ECs and other groups of PLWH at this level have not been performed to our knowledge.

References

1. Umesh, et al., *Case-Control Study of Risk Factors for Human Infection with a New Zoonotic Paramyxovirus, Nipah Virus, during a 1998–1999 Outbreak of Severe Encephalitis in Malaysia.* The Journal of Infectious Diseases, 2000. **181**(5): p. 1755-1759.
2. Ksiazek, T.G., et al., *A Novel Coronavirus Associated with Severe Acute Respiratory Syndrome.* New England Journal of Medicine, 2003. **348**(20): p. 1953-1966.
3. Drosten, C., et al., *Identification of a Novel Coronavirus in Patients with Severe Acute Respiratory Syndrome.* New England Journal of Medicine, 2003. **348**(20): p. 1967-1976.
4. Dawood, F.S., et al., *Emergence of a novel swine-origin influenza A (H1N1) virus in humans.* N Engl J Med, 2009. **360**(25): p. 2605-15.
5. Zaki, A.M., et al., *Isolation of a Novel Coronavirus from a Man with Pneumonia in Saudi Arabia.* New England Journal of Medicine, 2012. **367**(19): p. 1814-1820.
6. Gao, R., et al., *Human infection with a novel avian-origin influenza A (H7N9) virus.* N Engl J Med, 2013. **368**(20): p. 1888-97.
7. Baize, S., et al., *Emergence of Zaire Ebola Virus Disease in Guinea.* New England Journal of Medicine, 2014. **371**(15): p. 1418-1425.
8. Huang, C., et al., *Clinical features of patients infected with 2019 novel coronavirus in Wuhan, China.* The Lancet, 2020. **395**(10223): p. 497-506.
9. Huet, T., et al., *Genetic organization of a chimpanzee lentivirus related to HIV-1.* Nature, 1990. **345**(6273): p. 356-9.
10. Peeters, M., et al., *Isolation and partial characterization of an HIV-related virus occurring naturally in chimpanzees in Gabon.* Aids, 1989. **3**(10): p. 625-30.
11. Worobey, M., et al., *Direct evidence of extensive diversity of HIV-1 in Kinshasa by 1960.* Nature, 2008. **455**(7213): p. 661-664.
12. Barré-Sinoussi, F., et al., *Isolation of a T-Lymphotropic Retrovirus from a Patient at Risk for Acquired Immune Deficiency Syndrome (AIDS).* Science, 1983. **220**(4599): p. 868-871.
13. Popovic, M., et al., *Detection, Isolation, and Continuous Production of Cytopathic Retroviruses (HTLV-III) from Patients with AIDS and Pre-AIDS.* Science, 1984. **224**(4648): p. 497-500.
14. *Global HIV & AIDS statistics — Fact sheet*. 2021, UNAIDS.
15. *Kaposi's sarcoma and Pneumocystis pneumonia among homosexual men--New York City and California.* MMWR Morb Mortal Wkly Rep, 1981. **30**(25): p. 305-8.
16. Hymes, K., et al., *KAPOSI'S SARCOMA IN HOMOSEXUAL MEN—A REPORT OF EIGHT CASES.* The Lancet, 1981. **318**(8247): p. 598-600.
17. Friedman-Kien, A.E., *Disseminated Kaposi's sarcoma syndrome in young homosexual men.* Journal of the American Academy of Dermatology, 1981. **5**(4): p. 468-471.
18. Wallace, J.I., et al., *T-cell ratios in homosexuals.* Lancet, 1982. **1**(8277): p. 908.

19. Modlin, R.L., et al., *T-lymphocyte subsets in lymph nodes from homosexual men.* Jama, 1983. **250**(10): p. 1302-5.

20. Kornfeld, H., et al., *T-lymphocyte subpopulations in homosexual men.* N Engl J Med, 1982. **307**(12): p. 729-31.

21. Ammann, A.J., et al., *Acquired immune dysfunction in homosexual men: immunologic profiles.* Clin Immunol Immunopathol, 1983. **27**(3): p. 315-25.

22. Rasmussen, E.O., et al., *Immunosuppression in a homosexual man with Kaposi's sarcoma.* J Am Acad Dermatol, 1982. **6**(5): p. 870-9.

23. Urmacher, C., et al., *Outbreak of Kaposi's sarcoma with cytomegalovirus infection in young homosexual men.* Am J Med, 1982. **72**(4): p. 569-75.

24. Stahl, R.E., et al., *Immunologic abnormalities in homosexual men. Relationship to Kaposi's sarcoma.* Am J Med, 1982. **73**(2): p. 171-8.

25. Friedman-Kien, A.E., et al., *Disseminated Kaposi's sarcoma in homosexual men.* Ann Intern Med, 1982. **96**(6 Pt 1): p. 693-700.

26. Fauci, A.S., *The syndrome of Kaposi's sarcoma and opportunistic infections: an epidemiologically restricted disorder of immunoregulation.* Ann Intern Med, 1982. **96**(6 Pt 1): p. 777-9.

27. Durack, D.T., *Opportunistic infections and Kaposi's sarcoma in homosexual men.* N Engl J Med, 1981. **305**(24): p. 1465-7.

28. Drew, W.L., et al., *Cytomegalovirus and Kaposi's sarcoma in young homosexual men.* Lancet, 1982. **2**(8290): p. 125-7.

29. *Epidemiologic aspects of the current outbreak of Kaposi's sarcoma and opportunistic infections.* N Engl J Med, 1982. **306**(4): p. 248-52.

30. Masur, H., et al., *An outbreak of community-acquired Pneumocystis carinii pneumonia: initial manifestation of cellular immune dysfunction.* N Engl J Med, 1981. **305**(24): p. 1431-8.

31. Gottlieb, M.S., et al., *Pneumocystis carinii pneumonia and mucosal candidiasis in previously healthy homosexual men: evidence of a new acquired cellular immunodeficiency.* N Engl J Med, 1981. **305**(24): p. 1425-31.

32. *Follow-up on Kaposi's sarcoma and Pneumocystis pneumonia.* MMWR Morb Mortal Wkly Rep, 1981. **30**(33): p. 409-10.

33. Vilaseca, J., et al., *Kaposi's sarcoma and toxoplasma gondii brain abscess in a Spanish homosexual.* Lancet, 1982. **1**(8271): p. 572.

34. Zakowski, P., et al., *Disseminated Mycobacterium avium-intracellulare infection in homosexual men dying of acquired immunodeficiency.* Jama, 1982. **248**(22): p. 2980-2.

35. Follansbee, S.E., et al., *An outbreak of Pneumocystis carinii pneumonia in homosexual men.* Ann Intern Med, 1982. **96**(6 Pt 1): p. 705-13.

36. Schroff, R.W., et al., *Immunological studies of homosexual men with immunodeficiency and Kaposi's sarcoma.* Clin Immunol Immunopathol, 1983. **27**(3): p. 300-14.

37. Metroka, C.E., et al., *Generalized lymphadenopathy in homosexual men.* Ann Intern Med, 1983. **99**(5): p. 585-91.

38. Brynes, R.K., et al., *Value of lymph node biopsy in unexplained lymphadenopathy in homosexual men.* Jama, 1983. **250**(10): p. 1313-7.

39. Altman, L.K., *New homosexual disorder worries health officials*, in *The New York Times*. 1982. p. 1.

40. Marmor, M., et al., *Risk factors for Kaposi's sarcoma in homosexual men.* Lancet, 1982. **1**(8281): p. 1083-7.

41. Poon, M.C., et al., *Acquired immunodeficiency syndrome with Pneumocystis carinii pneumonia and Mycobacterium avium-intracellulare infection in a previously healthy patient with classic hemophilia. Clinical, immunologic, and virologic findings.* Ann Intern Med, 1983. **98**(3): p. 287-90.

42. Ammann, A.J., et al., *Acquired immunodeficiency in an infant: possible transmission by means of blood products.* Lancet, 1983. **1**(8331): p. 956-8.

43. Pitchenik, A.E., et al., *Opportunistic infections and Kaposi's sarcoma among Haitians: evidence of a new acquired immunodeficiency state.* Ann Intern Med, 1983. **98**(3): p. 277-84.

44. Piot, P., et al., *Acquired immunodeficiency syndrome in a heterosexual population in Zaire.* Lancet, 1984. **2**(8394): p. 65-9.

45. Harris, C., et al., *Immunodeficiency in female sexual partners of men with the acquired immunodeficiency syndrome.* N Engl J Med, 1983. **308**(20): p. 1181-4.

46. Guinan, M.E., et al., *Heterosexual and homosexual patients with the acquired immunodeficiency syndrome. A comparison of surveillance, interview, and laboratory data.* Ann Intern Med, 1984. **100**(2): p. 213-8.

47. Reitz, M.S., Jr., et al., *Characterization and distribution of nucleic acid sequences of a novel type C retrovirus isolated from neoplastic human T lymphocytes.* Proceedings of the National Academy of Sciences of the United States of America, 1981. **78**(3): p. 1887-1891.

48. Schüpbach, J., et al., *Serological Analysis of a Subgroup of Human T-Lymphotropic Retroviruses (HTLV-III) Associated with AIDS.* Science, 1984. **224**(4648): p. 503-505.

49. Sarngadharan, M.G., et al., *Antibodies reactive with human T-lymphotropic retroviruses (HTLV-III) in the serum of patients with AIDS.* Science, 1984. **224 4648**: p. 506-8.

50. Gallo, R., et al., *Frequent detection and isolation of cytopathic retrovirus (HTLV-III) from patients with AIDS and at risk for AIDS.* Science (New York, N.Y.), 1984. **224**: p. 500-3.

51. Coffin, J., et al., *Human Immunodeficiency Viruses.* Science, 1986. **232**(4751): p. 697-697.

52. Clavel, F., et al., *Isolation of a New Human Retrovirus from West African Patients with AIDS.* Science, 1986. **233**(4761): p. 343-346.

53. Clavel, F., et al., *Molecular cloning and polymorphism of the human immune deficiency virus type 2.* Nature, 1986. **324**(6098): p. 691-5.

54. Kanki, P.J., J.R. Hopper, and M. Essex, *The origins of HIV-1 and HTLV-4/HIV-2.* Ann N Y Acad Sci, 1987. **511**: p. 370-5.

55. Henrickson, R.V., et al., *Epidemic of acquired immunodeficiency in rhesus monkeys.* Lancet, 1983. **1**(8321): p. 388-90.

56. Daniel, M.D., et al., *Isolation of T-cell tropic HTLV-III-like retrovirus from macaques.* Science, 1985. **228**(4704): p. 1201-4.

57. Marx, P.A., et al., *Simian AIDS: isolation of a type D retrovirus and transmission of the disease.* Science, 1984. **223**(4640): p. 1083-6.

58. Kanki, P.J., et al., *Serologic identification and characterization of a macaque T-lymphotropic retrovirus closely related to HTLV-III.* Science, 1985. **228**(4704): p. 1199-201.

59. Hirsch, V., et al., *Cross-reactivity to human T-lymphotropic virus type III/lymphadenopathy-associated virus and molecular cloning of simian T-cell lymphotropic virus type III from African green monkeys.* Proc Natl Acad Sci U S A, 1986. **83**(24): p. 9754-8.

60. Fultz, P.N., et al., *Isolation of a T-lymphotropic retrovirus from naturally infected sooty mangabey monkeys (Cercocebus atys).* Proc Natl Acad Sci U S A, 1986. **83**(14): p. 5286-90.

61. Chakrabarti, L., et al., *Sequence of simian immunodeficiency virus from macaque and its relationship to other human and simian retroviruses.* Nature, 1987. **328**(6130): p. 543-547.

62. Franchini, G., et al., *Sequence of simian immunodeficiency virus and its relationship to the human immunodeficiency viruses.* Nature, 1987. **328**(6130): p. 539-543.

63. Gao, F., et al., *Origin of HIV-1 in the chimpanzee Pan troglodytes troglodytes.* Nature, 1999. **397**(6718): p. 436-41.

64. Van Heuverswyn, F., et al., *SIV infection in wild gorillas.* Nature, 2006. **444**(7116): p. 164-164.

65. Sharp, P.M., G.M. Shaw, and B.H. Hahn, *Simian Immunodeficiency Virus Infection of Chimpanzees.* Journal of Virology, 2005. **79**(7): p. 3891-3902.

66. Keele, B.F., et al., *Chimpanzee reservoirs of pandemic and nonpandemic HIV-1.* Science (New York, N.Y.), 2006. **313**(5786): p. 523-526.

67. Seiki, M., et al., *Characterization of simian retrovirus genome related to human T-cell leukemia virus type I.* Princess Takamatsu Symp, 1984. **15**: p. 241-9.

68. Pedersen, N.C., et al., *Isolation of a T-Lymphotropic Virus from Domestic Cats with an Immunodeficiency-Like Syndrome.* Science, 1987. **235**(4790): p. 790-793.

69. Gonda, M.A., *Bovine immunodeficiency virus.* AIDS (London, England), 1992. **6**(8): p. 759-76.

70. Roques, P., et al., *Phylogenetic characteristics of three new HIV-1 N strains and implications for the origin of group N.* Aids, 2004. **18**(10): p. 1371-81.

71. Robertson, D.L., et al., *HIV-1 Nomenclature Proposal.* Science, 2000. **288**(5463): p. 55-55.

72. Bbosa, N., P. Kaleebu, and D. Ssemwanga, *HIV subtype diversity worldwide.* Current Opinion in HIV and AIDS, 2019. **14**(3): p. 153-160.

73. Royce, R.A., et al., *Sexual Transmission of HIV.* New England Journal of Medicine, 1997. **336**(15): p. 1072-1078.

74. Sattentau, Q.J., et al., *Epitopes of the CD4 antigen and HIV infection.* Science, 1986. **234**(4780): p. 1120-3.

75. McDougal, J.S., et al., *Binding of the human retrovirus HTLV-III/LAV/ARV/HIV to the CD4 (T4) molecule: conformation dependence, epitope mapping, antibody inhibition, and potential for idiotypic mimicry.* J Immunol, 1986. **137**(9): p. 2937-44.

76. Lifson, J.D., et al., *Induction of CD4-dependent cell fusion by the HTLV-III/LAV envelope glycoprotein.* Nature, 1986. **323**(6090): p. 725-8.

77. Haase, A.T., *Perils at mucosal front lines for HIV and SIV and their hosts.* Nat Rev Immunol, 2005. **5**(10): p. 783-92.

78. Zhang, Z.Q., et al., *Sexual Transmission and Propagation of SIV and HIV in Resting and Activated CD4+ T Cells.* Science, 1999. **286**(5443): p. 1353-1357.

79. Whitney, J.B., et al., *Rapid seeding of the viral reservoir prior to SIV viraemia in rhesus monkeys.* Nature, 2014. **512**(7512): p. 74-77.

80. Whitney, J.B., et al., *Prevention of SIVmac251 reservoir seeding in rhesus monkeys by early antiretroviral therapy.* Nature Communications, 2018. **9**(1): p. 5429.

81. Lindbäck, S., et al., *Diagnosis of primary HIV-1 infection and duration of follow-up after HIV exposure.* AIDS, 2000. **14**(15).

82. Fiebig, E.W., et al., *Dynamics of HIV viremia and antibody seroconversion in plasma donors: implications for diagnosis and staging of primary HIV infection.* AIDS, 2003. **17**(13).

83. Mellors John, W., et al., *Plasma viral load and CD4+ lymphocytes as prognostic markers of HIV-1 infection.* Annals of Internal Medicine, 1997. **126**: p. 9.

84. Mellors John, W., et al., *Prognosis in HIV-1 Infection Predicted by the Quantity of Virus in Plasma.* Science, 1996. **272**(5265): p. 1167-1170.

85. O'Brien, T.R., et al., *Serum HIV-1 RNA Levels and Time to Development of AIDS in the Multicenter Hemophilia Cohort Study.* JAMA, 1996. **276**(2): p. 105-110.

86. O'Brien, W.A., et al., *Changes in plasma HIV-1 RNA and CD4+ lymphocyte counts and the risk of progression to AIDS. Veterans Affairs Cooperative Study Group on AIDS.* N Engl J Med, 1996. **334**(7): p. 426-31.

87. Günthard, H.F., et al., *Evolution of envelope sequences of human immunodeficiency virus type 1 in cellular reservoirs in the setting of potent antiviral therapy.* J Virol, 1999. **73**(11): p. 9404-12.

88. Maldarelli, F., et al., *ART suppresses plasma HIV-1 RNA to a stable set point predicted by pretherapy viremia.* PLoS Pathog, 2007. **3**(4): p. e46.

89. Palmer, S., et al., *Low-level viremia persists for at least 7 years in patients on suppressive antiretroviral therapy.* Proc Natl Acad Sci U S A, 2008. **105**(10): p. 3879-84.

90. Hatano, H., et al., *Prospective antiretroviral treatment of asymptomatic, HIV-1 infected controllers.* PLoS Pathog, 2013. **9**(10): p. e1003691.

91. Pantaleo, G., et al., *Studies in subjects with long-term nonprogressive human immunodeficiency virus infection.* N Engl J Med, 1995. **332**(4): p. 209-16.

92. Thiébaut, R., et al., *Long-term nonprogressors and elite controllers in the ANRS CO5 HIV-2 cohort.* Aids, 2011. **25**(6): p. 865-7.

93. Hatano, H., et al., *Evidence for Persistent Low-Level Viremia in Individuals Who Control Human Immunodeficiency Virus in the Absence of Antiretroviral Therapy.* Journal of Virology, 2009. **83**(1): p. 329-335.

94. Pereyra, F., et al., *Persistent Low-Level Viremia in HIV-1 Elite Controllers and Relationship to Immunologic Parameters.* The Journal of Infectious Diseases, 2009. **200**(6): p. 984-990.

95. Okulicz, J.F. and O. Lambotte, *Epidemiology and clinical characteristics of elite controllers.* Curr Opin HIV AIDS, 2011. **6**(3): p. 163-8.

96. Kamya, P., et al., *T cell Activation does not drive CD4 decline in longitudinally followed HIV-infected Elite Controllers.* AIDS Research and Therapy, 2011. **8**(1): p. 20.

97. Durand, S. and A. Cimarelli, *The inside out of lentiviral vectors.* Viruses, 2011. **3**(2): p. 132-159.

98. Pereira, L.A., et al., *A compilation of cellular transcription factor interactions with the HIV-1 LTR promoter.* Nucleic acids research, 2000. **28**(3): p. 663-668.

99. Berkowitz, R., J. Fisher, and S.P. Goff, *RNA Packaging*, in *Morphogenesis and Maturation of Retroviruses*, H.-G. Kräusslich, Editor. 1996, Springer Berlin Heidelberg: Berlin, Heidelberg. p. 177-218.

100. Nabel, G. and D. Baltimore, *An inducible transcription factor activates expression of human immunodeficiency virus in T cells.* Nature, 1987. **326**(6114): p. 711-713.

101. Krebs, F., et al., *Lentiviral LTR-directed expression, sequence variation, and disease pathogenesis.* HIV Sequence Compendium 2001, 2001.

102. Brown, P.H., L.S. Tiley, and B.R. Cullen, *Efficient polyadenylation within the human immunodeficiency virus type 1 long terminal repeat requires flanking U3-specific sequences.* Journal of virology, 1991. **65**(6): p. 3340-3343.

103. Bell, N.M. and A.M. Lever, *HIV Gag polyprotein: processing and early viral particle assembly.* Trends Microbiol, 2013. **21**(3): p. 136-44.

104. Hill, M., G. Tachedjian, and J. Mak, *The packaging and maturation of the HIV-1 Pol proteins.* Curr HIV Res, 2005. **3**(1): p. 73-85.

105. Hallenberger, S., et al., *Inhibition of furin-mediated cleavage activation of HIV-1 glycoprotein gpl60.* Nature, 1992. **360**(6402): p. 358-361.

106. Dalgleish, A.G., et al., *The CD4 (T4) antigen is an essential component of the receptor for the AIDS retrovirus.* Nature, 1984. **312**(5996): p. 763-7.

107. Kowalski, M., et al., *Functional regions of the envelope glycoprotein of human immunodeficiency virus type 1.* Science, 1987. **237**(4820): p. 1351-5.

108. Zhu, P., et al., *Cryoelectron tomography of HIV-1 envelope spikes: further evidence for tripod-like legs.* PLoS pathogens, 2008. **4**(11): p. e1000203-e1000203.

109. Sundquist, W.I. and H.-G. Kräusslich, *HIV-1 assembly, budding, and maturation.* Cold Spring Harbor perspectives in medicine, 2012. **2**(7): p. a006924-a006924.

110. Yu, X., et al., *The matrix protein of human immunodeficiency virus type 1 is required for incorporation of viral envelope protein into mature virions.* Journal of virology, 1992. **66**(8): p. 4966-4971.

111. Gallay, P., et al., *HIV-1 infection of nondividing cells: C-terminal tyrosine phosphorylation of the viral matrix protein is a key regulator.* Cell, 1995. **80**(3): p. 379-88.

112. Byeon, I.J., et al., *Structural convergence between Cryo-EM and NMR reveals intersubunit interactions critical for HIV-1 capsid function.* Cell, 2009. **139**(4): p. 780-90.

113. Yu, K.L., et al., *HIV-1 nucleocapsid protein localizes efficiently to the nucleus and nucleolus.* Virology, 2016. **492**: p. 204-212.

114. Sleiman, D., et al., *Initiation of HIV-1 reverse transcription and functional role of nucleocapsid-mediated tRNA/viral genome interactions.* Virus Research, 2012. **169**(2): p. 324-339.

115. Keane, S.C., et al., *RNA structure. Structure of the HIV-1 RNA packaging signal.* Science, 2015. **348**(6237): p. 917-21.

116. Freed, E.O. and M.A. Martin, *The role of human immunodeficiency virus type 1 envelope glycoproteins in virus infection.* J Biol Chem, 1995. **270**(41): p. 23883-6.

117. Sattentau, Q.J. and J.P. Moore, *The role of CD4 in HIV binding and entry.* Philos Trans R Soc Lond B Biol Sci, 1993. **342**(1299): p. 59-66.

118. Jordan, C.A., et al., *Infection of brain microglial cells by human immunodeficiency virus type 1 is CD4 dependent.* J Virol, 1991. **65**(2): p. 736-42.

119. Sekaly, R.P. and R. Rooke, *CD4*, in *Encyclopedia of Immunology (Second Edition)*, P.J. Delves, Editor. 1998, Elsevier: Oxford. p. 468-472.

120. Hladik, F., et al., *Initial events in establishing vaginal entry and infection by human immunodeficiency virus type-1.* Immunity, 2007. **26**(2): p. 257-270.

121. Spira, A.I., et al., *Cellular targets of infection and route of viral dissemination after an intravaginal inoculation of simian immunodeficiency virus into rhesus macaques.* J Exp Med, 1996. **183**(1): p. 215-25.

122. Kawamura, T., et al., *Candidate microbicides block HIV-1 infection of human immature Langerhans cells within epithelial tissue explants.* The Journal of experimental medicine, 2000. **192**(10): p. 1491-1500.

123. Hu, J., M.B. Gardner, and C.J. Miller, *Simian immunodeficiency virus rapidly penetrates the cervicovaginal mucosa after intravaginal inoculation and infects intraepithelial dendritic cells.* J Virol, 2000. **74**(13): p. 6087-95.

124. Gupta, P., et al., *Memory CD4(+) T cells are the earliest detectable human immunodeficiency virus type 1 (HIV-1)-infected cells in the female genital mucosal tissue during HIV-1 transmission in an organ culture system.* J Virol, 2002. **76**(19): p. 9868-76.

125. Naeim, F., *Chapter 2 - Principles of Immunophenotyping*, in *Hematopathology*, F. Naeim, P.N. Rao, and W.W. Grody, Editors. 2008, Academic Press: Oxford. p. 27-55.

126. He, J., et al., *CCR3 and CCR5 are co-receptors for HIV-1 infection of microglia.* Nature, 1997. **385**(6617): p. 645-9.

127. Maddon, P.J., et al., *The T4 gene encodes the AIDS virus receptor and is expressed in the immune system and the brain.* Cell, 1986. **47**(3): p. 333-348.

128. Clapham, P., et al., *Is CD4 sufficient for HIV entry? Cell surface molecules involved in HIV infection.* Philos Trans R Soc Lond B Biol Sci, 1993. **342**(1299): p. 67-73.

129. Oberlin, E., et al., *The CXC chemokine SDF-1 is the ligand for LESTR/fusin and prevents infection by T-cell-line-adapted HIV-1.* Nature, 1996. **382**(6594): p. 833-5.

130. Feng, Y., et al., *HIV-1 entry cofactor: functional cDNA cloning of a seven-transmembrane, G protein-coupled receptor.* Science, 1996. **272**(5263): p. 872-7.

131. Dragic, T., et al., *HIV-1 entry into CD4+ cells is mediated by the chemokine receptor CC-CKR-5.* Nature, 1996. **381**(6584): p. 667-673.

132. Choe, H., et al., *The β-Chemokine Receptors CCR3 and CCR5 Facilitate Infection by Primary HIV-1 Isolates.* Cell, 1996. **85**(7): p. 1135-1148.

133. Doranz, B.J., et al., *A Dual-Tropic Primary HIV-1 Isolate That Uses Fusin and the β-Chemokine Receptors CKR-5, CKR-3, and CKR-2b as Fusion Cofactors.* Cell, 1996. **85**(7): p. 1149-1158.

134. Lapham Cheryl, K., et al., *Evidence for Cell-Surface Association Between Fusin and the CD4-gp120 Complex in Human Cell Lines.* Science, 1996. **274**(5287): p. 602-605.

135. Trkola, A., et al., *CD4-dependent, antibody-sensitive interactions between HIV-1 and its co-receptor CCR-5.* Nature, 1996. **384**(6605): p. 184-187.

136. Speck, R.F., et al., *Selective employment of chemokine receptors as human immunodeficiency virus type 1 coreceptors determined by individual amino acids within the envelope V3 loop.* Journal of virology, 1997. **71**(9): p. 7136-7139.

137. Sullivan, N., et al., *Determinants of human immunodeficiency virus type 1 envelope glycoprotein activation by soluble CD4 and monoclonal antibodies.* J Virol, 1998. **72**(8): p. 6332-8.

138. Cardozo, T., et al., *Structural basis for coreceptor selectivity by the HIV type 1 V3 loop.* AIDS Res Hum Retroviruses, 2007. **23**(3): p. 415-26.

139. Shioda, T., J.A. Levy, and C. Cheng-Mayer, *Small amino acid changes in the V3 hypervariable region of gp120 can affect the T-cell-line and macrophage tropism of human immunodeficiency virus type 1.* Proceedings of the National Academy of Sciences of the United States of America, 1992. **89**(20): p. 9434-9438.

140. Weissenhorn, W., et al., *The ectodomain of HIV-1 env subunit gp41 forms a soluble, alpha-helical, rod-like oligomer in the absence of gp120 and the N-terminal fusion peptide.* Embo j, 1996. **15**(7): p. 1507-14.

141. Weissenhorn, W., et al., *Atomic structure of the ectodomain from HIV-1 gp41.* Nature, 1997. **387**(6631): p. 426-30.

142. Tan, K., et al., *Atomic structure of a thermostable subdomain of HIV-1 gp41.* Proc Natl Acad Sci U S A, 1997. **94**(23): p. 12303-8.

143. Furuta, R.A., et al., *Capture of an early fusion-active conformation of HIV-1 gp41.* Nature Structural Biology, 1998. **5**(4): p. 276-279.

144. Chan, D.C., et al., *Core structure of gp41 from the HIV envelope glycoprotein.* Cell, 1997. **89**(2): p. 263-73.

145. Bosch, M.L., et al., *Identification of the fusion peptide of primate immunodeficiency viruses.* Science, 1989. **244**(4905): p. 694-7.

146. Miyauchi, K., M.M. Kozlov, and G.B. Melikyan, *Early Steps of HIV-1 Fusion Define the Sensitivity to Inhibitory Peptides That Block 6-Helix Bundle Formation.* PLOS Pathogens, 2009. **5**(9): p. e1000585.

147. Arhel, N., *Revisiting HIV-1 uncoating.* Retrovirology, 2010. **7**(1): p. 96.

148. Ratner, L., et al., *Complete nucleotide sequence of the AIDS virus, HTLV-III.* Nature, 1985. **313**(6000): p. 277-284.

149. Kleiman, L., et al., *Incorporation of tRNA into normal and mutant HIV-1.* Biochemical and Biophysical Research Communications, 1991. **174**(3): p. 1272-1280.

150. Li, X., et al., *Human immunodeficiency virus Type 1 nucleocapsid protein (NCp7) directs specific initiation of minus-strand DNA synthesis primed by human tRNA(Lys3) in vitro: studies of viral RNA molecules mutated in regions that flank the primer binding site.* J Virol, 1996. **70**(8): p. 4996-5004.

151. De Rocquigny, H., et al., *Viral RNA annealing activities of human immunodeficiency virus type 1 nucleocapsid protein require only peptide domains outside the zinc fingers.* Proc Natl Acad Sci U S A, 1992. **89**(14): p. 6472-6.

152. DeStefano, J.J., et al., *Human immunodeficiency virus reverse transcriptase displays a partially processive 3' to 5' endonuclease activity.* J Biol Chem, 1991. **266**(36): p. 24295-301.

153. Hwang, C.K., E.S. Svarovskaia, and V.K. Pathak, *Dynamic copy choice: steady state between murine leukemia virus polymerase and polymerase-dependent RNase H activity determines frequency of in vivo template switching.* Proc Natl Acad Sci U S A, 2001. **98**(21): p. 12209-14.

154. Hu, W.S. and H.M. Temin, *Genetic consequences of packaging two RNA genomes in one retroviral particle: pseudodiploidy and high rate of genetic recombination.* Proc Natl Acad Sci U S A, 1990. **87**(4): p. 1556-60.

155. Charneau, P., M. Alizon, and F. Clavel, *A second origin of DNA plus-strand synthesis is required for optimal human immunodeficiency virus replication.* J Virol, 1992. **66**(5): p. 2814-20.

156. Katz, R.A. and A.M. Skalka, *Generation of diversity in retroviruses.* Annu Rev Genet, 1990. **24**: p. 409-45.

157. Lee, G.Q., et al., *HIV-1 DNA sequence diversity and evolution during acute subtype C infection.* Nature Communications, 2019. **10**(1): p. 2737.

158. Keele, B.F., et al., *Identification and characterization of transmitted and early founder virus envelopes in primary HIV-1 infection.* Proc Natl Acad Sci U S A, 2008. **105**(21): p. 7552-7.

159. Coffin, J.M., *HIV population dynamics in vivo: implications for genetic variation, pathogenesis, and therapy.* Science, 1995. **267**(5197): p. 483-9.

160. Vodicka, M.A., et al., *HIV-1 Vpr interacts with the nuclear transport pathway to promote macrophage infection.* Genes & development, 1998. **12**(2): p. 175-185.

161. Pluymers, W., et al., *Nuclear localization of human immunodeficiency virus type 1 integrase expressed as a fusion protein with green fluorescent protein.* Virology, 1999. **258**(2): p. 327-32.

162. Heinzinger, N.K., et al., *The Vpr protein of human immunodeficiency virus type 1 influences nuclear localization of viral nucleic acids in nondividing host cells.* Proc Natl Acad Sci U S A, 1994. **91**(15): p. 7311-5.

163. Bukrinsky, M.I., et al., *A nuclear localization signal within HIV-1 matrix protein that governs infection of non-dividing cells.* Nature, 1993. **365**(6447): p. 666-9.

164. Kamata, M., et al., *Importin-α Promotes Passage through the Nuclear Pore Complex of Human Immunodeficiency Virus Type 1 Vpr.* Journal of Virology, 2005. **79**(6): p. 3557-3564.

165. Haffar, O.K., et al., *Two nuclear localization signals in the HIV-1 matrix protein regulate nuclear import of the HIV-1 pre-integration complex.* J Mol Biol, 2000. **299**(2): p. 359-68.

166. Depienne, C., et al., *Characterization of the nuclear import pathway for HIV-1 integrase.* J Biol Chem, 2001. **276**(21): p. 18102-7.

167. Bouyac-Bertoia, M., et al., *HIV-1 Infection Requires a Functional Integrase NLS.* Molecular Cell, 2001. **7**(5): p. 1025-1035.

168. Fernandez, J., et al., *Transportin-1 binds to the HIV-1 capsid via a nuclear localization signal and triggers uncoating.* Nat Microbiol, 2019. **4**(11): p. 1840-1850.

169. De Iaco, A. and J. Luban, *Cyclophilin A promotes HIV-1 reverse transcription but its effect on transduction correlates best with its effect on nuclear entry of viral cDNA.* Retrovirology, 2014. **11**: p. 11.

170. Chin, C.R., et al., *Direct Visualization of HIV-1 Replication Intermediates Shows that Capsid and CPSF6 Modulate HIV-1 Intra-nuclear Invasion and Integration.* Cell Rep, 2015. **13**(8): p. 1717-31.

171. Burdick, R.C., et al., *HIV-1 uncoats in the nucleus near sites of integration.* Proc Natl Acad Sci U S A, 2020. **117**(10): p. 5486-5493.

172. Bejarano, D.A., et al., *HIV-1 nuclear import in macrophages is regulated by CPSF6-capsid interactions at the nuclear pore complex.* Elife, 2019. **8**.

173. Kane, M., et al., *Nuclear pore heterogeneity influences HIV-1 infection and the antiviral activity of MX2.* Elife, 2018. **7**.

174. Di Nunzio, F., et al., *Human nucleoporins promote HIV-1 docking at the nuclear pore, nuclear import and integration.* PLoS One, 2012. **7**(9): p. e46037.

175. Ciuffi, A., et al., *A role for LEDGF/p75 in targeting HIV DNA integration.* Nat Med, 2005. **11**(12): p. 1287-9.

176. Shun, M.C., et al., *LEDGF/p75 functions downstream from preintegration complex formation to effect gene-specific HIV-1 integration.* Genes Dev, 2007. **21**(14): p. 1767-78.

177. Marshall, H.M., et al., *Role of PSIP1/LEDGF/p75 in lentiviral infectivity and integration targeting.* PLoS One, 2007. **2**(12): p. e1340.

178. Knyazhanskaya, E., et al., *NHEJ pathway is involved in post-integrational DNA repair due to Ku70 binding to HIV-1 integrase.* Retrovirology, 2019. **16**(1): p. 30.

179. Siliciano, J.D., et al., *Long-term follow-up studies confirm the stability of the latent reservoir for HIV-1 in resting CD4+ T cells.* Nat Med, 2003. **9**(6): p. 727-8.

180. Cohn, L.B., N. Chomont, and S.G. Deeks, *The Biology of the HIV-1 Latent Reservoir and Implications for Cure Strategies.* Cell Host Microbe, 2020. **27**(4): p. 519-530.

181. Shukla, A., N.-G.P. Ramirez, and I. D'Orso, *HIV-1 Proviral Transcription and Latency in the New Era.* Viruses, 2020. **12**(5): p. 555.

182. Gaynor, R., *Cellular transcription factors involved in the regulation of HIV-1 gene expression.* Aids, 1992. **6**(4): p. 347-63.

183. Pereira, L.A., et al., *SURVEY AND SUMMARY A compilation of cellular transcription factor interactions with the HIV-1 LTR promoter.* Nucleic Acids Research, 2000. **28**(3): p. 663-668.

184. Li, Y., G. Mak, and B.R. Franza, Jr., *In vitro study of functional involvement of Sp1, NF-kappa B/Rel, and AP1 in phorbol 12-myristate 13-acetate-mediated HIV-1 long terminal repeat activation.* Journal of Biological Chemistry, 1994. **269**(48): p. 30616-30619.

185. Chan, J.K.L. and W.C. Greene, *NF-κB/Rel: agonist and antagonist roles in HIV-1 latency.* Current opinion in HIV and AIDS, 2011. **6**(1): p. 12-18.

186. Schiralli Lester, G.M. and A.J. Henderson, *Mechanisms of HIV Transcriptional Regulation and Their Contribution to Latency.* Molecular Biology International, 2012. **2012**: p. 614120.

187. Perkins, N.D., et al., *A cooperative interaction between NF-kappa B and Sp1 is required for HIV-1 enhancer activation.* The EMBO journal, 1993. **12**(9): p. 3551-3558.

188. Qu, D., et al., *The variances of Sp1 and NF-κB elements correlate with the greater capacity of Chinese HIV-1 B'-LTR for driving gene expression.* Scientific reports, 2016. **6**: p. 34532-34532.

189. Zhu, Y., et al., *Transcription elongation factor P-TEFb is required for HIV-1 tat transactivation in vitro.* Genes Dev, 1997. **11**(20): p. 2622-32.

190. Yang, X., et al., *TAK, an HIV Tat-associated kinase, is a member of the cyclin-dependent family of protein kinases and is induced by activation of peripheral blood lymphocytes and differentiation of promonocytic cell lines.* Proc Natl Acad Sci U S A, 1997. **94**(23): p. 12331-6.

191. Mancebo, H.S., et al., *P-TEFb kinase is required for HIV Tat transcriptional activation in vivo and in vitro.* Genes Dev, 1997. **11**(20): p. 2633-44.

192. Wimmer, J., et al., *Interactions between Tat and TAR and human immunodeficiency virus replication are facilitated by human cyclin T1 but not cyclins T2a or T2b.* Virology, 1999. **255**(1): p. 182-9.

193. Garber, M.E., P. Wei, and K.A. Jones, *HIV-1 Tat interacts with cyclin T1 to direct the P-TEFb CTD kinase complex to TAR RNA.* Cold Spring Harb Symp Quant Biol, 1998. **63**: p. 371-80.

194. Keen, N.J., M.J. Churcher, and J. Karn, *Transfer of Tat and release of TAR RNA during the activation of the human immunodeficiency virus type-1 transcription elongation complex.* Embo j, 1997. **16**(17): p. 5260-72.

195. Kao, S.Y., et al., *Anti-termination of transcription within the long terminal repeat of HIV-1 by tat gene product.* Nature, 1987. **330**(6147): p. 489-93.

196. Tazi, J., et al., *Alternative splicing: regulation of HIV-1 multiplication as a target for therapeutic action.* FEBS J, 2010. **277**(4): p. 867-76.

197. Rosen, C.A., et al., *Intragenic cis-acting art gene-responsive sequences of the human immunodeficiency virus.* Proceedings of the National Academy of Sciences of the United States of America, 1988. **85**(7): p. 2071-2075.

198. Sodroski, J., et al., *A second post-transcriptional trans-activator gene required for HTLV-III replication.* Nature, 1986. **321**(6068): p. 412-417.

199. Klotman, M.E., et al., *Kinetics of expression of multiply spliced RNA in early human immunodeficiency virus type 1 infection of lymphocytes and monocytes.* Proceedings of the National Academy of Sciences, 1991. **88**(11): p. 5011.

200. Fischer, U., et al., *Evidence that HIV-1 Rev directly promotes the nuclear export of unspliced RNA.* Embo j, 1994. **13**(17): p. 4105-12.

201. Stade, K., et al., *Exportin 1 (Crm1p) is an essential nuclear export factor.* Cell, 1997. **90**(6): p. 1041-50.

202. Fornerod, M., et al., *CRM1 is an export receptor for leucine-rich nuclear export signals.* Cell, 1997. **90**(6): p. 1051-60.

203. Askjaer, P., et al., *The specificity of the CRM1-Rev nuclear export signal interaction is mediated by RanGTP.* J Biol Chem, 1998. **273**(50): p. 33414-22.

204. Coffin, J., S. Hughes, and H. Varmus, *Retroviruses, Cold Spring Habour Laboratory Press, Plainview (NY)., DK; Gollackner, B.; Knosalla, C. and Ter how far have we come.* Transpl Immunol, 1997. **9**(2-4): p. 251-6.

205. Ono, A., J.M. Orenstein, and E.O. Freed, *Role of the Gag matrix domain in targeting human immunodeficiency virus type 1 assembly.* J Virol, 2000. **74**(6): p. 2855-66.

206. Hermida-Matsumoto, L. and M.D. Resh, *Localization of human immunodeficiency virus type 1 Gag and Env at the plasma membrane by confocal imaging.* J Virol, 2000. **74**(18): p. 8670-9.

207. Finzi, A., et al., *Productive human immunodeficiency virus type 1 assembly takes place at the plasma membrane.* Journal of virology, 2007. **81**(14): p. 7476-7490.

208. Zhou, W., et al., *Identification of a membrane-binding domain within the amino-terminal region of human immunodeficiency virus type 1 Gag protein which interacts with acidic phospholipids.* J Virol, 1994. **68**(4): p. 2556-69.

209. Ono, A., et al., *Phosphatidylinositol (4,5) bisphosphate regulates HIV-1 Gag targeting to the plasma membrane.* Proc Natl Acad Sci U S A, 2004. **101**(41): p. 14889-94.

210. Burniston, M.T., et al., *Human immunodeficiency virus type 1 Gag polyprotein multimerization requires the nucleocapsid domain and RNA and is promoted by the capsid-dimer interface and the basic region of matrix protein.* J Virol, 1999. **73**(10): p. 8527-40.

211. Clavel, F. and J.M. Orenstein, *A mutant of human immunodeficiency virus with reduced RNA packaging and abnormal particle morphology.* Journal of Virology, 1990. **64**(10): p. 5230-5234.

212. Gorelick, R.J., et al., *Noninfectious human immunodeficiency virus type 1 mutants deficient in genomic RNA.* Journal of Virology, 1990. **64**(7): p. 3207-3211.

213. McBride, M.S. and A.T. Panganiban, *Position dependence of functional hairpins important for human immunodeficiency virus type 1 RNA encapsidation in vivo.* Journal of virology, 1997. **71**(3): p. 2050-2058.

214. Paillart, J.C., et al., *A loop-loop "kissing" complex is the essential part of the dimer linkage of genomic HIV-1 RNA.* Proceedings of the National Academy of Sciences, 1996. **93**(11): p. 5572-5577.

215. Johnson, S.F. and A. Telesnitsky, *Retroviral RNA Dimerization and Packaging: The What, How, When, Where, and Why.* PLOS Pathogens, 2010. **6**(10): p. e1001007.

216. Göttlinger, H.G., et al., *Effect of mutations affecting the p6 gag protein on human immunodeficiency virus particle release.* Proceedings of the National Academy of Sciences of the United States of America, 1991. **88**(8): p. 3195-3199.

217. Meusser, B., B. Purfuerst, and F.C. Luft, *HIV-1 Gag release from yeast reveals ESCRT interaction with the Gag N-terminal protein region.* J Biol Chem, 2020. **295**(52): p. 17950-17972.

218. Garrus, J.E., et al., *Tsg101 and the vacuolar protein sorting pathway are essential for HIV-1 budding.* Cell, 2001. **107**(1): p. 55-65.

219. VerPlank, L., et al., *Tsg101, a homologue of ubiquitin-conjugating (E2) enzymes, binds the L domain in HIV type 1 Pr55(Gag).* Proc Natl Acad Sci U S A, 2001. **98**(14): p. 7724-9.

220. Meng, B. and A.M.L. Lever, *The Interplay between ESCRT and Viral Factors in the Enveloped Virus Life Cycle.* Viruses, 2021. **13**(2): p. 324.

221. UNAIDS, *90-90-90: An ambitious treatment target to help end the AIDS epidemic.* 2014. p. 1.

222. UNAIDS, *90–90–90: good progress, but the world is off-track for hitting the 2020 targets*. 2020.

223. (WHO), W.H.O., *The top 10 causes of death* 2020.

224. *Total number of AIDS-related deaths worldwide from 2000 to 2020 (in millions)*. 2022, Statista: Statista - The Statistics Portal.

225. Patterson, S., et al., *Life expectancy of HIV-positive individuals on combination antiretroviral therapy in Canada.* BMC infectious diseases, 2015. **15**: p. 274-274.

226. Marcus, J.L., et al., *Comparison of Overall and Comorbidity-Free Life Expectancy Between Insured Adults With and Without HIV Infection, 2000-2016.* JAMA network open, 2020. **3**(6): p. e207954-e207954.

227. Hogg, R.S., et al., *Health-adjusted life expectancy in HIV-positive and HIV-negative men and women in British Columbia, Canada: a population-based observational cohort study.* Lancet HIV, 2017. **4**(6): p. e270-e276.

228. (FDA), U.F.a.D.A., *FDA Approval of HIV Medicines*. 2021.

229. Arts, E.J. and D.J. Hazuda, *HIV-1 antiretroviral drug therapy.* Cold Spring Harbor perspectives in medicine, 2012. **2**(4): p. a007161-a007161.

230. Richman, D.D., *Resistance of clinical isolates of human immunodeficiency virus to antiretroviral agents.* Antimicrobial agents and chemotherapy, 1993. **37**(6): p. 1207-1213.

231. Smyth, R.P., M.P. Davenport, and J. Mak, *The origin of genetic diversity in HIV-1.* Virus Research, 2012. **169**(2): p. 415-429.

232. Staszewski, S., et al., *Efavirenz plus Zidovudine and Lamivudine, Efavirenz plus Indinavir, and Indinavir plus Zidovudine and Lamivudine in the Treatment of HIV-1 Infection in Adults.* New England Journal of Medicine, 1999. **341**(25): p. 1865-1873.

233. Lennox, J.L., et al., *Safety and efficacy of raltegravir-based versus efavirenz-based combination therapy in treatment-naive patients with HIV-1 infection: a multicentre, double-blind randomised controlled trial.* Lancet, 2009. **374**(9692): p. 796-806.

234. Walmsley, S.L., et al., *Dolutegravir plus abacavir-lamivudine for the treatment of HIV-1 infection.* N Engl J Med, 2013. **369**(19): p. 1807-18.

235. Canada, G.o., *HIV and AIDS: For health professionals*.

236. (HHS), U.S.D.o.H.a.H.S., *Guidelines for the Use of Antiretroviral Agents in Adults and Adolescents Living with HIV.*

237. Group, I.S.S., et al., *Initiation of Antiretroviral Therapy in Early Asymptomatic HIV Infection.* N Engl J Med, 2015. **373**(9): p. 795-807.

238. Zolopa, A., et al., *Early antiretroviral therapy reduces AIDS progression/death in individuals with acute opportunistic infections: a multicenter randomized strategy trial.* PLoS One, 2009. **4**(5): p. e5575.

239. Chen, J., et al., *The early bird gets the worm: benefits and future directions with early antiretroviral therapy initiation in primary HIV infection.* Future Virology, 2018. **13**(11): p. 779-786.

240. Violari, A., et al., *Early Antiretroviral Therapy and Mortality among HIV-Infected Infants.* New England Journal of Medicine, 2008. **359**(21): p. 2233-2244.

241. Zolla-Pazner, S., N.L. Michael, and J.H. Kim, *A tale of four studies: HIV vaccine immunogenicity and efficacy in clinical trials.* Lancet HIV, 2021. **8**(7): p. e449-e452.

242. Allan, J.S., et al., *Major Glycoprotein Antigens That Induce Antibodies in AIDS Patients Are Encoded by HTLV-III.* Science, 1985. **228**(4703): p. 1091-1094.

243. Bernstein, H.B., et al., *Human immunodeficiency virus type 1 envelope glycoprotein is modified by O-linked oligosaccharides.* Journal of virology, 1994. **68**(1): p. 463-468.

244. Leonard, C.K., et al., *Assignment of intrachain disulfide bonds and characterization of potential glycosylation sites of the type 1 recombinant human immunodeficiency virus envelope glycoprotein (gp120) expressed in Chinese hamster ovary cells.* J Biol Chem, 1990. **265**(18): p. 10373-82.

245. Wei, X., et al., *Antibody neutralization and escape by HIV-1.* Nature, 2003. **422**(6929): p. 307-312.

246. Zhou, T., et al., *Quantification of the Impact of the HIV-1-Glycan Shield on Antibody Elicitation.* Cell Rep, 2017. **19**(4): p. 719-732.

247. Mascola, J.R. and D.C. Montefiori, *HIV-1: nature's master of disguise.* Nature Medicine, 2003. **9**(4): p. 393-394.

248. Pinter, A., et al., *Oligomeric structure of gp41, the transmembrane protein of human immunodeficiency virus type 1.* Journal of virology, 1989. **63**(6): p. 2674-2679.

249. Earl, P.L., R.W. Doms, and B. Moss, *Oligomeric structure of the human immunodeficiency virus type 1 envelope glycoprotein.* Proceedings of the National Academy of Sciences of the United States of America, 1990. **87**(2): p. 648-652.

250. Song, Y.E., et al., *βTrCP is Required for HIV-1 Vpu Modulation of CD4, GaLV Env, and BST-2/Tetherin.* Viruses, 2018. **10**(10).

251. Schubert, U., et al., *CD4 glycoprotein degradation induced by human immunodeficiency virus type 1 Vpu protein requires the function of proteasomes and the ubiquitin-conjugating pathway.* J Virol, 1998. **72**(3): p. 2280-8.

252. Margottin, F., et al., *A novel human WD protein, h-beta TrCp, that interacts with HIV-1 Vpu connects CD4 to the ER degradation pathway through an F-box motif.* Mol Cell, 1998. **1**(4): p. 565-74.

253. Rowell, J.F., et al., *Lysosome-associated membrane protein-1-mediated targeting of the HIV-1 envelope protein to an endosomal/lysosomal compartment enhances its presentation to MHC class II-restricted T cells.* The Journal of Immunology, 1995. **155**(4): p. 1818.

254. Egan, M.A., et al., *Human immunodeficiency virus type 1 envelope protein endocytosis mediated by a highly conserved intrinsic internalization signal in the cytoplasmic domain of gp41 is*

suppressed in the presence of the Pr55gag precursor protein. Journal of virology, 1996. **70**(10): p. 6547-6556.

255. Zhu, P., et al., *Electron tomography analysis of envelope glycoprotein trimers on HIV and simian immunodeficiency virus virions.* Proceedings of the National Academy of Sciences of the United States of America, 2003. **100**(26): p. 15812-15817.

256. Schneider, J., et al., *Shedding and interspecies type sero-reactivity of the envelope glycopolypeptide gp120 of the human immunodeficiency virus.* Journal of General Virology, 1986. **67**(11): p. 2533-2538.

257. Willey, R.L., et al., *Identification of conserved and divergent domains within the envelope gene of the acquired immunodeficiency syndrome retrovirus.* Proc Natl Acad Sci U S A, 1986. **83**(14): p. 5038-42.

258. Starcich, B.R., et al., *Identification and characterization of conserved and variable regions in the envelope gene of HTLV-III/LAV, the retrovirus of AIDS.* Cell, 1986. **45**(5): p. 637-48.

259. Kwong, P.D., et al., *Structure of an HIV gp120 envelope glycoprotein in complex with the CD4 receptor and a neutralizing human antibody.* Nature, 1998. **393**(6686): p. 648-659.

260. Sagar, M., et al., *Human immunodeficiency virus type 1 V1-V2 envelope loop sequences expand and add glycosylation sites over the course of infection, and these modifications affect antibody neutralization sensitivity.* Journal of virology, 2006. **80**(19): p. 9586-9598.

261. Kitrinos, K.M., et al., *Turnover of env variable region 1 and 2 genotypes in subjects with late-stage human immunodeficiency virus type 1 infection.* J Virol, 2003. **77**(12): p. 6811-22.

262. Olshevsky, U., et al., *Identification of individual human immunodeficiency virus type 1 gp120 amino acids important for CD4 receptor binding.* J Virol, 1990. **64**(12): p. 5701-7.

263. Lasky, L.A., et al., *Delineation of a region of the human immunodeficiency virus type 1 gp120 glycoprotein critical for interaction with the CD4 receptor.* Cell, 1987. **50**(6): p. 975-85.

264. Trkola, A., et al., *CD4-dependent, antibody-sensitive interactions between HIV-1 and its co-receptor CCR-5.* Nature, 1996. **384**(6605): p. 184-7.

265. Madani, N., et al., *Localized changes in the gp120 envelope glycoprotein confer resistance to human immunodeficiency virus entry inhibitors BMS-806 and #155.* Journal of virology, 2004. **78**(7): p. 3742-3752.

266. Xiang, S.-H., et al., *Mutagenic stabilization and/or disruption of a CD4-bound state reveals distinct conformations of the human immunodeficiency virus type 1 gp120 envelope glycoprotein.* Journal of virology, 2002. **76**(19): p. 9888-9899.

267. Wu, L., et al., *CD4-induced interaction of primary HIV-1 gp120 glycoproteins with the chemokine receptor CCR-5.* Nature, 1996. **384**(6605): p. 179-83.

268. Wyatt, R., et al., *Analysis of the interaction of the human immunodeficiency virus type 1 gp120 envelope glycoprotein with the gp41 transmembrane glycoprotein.* J Virol, 1997. **71**(12): p. 9722-31.

269. Moore, J.P., et al., *Immunological evidence for interactions between the first, second, and fifth conserved domains of the gp120 surface glycoprotein of human immunodeficiency virus type 1.* J Virol, 1994. **68**(11): p. 6836-47.

270. Buzon, V., et al., *Crystal structure of HIV-1 gp41 including both fusion peptide and membrane proximal external regions.* PLoS pathogens, 2010. **6**(5): p. e1000880-e1000880.

271. Munro, J.B., et al., *Conformational dynamics of single HIV-1 envelope trimers on the surface of native virions.* Science (New York, N.Y.), 2014. **346**(6210): p. 759-763.

272. Aiken, C., et al., *Mutational analysis of HIV-1 Nef: identification of two mutants that are temperature-sensitive for CD4 downregulation.* Virology, 1996. **217**(1): p. 293-300.

273. Aiken, C., et al., *Nef induces CD4 endocytosis: requirement for a critical dileucine motif in the membrane-proximal CD4 cytoplasmic domain.* Cell, 1994. **76**(5): p. 853-64.

274. Willey, R.L., et al., *Human immunodeficiency virus type 1 Vpu protein induces rapid degradation of CD4.* J Virol, 1992. **66**(12): p. 7193-200.

275. Rhee, S.S. and J.W. Marsh, *Human immunodeficiency virus type 1 Nef-induced down-modulation of CD4 is due to rapid internalization and degradation of surface CD4.* J Virol, 1994. **68**(8): p. 5156-63.

276. Lama, J., A. Mangasarian, and D. Trono, *Cell-surface expression of CD4 reduces HIV-1 infectivity by blocking Env incorporation in a Nef- and Vpu-inhibitable manner.* Curr Biol, 1999. **9**(12): p. 622-31.

277. Moore, J.P., et al., *A monoclonal antibody to CD4 domain 2 blocks soluble CD4-induced conformational changes in the envelope glycoproteins of human immunodeficiency virus type 1 (HIV-1) and HIV-1 infection of CD4+ cells.* Journal of virology, 1992. **66**(8): p. 4784-4793.

278. Truneh, A., et al., *A region in domain 1 of CD4 distinct from the primary gp120 binding site is involved in HIV infection and virus-mediated fusion.* J Biol Chem, 1991. **266**(9): p. 5942-8.

279. Haim, H., et al., *Soluble CD4 and CD4-mimetic compounds inhibit HIV-1 infection by induction of a short-lived activated state.* PLoS pathogens, 2009. **5**(4): p. e1000360-e1000360.

280. Martin, L., et al., *Rational design of a CD4 mimic that inhibits HIV-1 entry and exposes cryptic neutralization epitopes.* Nature Biotechnology, 2003. **21**(1): p. 71-76.

281. Ma, X., et al., *HIV-1 Env trimer opens through an asymmetric intermediate in which individual protomers adopt distinct conformations.* eLife, 2018. **7**: p. e34271.

282. Xiang, S.H., et al., *Mutagenic stabilization and/or disruption of a CD4-bound state reveals distinct conformations of the human immunodeficiency virus type 1 gp120 envelope glycoprotein.* J Virol, 2002. **76**(19): p. 9888-99.

283. Labrijn, A.F., et al., *Access of antibody molecules to the conserved coreceptor binding site on glycoprotein gp120 is sterically restricted on primary human immunodeficiency virus type 1.* J Virol, 2003. **77**(19): p. 10557-65.

284. Xiang, S.-H., et al., *Characterization of CD4-Induced Epitopes on the HIV Type 1 gp120 Envelope Glycoprotein Recognized by Neutralizing Human Monoclonal Antibodies.* AIDS Research and Human Retroviruses, 2002. **18**(16): p. 1207-1217.

285. Prévost, J., et al., *Influence of the Envelope gp120 Phe 43 Cavity on HIV-1 Sensitivity to Antibody-Dependent Cell-Mediated Cytotoxicity Responses.* J Virol, 2017. **91**(7).

286. Angelis, K., et al., *Global Dispersal Pattern of HIV Type 1 Subtype CRF01_AE: A Genetic Trace of Human Mobility Related to Heterosexual Sexual Activities Centralized in Southeast Asia.* The Journal of Infectious Diseases, 2015. **211**(11): p. 1735-1744.

287. Ruxrungtham, K. and P. Phanuphak, *Update on HIV/AIDS in Thailand.* J Med Assoc Thai, 2001. **84 Suppl 1**: p. S1-17.

288. Weniger, B.G., et al., *The epidemiology of HIV infection and AIDS in Thailand.* Aids, 1991. **5 Suppl 2**: p. S71-85.

289. Alsahafi, N., et al., *An Asymmetric Opening of HIV-1 Envelope Mediates Antibody-Dependent Cellular Cytotoxicity.* Cell host & microbe, 2019. **25**(4): p. 578-587.e5.

290. Veillette, M., et al., *Interaction with cellular CD4 exposes HIV-1 envelope epitopes targeted by antibody-dependent cell-mediated cytotoxicity.* Journal of virology, 2014. **88**(5): p. 2633-2644.

291. Prévost, J., et al., *Incomplete Downregulation of CD4 Expression Affects HIV-1 Env Conformation and Antibody-Dependent Cellular Cytotoxicity Responses.* J Virol, 2018. **92**(13).

292. Alberti, M.O., et al., *Optimized Replicating Renilla Luciferase Reporter HIV-1 Utilizing Novel Internal Ribosome Entry Site Elements for Native Nef Expression and Function.* AIDS research and human retroviruses, 2015. **31**(12): p. 1278-1296.

293. Ferrari, G., et al., *An HIV-1 gp120 envelope human monoclonal antibody that recognizes a C1 conformational epitope mediates potent antibody-dependent cellular cytotoxicity (ADCC) activity and defines a common ADCC epitope in human HIV-1 serum.* Journal of virology, 2011. **85**(14): p. 7029-7036.

294. Richard, J., et al., *Flow cytometry-based assay to study HIV-1 gp120 specific antibody-dependent cellular cytotoxicity responses.* Journal of Virological Methods, 2014. **208**: p. 107-114.

295. Kant, S., et al., *Quantifying Anti-HIV Envelope-Specific Antibodies in Plasma from HIV Infected Individuals.* Viruses, 2019. **11**(6).

296. Dupuy, F.P., et al., *Antibody-Dependent Cellular Cytotoxicity-Competent Antibodies against HIV-1-Infected Cells in Plasma from HIV-Infected Subjects.* mBio, 2019. **10**(6).

297. Wang, Q., A. Finzi, and J. Sodroski, *The Conformational States of the HIV-1 Envelope Glycoproteins.* Trends in microbiology, 2020. **28**(8): p. 655-667.

298. Richard, J., et al., *Impact of HIV-1 Envelope Conformation on ADCC Responses.* Trends Microbiol, 2018. **26**(4): p. 253-265.

299. Baden, L.R., et al., *Efficacy and Safety of the mRNA-1273 SARS-CoV-2 Vaccine.* New England Journal of Medicine, 2020. **384**(5): p. 403-416.

300. Polack, F.P., et al., *Safety and Efficacy of the BNT162b2 mRNA Covid-19 Vaccine.* New England Journal of Medicine, 2020. **383**(27): p. 2603-2615.

301. Resch, B., *Product review on the monoclonal antibody palivizumab for prevention of respiratory syncytial virus infection.* Hum Vaccin Immunother, 2017. **13**(9): p. 2138-2149.

302. Chatterjee, A., K. Mavunda, and L.R. Krilov, *Current State of Respiratory Syncytial Virus Disease and Management.* Infectious diseases and therapy, 2021. **10**(Suppl 1): p. 5-16.

303. Pitisuttithum, P., et al., *Randomized, double-blind, placebo-controlled efficacy trial of a bivalent recombinant glycoprotein 120 HIV-1 vaccine among injection drug users in Bangkok, Thailand.* J Infect Dis, 2006. **194**(12): p. 1661-71.

304. Flynn, N.M., et al., *Placebo-controlled phase 3 trial of a recombinant glycoprotein 120 vaccine to prevent HIV-1 infection.* J Infect Dis, 2005. **191**(5): p. 654-65.

305. Karnasuta, C., et al., *Comparison of Antibody Responses Induced by RV144, VAX003, and VAX004 Vaccination Regimens.* AIDS research and human retroviruses, 2017. **33**(5): p. 410-423.

306. Balasubramanian, P., et al., *Functional Antibody Response Against V1V2 and V3 of HIV gp120 in the VAX003 and VAX004 Vaccine Trials.* Scientific Reports, 2018. **8**(1): p. 542.

307. Gray, G.E., et al., *Safety and efficacy of the HVTN 503/Phambili study of a clade-B-based HIV-1 vaccine in South Africa: a double-blind, randomised, placebo-controlled test-of-concept phase 2b study.* The Lancet. Infectious diseases, 2011. **11**(7): p. 507-515.

308. Buchbinder, S.P., et al., *Efficacy assessment of a cell-mediated immunity HIV-1 vaccine (the Step Study): a double-blind, randomised, placebo-controlled, test-of-concept trial.* Lancet (London, England), 2008. **372**(9653): p. 1881-1893.

309. Zak, D.E., et al., *Merck Ad5/HIV induces broad innate immune activation that predicts CD8⁺ T-cell responses but is attenuated by preexisting Ad5 immunity.* Proceedings of the National Academy of Sciences, 2012. **109**(50): p. E3503.

310. Letvin, N.L., et al., *Immune and Genetic Correlates of Vaccine Protection Against Mucosal Infection by SIV in Monkeys.* Science translational medicine, 2011. **3**(81): p. 81ra36-81ra36.

311. Hammer, S.M., et al., *Efficacy trial of a DNA/rAd5 HIV-1 preventive vaccine.* The New England journal of medicine, 2013. **369**(22): p. 2083-2092.

312. Janes, H.E., et al., *Higher T-Cell Responses Induced by DNA/rAd5 HIV-1 Preventive Vaccine Are Associated With Lower HIV-1 Infection Risk in an Efficacy Trial.* The Journal of Infectious Diseases, 2017. **215**(9): p. 1376-1385.

313. Neidich, S.D., et al., *Antibody Fc effector functions and IgG3 associate with decreased HIV-1 risk.* The Journal of clinical investigation, 2019. **129**(11): p. 4838-4849.

314. Fong, Y., et al., *Modification of the Association Between T-Cell Immune Responses and Human Immunodeficiency Virus Type 1 Infection Risk by Vaccine-Induced Antibody Responses in the HVTN 505 Trial.* The Journal of infectious diseases, 2018. **217**(8): p. 1280-1288.

315. Rerks-Ngarm, S., et al., *Vaccination with ALVAC and AIDSVAX to Prevent HIV-1 Infection in Thailand.* New England Journal of Medicine, 2009. **361**(23): p. 2209-2220.

316. Robb, M.L., et al., *Risk behaviour and time as covariates for efficacy of the HIV vaccine regimen ALVAC-HIV (vCP1521) and AIDSVAX B/E: a post-hoc analysis of the Thai phase 3 efficacy trial RV 144.* The Lancet. Infectious diseases, 2012. **12**(7): p. 531-537.

317. Plotkin, S.A., *Vaccines: correlates of vaccine-induced immunity.* Clin Infect Dis, 2008. **47**(3): p. 401-9.

318. Haynes, B.F., et al., *Immune-Correlates Analysis of an HIV-1 Vaccine Efficacy Trial.* New England Journal of Medicine, 2012. **366**(14): p. 1275-1286.

319. Chung Amy, W., et al., *Polyfunctional Fc-Effector Profiles Mediated by IgG Subclass Selection Distinguish RV144 and VAX003 Vaccines.* Science Translational Medicine, 2014. **6**(228): p. 228ra38-228ra38.

320. Carrasco, B., et al., *Crystallohydrodynamics for solving the hydration problem for multi-domain proteins: open physiological conformations for human IgG.* Biophysical Chemistry, 2001. **93**(2): p. 181-196.

321. Damelang, T., et al., *Role of IgG3 in Infectious Diseases.* Trends Immunol, 2019. **40**(3): p. 197-211.

322. Nascimento, E.J.M., et al., *Development of antibody biomarkers of long term and recent dengue virus infections.* Journal of Virological Methods, 2018. **257**: p. 62-68.

323. Roussilhon, C., et al., *Long-Term Clinical Protection from Falciparum Malaria Is Strongly Associated with IgG3 Antibodies to Merozoite Surface Protein 3.* PLOS Medicine, 2007. **4**(11): p. e320.

324. Dechavanne, C., et al., *Associations between an IgG3 polymorphism in the binding domain for FcRn, transplacental transfer of malaria-specific IgG3, and protection against Plasmodium falciparum malaria during infancy: A birth cohort study in Benin.* PLoS medicine, 2017. **14**(10): p. e1002403-e1002403.

325. Kallolimath, S., et al., *Highly active engineered IgG3 antibodies against SARS-CoV-2.* Proceedings of the National Academy of Sciences, 2021. **118**(42): p. e2107249118.

326. Kober, C., et al., *IgG3 and IgM Identified as Key to SARS-CoV-2 Neutralization in Convalescent Plasma Pools.* PLOS ONE, 2022. **17**(1): p. e0262162.

327. Luo, H., et al., *The Characterization of Disease Severity Associated IgG Subclasses Response in COVID-19 Patients.* Frontiers in Immunology, 2021. **12**.

328. Bindon, C.I., et al., *Human monoclonal IgG isotypes differ in complement activating function at the level of C4 as well as C1q.* Journal of Experimental Medicine, 1988. **168**(1): p. 127-142.

329. Bruhns, P., et al., *Specificity and affinity of human Fcγ receptors and their polymorphic variants for human IgG subclasses.* Blood, 2009. **113**(16): p. 3716-3725.

330. Yates, N.L., et al., *Multiple HIV-1-specific IgG3 responses decline during acute HIV-1: implications for detection of incident HIV infection.* Aids, 2011. **25**(17): p. 2089-97.

331. Dugast, A.-S., et al., *Independent evolution of Fc- and Fab-mediated HIV-1-specific antiviral antibody activity following acute infection.* European journal of immunology, 2014. **44**(10): p. 2925-2937.

332. Sadanand, S., et al., *Temporal variation in HIV-specific IgG subclass antibodies during acute infection differentiates spontaneous controllers from chronic progressors.* AIDS, 2018. **32**(4).

333. Yates Nicole, L., et al., *Vaccine-Induced Env V1-V2 IgG3 Correlates with Lower HIV-1 Infection Risk and Declines Soon After Vaccination.* Science Translational Medicine, 2014. **6**(228): p. 228ra39-228ra39.

334. Chung, A.W., et al., *Dissecting Polyclonal Vaccine-Induced Humoral Immunity against HIV Using Systems Serology.* Cell, 2015. **163**(4): p. 988-998.

335. Baden, L.R., et al., *First-in-human evaluation of the safety and immunogenicity of a recombinant adenovirus serotype 26 HIV-1 Env vaccine (IPCAVD 001).* The Journal of infectious diseases, 2013. **207**(2): p. 240-247.

336. Rolland, M., et al., *Increased HIV-1 vaccine efficacy against viruses with genetic signatures in Env V2.* Nature, 2012. **490**(7420): p. 417-420.

337. ClinicalTrials.gov, *Phase 1b Randomized Double Blind Placebo Controlled Clinical Trial to Evaluate the Safety and Immunogenicity of the Vaccine Regimen ALVAC-HIV (vCP1521) Followed by AIDSVAX® B/E in Healthy, HIV-1 Uninfected Adult Participants in South Africa*. 2019, ClinicalTrials.gov: ClinicalTrials.gov.

338. Gray, G.E., et al., *Immune correlates of the Thai RV144 HIV vaccine regimen in South Africa.* Science translational medicine, 2019. **11**(510): p. eaax1880.

339. ClinicalTrials.gov, *A Pivotal Phase 2b/3 Multisite, Randomized, Double-blind, Placebo-controlled Clinical Trial to Evaluate the Safety and Efficacy of ALVAC-HIV (vCP2438) and Bivalent Subtype C gp120/MF59 in Preventing HIV-1 Infection in Adults in South Africa*. 2021, ClinicalTrials.gov.

340. Gray, G.E., et al., *Vaccine Efficacy of ALVAC-HIV and Bivalent Subtype C gp120-MF59 in Adults.* The New England journal of medicine, 2021. **384**(12): p. 1089-1100.

341. *Experimental HIV Vaccine Regimen Ineffective in Preventing HIV*. 2020, National Institute of Allergy and Infectious Diseases (NIAID).

342. Richard, J., et al., *Uninfected Bystander Cells Impact the Measurement of HIV-Specific Antibody-Dependent Cellular Cytotoxicity Responses.* mBio, 2018. **9**(2).

343. Francica, J.R., et al., *Innate transcriptional effects by adjuvants on the magnitude, quality, and durability of HIV envelope responses in NHPs.* Blood Advances, 2017. **1**(25): p. 2329-2342.

344. Zoubchenok, D., et al., *Histidine 375 Modulates CD4 Binding in HIV-1 CRF01_AE Envelope Glycoproteins.* Journal of virology, 2017. **91**(4): p. e02151-16.

345. ClinicalTrials.gov, *A Study to Assess the Efficacy of a Heterologous Prime/Boost Vaccine Regimen of Ad26.Mos4.HIV and Aluminum Phosphate-Adjuvanted Clade C gp140 in Preventing Human Immunodeficiency Virus (HIV) -1 Infection in Women in Sub-Saharan Africa*. 2021, ClinicalTrials.gov: ClinicalTrials.gov.

346. ClinicalTrials.gov, *A Study of Heterologous Vaccine Regimen of Adenovirus Serotype 26 Mosaic4 Human Immunodeficiency Virus(Ad26.Mos4.HIV), Adjuvanted Clade C gp140 and Mosaic gp140 to Prevent HIV-1 Infection Among Cis-gender Men and Transgender Individuals Who Have Sex With Cis-gender Men and/or Transgender Individuals (MOSAICO)*. 2021, ClinicalTrials.gov: ClinicalTrials.gov.

347. ClinicalTrials.gov, *A Phase 2b Study to Evaluate the Safety and Efficacy of VRC01 Broadly Neutralizing Monoclonal Antibody in Reducing Acquisition of HIV-1 Infection in Women in Sub-Saharan Africa*. 2021, ClinicalTrials.gov: ClinicalTrials.gov.

348. ClinicalTrials.gov, *A Phase 2b Study to Evaluate the Safety and Efficacy of VRC01 Broadly Neutralizing Monoclonal Antibody in Reducing Acquisition of HIV-1 Infection Among Men and Transgender Persons Who Have Sex With Men*. 2021, ClinicalTrials.gov: ClinicalTrials.gov.

349. Barouch, D.H., et al., *Mosaic HIV-1 vaccines expand the breadth and depth of cellular immune responses in rhesus monkeys.* Nature medicine, 2010. **16**(3): p. 319-323.

350. Barouch, D.H., et al., *Evaluation of a mosaic HIV-1 vaccine in a multicentre, randomised, double-blind, placebo-controlled, phase 1/2a clinical trial (APPROACH) and in rhesus monkeys (NHP 13-19).* Lancet (London, England), 2018. **392**(10143): p. 232-243.

351. (NIAID), N.I.o.A.a.I.D., *HIV Vaccine Candidate Does Not Sufficiently Protect Women Against HIV Infection*. 2021: National Institute of Allergy and Infectious Diseases (NIAID).

352. Corey, L., et al., *Two Randomized Trials of Neutralizing Antibodies to Prevent HIV-1 Acquisition.* New England Journal of Medicine, 2021. **384**(11): p. 1003-1014.

353. ClinicalTrials.gov, *Safety and Pharmacokinetics of the Combination Broadly Neutralizing Antibodies, 3BNC117-LS-J and 10-1074-LS-J, in Healthy American and African Adults*. 2020, ClinicalTrials.gov: ClinicalTrials.gov.

354. ClinicalTrials.gov, *A Phase 1 Dose-escalation Clinical Trial to Evaluate the Safety, Tolerability, Pharmacokinetics, and Antiviral Activity of the Monoclonal Antibody PGT121.414.LS Administered Alone and in Combination With VRC07-523LS Via Intravenous or Subcutaneous Infusions in Healthy, HIV-uninfected Adult Participants*. 2021, ClinicalTrials.gov: ClinicalTrials.gov.

355. ClinicalTrials.gov, *A Phase 1 Clinical Trial to Evaluate the Safety, Tolerability, Pharmacokinetics, and Antiviral Activity of Combinations of Monoclonal Antibodies PGT121, PGDM1400, 10-1074, and VRC07-523LS Administered Via Intravenous Infusion in Healthy, HIV-uninfected Adult Participants*. 2021, ClinicalTrials.gov: ClinicalTrials.gov.

356. Burton, D.R., et al., *HIV vaccine design and the neutralizing antibody problem.* Nature Immunology, 2004. **5**(3): p. 233-236.

357. Binley, J.M., et al., *A recombinant human immunodeficiency virus type 1 envelope glycoprotein complex stabilized by an intermolecular disulfide bond between the gp120 and gp41 subunits is an antigenic mimic of the trimeric virion-associated structure.* Journal of virology, 2000. **74**(2): p. 627-643.

358. Sanders, R.W., et al., *Stabilization of the soluble, cleaved, trimeric form of the envelope glycoprotein complex of human immunodeficiency virus type 1.* Journal of virology, 2002. **76**(17): p. 8875-8889.

359. Dey, A.K., et al., *Biochemical and biophysical comparison of cleaved and uncleaved soluble, trimeric HIV-1 envelope glycoproteins.* Virology, 2009. **385**(1): p. 275-81.

360. Sanders, R.W., et al., *A next-generation cleaved, soluble HIV-1 Env trimer, BG505 SOSIP.664 gp140, expresses multiple epitopes for broadly neutralizing but not non-neutralizing antibodies.* PLoS pathogens, 2013. **9**(9): p. e1003618-e1003618.

361. Sanders, R.W., et al., *HIV-1 VACCINES. HIV-1 neutralizing antibodies induced by native-like envelope trimers.* Science (New York, N.Y.), 2015. **349**(6244): p. aac4223-aac4223.

362. de Taeye, S.W., et al., *Immunogenicity of Stabilized HIV-1 Envelope Trimers with Reduced Exposure of Non-neutralizing Epitopes.* Cell, 2015. **163**(7): p. 1702-1715.

363. Klasse, P.J., et al., *Sequential and Simultaneous Immunization of Rabbits with HIV-1 Envelope Glycoprotein SOSIP.664 Trimers from Clades A, B and C.* PLoS pathogens, 2016. **12**(9): p. e1005864-e1005864.

364. Torrents de la Peña, A., et al., *Immunogenicity in Rabbits of HIV-1 SOSIP Trimers from Clades A, B, and C, Given Individually, Sequentially, or in Combination.* J Virol, 2018. **92**(8).

365. Pauthner, M.G., et al., *Vaccine-Induced Protection from Homologous Tier 2 SHIV Challenge in Nonhuman Primates Depends on Serum-Neutralizing Antibody Titers.* Immunity, 2019. **50**(1): p. 241-252.e6.

366. ClinicalTrials.gov, *A Randomized, Double-blinded, Placebo-controlled, Dose-escalation Phase 1 Clinical Trial to Evaluate the Safety and Immunogenicity of Recombinant HIV-1 Envelope Protein BG505 SOSIP.GT1.1 gp140 Vaccine, Adjuvanted in Healthy, HIV-uninfected Adults*. 2020, ClinicalTrials.gov: ClinicalTrials.gov.

367. ClinicalTrials.gov, *Evaluating the Safety and Immunogenicity of HIV-1 BG505 SOSIP.664 gp140 With TLR Agonist and/or Alum Adjuvants in Healthy, HIV-uninfected Adults*. 2021, ClinicalTrials.gov: ClinicalTrials.gov.

368. Zhang, C., et al., *Advances in mRNA Vaccines for Infectious Diseases.* Frontiers in Immunology, 2019. **10**.

369. Moyo, N., et al., *Efficient Induction of T Cells against Conserved HIV-1 Regions by Mosaic Vaccines Delivered as Self-Amplifying mRNA.* Molecular therapy. Methods & clinical development, 2018. **12**: p. 32-46.

370. Pardi, N., et al., *Characterization of HIV-1 Nucleoside-Modified mRNA Vaccines in Rabbits and Rhesus Macaques.* Molecular therapy. Nucleic acids, 2019. **15**: p. 36-47.

371. Saunders, K.O., et al., *Lipid nanoparticle encapsulated nucleoside-modified mRNA vaccines elicit polyfunctional HIV-1 antibodies comparable to proteins in nonhuman primates.* NPJ vaccines, 2021. **6**(1): p. 50-50.

372. Zhang, P., et al., *A multiclade env-gag VLP mRNA vaccine elicits tier-2 HIV-1-neutralizing antibodies and reduces the risk of heterologous SHIV infection in macaques.* Nat Med, 2021. **27**(12): p. 2234-2245.

373. *IAVI and Moderna launch trial of HIV vaccine antigens delivered through mRNA technology*. 2022, Moderna.

374. A., S., *First patients vaccinated in clinical trial of HIV experimental vaccine that uses Moderna's mRNA technology*, in *CTV News*. 2022, CTV News.

375. Lifson, A.R., et al., *Longterm Human Immunodeficiency Virus Infection in Asymptomatic Homosexual and Bisexual Men with Normal CD4⁺ Lymphocyte Counts: Immunologic and Virologic Characteristics.* The Journal of Infectious Diseases, 1991. **163**(5): p. 959-965.

376. Rutherford, G.W., et al., *Course of HIV-I infection in a cohort of homosexual and bisexual men: an 11 year follow up study.* BMJ (Clinical research ed.), 1990. **301**(6762): p. 1183-1188.

377. Cao, Y., et al., *Virologic and Immunologic Characterization of Long-Term Survivors of Human Immunodeficiency Virus Type 1 Infection.* New England Journal of Medicine, 1995. **332**(4): p. 201-208.

378. Pantaleo, G., et al., *Studies in Subjects with Long-Term Nonprogressive Human Immunodeficiency Virus Infection.* New England Journal of Medicine, 1995. **332**(4): p. 209-216.

379. Lefrère, J.-J., et al., *Even Individuals Considered as Long-Term Nonprogressors Show Biological Signs of Progression After 10 Years of Human Immunodeficiency Virus Infection.* Blood, 1997. **90**(3): p. 1133-1140.

380. Rodés, B., et al., *Differences in disease progression in a cohort of long-term non-progressors after more than 16 years of HIV-1 infection.* AIDS, 2004. **18**(8).

381. Gilbert, P.B., et al., *Virologic and Regimen Termination Surrogate End Points in AIDS Clinical Trials.* JAMA, 2001. **285**(6): p. 777-784.

382. Hirsch, M.S., et al., *Antiretroviral drug resistance testing in adults infected with human immunodeficiency virus type 1: 2003 recommendations of an International AIDS Society-USA Panel.* Clinical Infectious Diseases, 2003. **37**(1): p. 113-128.

383. Doyle, T., et al., *Plasma HIV-1 RNA Detection Below 50 Copies/mL and Risk of Virologic Rebound in Patients Receiving Highly Active Antiretroviral Therapy.* Clinical Infectious Diseases, 2012. **54**(5): p. 724-732.

384. Alvarez, M., et al., *Improving Clinical Laboratory Efficiency: Introduction of Systems for the Diagnosis and Monitoring of HIV Infection.* The open virology journal, 2012. **6**: p. 135-143.

385. Charpentier, C., et al., *Persistent low-level HIV-1 RNA between 20 and 50 copies/mL in antiretroviral-treated patients: associated factors and virological outcome.* Journal of Antimicrobial Chemotherapy, 2012. **67**(9): p. 2231-2235.

386. Álvarez Estévez, M., et al., *Quantification of viral loads lower than 50 copies per milliliter by use of the Cobas AmpliPrep/Cobas TaqMan HIV-1 test, version 2.0, can predict the likelihood of subsequent virological rebound to >50 copies per milliliter.* Journal of clinical microbiology, 2013. **51**(5): p. 1555-1557.

387. Deeks, S.G. and B.D. Walker, *Human immunodeficiency virus controllers: mechanisms of durable virus control in the absence of antiretroviral therapy.* Immunity, 2007. **27**(3): p. 406-16.

388. Gurdasani, D., et al., *A systematic review of definitions of extreme phenotypes of HIV control and progression.* AIDS (London, England), 2014. **28**(2): p. 149-162.

389. Noel, N., et al., *Immunologic and Virologic Progression in HIV Controllers: The Role of Viral "Blips" and Immune Activation in the ANRS CO21 CODEX Study.* PloS one, 2015. **10**(7): p. e0131922-e0131922.

390. Rosás-Umbert, M., et al., *Mechanisms of Abrupt Loss of Virus Control in a Cohort of Previous HIV Controllers.* Journal of virology, 2019. **93**(4): p. e01436-18.

391. Gebara, N.Y., V. El Kamari, and N. Rizk, *HIV-1 elite controllers: an immunovirological review and clinical perspectives.* Journal of virus eradication, 2019. **5**(3): p. 163-166.

392. Pernas, M., et al., *Factors Leading to the Loss of Natural Elite Control of HIV-1 Infection.* Journal of virology, 2018. **92**(5): p. e01805-17.

393. Hubert, J.-B., et al., *Natural history of serum HIV-1 RNA levels in 330 patients with a known date of infection.* AIDS, 2000. **14**(2).

394. Madec, Y., et al., *Undetectable Viremia without Antiretroviral Therapy in Patients with HIV Seroconversion: An Uncommon Phenomenon?* Clinical Infectious Diseases, 2005. **40**(9): p. 1350-1354.

395. Madec, Y., et al., *Spontaneous control of viral load and CD4 cell count progression among HIV-1 seroconverters.* AIDS, 2005. **19**(17).

396. Grabar, S., et al., *Prevalence and comparative characteristics of long-term nonprogressors and HIV controller patients in the French Hospital Database on HIV.* AIDS, 2009. **23**(9): p. 1163-1169.

397. Okulicz, J.F., et al., *Clinical outcomes of elite controllers, viremic controllers, and long-term nonprogressors in the US Department of Defense HIV natural history study.* J Infect Dis, 2009. **200**(11): p. 1714-23.

398. Marzo, A.L., et al., *Fully functional memory CD8 T cells in the absence of CD4 T cells.* J. Immunol, 2004. **173**(2): p. 969-975.

399. El-Far, M., et al., *Proinflammatory isoforms of IL-32 as novel and robust biomarkers for control failure in HIV-infected slow progressors.* Scientific reports, 2016. **6**: p. 22902-22902.

400. Mehraj, V., et al., *Socio-economic status and time trends associated with early ART initiation following primary HIV infection in Montreal, Canada: 1996 to 2015.* Journal of the International AIDS Society, 2018. **21**(2): p. e25034.

401. Learmont, J., et al., *Long-term symptomless HIV-1 infection in recipients of blood products from a single donor.* The Lancet, 1992. **340**(8824): p. 863-867.

402. Deacon, N.J., et al., *Genomic Structure of an Attenuated Quasi Species of HIV-1 from a Blood Transfusion Donor and Recipients.* Science, 1995. **270**(5238): p. 988-991.

403. McIntyre, L.B., et al., *The Sydney Blood Bank Cohort: A Case-Control Study Using a Transfused HIV-1 Seronegative Group.* Annals of Epidemiology, 1999. **9**(7): p. 436-440.

404. Kirchhoff, F., et al., *Absence of Intact nef Sequences in a Long-Term Survivor with Nonprogressive HIV-1 Infection.* New England Journal of Medicine, 1995. **332**(4): p. 228-232.

405. Learmont, J.C., et al., *Immunologic and Virologic Status after 14 to 18 Years of Infection with an Attenuated Strain of HIV-1 — A Report from the Sydney Blood Bank Cohort.* New England Journal of Medicine, 1999. **340**(22): p. 1715-1722.

406. Kirchhoff, F., et al., *Sequence variations in human immunodeficiency virus type 1 Nef are associated with different stages of disease.* Journal of virology, 1999. **73**(7): p. 5497-5508.

407. Tolstrup, M., et al., *Cysteine 138 mutation in HIV-1 Nef from patients with delayed disease progression.* Sex Health, 2006. **3**(4): p. 281-6.

408. Premkumar, D.R., et al., *The nef gene from a long-term HIV type 1 nonprogressor.* AIDS Res Hum Retroviruses, 1996. **12**(4): p. 337-45.

409. Corró, G., et al., *Genetic and functional analysis of HIV type 1 nef gene derived from long-term nonprogressor children: association of attenuated variants with slow progression to pediatric AIDS.* AIDS Res Hum Retroviruses, 2012. **28**(12): p. 1617-26.

410. Alsahafi, N., et al., *Nef Proteins from HIV-1 Elite Controllers Are Inefficient at Preventing Antibody-Dependent Cellular Cytotoxicity.* J Virol, 2015. **90**(6): p. 2993-3002.

411. Alsahafi, N., et al., *Impaired Downregulation of NKG2D Ligands by Nef Proteins from Elite Controllers Sensitizes HIV-1-Infected Cells to Antibody-Dependent Cellular Cytotoxicity.* Journal of Virology. **91**(16): p. e00109-17.

412. Caly, L., et al., *Impaired nuclear import and viral incorporation of Vpr derived from a HIV long-term non-progressor.* Retrovirology, 2008. **5**: p. 67.

413. Mologni, D., et al., *Vpr and HIV-1 disease progression: R77Q mutation is associated with long-term control of HIV-1 infection in different groups of patients.* Aids, 2006. **20**(4): p. 567-74.

414. Chen, J., et al., *Modest Attenuation of HIV-1 Vpu Alleles Derived from Elite Controller Plasma.* PLOS ONE, 2015. **10**(3): p. e0120434.

415. Churchill, M.J., et al., *Persistence of attenuated HIV-1 rev alleles in an epidemiologically linked cohort of long-term survivors infected with nef-deleted virus.* Retrovirology, 2007. **4**(1): p. 43.

416. Lassen, K.G., et al., *Elite suppressor-derived HIV-1 envelope glycoproteins exhibit reduced entry efficiency and kinetics.* PLoS Pathog, 2009. **5**(4): p. e1000377.

417. Huang, Y., L. Zhang, and D.D. Ho, *Characterization of nef sequences in long-term survivors of human immunodeficiency virus type 1 infection.* Journal of virology, 1995. **69**(1): p. 93-100.

418. Liu, R., et al., *Homozygous Defect in HIV-1 Coreceptor Accounts for Resistance of Some Multiply-Exposed Individuals to HIV-1 Infection.* Cell, 1996. **86**(3): p. 367-377.

419. Dean, M., et al., *Genetic Restriction of HIV-1 Infection and Progression to AIDS by a Deletion Allele of the CKR5 Structural Gene.* Science, 1996. **273**(5283): p. 1856-1862.

420. Samson, M., et al., *Resistance to HIV-1 infection in Caucasian individuals bearing mutant alleles of the CCR-5 chemokine receptor gene.* Nature, 1996. **382**(6593): p. 722-725.

421. Klein, M.R. and F. Miedema, *Long-term survivors of HIV-1 infection.* Trends in Microbiology, 1995. **3**(10): p. 386-391.

422. Kaslow, R.A., et al., *Influence of combinations of human major histocompatibility complex genes on the course of HIV–1 infection.* Nature Medicine, 1996. **2**(4): p. 405-411.

423. Goulder, P.J.R., et al., *Novel, Cross-Restricted, Conserved, and Immunodominant Cytotoxic T Lymphocyte Epitopes in Slow Progressors in HIV Type 1 Infection.* AIDS Research and Human Retroviruses, 1996. **12**(18): p. 1691-1698.

424. Migueles, S.A., et al., *HLA B*5701 is highly associated with restriction of virus replication in a subgroup of HIV-infected long term nonprogressors.* Proceedings of the National Academy of Sciences of the United States of America, 2000. **97**(6): p. 2709-2714.

425. Migueles, S.A., et al., *CD8(+) T-cell Cytotoxic Capacity Associated with Human Immunodeficiency Virus-1 Control Can Be Mediated through Various Epitopes and Human Leukocyte Antigen Types.* EBioMedicine, 2014. **2**(1): p. 46-58.

426. Kiepiela, P., et al., *Dominant influence of HLA-B in mediating the potential co-evolution of HIV and HLA.* Nature, 2004. **432**(7018): p. 769-775.

427. Fellay, J., et al., *Common genetic variation and the control of HIV-1 in humans.* PLoS genetics, 2009. **5**(12): p. e1000791-e1000791.

428. Fellay, J., et al., *A Whole-Genome Association Study of Major Determinants for Host Control of HIV-1.* Science, 2007. **317**(5840): p. 944-947.

429. Migueles, S.A., et al., *HIV-specific CD8+ T cell proliferation is coupled to perforin expression and is maintained in nonprogressors.* Nature Immunology, 2002. **3**(11): p. 1061-1068.

430. Betts, M.R., et al., *HIV nonprogressors preferentially maintain highly functional HIV-specific CD8+ T cells.* Blood, 2006. **107**(12): p. 4781-9.

431. Bailey, J.R., et al., *Maintenance of viral suppression in HIV-1-infected HLA-B*57+ elite suppressors despite CTL escape mutations.* The Journal of experimental medicine, 2006. **203**(5): p. 1357-1369.

432. O'Connell, K.A., et al., *Control of HIV-1 in elite suppressors despite ongoing replication and evolution in plasma virus.* Journal of virology, 2010. **84**(14): p. 7018-7028.

433. Abdel-Mohsen, M., et al., *Expression profile of host restriction factors in HIV-1 elite controllers.* Retrovirology, 2013. **10**: p. 106.

434. Malim, M.H. and P.D. Bieniasz, *HIV Restriction Factors and Mechanisms of Evasion.* Cold Spring Harbor perspectives in medicine, 2012. **2**(5): p. a006940-a006940.

435. Colomer-Lluch, M., et al., *Restriction Factors: From Intrinsic Viral Restriction to Shaping Cellular Immunity Against HIV-1.* Frontiers in Immunology, 2018. **9**.

436. Sheehy, A.M., et al., *Isolation of a human gene that inhibits HIV-1 infection and is suppressed by the viral Vif protein.* Nature, 2002. **418**(6898): p. 646-650.

437. Chen, K.-M., et al., *Structure of the DNA deaminase domain of the HIV-1 restriction factor APOBEC3G.* Nature, 2008. **452**(7183): p. 116-119.

438. Kikuchi, T., et al., *Anti-APOBEC3G Activity of HIV-1 Vif Protein Is Attenuated in Elite Controllers.* Journal of Virology. **89**(9): p. 4992-5001.

439. Merindol, N., et al., *HIV-1 capsids from B27/B57+ elite controllers escape Mx2 but are targeted by TRIM5α, leading to the induction of an antiviral state.* PLoS pathogens, 2018. **14**(11): p. e1007398-e1007398.

440. Van Hecke, C., et al., *Early treated HIV-1 positive individuals demonstrate similar restriction factor expression profile as long-term non-progressors.* EBioMedicine, 2019. **41**: p. 443-454.

441. Saunders, K.O., *Conceptual Approaches to Modulating Antibody Effector Functions and Circulation Half-Life.* Frontiers in Immunology, 2019. **10**.

442. Vidarsson, G., G. Dekkers, and T. Rispens, *IgG subclasses and allotypes: from structure to effector functions.* Frontiers in immunology, 2014. **5**: p. 520-520.

443. Checkley, M.A., B.G. Luttge, and E.O. Freed, *HIV-1 envelope glycoprotein biosynthesis, trafficking, and incorporation.* Journal of molecular biology, 2011. **410**(4): p. 582-608.

444. Liu, L., *Antibody Glycosylation and Its Impact on the Pharmacokinetics and Pharmacodynamics of Monoclonal Antibodies and Fc-Fusion Proteins.* Journal of Pharmaceutical Sciences, 2015. **104**(6): p. 1866-1884.

445. Richards, J.O., et al., *Optimization of antibody binding to FcγRIIa enhances macrophage phagocytosis of tumor cells.* Molecular cancer therapeutics, 2008. **7**(8): p. 2517-2527.

446. Niwa, R., et al., *Enhancement of the antibody-dependent cellular cytotoxicity of low-fucose IgG1 is independent of FcγRIIIa functional polymorphism.* Clinical Cancer Research, 2004. **10**(18): p. 6248-6255.

447. Shinkawa, T., et al., *The absence of fucose but not the presence of galactose or bisecting N-acetylglucosamine of human IgG1 complex-type oligosaccharides shows the critical role of enhancing antibody-dependent cellular cytotoxicity.* J Biol Chem, 2003. **278**(5): p. 3466-73.

448. Shields, R.L., et al., *Lack of fucose on human IgG1 N-linked oligosaccharide improves binding to human Fcgamma RIII and antibody-dependent cellular toxicity.* J Biol Chem, 2002. **277**(30): p. 26733-40.

449. Ferrara, C., et al., *Unique carbohydrate-carbohydrate interactions are required for high affinity binding between FcgammaRIII and antibodies lacking core fucose.* Proc Natl Acad Sci U S A, 2011. **108**(31): p. 12669-74.

450. Moldt, B., et al., *A nonfucosylated variant of the anti-HIV-1 monoclonal antibody b12 has enhanced FcγRIIIa-mediated antiviral activity in vitro but does not improve protection against mucosal SHIV challenge in macaques.* Journal of virology, 2012. **86**(11): p. 6189-6196.

451. Anand, S.P., et al., *Enhanced Ability of Plant-Derived PGT121 Glycovariants To Eliminate HIV-1-Infected Cells.* Journal of virology, 2021. **95**(18): p. e0079621-e0079621.

452. Larsen Mads, D., et al., *Afucosylated IgG characterizes enveloped viral responses and correlates with COVID-19 severity.* Science, 2021. **371**(6532): p. eabc8378.

453. Wang, T.T., et al., *IgG antibodies to dengue enhanced for FcγRIIIA binding determine disease severity.* Science, 2017. **355**(6323): p. 395-398.

454. Lux, A., et al., *Impact of immune complex size and glycosylation on IgG binding to human FcγRs.* J Immunol, 2013. **190**(8): p. 4315-23.

455. Bruhns, P., et al., *Specificity and affinity of human Fcgamma receptors and their polymorphic variants for human IgG subclasses.* Blood, 2009. **113**(16): p. 3716-25.

456. Roux, K.H., L. Strelets, and T.E. Michaelsen, *Flexibility of human IgG subclasses.* J Immunol, 1997. **159**(7): p. 3372-82.

457. Michaelsen, T.E., L.M. Naess, and A. Aase, *Human IgG3 is decreased and IgG1, IgG2 and IgG4 are unchanged in molecular size by mild reduction and reoxidation without any major change in effector functions.* Mol Immunol, 1993. **30**(1): p. 35-45.

458. Javaherian, K., et al., *Broadly Neutralizing Antibodies Elicited by the Hypervariable Neutralizing Determinant of HIV-1.* Science, 1990. **250**(4987): p. 1590-1593.

459. Moore, J.P., et al., *Primary isolates of human immunodeficiency virus type 1 are relatively resistant to neutralization by monoclonal antibodies to gp120, and their neutralization is not predicted by studies with monomeric gp120.* J Virol, 1995. **69**(1): p. 101-9.

460. McCoy, L.E. and Á. McKnight, *Lessons learned from humoral responses of HIV patients.* Curr Opin HIV AIDS, 2017. **12**(3): p. 195-202.

461. Richman, D.D., et al., *Rapid evolution of the neutralizing antibody response to HIV type 1 infection.* Proceedings of the National Academy of Sciences of the United States of America, 2003. **100**(7): p. 4144-4149.

462. Deeks, S.G., et al., *Neutralizing antibody responses against autologous and heterologous viruses in acute versus chronic human immunodeficiency virus (HIV) infection: evidence for a constraint on the ability of HIV to completely evade neutralizing antibody responses.* J Virol, 2006. **80**(12): p. 6155-64.

463. Carotenuto, P., et al., *Neutralizing antibodies are positively associated with CD4+ T-cell counts and T-cell function in long-term AIDS-free infection.* Aids, 1998. **12**(13): p. 1591-600.

464. Pilgrim, A.K., et al., *Neutralizing antibody responses to human immunodeficiency virus type 1 in primary infection and long-term-nonprogressive infection.* J Infect Dis, 1997. **176**(4): p. 924-32.

465. Pereyra, F., et al., *Genetic and immunologic heterogeneity among persons who control HIV infection in the absence of therapy.* J Infect Dis, 2008. **197**(4): p. 563-71.

466. Loomis-Price, L.D., et al., *Correlation between humoral responses to human immunodeficiency virus type 1 envelope and disease progression in early-stage infection.* J Infect Dis, 1998. **178**(5): p. 1306-16.

467. Harrer, T., et al., *Strong cytotoxic T cell and weak neutralizing antibody responses in a subset of persons with stable nonprogressing HIV type 1 infection.* AIDS Res Hum Retroviruses, 1996. **12**(7): p. 585-92.

468. Landais, E., et al., *Broadly Neutralizing Antibody Responses in a Large Longitudinal Sub-Saharan HIV Primary Infection Cohort.* PLoS Pathog, 2016. **12**(1): p. e1005369.

469. Gray, E.S., et al., *The neutralization breadth of HIV-1 develops incrementally over four years and is associated with CD4+ T cell decline and high viral load during acute infection.* J Virol, 2011. **85**(10): p. 4828-40.

470. Liao, H.X., et al., *Co-evolution of a broadly neutralizing HIV-1 antibody and founder virus.* Nature, 2013. **496**(7446): p. 469-76.

471. de Bree, G.J., et al., *Longitudinal dynamics of the HIV-specific B cell response during intermittent treatment of primary HIV infection.* PLoS One, 2017. **12**(3): p. e0173577.

472. Bonsignori, M., et al., *Staged induction of HIV-1 glycan-dependent broadly neutralizing antibodies.* Sci Transl Med, 2017. **9**(381).

473. Chaillon, A., et al., *Human immunodeficiency virus type-1 (HIV-1) continues to evolve in presence of broadly neutralizing antibodies more than ten years after infection.* PLoS One, 2012. **7**(8): p. e44163.

474. Burton, D.R., et al., *Efficient neutralization of primary isolates of HIV-1 by a recombinant human monoclonal antibody.* Science, 1994. **266**(5187): p. 1024-7.

475. Trkola, A., et al., *Human monoclonal antibody 2G12 defines a distinctive neutralization epitope on the gp120 glycoprotein of human immunodeficiency virus type 1.* J Virol, 1996. **70**(2): p. 1100-8.

476. Moldt, B., et al., *A panel of IgG1 b12 variants with selectively diminished or enhanced affinity for Fcγ receptors to define the role of effector functions in protection against HIV.* J Virol, 2011. **85**(20): p. 10572-81.

477. Spencer, D.A., et al., *Advancing HIV Broadly Neutralizing Antibodies: From Discovery to the Clinic.* Frontiers in Public Health, 2021. **9**.

478. Sievers, S.A., et al., *Antibody engineering for increased potency, breadth and half-life.* Current opinion in HIV and AIDS, 2015. **10**(3): p. 151-159.

479. Hessell, A.J., et al., *Fc receptor but not complement binding is important in antibody protection against HIV.* Nature, 2007. **449**(7158): p. 101-104.

480. Hessell, A.J., et al., *Effective, low-titer antibody protection against low-dose repeated mucosal SHIV challenge in macaques.* Nature Medicine, 2009. **15**(8): p. 951-954.

481. Moldt, B., et al., *Highly potent HIV-specific antibody neutralization in vitro translates into effective protection against mucosal SHIV challenge in vivo.* Proc Natl Acad Sci U S A, 2012. **109**(46): p. 18921-5.

482. Pegu, A., et al., *Neutralizing antibodies to HIV-1 envelope protect more effectively in vivo than those to the CD4 receptor.* Sci Transl Med, 2014. **6**(243): p. 243ra88.

483. Shingai, M., et al., *Passive transfer of modest titers of potent and broadly neutralizing anti-HIV monoclonal antibodies block SHIV infection in macaques.* J Exp Med, 2014. **211**(10): p. 2061-74.

484. Walker, B.D., *The AMP Trials — A Glass Half Full.* New England Journal of Medicine, 2021. **384**(11): p. 1068-1069.

485. Hessell, A.J., et al., *Early short-term treatment with neutralizing human monoclonal antibodies halts SHIV infection in infant macaques.* Nat Med, 2016. **22**(4): p. 362-8.

486. Shapiro, M.B., et al., *Single-dose bNAb cocktail or abbreviated ART post-exposure regimens achieve tight SHIV control without adaptive immunity.* Nat Commun, 2020. **11**(1): p. 70.

487. Mendoza, P., et al., *Combination therapy with anti-HIV-1 antibodies maintains viral suppression.* Nature, 2018. **561**(7724): p. 479-484.

488. Bournazos, S., et al., *Broadly neutralizing anti-HIV-1 antibodies require Fc effector functions for in vivo activity.* Cell, 2014. **158**(6): p. 1243-1253.

489. Asokan, M., et al., *Fc-mediated effector function contributes to the in vivo antiviral effect of an HIV neutralizing antibody.* Proceedings of the National Academy of Sciences, 2020. **117**(31): p. 18754-18763.

490. Parsons, M.S., et al., *Fc-dependent functions are redundant to efficacy of anti-HIV antibody PGT121 in macaques.* J Clin Invest, 2019. **129**(1): p. 182-191.

491. Anand, S.P., et al., *Enhanced Ability of Plant-Derived PGT121 Glycovariants To Eliminate HIV-1-Infected Cells.* J Virol, 2021. **95**(18): p. e0079621.

492. Blazkova, J., et al., *Glycan-dependent HIV-specific neutralizing antibodies bind to cells of uninfected individuals.* J Clin Invest, 2019. **129**(11): p. 4832-4837.

493. Ben Mkaddem, S., M. Benhamou, and R.C. Monteiro, *Understanding Fc Receptor Involvement in Inflammatory Diseases: From Mechanisms to New Therapeutic Tools.* Frontiers in Immunology, 2019. **10**.

494. Goldberg, B.S. and M.E. Ackerman, *Antibody-mediated complement activation in pathology and protection.* Immunol Cell Biol, 2020. **98**(4): p. 305-317.

495. Duncan, A.R. and G. Winter, *The binding site for C1q on IgG.* Nature, 1988. **332**(6166): p. 738-40.

496. Bernard, N.F., et al., *Natural Killer (NK) Cell Education Differentially Influences HIV Antibody-Dependent NK Cell Activation and Antibody-Dependent Cellular Cytotoxicity.* Frontiers in immunology, 2017. **8**: p. 1033-1033.

497. Chung, A.W., et al., *Dissecting Polyclonal Vaccine-Induced Humoral Immunity against HIV Using Systems Serology.* Cell, 2015. **163**(4): p. 988-98.

498. Drexler, A.M., *Tumor necrosis factor: its role in HIV/AIDS.* STEP Perspect, 1995. **7**(1): p. 13-5.

499. Tau, G. and P. Rothman, *Biologic functions of the IFN-gamma receptors.* Allergy, 1999. **54**(12): p. 1233-1251.

500. Oliva, A., et al., *Natural killer cells from human immunodeficiency virus (HIV)-infected individuals are an important source of CC-chemokines and suppress HIV-1 entry and replication in vitro.* J Clin Invest, 1998. **102**(1): p. 223-31.

501. Alter, G., J.M. Malenfant, and M. Altfeld, *CD107a as a functional marker for the identification of natural killer cell activity.* J Immunol Methods, 2004. **294**(1-2): p. 15-22.

502. Stratov, I., A. Chung, and J. Kent Stephen, *Robust NK Cell-Mediated Human Immunodeficiency Virus (HIV)-Specific Antibody-Dependent Responses in HIV-Infected Subjects.* Journal of Virology, 2008. **82**(11): p. 5450-5459.

503. Nelson, D.L., C.C. Kurman, and D.E. Serbousek, *51Cr Release Assay of Antibody-Dependent Cell-Mediated Cytotoxicity (ADCC).* Current Protocols in Immunology, 1993. **8**(1): p. 7.27.1-7.27.8.

504. Baum, L.L., et al., *HIV-1 gp120-specific antibody-dependent cell-mediated cytotoxicity correlates with rate of disease progression.* The Journal of Immunology, 1996. **157**(5): p. 2168-2173.

505. Forthal, D.N. and A. Finzi, *Antibody-dependent cellular cytotoxicity in HIV infection.* AIDS (London, England), 2018. **32**(17): p. 2439-2451.

506. Wu, X., et al., *Rational Design of Envelope Identifies Broadly Neutralizing Human Monoclonal Antibodies to HIV-1.* Science, 2010. **329**(5993): p. 856-861.

507. Edmonds, T.G., et al., *Replication competent molecular clones of HIV-1 expressing Renilla luciferase facilitate the analysis of antibody inhibition in PBMC.* Virology, 2010. **408**(1): p. 1-13.

508. Pollara, J., et al., *High-throughput quantitative analysis of HIV-1 and SIV-specific ADCC-mediating antibody responses.* Cytometry. Part A : the journal of the International Society for Analytical Cytology, 2011. **79**(8): p. 603-612.

509. Ding, S., et al., *A Highly Conserved Residue of the HIV-1 gp120 Inner Domain Is Important for Antibody-Dependent Cellular Cytotoxicity Responses Mediated by Anti-cluster A Antibodies.* Journal of virology, 2015. **90**(4): p. 2127-2134.

510. Veillette, M., et al., *Interaction with Cellular CD4 Exposes HIV-1 Envelope Epitopes Targeted by Antibody-Dependent Cell-Mediated Cytotoxicity.* Journal of Virology, 2014. **88**(5): p. 2633-2644.

511. Veillette, M., et al., *The HIV-1 gp120 CD4-Bound Conformation Is Preferentially Targeted by Antibody-Dependent Cellular Cytotoxicity-Mediating Antibodies in Sera from HIV-1-Infected Individuals.* Journal of Virology. **89**(1): p. 545-551.

512. Kramski, M., et al., *Role of monocytes in mediating HIV-specific antibody-dependent cellular cytotoxicity.* Journal of Immunological Methods, 2012. **384**(1): p. 51-61.

513. Kramski, M., et al., *HIV-specific antibody immunity mediated through NK cells and monocytes.* Curr HIV Res, 2013. **11**(5): p. 388-406.

514. Gómez-Román, V.R., et al., *A simplified method for the rapid fluorometric assessment of antibody-dependent cell-mediated cytotoxicity.* Journal of Immunological Methods, 2006. **308**(1): p. 53-67.

515. Ferrari, G., et al., *An HIV-1 gp120 envelope human monoclonal antibody that recognizes a C1 conformational epitope mediates potent antibody-dependent cellular cytotoxicity (ADCC) activity and defines a common ADCC epitope in human HIV-1 serum.* J Virol, 2011. **85**(14): p. 7029-36.

516. Smalls-Mantey, A., et al., *Antibody-dependent cellular cytotoxicity against primary HIV-infected CD4+ T cells is directly associated with the magnitude of surface IgG binding.* J Virol, 2012. **86**(16): p. 8672-80.

517. Richardson, S.I., et al., *HIV-specific Fc effector function early in infection predicts the development of broadly neutralizing antibodies.* PLOS Pathogens, 2018. **14**(4): p. e1006987.

518. Alpert, M.D., et al., *A novel assay for antibody-dependent cell-mediated cytotoxicity against HIV-1- or SIV-infected cells reveals incomplete overlap with antibodies measured by neutralization and binding assays.* Journal of virology, 2012. **86**(22): p. 12039-12052.

519. Richard, J., et al., *CD4 mimetics sensitize HIV-1-infected cells to ADCC.* Proceedings of the National Academy of Sciences of the United States of America, 2015. **112**(20): p. E2687-E2694.

520. Baum, L.L., et al., *HIV-1 gp120-specific antibody-dependent cell-mediated cytotoxicity correlates with rate of disease progression.* The Journal of Immunology, 1996. **157**(5): p. 2168.

521. Lambotte, O., et al., *Heterogeneous neutralizing antibody and antibody-dependent cell cytotoxicity responses in HIV-1 elite controllers.* AIDS (London, England), 2009. **23**(8): p. 897-906.

522. Wren, L.H., et al., *Specific antibody-dependent cellular cytotoxicity responses associated with slow progression of HIV infection.* Immunology, 2013. **138**(2): p. 116-123.

523. Madhavi, V., et al., *Breadth of HIV-1 Env-specific antibody-dependent cellular cytotoxicity: relevance to global HIV vaccine design.* AIDS (London, England), 2014. **28**(13): p. 1859-70.

524. Madhavi, V., et al., *HIV-1 Env- and Vpu-Specific Antibody-Dependent Cellular Cytotoxicity Responses Associated with Elite Control of HIV.* Journal of virology, 2017. **91**(18): p. e00700-17.

525. Ackerman, M.E., et al., *Natural variation in Fc glycosylation of HIV-specific antibodies impacts antiviral activity.* The Journal of clinical investigation, 2013. **123**(5): p. 2183-2192.

526. Ackerman, M.E., et al., *Polyfunctional HIV-Specific Antibody Responses Are Associated with Spontaneous HIV Control.* PLoS pathogens, 2016. **12**(1): p. e1005315-e1005315.

527. Huang, Y., et al., *Diversity of Antiviral IgG Effector Activities Observed in HIV-Infected and Vaccinated Subjects.* J Immunol, 2016. **197**(12): p. 4603-4612.

528. Buckner, C.M., et al., *Maintenance of HIV-Specific Memory B-Cell Responses in Elite Controllers Despite Low Viral Burdens.* J Infect Dis, 2016. **214**(3): p. 390-8.

529. Rouers, A., et al., *HIV-Specific B Cell Frequency Correlates with Neutralization Breadth in Patients Naturally Controlling HIV-Infection.* EBioMedicine, 2017. **21**: p. 158-169.

530. Sáez-Cirión, A., et al., *Post-Treatment HIV-1 Controllers with a Long-Term Virological Remission after the Interruption of Early Initiated Antiretroviral Therapy ANRS VISCONTI Study.* PLOS Pathogens, 2013. **9**(3): p. e1003211.

531. Namazi, G., et al., *The Control of HIV After Antiretroviral Medication Pause (CHAMP) Study: Posttreatment Controllers Identified From 14 Clinical Studies.* The Journal of Infectious Diseases, 2018. **218**(12): p. 1954-1963.

532. Persaud, D., et al., *Absence of detectable HIV-1 viremia after treatment cessation in an infant.* N Engl J Med, 2013. **369**(19): p. 1828-35.

533. Luzuriaga, K., et al., *Viremic relapse after HIV-1 remission in a perinatally infected child.* The New England journal of medicine, 2015. **372**(8): p. 786-788.

534. Hütter, G., et al., *Long-Term Control of HIV by CCR5 Delta32/Delta32 Stem-Cell Transplantation.* New England Journal of Medicine, 2009. **360**(7): p. 692-698.

535. Allers, K., et al., *Evidence for the cure of HIV infection by CCR5Δ32/Δ32 stem cell transplantation.* Blood, 2011. **117**(10): p. 2791-2799.

536. Gupta, R.K., et al., *Evidence for HIV-1 cure after CCR5Δ32/Δ32 allogeneic haemopoietic stem-cell transplantation 30 months post analytical treatment interruption: a case report.* The Lancet HIV, 2020. **7**(5): p. e340-e347.

537. Hsu, J., et al. *HIV-1 REMISSION WITH CCR5delta32/delta32 HAPLO-CORD TRANSPLANT IN A US WOMAN: IMPAACT P1107*. in *Conference on Retroviruses and Opportunistic Infection (CROI)*. 2022. Colorado, Denver, USA.

538. Blankson, J.N., D. Persaud, and R.F. Siliciano, *The challenge of viral reservoirs in HIV-1 infection.* Annu Rev Med, 2002. **53**: p. 557-93.

539. Mens, H., et al., *HIV-1 continues to replicate and evolve in patients with natural control of HIV infection.* J Virol, 2010. **84**(24): p. 12971-81.

540. Pereyra, F., et al., *Persistent low-level viremia in HIV-1 elite controllers and relationship to immunologic parameters.* J Infect Dis, 2009. **200**(6): p. 984-90.

541. Dinoso, J.B., et al., *A Comparison of Viral Loads between HIV-1–Infected Elite Suppressors and Individuals Who Receive Suppressive Highly Active Antiretroviral Therapy.* Clinical Infectious Diseases, 2008. **47**(1): p. 102-104.

542. Woldemeskel, B.A., A.K. Kwaa, and J.N. Blankson, *Viral reservoirs in elite controllers of HIV-1 infection: Implications for HIV cure strategies.* eBioMedicine, 2020. **62**.

543. van Zyl, G., M.J. Bale, and M.F. Kearney, *HIV evolution and diversity in ART-treated patients.* Retrovirology, 2018. **15**(1): p. 14.

544. Kulpa, D.A. and N. Chomont, *HIV persistence in the setting of antiretroviral therapy: when, where and how does HIV hide?* Journal of Virus Eradication, 2015. **1**(2): p. 59-66.

545. Reeves, D.B., et al., *A majority of HIV persistence during antiretroviral therapy is due to infected cell proliferation.* Nature Communications, 2018. **9**(1): p. 4811.

546. Martinez-Picado, J. and S.G. Deeks, *Persistent HIV-1 replication during antiretroviral therapy.* Current Opinion in HIV and AIDS, 2016. **11**(4).

547. Chaillon, A., et al., *HIV persists throughout deep tissues with repopulation from multiple anatomical sources.* The Journal of Clinical Investigation, 2020. **130**(4): p. 1699-1712.

548. Ganor, Y., et al., *HIV-1 reservoirs in urethral macrophages of patients under suppressive antiretroviral therapy.* Nature Microbiology, 2019. **4**(4): p. 633-644.

549. Wong, M.E., A. Jaworowski, and A.C. Hearps, *The HIV Reservoir in Monocytes and Macrophages.* Frontiers in Immunology, 2019. **10**.

550. Siliciano, J.D. and R.F. Siliciano, *Enhanced Culture Assay for Detection and Quantitation of Latently Infected, Resting CD4+ T-Cells Carrying Replication-Competent Virus in HIV-1-Infected Individuals*, in *Human Retrovirus Protocols: Virology and Molecular Biology*, T. Zhu, Editor. 2005, Humana Press: Totowa, NJ. p. 3-15.

551. Finzi, D., et al., *Identification of a Reservoir for HIV-1 in Patients on Highly Active Antiretroviral Therapy.* Science, 1997. **278**(5341): p. 1295-1300.

552. Chomont, N., et al., *HIV reservoir size and persistence are driven by T cell survival and homeostatic proliferation.* Nature Medicine, 2009. **15**(8): p. 893-900.

553. Bruner, K.M., et al., *A quantitative approach for measuring the reservoir of latent HIV-1 proviruses.* Nature, 2019. **566**(7742): p. 120-125.

554. Bruner, K.M., et al., *Defective proviruses rapidly accumulate during acute HIV-1 infection.* Nature medicine, 2016. **22**(9): p. 1043-1049.

555. Procopio, F.A., et al., *A Novel Assay to Measure the Magnitude of the Inducible Viral Reservoir in HIV-infected Individuals.* EBioMedicine, 2015. **2**(8): p. 874-883.

556. Baxter, A.E., et al., *Single-Cell Characterization of Viral Translation-Competent Reservoirs in HIV-Infected Individuals.* Cell Host Microbe, 2016. **20**(3): p. 368-380.

557. Pardons, M., et al., *Single-cell characterization and quantification of translation-competent viral reservoirs in treated and untreated HIV infection.* PLOS Pathogens, 2019. **15**(2): p. e1007619.

558. Baxter, A.E., et al., *Multiparametric characterization of rare HIV-infected cells using an RNA-flow FISH technique.* Nature Protocols, 2017. **12**(10): p. 2029-2049.

559. Kinloch, N.N., et al., *HIV-1 diversity considerations in the application of the Intact Proviral DNA Assay (IPDA).* Nature Communications, 2021. **12**(1): p. 165.

560. Simonetti Francesco, R., et al., *Intact proviral DNA assay analysis of large cohorts of people with HIV provides a benchmark for the frequency and composition of persistent proviral DNA.* Proceedings of the National Academy of Sciences, 2020. **117**(31): p. 18692-18700.

561. Siliciano, J.D., et al., *Long-term follow-up studies confirm the stability of the latent reservoir for HIV-1 in resting CD4+ T cells.* Nature Medicine, 2003. **9**(6): p. 727-728.

562. Archin, N.M., et al., *Administration of vorinostat disrupts HIV-1 latency in patients on antiretroviral therapy.* Nature, 2012. **487**(7408): p. 482-5.

563. Elliott, J.H., et al., *Activation of HIV transcription with short-course vorinostat in HIV-infected patients on suppressive antiretroviral therapy.* PLoS Pathog, 2014. **10**(10): p. e1004473.

564. Archin, N.M., et al., *HIV-1 expression within resting CD4+ T cells after multiple doses of vorinostat.* J Infect Dis, 2014. **210**(5): p. 728-35.

565. Søgaard, O.S., et al., *The Depsipeptide Romidepsin Reverses HIV-1 Latency In Vivo.* PLoS Pathog, 2015. **11**(9): p. e1005142.

566. Doyon, G., et al., *Disulfiram reactivates latent HIV-1 expression through depletion of the phosphatase and tensin homolog.* Aids, 2013. **27**(2): p. F7-f11.

567. Spivak, A.M., et al., *A pilot study assessing the safety and latency-reversing activity of disulfiram in HIV-1-infected adults on antiretroviral therapy.* Clin Infect Dis, 2014. **58**(6): p. 883-90.

568. Lee, S.A., et al., *Population Pharmacokinetics and Pharmacodynamics of Disulfiram on Inducing Latent HIV-1 Transcription in a Phase IIb Trial.* Clin Pharmacol Ther, 2019. **105**(3): p. 692-702.

569. Kula, A., et al., *Heterogeneous HIV-1 Reactivation Patterns of Disulfiram and Combined Disulfiram+Romidepsin Treatments.* Journal of acquired immune deficiency syndromes (1999), 2019. **80**(5): p. 605-613.

570. Gutiérrez, C., et al., *Bryostatin-1 for latent virus reactivation in HIV-infected patients on antiretroviral therapy.* Aids, 2016. **30**(9): p. 1385-92.

571. López-Huertas, M.R., et al., *The CCR5-antagonist Maraviroc reverses HIV-1 latency in vitro alone or in combination with the PKC-agonist Bryostatin-1.* Scientific reports, 2017. **7**(1): p. 2385-2385.

572. Pardons, M., et al., *Latency-Reversing Agents Induce Differential Responses in Distinct Memory CD4 T Cell Subsets in Individuals on Antiretroviral Therapy.* Cell reports, 2019. **29**(9): p. 2783-2795.e5.

573. Kim, Y., J.L. Anderson, and S.R. Lewin, *Getting the "Kill" into "Shock and Kill": Strategies to Eliminate Latent HIV.* Cell host & microbe, 2018. **23**(1): p. 14-26.

574. Hattori, S.I., et al., *Combination of a Latency-Reversing Agent With a Smac Mimetic Minimizes Secondary HIV-1 Infection in vitro.* Front Microbiol, 2018. **9**: p. 2022.

575. Kim, J.T., et al., *Latency reversal plus natural killer cells diminish HIV reservoir in vivo.* Nature Communications, 2022. **13**(1): p. 121.

576. Mousseau, G., et al., *An analog of the natural steroidal alkaloid cortistatin A potently suppresses Tat-dependent HIV transcription.* Cell Host Microbe, 2012. **12**(1): p. 97-108.

577. Mousseau, G., et al., *The Tat Inhibitor Didehydro-Cortistatin A Prevents HIV-1 Reactivation from Latency.* mBio, 2015. **6**(4): p. e00465.

578. Kant, S., et al., *Polyfunctional Fc Dependent Activity of Antibodies to Native Trimeric Envelope in HIV Elite Controllers.* Front Immunol, 2020. **11**: p. 583820.

579. Banerjee, K., et al., *IgG subclass profiles in infected HIV type 1 controllers and chronic progressors and in uninfected recipients of Env vaccines.* AIDS research and human retroviruses, 2010. **26**(4): p. 445-458.

580. Klingler, J., et al., *Distinct antibody profiles in HLA-B∗57+, HLA-B∗57- HIV controllers and chronic progressors.* AIDS (London, England), 2022. **36**(4): p. 487-499.

581. Pittala, S., et al., *Antibody Fab-Fc properties outperform titer in predictive models of SIV vaccine-induced protection.* Molecular systems biology, 2019. **15**(5): p. e8747-e8747.

582. Heß, R., et al., *Glycosylation of HIV Env Impacts IgG Subtype Responses to Vaccination.* Viruses, 2019. **11**(2): p. 153.

583. Chung, A.W., et al., *Viral control in chronic HIV-1 subtype C infection is associated with enrichment of p24 IgG1 with Fc effector activity.* AIDS (London, England), 2018. **32**(10): p. 1207-1217.

584. Brown, E.P., et al., *High-throughput, multiplexed IgG subclassing of antigen-specific antibodies from clinical samples.* Journal of immunological methods, 2012. **386**(1-2): p. 117-123.

585. Tomaras, G.D., et al., *Initial B-cell responses to transmitted human immunodeficiency virus type 1: virion-binding immunoglobulin M (IgM) and IgG antibodies followed by plasma anti-gp41 antibodies with ineffective control of initial viremia.* Journal of virology, 2008. **82**(24): p. 12449-12463.

586. Wang, S., et al., *Broadly binding and functional antibodies and persisting memory B cells elicited by HIV vaccine PDPHV.* NPJ vaccines, 2022. **7**(1): p. 18-18.

587. Ackerman, M.E., et al., *A robust, high-throughput assay to determine the phagocytic activity of clinical antibody samples.* Journal of Immunological Methods, 2011. **366**(1): p. 8-19.

588. Nduati, E.W., et al., *Coordinated Fc-effector and neutralization functions in HIV-infected children define a window of opportunity for HIV vaccination.* AIDS (London, England), 2021. **35**(12): p. 1895-1905.

589. Fischinger, S., et al., *IgG3 collaborates with IgG1 and IgA to recruit effector function in RV144 vaccinees.* JCI insight, 2020. **5**(21): p. e140925.

590. Boivin, W.A., et al., *Intracellular versus extracellular granzyme B in immunity and disease: challenging the dogma.* Laboratory Investigation, 2009. **89**(11): p. 1195-1220.

591. Lewis, G.K., et al., *Knowns and Unknowns of Assaying Antibody-Dependent Cell-Mediated Cytotoxicity Against HIV-1.* Frontiers in Immunology, 2019. **10**.

592. Alrubayyi, A., et al., *A flow cytometry based assay that simultaneously measures cytotoxicity and monocyte mediated antibody dependent effector activity.* J Immunol Methods, 2018. **462**: p. 74-82.

593. Fischinger, S., et al., *A high-throughput, bead-based, antigen-specific assay to assess the ability of antibodies to induce complement activation.* Journal of immunological methods, 2019. **473**: p. 112630-112630.

594. Pušnik, J., et al., *Production of HIV-1 Env-specific antibodies mediating innate immune functions depends on cognate IL-21- secreting CD4+ T cells.* Journal of virology, 2021. **95**(8): p. e02097-20.

595. Dufloo, J., et al., *Anti-HIV-1 antibodies trigger non-lytic complement deposition on infected cells.* EMBO reports, 2020. **21**(2): p. e49351.

596. Goldberg, B.S., et al., *Revisiting an IgG Fc Loss-of-Function Experiment: the Role of Complement in HIV Broadly Neutralizing Antibody b12 Activity.* mBio, 2021. **12**(5): p. e0174321-e0174321.

597. Thielen, A.J.F., et al., *CRISPR/Cas9 generated human CD46, CD55 and CD59 knockout cell lines as a tool for complement research.* J Immunol Methods, 2018. **456**: p. 15-22.

598. Schmitz, J., et al., *Antibody-dependent complement-mediated cytotoxicity in sera from patients with HIV-1 infection is controlled by CD55 and CD59.* The Journal of clinical investigation, 1995. **96**(3): p. 1520-1526.

599. Saifuddin, M., et al., *Role of virion-associated glycosylphosphatidylinositol-linked proteins CD55 and CD59 in complement resistance of cell line-derived and primary isolates of HIV-1.* The Journal of experimental medicine, 1995. **182**(2): p. 501-509.

600. Richardson, S.I., et al., *Measuring the ability of HIV-specific antibodies to mediate trogocytosis.* Journal of Immunological Methods, 2018. **463**: p. 71-83.

601. Pollara, J., et al., *Application of area scaling analysis to identify natural killer cell and monocyte involvement in the GranToxiLux antibody dependent cell-mediated cytotoxicity assay.* Cytometry A, 2018. **93**(4): p. 436-447.

602. Suzuki, E., et al., *Trogocytosis-mediated expression of HER2 on immune cells may be associated with a pathological complete response to trastuzumab-based primary systemic therapy in HER2-overexpressing breast cancer patients.* BMC Cancer, 2015. **15**(1): p. 39.

603. Boross, P., et al., *Both activating and inhibitory Fc gamma receptors mediate rituximab-induced trogocytosis of CD20 in mice.* Immunology Letters, 2012. **143**(1): p. 44-52.

604. Beum, P.V., et al., *Loss of CD20 and Bound CD20 Antibody from Opsonized B Cells Occurs More Rapidly Because of Trogocytosis Mediated by Fc Receptor-Expressing Effector Cells Than Direct Internalization by the B Cells.* The Journal of Immunology, 2011. **187**(6): p. 3438.

605. Maldarelli, F., *The role of HIV integration in viral persistence: no more whistling past the proviral graveyard.* J Clin Invest, 2016. **126**(2): p. 438-47.

606. Marras, F., et al., *Control of the HIV-1 DNA Reservoir Is Associated In Vivo and In Vitro with NKp46/NKp30 (CD335 CD337) Inducibility and Interferon Gamma Production by Transcriptionally Unique NK Cells.* Journal of Virology. **91**(23): p. e00647-17.

607. Wagner Thor, A., et al., *Proliferation of cells with HIV integrated into cancer genes contributes to persistent infection.* Science, 2014. **345**(6196): p. 570-573.

608. Maldarelli, F., et al., *Specific HIV integration sites are linked to clonal expansion and persistence of infected cells.* Science, 2014. **345**(6193): p. 179-183.

609. Jiang, C., et al., *Distinct viral reservoirs in individuals with spontaneous control of HIV-1.* Nature, 2020. **585**(7824): p. 261-267.

610. Thornhill, J.P., et al., *The Role of CD4+ T Follicular Helper Cells in HIV Infection: From the Germinal Center to the Periphery.* Frontiers in Immunology, 2017. **8**.

611. Aid, M., et al., *Follicular CD4 T Helper Cells As a Major HIV Reservoir Compartment: A Molecular Perspective.* Frontiers in immunology, 2018. **9**: p. 895-895.

612. García, M., et al., *Peripheral T follicular helper Cells Make a Difference in HIV Reservoir Size between Elite Controllers and Patients on Successful cART.* Scientific Reports, 2017. **7**(1): p. 16799.

613. Banga, R., et al., *PD-1(+) and follicular helper T cells are responsible for persistent HIV-1 transcription in treated aviremic individuals.* Nat Med, 2016. **22**(7): p. 754-61.

614. Perreau, M., et al., *Follicular helper T cells serve as the major CD4 T cell compartment for HIV-1 infection, replication, and production.* J Exp Med, 2013. **210**(1): p. 143-56.

615. Fletcher, C.V., et al., *Persistent HIV-1 replication is associated with lower antiretroviral drug concentrations in lymphatic tissues.* Proc Natl Acad Sci U S A, 2014. **111**(6): p. 2307-12.

616. Breitfeld, D., et al., *Follicular B Helper T Cells Express Cxc Chemokine Receptor 5, Localize to B Cell Follicles, and Support Immunoglobulin Production.* Journal of Experimental Medicine, 2000. **192**(11): p. 1545-1552.

617. Yamamoto, T., et al., *Quality and quantity of TFH cells are critical for broad antibody development in SHIVAD8 infection.* Science Translational Medicine, 2015. **7**(298): p. 298ra120-298ra120.

618. Buranapraditkun, S., et al., *Preservation of Peripheral T Follicular Helper Cell Function in HIV Controllers.* Journal of virology, 2017. **91**(14): p. e00497-17.

619. Jefferis, R., *Isotype and glycoform selection for antibody therapeutics.* Arch Biochem Biophys, 2012. **526**(2): p. 159-66.

620. Ackerman, M.E., A.S. Dugast, and G. Alter, *Emerging concepts on the role of innate immunity in the prevention and control of HIV infection.* Annu Rev Med, 2012. **63**: p. 113-30.

621. de Taeye, S.W., et al., *FcγR Binding and ADCC Activity of Human IgG Allotypes.* Frontiers in Immunology, 2020. **11**.

622. Thomann, M., et al., *Fc-galactosylation modulates antibody-dependent cellular cytotoxicity of therapeutic antibodies.* Molecular Immunology, 2016. **73**: p. 69-75.

623. Das, J., et al., *Mining for humoral correlates of HIV control and latent reservoir size.* PLoS pathogens, 2020. **16**(10): p. e1008868-e1008868.

624. Bartsch Yannic, C., et al., *Viral Rebound Kinetics Correlate with Distinct HIV Antibody Features.* mBio. **12**(2): p. e00170-21.

625. Leon, A., et al., *Rate and predictors of progression in elite and viremic HIV-1 controllers.* Aids, 2016. **30**(8): p. 1209-20.

626. Pereyra, F., et al., *Increased coronary atherosclerosis and immune activation in HIV-1 elite controllers.* AIDS (London, England), 2012. **26**(18): p. 2409-2412.

627. Okulicz, J.F., et al., *Cancers in elite controllers: appropriate follow-up is essential.* AIDS, 2016. **30**(11).

628. Poizot-Martin, I., et al., *Cancer risk in HIV-infected patients: elite controllers are also concerned.* Aids, 2018. **32**(5): p. 673-675.

629. Crowell, T.A., et al., *Hospitalization Rates and Reasons Among HIV Elite Controllers and Persons With Medically Controlled HIV Infection.* J Infect Dis, 2015. **211**(11): p. 1692-702.

630. Chun, T.-W., et al., *Effect of antiretroviral therapy on HIV reservoirs in elite controllers.* The Journal of infectious diseases, 2013. **208**(9): p. 1443-1447.

631. Boufassa, F., et al., *Blunted response to combination antiretroviral therapy in HIV elite controllers: an international HIV controller collaboration.* PloS one, 2014. **9**(1): p. e85516-e85516.

632. Sedaghat, A.R., et al., *T cell dynamics and the response to HAART in a cohort of HIV-1-infected elite suppressors.* Clinical infectious diseases : an official publication of the Infectious Diseases Society of America, 2009. **49**(11): p. 1763-1766.